Regulation of START domain-containing proteins through membrane interaction

Von der Fakultät Energie-, Verfahrens- und Biotechnik der

Universität Stuttgart zur Erlangung der Würde eines

Doktors der Naturwissenschaften (Dr. rer. nat.)

genehmigte Abhandlung

vorgelegt von

Patrik Erlmann

aus Filderstadt

Hauptberichter: Prof. Dr. Klaus Pfizenmaier

Mitberichter: Prof. Dr. Thomas Günther-Pomorski

Tag der mündlichen Prüfung:

26.06.2009

Institut für Zellbiologie und Immunologie

Universität Stuttgart

2009

"It doesn't matter how beautiful your theory is, it doesn't matter how smart you are. If it doesn't agree with the experiment, it's wrong."

Richard Feynman (1918-1988)

Index

1. Zusammenfassung

In Säugern sind 15 Proteine mit einer lipidbindenden START-Domäne bekannt. Die bislang charakterisierten Mitglieder dieser Proteinfamilie können Lipide *in vitro* zwischen Membranen transportieren. Um ihre Transportfunktion auszuüben, müssen START-Domänen-Proteine mit Zellmembranen direkt wechselwirken. Das Ziel der Arbeit war es aufzuklären, wie diese Wechselwirkung mit Membranen reguliert wird und ob sie eine Auswirkung auf die Proteinfunktion hat. Drei Proteine mit START-Domäne wurden näher untersucht: STARD10, CERT/StarD11 und DLC1/StarD12.

StarD10 ist ein „minimales" START-Domänen-Protein, welches keine weiteren Lokalisationsmotive besitzt. Es wurde bereits gezeigt, dass StarD10 *in vitro* Phosphatidylcholin (PC) und in geringerem Maße Phosphatidylethanolamin (PE) transportiert. Mit Hilfe massenspektrometrischer Analysen haben wir Serin 284 als eine neue Phosphorylierungsstelle in StarD10 identifiziert. Phosphorylierung dieses Serins durch Casein-Kinase II führte zu einer Abnahme des Lipidtransports *in vitro* und reduzierte die Membranbindung des Proteins *in vivo*. Zwischen welchen zellulären Membranen der StarD10-vermittelte Lipidtransfer erfolgt, ist jedoch noch unbekannt.

Hingegen ist das Ceramidtransferprotein CERT für den Transport von Ceramid vom Endoplasmatischen Retikulum (ER) zum Golgi-Komplex verantwortlich. CERT assoziiert über ein FFAT-Motiv mit dem ER-ständigen VAP-Protein, während die PH-Domäne an Phosphatidylinositol-4-Phosphat (PI(4)P) bindet, welches in Golgi-Membranen angereichert ist. Wir konnten zeigen, dass CERT als Substrat der Proteinkinase D (PKD) am Golgi-Komplex dient. PKD-vermittelte Phosphorylierung an Serin 132 verminderte sowohl die PH-Domänen-abhängige Bindung des Proteins an PI(4)P-haltige Membranen als auch den Ceramidtransport. Zusammenfassend lässt sich sagen, dass die Membranbindung von StarD10 und CERT durch Phosphorylierung negativ reguliert wird und dies zur Reduktion ihrer Lipidtransferaktivitäten führt.

Das Tumorsuppressor-Protein Deleted in Liver Cancer 1 (DLC1) ist ein GTPase-inaktivierendes Protein (GAP), das eine START-Domäne besitzt, deren Ligand und Funktion noch nicht identifiziert worden sind. Durch seine GAP-Domäne inaktiviert DLC1 kleine GTPasen der Rho-Familie und beeinflusst so die Remodellierung des Aktin-Zytoskeletts und biologische Prozesse wie Zellmigration und Zellproliferation. In dieser Arbeit konnte in DLC1 eine bisher unbekannte basische Region (PBR) identifiziert werden, über die das GAP-Protein mit dem Lipid Phosphatidylinositol-(4,5)-Biphosphat (PI(4,5)P_2) interagiert. Die funktionelle Bedeutung dieser Interaktion konnte sowohl in zellfreien Systemen also auch in lebenden Zellen aufgezeigt werden: Die Anwesenheit von PI(4,5)P_2-angereicherten Membranen steigerte die RhoGAP-Aktivität von DLC1 *in vitro*. Darüberhinaus wurde in lebenden Zellen die Rho-abhängige Signaltransduktion

durch eine DLC1 Mutante, in der die PBR deletiert war, weniger stark reduziert als durch das Wildtyp-Protein. Weiterhin war diese Deletionsmutante in ihrer Aktivität hinsichtlich der Unterdrückung von Zellausbreitung, gerichteter Migration und Proliferation stark eingeschränkt. $PI(4,5)P_2$ ist somit ein wichtiger Kofaktor der Regulation von DLC1-Aktivität. Interessanterweise war die PBR weder für die Rekrutierung von DLC1 an Membranen ausreichend, noch war die subzelluläre Verteilung von DLC1 durch die Deletion der PBR verändert. Stattdessen haben wir Hinweise dafür, dass die Lokalisation von DLC1 über andere Mechanismen geregelt wird. Die Bindung an die Lipidphosphatase PTEN könnte zur Rekrutierung von DLC1 an die Plasmamembran beitragen, während 14-3-3 Adaptorproteine DLC1 im Zytosol sequestrieren.

2. Summary

In mammals, there are 15 proteins that contain a lipid-binding START domain and those that have been characterized are able to transfer lipids between membranes *in vitro*. A prerequisite for START domains to act as lipid carriers is the interaction of the protein with cellular membranes. The goal of this thesis was to investigate how membrane targeting of these START domain-containing proteins is regulated and affects protein function. Three START family members were studied in greater detail: StarD10, CERT/StarD11 and DLC1/StarD12.

StarD10 is a minimal START domain protein with no additional targeting sequences, which was previously shown to transfer phosphatidylcholine (PC) and to a lesser extent phosphatidylethanolamine (PE) *in vitro*. By mass spectrometry, we identified a novel phosphorylation site in StarD10 at serine 284. We were able to show that casein kinase II-mediated phosphorylation of this site reduced lipid transfer *in vitro* and membrane binding *in vivo*. However, the intracellular route of lipid transfer by StarD10 still remains to be determined. By contrast, the ceramide transfer protein CERT is known to shuttle ceramide from the endoplasmatic reticulum (ER) to the Golgi complex. Targeting to these organelles is mediated via the FFAT motif that binds to the ER-resident protein VAP and the PH domain that binds phosphatidylinositol-(4)-phosphate (PI(4)P) enriched in Golgi membranes. Here we identified CERT as a novel substrate for Protein Kinase D (PKD) at the Golgi. PKD-mediated phosphorylation at serine 132 is shown to reduce the PH domain-dependent interaction of CERT with PI(4)P-containing membranes and ceramide transfer. Thus, membrane binding of both StarD10 and CERT is negatively regulated by phosphorylation and this results in decreased lipid transfer efficiency.

The tumor suppressor protein DLC1 (Deleted in Liver Cancer 1) is a Rho GTPase activating protein (GAP), which contains a START domain of unknown specificity and function. Through its GAP domain DLC1 inactivates the small GTPase RhoA to control actin cytoskeletal remodeling and biological processes such as cell migration and proliferation. In this thesis, DLC1 was found to interact with phosphatidylinositol-(4,5)-bisphosphate ($PI(4,5)P_2$) through a previously unrecognized polybasic region (PBR). Interestingly, $PI(4,5)P_2$-containing membranes enhanced DLC1 RhoGAP activity *in vitro*. In living cells, a DLC1 mutant lacking an intact PBR inactivated Rho signaling less efficiently and was severely compromised in suppressing cell spreading, directed migration and proliferation. $PI(4,5)P_2$ thus appears to be an important cofactor in DLC1 regulation *in vivo*. The PBR, however, was not sufficient to recruit DLC1 to membranes and its deletion did not alter DLC1 subcellular localization. Instead, we provide evidence for alternative mechanisms towards the regulation of DLC1 localization. DLC1 interaction with the lipid phosphatase PTEN may contribute to plasma membrane localization, while interaction with 14-3-3 adaptor proteins sequesters the protein in the cytoplasm.

3. Introduction

3.1. Cellular membranes

The eukaryotic cell as well as its organelles are surrounded by a double layer of lipids. Besides the lipids, various proteins interact with and are incorporated into these membranes. These double layer membranes have special physical and chemical properties, providing the cell with a self-assembling, stable and water-impermeable barrier that is still very flexible and allows easy partitioning. These characteristics are essential for cell division, biological reproduction and intracellular trafficking (van Meer et al., 2008).

3.1.1. The lipids of the membrane

The most abundant lipids in mammalian membranes are the glycerophospholipids: PC, PE, phosphatidylserine, phosphatidylinositol (PI) and phosphatidic acid. In these lipids, two fatty acyl chains of different length and saturation as well as a polar headgroup are attached to a glycerol backbone. The sphingolipids are comprised of ceramide as the hydrophobic backbone and a variety of headgroups such as myelin, mono-, di-, or oligosaccharides and sialic acids. The major non-polar lipid components are the sterols, and in mammalian cells cholesterol is predominant (van Meer et al., 2008). Additionally, there exist a large number of hydrolysis products or modified lipids that, although small in number, are known to play an important role in cell signaling. The main site of lipid biogenesis is the endoplasmatic reticulum (ER), but modification and processing of the lipids takes place at all organelles. All in all, the variation of headgroups and aliphatic side chains alone allow the existence of over 1000 different lipid species (van Meer et al., 2008).

3.1.2. Lipid distribution

Interestingly, these different lipids and their subspecies are distributed non-randomly between the plasma membrane, the membranes of cellular organelles, as well as between the two sheets of the bilayer. Even within an organelle membrane, the lipid composition varies forming so-called microdomains that are enriched in distinct lipid species and thus possess special properties, due to differences in charge or membrane fluidity. In addition to the barrier function and as a result of the non-random distribution, membranes act as signaling platforms with lipids being versatile and dynamic regulators of numerous cellular processes, including cell growth, cell survival, intracellular signaling, cargo sorting, vesicle fission and membrane transport (Holthuis and Levine, 2005). For the less abundant lipid species the non-random distribution can be explained by local metabolism. This is the case for the phosphoinositides, phosphorylated sphingosines and bioactive metabolites such as phosphatidic acid and lysophospholipids (Wymann and Schneiter, 2008). But the major lipid components of the cellular membrane are non-randomly distributed, too, in spite of the heavy vesicular traffic between organelles and their ability to diffuse freely within the membrane. To keep

up this segregation, active protein-driven lipid sorting is necessary (Holthuis and Levine, 2005). Concerning the transport of lipids between organelles, so-called "membrane contact sites" (MCS) might play an important role. Here, small patches of membrane from two different organelles are in close proximity, probably stabilized by proteins, allowing for a rapid exchange of lipids by transfer proteins shuttling between the two membranes (Levine and Loewen, 2006). The bulk way of
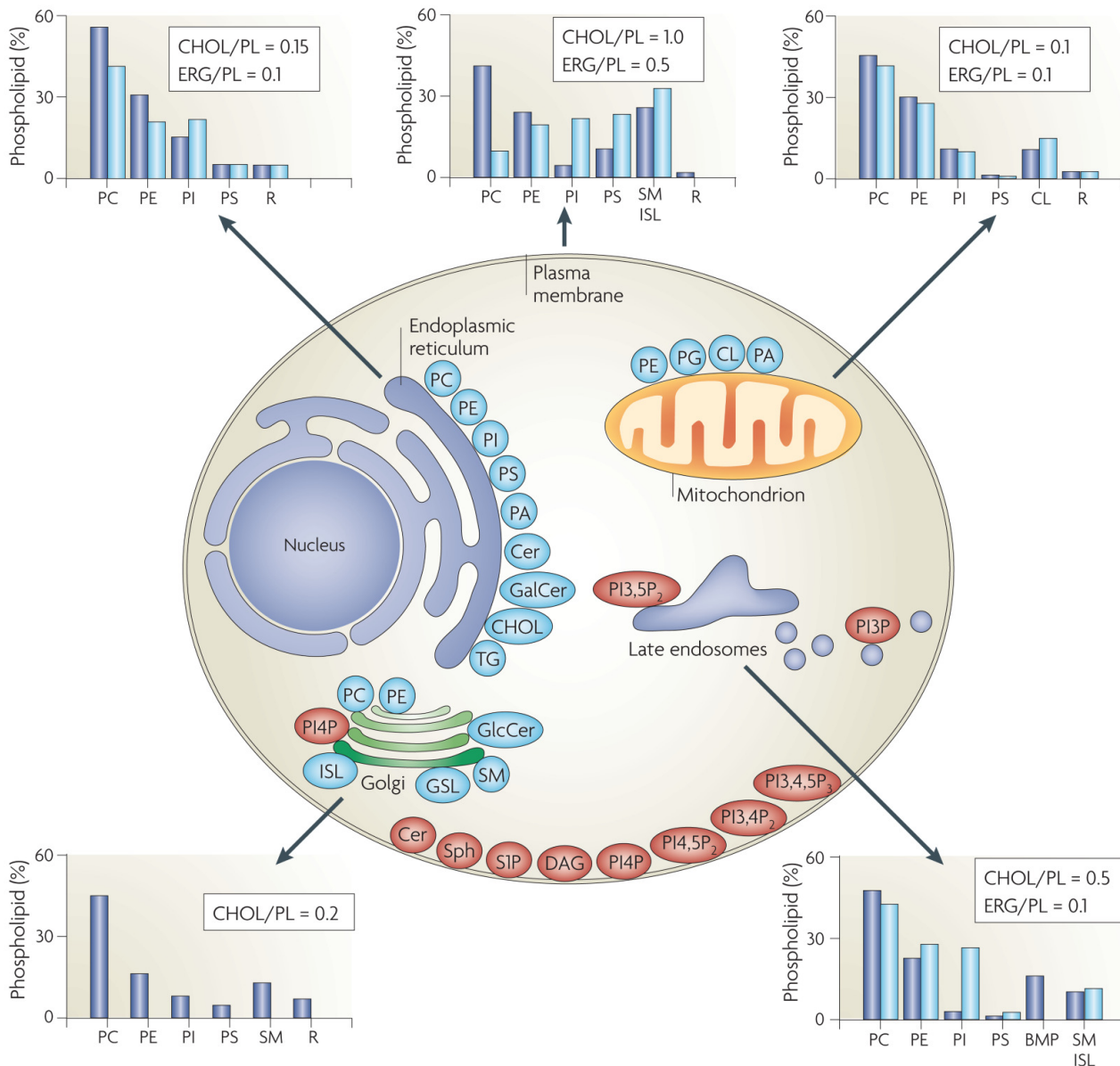
Figure 1: Lipid synthesis and steady-state composition of cell membranes: The lipid compositional data are expressed as a percentage of the total phospholipid (PL) in mammals (blue) and yeast (light blue). As a measure of sterol content, the molar ratio of cholesterol (CHOL; in mammals) and ergosterol (ERG; in yeast) to phospholipid is also included. The main panel shows the site of synthesis of the major phospholipids (blue) and lipids that are involved in signaling and organelle recognition pathways (red). Abbreviations: phosphatidylcholine (PtdCho; PC), phosphatidylethanolamine (PtdEtn; PE), phosphatidylinositol (PtdIns; PI), phosphatidylserine (PtdSer; PS), ceramide (Cer), phosphatidic acid (PA), galactosylceramide (GalCer), triacylglycerol (TG) synthesis, sphingomyelin (SM), complex glycosphingolipids (GSLs), yeast inositol sphingolipid (ISL), diacylglycerol (DAG), cardiolipin (CL), BMP (bis(monoacylglycero)phosphate), phosphatidylinositol-(3,5)-bisphosphate (PI(3,5)P$_2$), phosphatidylinositol-(4,5)-bisphosphate (PI(4,5)P$_2$), phosphatidylinositol-(3,4,5)- trisphosphate (PI(3,4,5)P$_3$), phosphatidylinositol-4-phosphate (PI4P), remaining lipids (R) and sphingosine-1-phosphate (S1P). From (van Meer et al., 2008)

distributing lipids is by vesicle transport between the organelles and between organelles and the plasma membrane. Here, active segregation of lipids into the vesicle membrane also takes place (Holthuis and Levine, 2005). The lipid distribution between the organelles is displayed in Figure1.

3.1.3.   Lipid signaling

Lipid phosphorylation

Phosphorylation has proven to be a versatile transient secondary modification used by eukaryotic cells in a wide range of processes from activity control, localization and interactions of proteins to the activation of substrates. Less known but equally important is the phosphorylation of lipids. Two types of lipids are phosphorylated, sphingolipids and PI. These lipids function either as versatile, short-lived second messengers themselves or act as a signaling platform (Di Paolo and De Camilli, 2006).

Phosphoinositides have been studied in great detail and it has been shown that they play a role in virtually all cellular signaling processes that involve the membrane. The inositol ring can be phosporylated at three positions 3', 4' and 5' and at one, two or three sites at one time. This results in seven different combinations that are shown in Figure 2. It has been shown that all have a definite function rather than being an intermediate synthesis product (Vicinanza et al., 2008).

Most important and present in the highest quantity in the cell is $PI(4,5)P_2$, which accounts for up to 0,5% of the membrane lipids. The highest $PI(4,5)P_2$ concentrations are found at the inner leaflet of
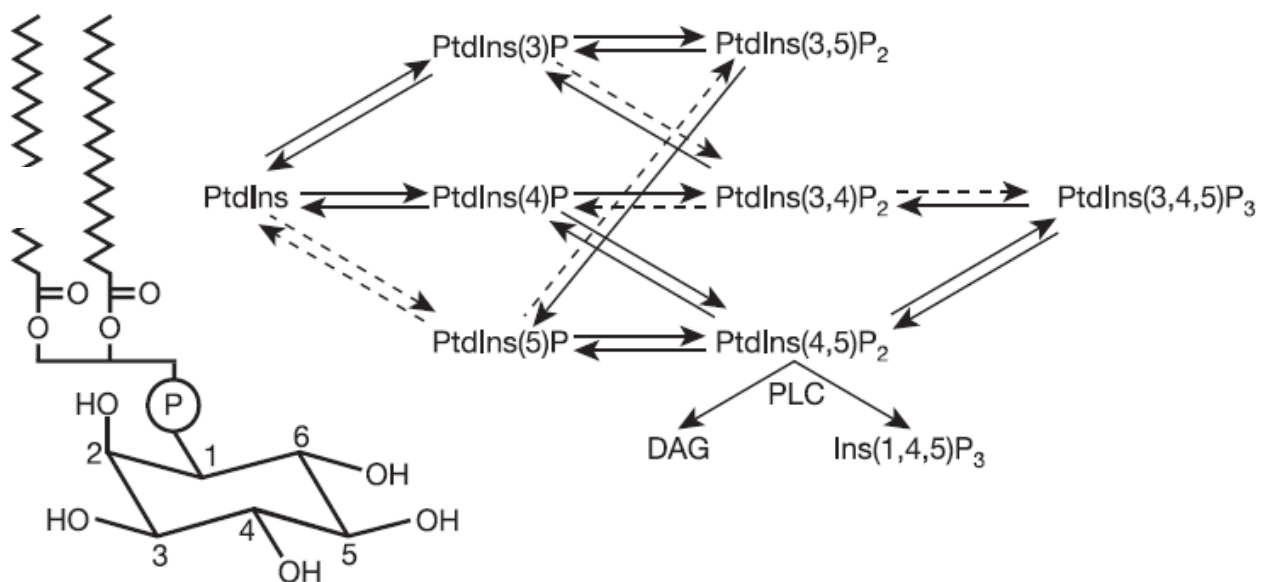
Figure 2: The phosphorylated phosphatidylinositols: Drawing of phosphatidylinositol, the numbers indicating the possible phosphorylation sites. Metabolic reactions leading to the generation of the seven phosphorylated phospohoinositides. Solid arrows indicate in vivo and broken arrows in vitro only characterized reactions. Abbreviations: phosphatidylinositol (PtdIns), phospholipase C (PLC), inositol-(1,4,5)- trisphosphate (Ins(1,4,5)P3), diacylglycerol (DAG). From (Di Paolo and De Camilli, 2006).

the plasma membrane. There, PI(4,5)P$_2$ is involved in the regulation of the structural components of the cell, which will be discussed in more detail later, and signal transduction at the plasma membrane. The activation of phospholipases and PI(4,5)P$_2$ is the source for active metabolites such as diacylglycerol (DAG), phosphorylated inositol (IP$_3$) and PI(3,4,5)P$_3$. Additionally, PI(4,5)P$_2$ plays a role in endocytosis, exocytosis, phagocytosis and the regulation of ion channels (Niggli, 2005).

PI(4)P is the predominant phosphoinositide at the Golgi complex. PI(4)P is necessary for Golgi to plasma membrane transport processes as well as maintenance of the Golgi structural and functional organization. PI(3)P and PI(3,5)P$_2$ play a crucial role in endosome dynamics. PI(3)P is a major determinant of the early endosome, whereas PI(3,5)P$_2$ is suggested to play a role in induction of vesicle budding from endosomes and in yeast it is the major phosphoinositide at the vacuole (Vicinanza et al., 2008). The spatio-temporal regulation of the phosphoinositides is maintained by a large set of lipid kinases, such as the phosphoinositol-4-kinase IIIβ (PI4K IIIβ) that produces PI(4)P exclusively at the Golgi complex and lipid phosphatases such as Sac1 that clears vesicles leaving the Golgi complex of residual PI(4)P (Behnia and Munro, 2005).

Less is known about the sphingolipid phosphates, ceramide-1-phosphate (C1P) and sphingosine-1-phosphate (S1P). C1P plays a role in inflammation and vesicular trafficking whereas S1P is involved in cell growth, cell survival, angiogenesis, vasculogenesis, neuritogenesis and immune function (Chalfant and Spiegel, 2005). Thus far no domains binding to or interacting specifically with S1P are known while C1P is known to be bound by the C2 domain of the cytocolic phospholipase A2 (cPLA2) in a Ca^{2+} dependant manner (Stahelin et al., 2007).

Active lipid metabolites

Products of lipid metabolism are also used as signaling compounds by the cell. A prominent example is the degradation of PI(4,5)P$_2$ by the phospholipase C (PLC). PLC cleaves the phospholipid, releasing the hydrophilic second messenger IP$_3$ into the cytosol. There, it leads to the release of Ca^{2+}, the second metabolite DAG remains in the membrane where it activates protein kinase C (PKC). cPLA2 cleaves phospholipids releasing one polyunsaturated fatty acid that is used for the production of eicosanoids, and the remaining lyso-phospholipid is also thought to be used as a signaling molecule (Wymann and Schneiter, 2008).

3.1.4. Regulation of the actin cytoskeleton and the cell-matrix contacts by phosphoinositides

Naturally it is more likely that events taking place at or near cellular membranes are prone to be regulated by lipid signaling. At the plasma membrane, a number of proteins that are involved in the regulation of the actin cytoskeleton have been shown to be regulated by phosphoinositides. An example is the regulation of actin assembly and disassembly, where on the one hand, gelsolin, villin, cofilin and profilin, which sever or depolymerize actin, are negatively regulated by $PI(4,5)P_2$. On the other hand, this lipid activates proteins responsible for ignition of actin polymerization (N-WASP), crosslinking of filaments and linking filaments to the membrane (vinculin, talin, ezrin) (Janmey and Lindberg, 2004; Niggli, 2005). The same lipid plays an important role in connecting the cell to the matrix via so-called "focal adhesions". Focal adhesions arise when integrin-matrix contacts get connected to the actin cytoskeleton, leading to resilient contacts important for stress fiber formation, cell movement and shape (Sechi and Wehland, 2000; Worth and Parsons, 2008). $PI(3,4,5)P_3$ is also mainly seen at the plasma membrane, where it plays a role in the regulation of the actin cytoskeleton. Most of the mentioned actin regulating proteins also bind to $PI(3,4,5)P_3$ and some like WAVE2 bind it exclusively (Niggli, 2005).

3.2. Protein-membrane interaction

Association of proteins with intracellular membranes is essential for a variety of cellular functions, including lipid transport, signaling, vesicle trafficking and maintenance of the cell structure. This calls for a wide range of different membrane interaction motifs with different specificities and physical properties. These are subgrouped into unspecific membrane targeting domains that target the protein to any given membrane, domains that bind one specific lipid ligand, domains that require cofactors for membrane binding and domains that bind to membranes that reveal certain physical properties (Lemmon, 2008). In the following section I carefully distinguish between interaction and binding. The term binding is only used when a domain is able to extract a lipid from a membrane, securely binding it.

3.2.1. Unspecific membrane targeting domains

Transmembrane proteins

The most common way to target a protein to the plasma membrane are membrane-spanning helices. These "transmembrane" proteins are inserted into the membrane during their translation at the ER. Common to these proteins is a α-helix comprised of 19-21 hydrophobic amino acids that interact with the hydrocarbon environment of the lipid acyl side chains. Transmembrane proteins are distinguished by the number of membrane-spanning helices. They are not very mobile and unable to dissociate from the intact membrane, but can be recruited to membrane microdomains such as lipid rafts (Shima et al., 2003). Hence, membrane-spanning proteins mostly act as

structural components or, if they are involved in signaling processes, they either transport the signal across the membrane or they are partially cleaved to allow for signal transduction into the cytosol.

Acylation and prenylation

These are secondary modifications that target proteins to the plasma membrane by covalently adding apolar groups to amino acids. The N-myristoyl-transferase catalyzes the addition of myristoyl-CoA to an N-terminal glycine residue, and in a similar way, palmitoyl-CoA is transferred to cysteine residues. Pyrophosphate forms of farnesyl and geranylgeranyl are covalently bound to C-terminal cysteine residues. The amino acid sequence of the protein dictates whether farnesyl or geranylgeranyl is bound. Farnesylation occurs at carboxy-terminal CaaX (C is cysteine, a is any aliphatic amino acid and X is any amino acid), whereas geranylgeranylation occurs at CC, CXC or CCXX amino acid clusters The prenyl or acyl anchor is a general membrane-targeting motif with no preferences for lipid composition of the membrane. Proteins modified in this way can diffuse on and off the membrane if the hydrophobic group is protected from the cytosol, for example by another protein or a hydrophobic pocket within the protein itself (Fivaz and Meyer, 2003; Resh, 2004). The most prominent prenylated proteins are among the 125 members of the small GTPase family of proteins, 48 of which are localized at the membrane, and 43 possess one or more prenylation or acylation sites (Heo et al., 2006). Inhibition of this modification renders most of these proteins inactive, proving the importance of the modification (Roberts et al., 2008).

3.2.2.   Lipid-specific membrane targeting domains

These membrane targeting domains interact with one or more specific lipids tethering the domain to the surface of the membrane. Some of these domains show a very specific targeting, recognizing the headgroup of a distinct lipid even in a stereo-specific way. Most of these domains utilize phosphoinositides as binding partners. Because of their spatio-temporal regulation and their restriction to certain organelles in the cell phosphoinositides are ideal targets for specific domains (Lemmon, 2008).

C1 and FYVE domains

C1 and FYVE domains are zinc finger domains that interact with lipids through a conserved region. Both harbor additional hydrophobic side chains encircling the lipid interaction domain. These side chains penetrate into the apolar membrane and strengthen the interaction with lipids incorporated into the membrane. For C1 (conserved region-1) domains, the conserved motif is $HX_{12}CX_2CX_{13-14}CX_2CX_4HX_2CX_7C$, where C is cysteine, H is histidine and X is any residue. The domain ensures for a very strong binding of the ligand DAG or phorbol esters. The prototype C1 domain is found in PKC, where it controls PKC activation by DAG and phorbol esters. In the case of FYVE (Fab1, YOTB, Vac1, and EEA1) domains, the conserved motif RR/KHHCR forms a weak positively charged binding pocket. Because binding to the ligand PI(3)P is weak, membrane binding of some

FYVE domain-containing proteins require dimerization to allow multivalent binding (Lemmon, 2008; Stahelin, 2008).

PX and PROPPINS domains

PX (Phox-homology) domains have a $\alpha+\beta$ structure and interact with PI(3)P. PROPPINS (β-propellers that bind phosphoinositides) is a β-propeller domain that binds PI(3,5)P_2. Both domains have hydrophobic side chains penetrating the membrane, leading to strong membrane interaction (Lemmon, 2008).

PH domain

The PH (pleckstrin homology) domains are 100 amino acids in length and form a α–β sandwich that possesses a deep interacting pocket for lipid headgroups and contains the sequence motif $KX_n(K/R)XR$. PH domains lack the apolar side chains that support membrane insertion, thus they readily bind to free lipids or headgroups only. The ligands for PH domains are phosphoinositides such as PI(3)P, PI(4,5)P_2 or PI(3,4,5)P_3. Some of the domains display a strong specificity for one PI(X)P_X, whereas others recognize several. PH domains are the most abundant lipid interacting domains in mammals, and they are found in their name-giving protein pleckstrin, PLCδ as well as in the lipid transfer protein CERT that will be discussed later in more detail (Lemmon, 2008; Stahelin, 2008).

3.2.3. Cofactor-dependant membrane binding domains

C2 domain

The C2 domain is a Ca^{2+}-dependant phospholipid binding domain that comprises a characteristic 8-stranded antiparallel β sandwich of 130 amino acid. C2 (conserved region-2) domains lack a basic binding pocket. In fact, addition of positively charged Ca^{2+} ions is sufficient to lead to a change in the electrostatic characteristics of the domain, allowing for interaction with the negatively charged membrane. C2 domains have no common ligand, some interact with phosphatidylserine, whereas others interact with all anionic or even zwitterionic phospholipids. The C2 domain was first described in PLC (Lemmon, 2008; Stahelin, 2008).

3.2.4. Membrane binding domains that require special physical properties

ENTH, ANTH and BAR domains

All these domains interact more or less specifically with acidic phospholipids. Due to their structure and/or capacity to bind to structural proteins, these domains are involved in membrane deformation. ENTH domains possess an amphiphatic helix that becomes ordered upon membrane interaction, and with this helix the protein inserts into and deforms the membrane. The BAR (F-BAR, N-BAR) domains have an extended coiled-coil structure and form "banana"-shaped dimers that have been proposed to touch the membrane with their whole concave face, promoting or

sensing membrane curvature. Isolated BAR domains have been shown to bind to and tubulate membranes *in vitro* (Lemmon, 2008)*.*

Polybasic regions

PBRs consist of multiple positively charged amino acids that bind to the headgroups of acidic phospholipids. They are often accompanied by hydrophobic amino acids that are speculated to penetrate into the apolar membrane. In some cases it has been shown that these hydrophobic amino acids are essential for membrane targeting (Heo et al., 2006). It is unclear whether PBRs are able to bind to a specific phospholipid or just recognize the charged lipid surface of the membrane (Papayannopoulos et al., 2005). They generally have a rather low affinity to membranes and are therefore often accompanied by a second membrane targeting motif, such as prenyl groups attached to small GTPases (Heo et al., 2006). As there is no consensus in sequence or structure for the PBRs, they are hard to identify, but it is speculated that these low affinity binding sites are frequent in proteins having a function in the vicinity of membranes (Fivaz and Meyer, 2003).

3.3. Lipid binding domains

All lipid binding domains share a certain structural phenomenon by forming a hydrophobic cavity large enough to take up a specific lipid ligand. Besides this, the primary structure of these domains is not homologous. The domains themselves do not necessarily bind to membranes, but they need to be in close contact with membranes in order to exchange the bound lipid molecule. Most proteins harboring such domains have been postulated to transfer lipids from one membrane in the cell to another. Lipid transfer between membranes has been shown for almost all lipid binding domains *in vitro* but their *in vivo* function is poorly understood. An expectation is the CERT protein that transfers ceramide from the ER to the Golgi complex (Wirtz, 2006). It has been proposed that these proteins predominantly act at MCS where different organelles are in close contact. Whether MCS really exist and lipid binding proteins fulfill their function at these sites remains to be proven (Levine and Loewen, 2006).

3.3.1.   SCP-2, PI-TP and Sec14 domains

The sterol carrier-2 (SCP-2) domain lacks specificity for a lipid ligand and is able to transport a large variety of lipids, e.g. phospholipids, acyl-CoA esters, fatty acids as well as sterols in *in vitro* assays. In mammals, there are only two proteins known that harbor a SCP-2 domain, the peroxisomal SCP-X and the cytosolic SCP-2 proteins (Wirtz, 2006).

PI transfer proteins (PI-TPs) act as carriers for PI, PC and in some cases sphingomyelin. Examples of PI-TP domains are found in the name-giving cytosolic PI-TP proteins, as well as in the family of Nir tyrosine kinases. The yeast homolog Sec14 possesses a 32% sequence identity and by computational analysis more than 500 Sec14-like proteins were found, reaching from plants to mammals (Schaaf et al., 2008).

3.3.2. START domains

The steroidogenic acute regulatory protein related transfer (START) domain is a 210 amino acid helix-grip domain that is conserved from plants to mammals. START domains are known to transport sterols, phospholipids and sphingolipids, and most START domains are ligand specific (Alpy and Tomasetto, 2005). In plants, START domains are more common than in mammals with Arabidopsis containing 35 START proteins. Specialities of plants are homeodomain-containing transcription factors with a START domain, which might act as metabolic sensors (Schrick et al., 2004). The 15 mammalian proteins are discussed in greater detail in the following section.

3.4. The family of START domain proteins

The START domain is conserved from plants to mammals. It is also present in yeast, some bacteria and protists but is absent in archea. Here I will discuss the mammalian START domain proteins as well as the Drosophila DLC1 homolog RhoGAP88C.

Special attention will be devoted to StarD10, CERT and DLC1, as these proteins are the focus of this thesis. The mammalian START domains are grouped into subfamilies by sequence alignment and the phylogenic tree is shown in Figure 3. Some START domain-containing proteins were
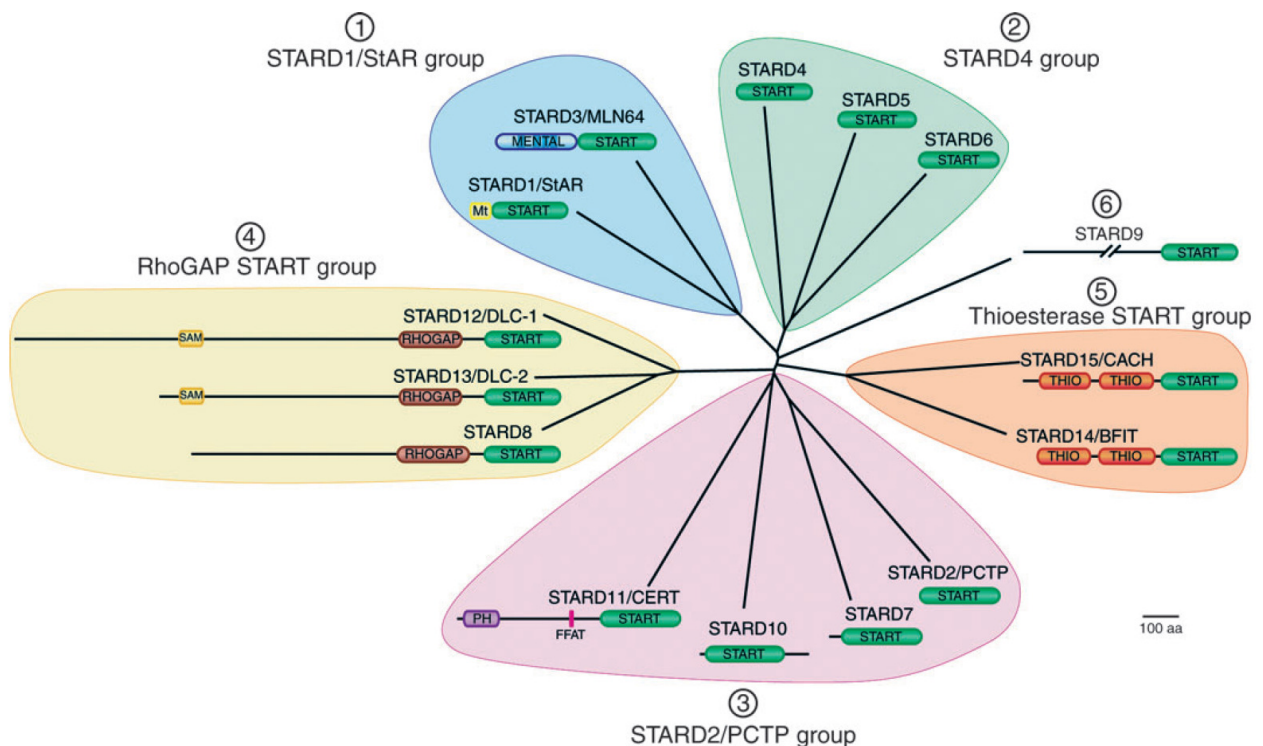
Figure 3: Phylogenetic tree and domain organizations of the 15 START-domain proteins in humans. START domain sequences were aligned by the Eclustalw program (Genetics Computer Group, Madison, WI). The phylogenetic tree was drawn with the drawtree software [J. Felsenstein, 1993, PHYLIP (Phylogeny Inference Package) v.3.5c, Department of Genome Sciences, University of Washington, Seattle, WA].Abbreviations: Mt, mitochondrial targeting motif; MENTAL, MLN64 N-terminal domain; PH, pleckstrin homology domain; FFAT, two phenylalanines in an acidic tract motif responsible for ER targeting; RHOGAP, Rho-GTPase-activating-protein domain; SAM, sterile alpha motif; THIO, acyl-CoA thioesterase domain. From (Alpy and Tomasetto, 2005).

shown to transfer lipids *in vitro*. It is still a controversy, however, whether these proteins also transfer lipids between membranes *in vivo*, because most of them lack membrane targeting sequences. It is being discussed that some START domain proteins are more likely to act as lipid sensors or "mobilize" lipids, making them available for other proteins (Alpy and Tomasetto, 2005).

3.4.1.   StarD1/StAR group

The StarD1/StAR group comprises two members that both transfer cholesterol. In addition to the START domain, StarD1/StAR has a mitochondrial targeting sequence. StAR seems to be essential for the transfer of cholesterol from the outer to the inner mitochondrial membrane where it is used to generate the hormone pregnenolone by enzymatic cleavage through p450scc. Ectopic expression of StAR leads to increased pregnenolone production in the absence of a stimulus (Arakane et al., 1997). When the StAR gene is mutated, patients develop congenital lipoid adrenal hyperplasia (lipoid CAH) resulting from accumulation of cholesterol in the gonads and the adrenal glands and decreased steroid synthesis. These patients suffer from severe adrenal insufficiency in both sexes and complete female external genitalia in genetic males (Kaku et al., 2008).

StarD3/MLN64 is targeted to the endosomal membrane by a MENTAL domain, where it is thought to mediate mobilization and regulate levels of endosomal cholesterol. The protein was first discovered as a gene overexpressed in malignant breast tumors (Alpy and Tomasetto, 2005).

3.4.2.   StarD4 group

This group is comprised of three minimal START domain proteins. StarD4 and StarD5 are believed to transfer cholesterol, whereas the lipid ligand for StarD6 is unknown. StarD4 and StarD5 are expressed ubiquitously but are differentially regulated, with StarD4 being regulated by sterol-regulatory binding proteins and StarD5 in response to ER stress. By contrast, StarD6 is restricted to the testes where it is expressed during spermatogenesis in spermides but not in steroidogenic cells (Alpy and Tomasetto, 2005).

3.4.3.   StarD2/PCTP group

This group is more heterogeneous concerning the lipid ligands as well as the domain structure.

StarD2/PCTP

StarD2/PCTP is a cytosolic protein capable of rapidly transferring PC between membranes. Several possible lipid transfer routes have been suggested but a knock-out mouse showed no phenotype other than the impaired secretion of bile salts and bile cholesterol when fed a high-fat, high-cholesterol lithogenic diet. Thus a function for StarD2 in transporting PC to the hepatocytic canalicular membrane where PC is secreted into bile is the most likely, especially as the liver expresses relatively high amounts of StarD2. The absence of a solid phenotype in the knock-out mouse raises the possibility that other START domain-containing proteins, especially StarD10 and to a lesser extent StarD7, may compensate for StarD2 (Alpy and Tomasetto, 2005). It has also

been postulated that interaction partners might dictate the function of STARD2. A yeast two hybrid screen revealed two possible binding partners for PCTP, the thioesterase Them2 and the homeodomain transcription factor Pax3. StarD2 enhanced both the thioesterase activity of Them1 *in vitro* and Pax3-mediated activation of transcription in a reporter gene assay (Kanno et al., 2007).

StarD7

The lipid ligand of StarD7 is unknown. StarD7 is broadly expressed and the sequence is similar to that of StarD2 and StarD10, making a role as a phospholipid transporter possible. However, we did not observe any phospholipid transfer activity nor were we able to identify phospholipids bound to StarD7 by mass spectrometry (T. Pomorski, personal communication). It seems possible that StarD7 has a non-phospholipid ligand unlike the other members of the group. As the protein is also overexpressed in cancer cell lines, a role in lipid-mediated tumor signaling has been implicated (Alpy and Tomasetto, 2005).

StarD10

StarD10 effectively transfers PC and to a lesser extent PE *in vitro* and was shown to bind these lipids *in vivo*. In addition to the START domain, StarD10 comprises a 65 amino acid C-terminal tail of unknown function. The protein is highly expressed in human liver, heart, skeletal muscle and kidney, where it is detected in the cytoplasm and the nucleus. The expression is upregulated in testes and during mammary gland development. In the mammary gland the highest expression levels are seen during gestation and lactation (Olayioye et al., 2005). StarD10 was first discovered as a phosphoprotein upregulated in breast carcinoma samples and cell lines, where it was speculated to cooperate with the receptor tyrosine kinase ErbB2 in cell transformation. It remains unclear whether StarD10-mediated lipid transfer contributes to tumor progression or if StarD10 has additional functions in tumor cells (Olayioye et al., 2004).

StarD11/CERT

The ceramide transfer protein StarD11/CERT is the best explored protein of the START domain family concerning its *in vivo* function. There are two transcript variants of the protein: CERT$_L$, also called Goodpasture-antigen-binding protein (GPBP), and the more abundant shorter version lacking 26 amino acids named CERT or GPBPΔ26. In humans, CERT is expressed in a number of tissues including skeletal muscle, heart, brain, kidney, pancreas and placenta. In addition to its START domain, CERT harbors a PH domain that binds specifically to PI(4)P, and an FFAT motif. The FFAT motif targets the protein to the ER by binding to the ER membrane protein VAP. Binding to Golgi membranes occurs via PI(4)P. CERT was originally discovered to rescue LY-A cells, mutant Chinese hamster ovary cells that have a defect in *de novo* sphingomyelin synthesis. It was shown that CERT transfers ceramide from its site of synthesis at the ER to Golgi membranes where it is used for the *de novo* synthesis of sphingomyelin. The START domain of CERT is

necessary for transfer of ceramide *in vivo* and sufficient for transfer *in vitro* (Hanada et al., 2003). Just recently it was shown that genetic ablation of CERT in mice leads to severe degeneration and is lethal around E11. Embryonic death is rather due to accumulation of ceramide in the ER leading to ER stress than a result of reduced levels of sphingomyelin at the Golgi complex. A typical response to ER stress would be apoptosis, but in CERT-deficient embryos no apoptotic cells were observed. In these *in vivo* conditions, ER stress effected mitochondrial structure and function, leading to the assumption that lethality results from insufficient energy production by mitochondria in heart muscle cells (Wang et al., 2009).

3.4.4.   StarD9

StarD9 is a predicted 1820 amino acid protein, with no other known domains apart from the C-terminal START domain. Its lipid ligand is unknown (Alpy and Tomasetto, 2005).

3.4.5.   RhoGAP START group

The three members of this family show a great homology in their domain structure, as they all contain a N-terminal sterile α motif (SAM), a RhoGAP and a C-terminal START domain. The function of the START domain in the DLC proteins remains unclear and so far no ligand for any of the DLC START domains has been discovered. The RhoGAP domain facilitates the inactivation of Rho family proteins by accelerating GTP hydrolysis, this domain is the most conserved domain among the three DLC family members. In all three proteins this domain has been shown to accelerate the inactivation of RhoA and to a lesser extent Cdc42 *in vitro* and StarD12/Deleted in liver cancer 1 (DLC1) and StarD13/Deleted in liver cancer 2 (DLC2) have also been shown to do so *in vivo* (Durkin et al., 2007; Kawai et al., 2007). DLC1 also accelerates the inactivation of RhoB and RhoC *in vitro* (Healy et al., 2008). RhoA, RhoB, RhoC and Cdc42 all belong to the Rho family of small GTPases. These proteins act as molecular switches and their function is described in greater detail below. N-terminally, DLC proteins posses a SAM domain, however, there are reports on variant transcripts lacking this domain for DLC2 and StarD8/Deleted in liver cancer 3 (DLC3). SAM domains are 70 amino acids in size and they occur in more than 200 human proteins. SAM domains are thought to be mainly involved in protein-protein interactions of homo- or heterotypic fashion, but SAM-RNA and SAM-membrane interactions have also been described. The function of the SAM domain in the DLC proteins is unclear, but as deletion of the SAM domain leaves a more active form of DLC1 and DLC3, it is speculated that the SAM domain is involved in auto-inhibition of the RhoGAP activity (Kim et al., 2009). The RhoGAP and the SAM domains are linked via a long unstructured region, which shows the least homology with 48% homology between DLC1 and DLC2 and only 29% homology between DLC1 and DLC3 (Durkin et al., 2007).

RhoGTPases

The proteins of the small Rho GTPase family are molecular switches that play an important role in regulating such diverse processes as actin and microtubule rearrangements, the cell cycle, cell morphogenesis and cell migration. These proteins cycle between an inactive GDP-bound and an active GTP-bound state. In the active state, most Rho proteins translocate to a membrane via membrane interaction through a prenyl group. There, they interact with and activate effector proteins that range from serine/threonine and lipid kinases to oxidases and scaffolding proteins (Sahai and Marshall, 2002). Due to their important roles, the Rho proteins themselves need to be tightly regulated in a spatio-temporal manner. RhoA, for example, is activated during cytokinesis exactly at the site of the cleavage furrow. Three levels of regulation have been described: In the inactive state, Rho proteins can be sequester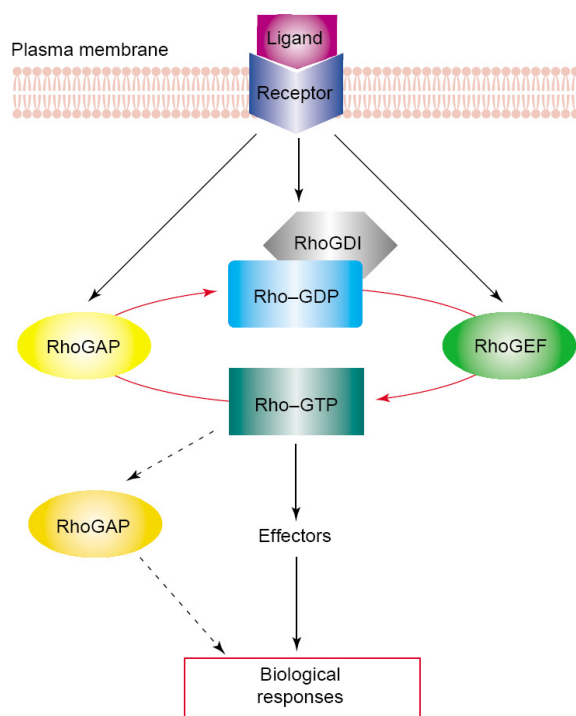ed by guanine nucleotide dissociation inhibitors (GDI) that bind the prenyl group, shield the bound GDP and thus keep the protein in an inactive state away from the membrane. To activate the Rho protein, GDP has to be exchanged for GTP and in a physiological environment this requires a guanine nucleotide exchange factor (GEF) protein. As the name suggests, Rho GTPases have an intrinsic GTPase activity that leads to their slow auto-inactivation. Fast inactivation, however, relies on GTPase activating proteins (GAP) that strongly enhance the intrinsic Rho GTPase activity. The Rho GTPase cycle is depicted in Figure 4. To emphasize the complexity of the Rho system it should be mentioned that so far in the human genome 22 Rho family GTPases, three GDIs, 82 GEFs, 67 GAPs and over 100 putative targets have been discovered (Bos et al., 2007).

Figure 4: A biochemical model of Rho GTPase-activating protein (RhoGAP) function in the signaling scheme of Rho GTPases. (Moon and Zheng, 2003)

DLC1

DLC1 was shown to be deleted in a number of hepatocellular carcinomas (HCC) by a PCR-based subtractive hybridization technique. DLC1 is localized at chromosome 8p21.3-2. This region shows a frequent loss of heterozygosity (LOH) in a wide range of human tumors, including prostate, colon, breast, ovarian, liver, lung, bladder, and head and neck. In addition, downregulation of DLC1 expression in some cancer types seems to be mediated by DNA hypermethylation, suggesting that DLC1 may serve a tumor suppressor function. In addition to the deletion and downregulation (Durkin et al., 2007), DLC1 missense and nonsense mutations have been

characterized (Liao et al., 2008). By using GAP-deficient DLC1 mutants and dominantly active RhoA variants it was shown that the GAP activity is necessary for DLC1's tumor suppressive function. Less is known about the regulation of DLC1 function.

Ectopic expression of DLC1 in most cultured cell lines leads to a reduction in the number and size of focal adhesions as well as a reduction of the actin stress fiber content. Above a certain expression level cells begin to show a "neurite like" phenotype. This is due to failure in the retracting tail movement and enhanced protrusive activity. This change in morphology is dependent on a functional RhoGAP domain and co-expression of active RhoA was shown to revert this phenotype (Kim et al., 2008). DLC1 overexpression also inhibits cell proliferation, colony formation, cell migration and soft agar growth in a wide range of tumor cell lines (Durkin et al., 2007). Mutation of the RhoGAP domain leads to a total loss of *in vitro* Rho GTPase activation. Interestingly, cells transfected with a GAP inactive mutant still showed a reduced invasive potential and a reduced ability to form colonies in soft agar, raising the possibility that DLC1 fulfills additional RhoGAP-independent functions (Healy et al., 2007). Concerning DLC1 function in animals it was shown that expression of DLC1 reduced tumor size in athymic nude mouse xenograft models. Knock-out of DLC1 in mice led to embryonic lethality around day 10 of gestation. The death is the consequence of a severe failure in organ development, including abnormalities in the brain neuroepithelium, the heart, defective fetal blood vessels and an open anterior neuronal tube (Durkin et al., 2005). It was recently shown that downregulation of DLC1 by a short hairpin RNA induces tumor formation in a mouse model using p53$^{-/-}$ liver progenitor cells that co-express c-Myc (Xue et al., 2008). This was a milestone for DLC1 research, because it proved that DLC1 is indeed a tumor suppressor.

Initially the rat (p122/RhoGAP) DLC1 isoform was discovered as a protein interacting with and stimulating PLCδ1 activity *in vitro* (Homma and Emori, 1995), although this has not been confirmed for the human protein. In most tested cell lines DLC1 localizes to focal adhesions via binding to tensin family proteins. In its linker region DLC1 harbors a binding site that interacts with the SH2 domain of the tensin family proteins in a phosphorylation-independent manner. The binding site was mapped to amino acids 440-445 and either mutation of serine 440 or tyrosine 442 inhibited binding. These mutations exclude the protein from focal adhesions and reduce DLC1-mediated inhibition of colony formation as well as growth suppression. There is some evidence that DLC1 interacts with caveolin-1 (Liao et al., 2006; Yam et al., 2006), but the relevance and impact on activity needs to be further investigated. Recently, two new interaction partners of DLC1 have been discovered. The RasGAP protein p120Ras-GAP binds to the RhoGAP domain of DLC1 with its SH3 domain, lowering DLC1's RhoGAP activity and growth inhibition (Yang et al., 2009). Via the SAM domain, DLC1 interacts with the elongation factor 1A1. This targets the transcription factor to the plasma membrane upon growth factor stimulation (Zhong et al., 2009).

DLC2

DLC2 was identified by analysis of genomic and cDNA sequences. It is situated on chromosome 13q13, which is another LOH site. DLC2 is downregulated in a significant fraction of primary lung, ovary, kidney, breast and uterine tumors, as well as in many tumor-derived cell lines. Ectopic expression of DLC2 leads to a phenotype reminiscent of DLC1-expressing cells. The phenotype is dependent on the RhoGAP function (Durkin et al., 2007). Recently it was shown that the activation of phosphatidylglycerolphosphate synthase by ceramide is mediated by DLC2 and that DLC2 knockdown alters the cellular response to chemotherapeutics (Hatch et al., 2008). There are controversial findings about the localization of DLC2. In HCC, HeLa and NIH3T3 cells, DLC2 localized to mitochondria via its START domain (Ng et al., 2006), and in HeLa cells focal adhesion localization was shown (Kawai et al., 2009).

DLC3

DLC3 was isolated from a human myeloid cell line library. It is situated on the X chromosome and DLC3 is downregulated and possibly also deleted in many human breast, ovarian and prostate cancer cell lines as well as in primary tumors of these tissues (Durkin et al., 2007).

DLC3 localizes to focal adhesions, probably due to the interaction with proteins of the tensin family. DLC3 has also been shown to activate PLCδ1 *in vitro* (Kawai et al., 2007). Cells ectopicly expressing DLC3 show a similar phenotype to DLC1 expressing cells, which is also dependent on the RhoGAP function.

crossveinless-c

The Drosophila homolog shows greatest homology to DLC2, and it is able to inactivate Rho1 and probably Rac1 and Rac2. Crossveinless-c (cv-c) expression is differentially regulated during embryonic development in multiple tissues. Mutation of cv-c is lethal in the embryonic/larval stage due to severe defects in morphogenesis. It has been shown that cv-c is required for the regulation of F-actin structures during morphogenesis (Denholm et al., 2005).

4. Results and discussion

4.1. Aim of the study

The aim of this study was to shed light onto the mechanisms by which proteins that contain START domains are recruited to membranes and how this membrane interaction is regulated. In addition, we investigated whether regulation of membrane interaction might have an impact on protein function.

We analyzed three members of the START domain family, of which StarD10 and CERT show lipid transfer activity *in vitro*. As both proteins transfer lipids, they must interact with membranes to exchange lipids from their binding pocket. StarD10 is a minimal START domain protein that lacks membrane targeting motifs and shows a cytosolic distribution. Neither the target membrane nor the lipid transport route are known. By contrast, CERT harbors two targeting sequences: an ER targeting FFAT motif and a PI(4)P binding PH domain that locates the protein to the Golgi complex. One possibility of regulating proteins comprising such additional targeting sequences is to alter the target. This is a more global mode of regulation because different proteins use the same target and all would be affected. Availability of the substrate is a way of regulating lipid transfer proteins independently of targeting motifs. As all known lipid transfer proteins work in an energy independent way along a gradient, regulation can occur via synthesis of the transported lipid at the donor membrane or via its metabolism at the acceptor membrane. Post-translational modification of the lipid transfer protein by phosphorylation is another mechanism by which membrane binding and lipid transfer can be regulated. For example, the PI-TP domain-containing protein Nir2 has been shown to be targeted to lipid droplets only upon phosphorylation (Litvak et al., 2002). A change of lipid binding affinity by phosphorylation has also been described to affect lipid transfer of PI-TP. This protein binds and transfers PI and with a lower affinity PC. Here, phosphorylation of a distinct serine residue inhibits PI transfer but still allows PC transfer (Morgan et al., 2004). Phosphorylation has also been shown to alter the steroidogenic activity of StAR, but the mechanism remains unclear (Arakane et al., 1997).

Finally, the third protein studied in this thesis is the tumor suppressor protein DLC1, which is unlikely to act as a classical lipid transfer protein due to its domain structure. The known function of DLC1 is the acceleration of RhoA inactivation via the RhoGAP domain. This is also the case for the other DLC family members. Neither protein of the DLC family has been shown to transfer lipids and membrane association has so far only been described for the isolated DLC2 SAM domain. Thus, it is widely accepted that DLC family members act as signaling proteins. Because active Rho GTPases are associated with membranes, we asked the question whether membrane interaction is a prerequisite for DLC1 function and investigated how this interaction is regulated.

4.2. Phosphorylation of StarD10 modulates its lipid transfer activity

Post-translational modification by phosphorylation is a common mechanism that regulates protein function. Originally, StarD10 was discovered as a phosphoprotein that cross-reacted with a phospho-FKHR antibody. However, the phosphorylation at serine 259, detected by the phosphospecific antibody did not alter StarD10 activity (Olayioye et al., 2004). With a mass spectrometry approach we identified that StarD10 was additionally phosphorylated at serine 284. This site was phosphorylated by casein kinase II (CKII) *in vitro* and serine to alanine mutation prevented CKII-mediated phosphorylation of StarD10 (Olayioye et al., 2008). CKII is a tetrameric serine/threonine kinase that is ubiquitously expressed. CKII is thought to be active independently of any stimulus. It has been postulated that CKII plays a role in cell cycle regulation, cell division, apoptosis and cancer cell survival (Litchfield, 2003). We could show that phosphorylation at serine 284 significantly reduced *in vitro* lipid transfer activity of StarD10. The decrease in lipid transfer was accompanied by a decrease of StarD10 membrane interaction. Hence, we could show that phosphorylation regulates the transfer activity of StarD10 and this regulation works via the reduction of membrane binding (Olayioye et al., 2008).

Compared to the serine to alanine exchange mutant, lipid transfer and membrane binding of a StarD10 mutant lacking eight C-terminal amino acids was increased even further. These eight terminal amino acids comprise the phosphorylated serine 284 and three additional negatively charged amino acids. It can be speculated that these terminal amino acids are important for StarD10 membrane disassociation. Cellular membranes are normally negatively charged due to acidic phospholipids such as phosphatidylserine and phosphorylated phosphatidylinositols (Yeung et al., 2008). The negatively charged C-terminus and the additional negative charge introduced by the phosphorylation might lower the dissociation energy needed to separate StarD10 from the membrane. The short-lived membrane interaction would then hinder the exchange of lipids from the START domain leading to a reduction of lipid transfer. A similar regulatory mechanism was described for the PKC substrate myristoylated alanine-rich C kinase substrate (MARCKS), which binds via positively charged amino acids to PI(4,5)P$_2$ in the plasma membrane and dislocates upon phosphorylation of serine residues (Arbuzova, Schmitz and Vergères, 2002).

As StarD10 seems to be constitutively phosphorylated at serine 284 and thus kept in a less active state, the important question is: Are there any tissues, stimuli or cellular events that alter StarD10 phosphorylation and thereby alter the protein's transfer activity? Most promising would be the analysis of the StarD10 phosphorylation status in mammary gland tissue of lactating animals as well as in liver upon bile secretion. As StarD10 might be involved in cancer progression, it would also be interesting to know if in addition to the higher expression level the protein is also phosphorylated to a lower extent in cancer cells. The characterization of the phosphorylation might then shed some light onto the *in vivo* function of StarD10.

4.3. Regulation of secretory transport by phosphorylation of the ceramide transfer protein

4.3.1. Protein Kinase D

The Protein Kinase D (PKD) family of serine/threonine kinases consists of three members, PKD 1, 2 and 3 that are structurally related. PKD family members contain two zinc-finger like cysteine-rich motifs that bind DAG, a PH domain and a kinase domain. PKD localizes to the cytosol, the nucleus, the Golgi complex and the plasma membrane. There, the kinase regulates diverse cellular processes such as vesicle trafficking, cell survival, migration, differentiation and proliferation (Wang, 2006). So far the only known PKD substrate at the Golgi complex is the lipid kinase PI4KIIIβ. Upon phosphorylation of PI4KIIIβ by PKD, PI(4)P production is increased, leading to increased Golgi complex to plasma membrane vesicle transport (Hausser et al., 2005).

4.3.2. CERT phosphorylation inhibits ceramide transfer

Here we identified CERT as a novel substrate for PKD at the Golgi complex. We could show that CERT is phosphorylated at serine 132 and that phosphorylation depends on the presence of the PKD isoforms 1 and 2. Mutation of serine 132 to alanine resulted in a loss of PKD-dependent phosphorylation *in vitro* and *in vivo*. As serine 132 is in close proximity of the PI(4)P binding PH domain, we speculated that phosphorylation at this site might alter PH domain-dependent Golgi complex association of CERT. Indeed mutation of serine 132 to alanine led to an increased binding to nitrocellulose membrane bound PI(4)P and to lipid vesicles comprising PI(4)P. This correlated with increased membrane interaction of the S132A mutant in intact cells compared to the wild type protein. We then analyzed the impact of phosphorylation on *in vitro* ceramide transfer. Interestingly, the S132A mutant demonstrated a higher rate of ceramide transfer, which is similar to the data obtained for the StarD10 S284A phosphorylation site mutant (Fugmann et al., 2007).

Ceramide together with PC is used at the Golgi complex to generate sphingomyelin and DAG. This implicates a negative feedback loop, as DAG activates PKD, which in turn phosphorylates CERT inhibiting further ceramide transfer. We therefore tested whether CERT influenced vesicle transport from the Golgi complex to the plasma membrane and were able to show that ectopic expression of CERT led to increased, while siRNA-mediated knock-down of CERT drastically reduced secretory transport (Fugmann et al., 2007). With our results we could show that CERT is a crucial player in the regulation of lipid homeostasis at Golgi membranes required for proper organelle function.

4.3.3. Serine 132 phosphorylation of CERT leads to hyperphosphorylation

An independent paper published showed that CERT phosphorylation at serine 132 leads to hyperphosphorylation of downstream serine and threonine residues with up to ten phosphorylated sites mapped by mass spectrometry (Kumagai et al., 2007). Casein kinase Iγ2 was identified to be

responsible for this hyperphosphorylation following the initial PKD-mediated phosphorylation of serine 132. Casein kinases are ideal candidate kinases because their consensus site requires one or two negatively charged residues, for example a phosphorylated residue in the -2 or -3 position relative the phosphorylated serine or threonine (Tomishige et al., 2008). This massive concentration of negative charge might be the reason for the decrease in PI(4)P and subsequently membrane binding (Kumagai et al., 2007). Furthermore, the protein phosphatase 2Cε (PP2Cε) was shown to be responsible for CERT dephosphorylation. PP2Cε is an integral membrane protein that resides at the ER and like CERT, interacts with VAP. The CERT-VAP interaction appears to depend on PP2Cε-mediated dephosphorylation, therefore, hyperphosphorylation might inhibit binding of CERT to both target organelles (Saito et al., 2007). The authors further postulated that phosphorylation of CERT leads to the intra-molecular association of its domains, forming a closed conformation that inhibits membrane binding and thus lipid transfer (Kumagai et al., 2007). Whether phosphorylation directly affects membrane binding or if it leads to a closed conformation could be addressed by modulating the so far unknown intra-molecular binding site, or by assaying the PH domain-dependant PI(4)P binding using constructs consisting only of the PH domain and the phosphorylation sites. As phosphorylation seems to inhibit the binding of CERT to both target membranes it could be argued that this leads to the exclusion from MCS, a hypothesis that needs to be further elucidated.

4.4. Membrane interaction of DLC1

DLC1 is a RhoGAP protein whose biological activity is thought to require focal adhesion localization. However, there are indications that DLC1-mediated RhoA inactivation takes place at the tip of the leading edge where active RhoA is also present (Healy et al., 2008; Kurokawa et al., 2005). This suggests that there is a focal adhesion-independent pool of active DLC1 at the plasma membrane. In initial experiments we observed that a small proportion of ectopically expressed GFP-DLC1 is associated with the plasma membrane. We therefore investigated whether DLC1 may interact with specific phospholipids. Interestingly, DLC1 was found to interact with immobilized $PI(4,5)_2$ and $PI(4,5)P_2$–containing membranes independently of the START and SAM domains. The binding was identified to be mediated by a polybasic region (PBR) that is conserved in human, mouse and rat DLC1, in human DLC2 and DLC3 as well as in the Xenopus and Drosophila DLC homologs (Erlmann et al., in revision).

4.4.1. Differential activation of DLC1 and DLC2

To get an insight into DLC protein function we compared the two family members DLC1 and DLC2 in their ability to lower intracellular active RhoA levels. Indeed, overexpression of DLC1 and DLC2 reduced RhoA-GTP levels and knock-down of either family member by siRNA led to an increase in active RhoA levels. While deletion of DLC1 led to enhanced stress fibres, focal adhesions, acceleration of wound closure and enhanced migration, knock-down of DLC2 only resulted in a

weak increase in stress fibres and focal adhesions and had no effect on wound closure and migration (Holeiter et al., 2008). DLC1-mediated regulation of RhoA signaling was shown to require the effector protein mDia, which was found to accumulate at the leading edge in cells lacking DLC1 (Holeiter et al., 2008). This finding provided further evidence that DLC1 is active at the cell membrane, especially at the leading edge of cells.

If knock-down of both DLC1 and DLC2 lead to higher active RhoA levels, the question arises why only cells lacking DLC1 show enhanced mobility. A possible explanation might be that the two family members locate to different compartments of the cell. It is likely that the RhoGAP activity of either DLC isoform is regulated in a spatio-temporal manner, leading to the inactivation of distinct pools of active RhoA proteins. It is now widely accepted that DLC1 is partly cytosolic, localizes to focal adhesions and, in some cells, to the nucleus (Yuan et al., 2007; Kim et al., 2009). DLC2 location is more controversially discussed. There is a report on DLC2 association with mitochondria (Ng et al., 2006), another on localization to focal adhesions (Kawai et al., 2009) and the DLC2 SAM domain was proposed to interact with membranes (Li et al., 2007). In contrast to these reports, in our hands DLC2 was exclusively cytosolic in MCF7 cells (Holeiter et al., 2008).

4.4.2.   Effect of membrane interaction on RhoGAP activity

Due to the increasing body of evidence that DLC1 is active at the cell membrane and because the PBR identified in our studies is located close to the RhoGAP domain we examined the effect of membrane-PBR interaction on RhoGAP activity. To this end, we performed *in vitro* RhoGTPase assays using geranylgeranylated RhoA, which in the active state associates with membranes. These assays revealed that DLC1 inactivated, geranylgeranylated membrane-bound RhoA more rapidly than unmodified RhoA in the absence of membranes. This increase in RhoGAP activity was dependent on the presence of the PBR. By contrast, the presence of membranes had no effect on RhoA inactivation by a DLC1 mutant lacking the PBR. Interestingly, addition of $PI(4,5)P_2$ further increased DLC1-mediated RhoA inactivation, indicating that DLC1 RhoGAP function might be regulated by the presence of the signaling lipid $PI(4,5)P_2$ (Erlmann et al., in revision).

4.4.3.   Functional consequences of DLC1 PBR deletion

Compared with wild type DLC1, a deletion mutant lacking the PBR led to decreased cellular RhoA inactivation in transiently transfected cells (Erlmann et al., in revision). Wild type DLC1 localizes to focal adhesions and reduces their number and size or eliminates them, dependent on the cell type (Durkin et al., 2007). Deletion of the PBR did not alter DLC1 focal adhesion localization, but the protein no longer affected the amount or size of focal adhesions. Deletion of the PBR also impaired the ability of DLC1 to induce changes in morphology, and inhibit growth and migration, proving the importance of the PBR for DLC1 cellular function. When cells expressing wild type DLC1 were plated onto collagen-coated surfaces, they adhered normally but then showed severe spreading

defects, lacked lamellipodia formation and showed abnormal outgrowths. Cells expressing a DLC1 variant lacking the PBR spread more like control cells (Erlmann et al., in revision). Membrane localization of DLC1, however, was not altered by PBR deletion (data not shown). Interestingly this is consistent with the PBR-containing yeast Cdc42 effector proteins Ste20 and Gic2. There it was shown that both the PBR and the GRIP domain that binds Cdc42 are necessary to localize and activate the protein at the plasma membrane while either alone were not sufficient for activation (Takahashi and Pryciak, 2007; Orlando et al., 2008). A similar mechanism would also be conceivable for DLC1 but this would ask for prolonged binding of DLC1 to RhoA, which is highly speculative and needs to be demonstrated.

The signaling lipid $PI(4,5)P_2$ regulates membrane-cytoskeleton interactions, for example at forming lamellipodia (Di Paolo and De Camilli, 2006). We were able to show that DLC1-mediated RhoA inactivation is accelerated in the presence of $PI(4,5)P_2$-containing membranes. Thus, DLC1 RhoGAP activity in cells might be regulated dynamically by local changes in $PI(4,5)P_2$ levels. The reduction of intracellular $PI(4,5)P_2$ levels by various means, such as expression of targeted lipid phosphatases or the use of small molecular inhibitors, did not alter DLC1 RhoGAP activity as measured with Raichu-RhoA biosensor assays. This may be explained by the fact that $PI(4,5)P_2$–dependent changes in DLC1 activity might be restricted to specific pools of DLC1 at the plasma membrane. In order to resolve these changes DLC1 activity needs to be followed in a spatiotemporal fashion by imaging of single cells.

4.4.4.   Regulation of DLC1 membrane interaction

As it is unclear how DLC1 associates with membranes we searched for possible binding sites or interactions that would tether DLC1 to the cell membrane. In this respect, the DLC1 SAM domain was an attractive candidate, either through direct SAM-membrane binding as it has been demonstrated for the DLC2 SAM domain (Li et al., 2007), or via interaction with a protein that is bound to the membrane. We were able to demonstrate that DLC1 interacts with the tumor suppressor PTEN in response to PDGF stimulation. The interaction with PTEN was confirmed to be dependent on the DLC1 SAM domain by co-immunoprecipitation and GST pull-downs. PTEN contains an N-terminal phosphatase domain that acts on both protein and lipid substrates, a C2 domain that interacts in a Ca^{2+}-independent manner with phospholipid substrates to mediate recruitment to the membrane and a C-terminal PDZ binding motif. Interestingly, active PTEN is recruited to the plasma membrane and there we observed DLC1 and PTEN colocalization (Heering et al., in revision). It is therefore intriguing to speculate that PTEN is a critical factor in DLC1 recruitment to the plasma membrane. PTEN may further be involved in the regulation of DLC1 activity by dephosphorylating $PI(3,4,5)P_3$, leading to the local production of $PI(4,5)P_2$, which may then in turn activate DLC1. Because DLC1 and PTEN both negatively regulate cell migration, a complex of the two proteins may function to coordinate signaling events underlying the different steps of the migratory progress.

Our studies furthermore identified the ubiquitously expressed 14-3-3 adaptor proteins as novel DLC1 interactors. Coexpression of 14-3-3 proteins reduced DLC1 RhoGAP activity and prevented DLC1-mediated changes in cell morphology. 14-3-3 proteins form homo- and heterodimers, which specifically bind to motifs containing a phosphorylated serine or threonine residue (consensus motifs: RSXpSXP or RXXXpSXP) (Bridges and Moorhead, 2004). The DLC1 14-3-3 interaction was enhanced by activating the PKC/PKD pathway or by inhibiting serine/threonine phosphatases, which indicated that the interaction was phosphorylation dependent. Within the DLC1 linker region we mapped two serines (S327 and S431) that were phosphorylated by PKD and served as 14-3-3 binding sites. Stable expression of a DLC1 S327/431 mutant suppressed cell growth more efficiently than that of the wild type protein, which is in agreement with the inhibitory effect of 14-3-3 binding on DLC1 RhoGAP activity (Scholz et al., 2008). In many cases, binding of 14-3-3 dimers to target proteins has been shown to alter their localization (Bridges and Moorhead, 2004). We were able to show that DLC1 translocation to the nucleus is inhibited by 14-3-3 binding, indicating that 14-3-3 interaction can indeed regulate DLC1 localization (Scholz et al., 2008). However, it remains to be determined whether plasma membrane binding of DLC1 is also modulated by 14-3-3 binding.

4.5. Conclusion

The function of the START domain in the DLC1 protein remains unclear and so far no ligand for any of the DLC START domains has been discovered. It is not uncommon that signaling proteins contain lipid interaction domains, but lipid binding domains are less frequent. Examples of START domains in non-transfer proteins are seen in plants, where several transcription factors comprising a START domain are thought to sense lipid levels (Schrick et al., 2004). For other START domains, such as the yeast Sec14 proteins, it has been postulated that they "present" lipids for further processing rather than fulfill a transport function (Schaaf et al., 2008). As DLC1 might act in a signaling complex together with PTEN and probably further proteins, its START domain may also present lipids. Moreover, DLC1 membrane binding could also be facilitated by the START domain. Minimal START domain proteins are able to bind to membranes and we observed that the isolated START domain of DLC1 binds membranes, too (unpublished data). The function of the DLC family START domain thus remains to be characterized in future studies.

Taken together, we were able to show that both StarD10 and CERT are regulated by phosphorylation and provided further insights into the mechanism of this regulation. Phosphorylation reduced the membrane affinity of these proteins. It is neither obvious nor clear why prolonged membrane interaction accelerates lipid transfer but it could be speculated that lipid exchange from the START domain might take some time. It would thus be interesting to compare membrane disassociation rates of phosphorylated and non-phosphorylated START domain proteins. Because phosphorylation of CERT regulates PH domain-dependent membrane

interaction and phosphorylation of StarD10 regulates membrane interaction via the C-terminal tail, phosphorylation could be seen as a more general mechanism that regulates membrane interaction of START domain proteins.

In the case of DLC1, we identified a previously unrecognized polybasic region with affinity for $PI(4,5)P_2$ that is essential for DLC1 RhoGAP activity and cellular function. The PBR, however, was not sufficient for DLC1 recruitment to cellular membranes, indicating that additional factors determine DLC1 localization to these sites. We identified 14-3-3 proteins and PTEN as novel DLC1 binding partners, both of which may influence DLC1 membrane localization, the former in a negative and the latter in a positive manner. Figure 5 summarizes the possible connections that were discussed in this thesis.

Membrane binding is of dual importance for DLC1. Active RhoA localizes to the membrane and there DLC1 needs to exert its RhoGAP function. Furthermore, RhoGAP activity of DLC1 depends on the interaction of the protein with membranes via the PBR and RhoGAP activity is modulated at least *in vitro* by the presence of the signaling lipid $PI(4,5)P_2$. Secondly, any suggested function of
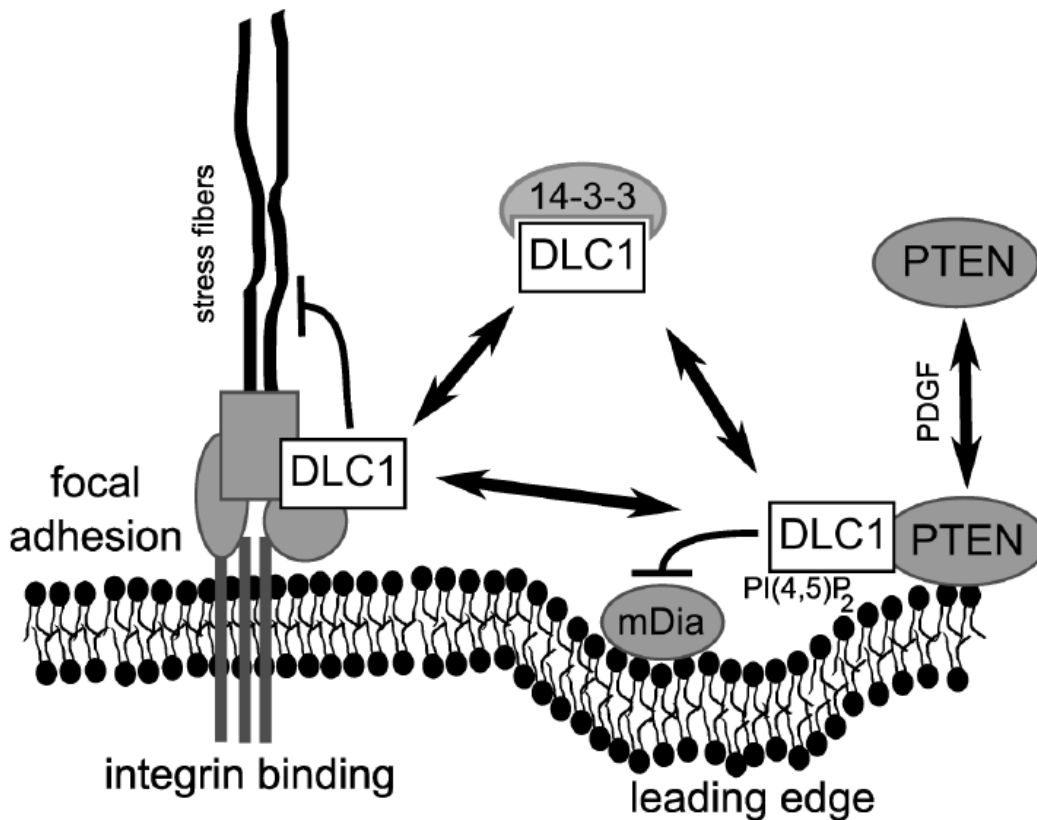

Figure 5: Scheme of DLC1 regulation. DLC1 is localized to focal adhesions via binding to tensin proteins. Besides, there is a pool of DLC1 located at the plasma membrane possibly enriched at the leading edge. Recruitment of DLC1 to the plasma membrane could be mediated by direct interaction with PTEN. Membrane bound DLC1 is activated by PI(4,5)P2 and inhibits RhoA signaling through mDia. Upon phosphorylation DLC1 binds to 14-3-3 proteins and is retained in the cytosol.

the START domain, whether it might be lipid transfer, lipid sensing or membrane binding would require DLC1 to be at the membrane. Therefore, it is now most important to identify the molecular mechanisms that control DLC1 membrane binding.

5. Abbreviations

BAR	Bin–Amphiphysin–Rvs
C1	Conserved region-1
C1P	Ceramide-1-phosphate
C2	Conserved region-2
Ca	Calcium
cDNA	Complementary DNA
Cer	Ceramide
CHA	Congenital adrenal hyperplasia
CHOL	Cholesterol
CKII	Casein kinase II
CL	Cardiolipin
c-Myc	Cellular myelocytomatosis oncogene
CoA	Coenzym-A
cPLA2	Cytosolic phospholipase A2
cv-c	Crossvainless-c
DAG	Diacylglycerol
DLC	Deleted in liver cancer
DNA	Deoxyribonucleic acid
ENTH	Epsin N-terminal homology
ER	Endoplasmatic riticulum
ErbB2	Epidermal growth factor (EGF)-receptor related protein tyrosine kinase B2
ERG	Ergosterol
F-actin	Filamentous actin
F-BAR	FCH BAR
FFAT	Two phenylalanines in an acidic tract
FKHR	Forkhead receptor
FYVE	Fab1, YOTB, Vac1 and EEA1
GalCer	Galactosylceramide

(Rho)GAP	(Rho)GTPase activating protein
GDI	Guanine nucleotide dissociation inhibitors
GDP	Guanosin diphosphate
GEF	Guanine nucleotide exchange factor
GPBP	Goodpasteur binding protein
GRIP	Golgin-97, RanBP2α, Imh1p and p230/golgin-245
GSLs	Complex glycosphingolipids
GST	Glutathion-S-transferase
GTP	Guanosin triphosphate
GTPase	GTP hydrolysing
HCC	Hepatocellular carcinoma
IP$_3$	Inositol-trisphosphate
ISL	Yeast inositol sphingolipid
kDa	Kilo dalton
LOH	Loss of heterozygosity
MARCKS	Myristoylated alanine-rich C kinase substrate
MCS	Membrane contact site
mDia	Mammalian diaphanous
MENTAL	MLN64 N-terminal domain
Mt	Mitochondrial trageting
N-BAR	N-terminal amphipathic helix BAR
Nir2	Pyk2 N-terminal domain-interacting receptor 2
N-WASP	Neuronal Wiskott-Aldrich Syndrome protein
PA	Phosphatidic acid
Pax-3	Paired box-3
PBR	Polybasic region
PC/PdtCho	Phosphatidylcholine
PCR	Polymerase chain reaction
PCTP	Phosphatidylcholine transfer protein
PDGF	Platlet derived growth factor
PDZ	PSD95/SAP90, Protein Discs large, Zonula occludentes-1

PE/PtdEtn	Phosphatidylethanolamine
PH	Plextrin homology
PI(3)P/ PtdIns(3)P	Phosphatidylinositol-3-phosphate
PI(3,4,5)P$_3$/PtdIns(3,4,5)P$_3$	Phosphatidylinositol-3,4,5-trisphosphate
PI(3,5)P$_2$/PtdIns(3,5)P$_2$	Phosphatidylinositol-3,5-bisphosphate
PI(4)P/PtdIns(4)P	Phosphatidylinositol-4-phosphate
PI(4,5)P$_2$/PtdIns(4,5)P$_2$	Phosphatidylinositol-4,5-bisphosphate
PI/PtdIns	Phosphatidylinositol
PI4K IIIβ	Phosphatidylinositol-4-kinase IIIβ
PI-TP	Phosphatidylinositol-transfer protein
PKC	Protein kinase C
PKD	Protein kinase D
PL	Phospholipid
PLC	Phospholipase C
PP2Cε	Protein phosphatase 2Cε
PROPPINS	β-Propellers that bind phosphoinositides
PS/PtdSer	Phosphatidylserine
PX	Phox-homology
Raichu	Ras and interacting protein chimeric unit
RNA	Ribonucleic acid
S1P	Sphingosine-1-phosphate
SAM	Steril alpha motive
scc	Side-chain cleavage
SCP-2	Sterol carrier protein-2
SCP-X	Sterol carrier protein-X
SH2	Src homology2
SH3	Src homology3
siRNA	Small interfering RNA
SM	Sphingomyelin
StAR	Steroidogenic acute regulatory

START	StAR protein related transfer
TG	Triacylglycerol
Them	Thioesterase superfamily member
THIO	Acyl-CoA thioesterase domain
VAP	Vesicle associated protein

6. References

Alpy,F. and Tomasetto,C. (2005) Give lipids a START: the StAR-related lipid transfer (START) domain in mammals. JCS 118 pp2791-2801

Arakane,F., King,S.R., Du,Y., Kallan,C.B., Walsh,L.O., Watari,H., Stocco,D.M. and Strauss III,J.F. (1997) Phosphorylation of steroidogenic acute regulatory protein (StAR) modulates its steroidogenic acivity. JBC 272; 51 pp32656-32662

Arbuzova,A., Schmitz,A.A. and Vergères,G. (2002) Cross-talk unfolded: MARCKS proteins. Biochem J. 362 1-12.

Behnia,R. and Munro,S. (2005) Organelle identity and the signposts for membrane traffic. Nature 438 pp597-604

Bos,J.L., Rehmann,H. and Wittinghofer,A. (2007) GEFs and GAPs: Critical elements in the control of small G proteins. Cell 129 pp865-877

Bridges,D. and Moorhead,G.B. (2004) 14-3-3 proteins: a number of functions for a numbered protein. Sci STKE. 242 re10

Chalfant,C.E. and Spiegel,S. (2005) Sphingosine 1-phosphate and ceramide 1-phosphate: expanding roles in cell signaling. JCS 118 pp4605-4612

Denholm,B., Brown,S., Ray,R.P., Ruiz-Gómez,M., Skaer,H. and Hombría,J.C.-G. (2005) crossvainless-c is a RhoGAP required for actin reorganization during morphogenesis. Development 132 pp2389-2400

Di Paolo,G. and De Camilli,P. (2006) Phosphoinositides in cell regulation and membrane dynamics. Nature 443 pp651-657

Durkin,M.E., Yuan,B.-Z., Zhou,X., Zimonjic,D.B., Lowy,D.R., Thorgeirsson,S.S. and Popescu,N.C. (2007) DLC-1: a Rho GTPase-activating protein and tumor suppressor. J.Cell.Mol.Med 11; 5 pp1185-1207

Durkin,M.E., Avner,M.R., HuhC.-G., Yuan,B.-Z., Thorgeirsson,S.S. and Popescu,N.C. (2005) DLC-1, a Rho GTPase-activating protein with tumor suppressor function, is essential for embryonic development. FEBS Letters 579 pp 1191-1196

Erlmann,P., Schmid,S., Horenkamp,F.A., Geyer,M., Pomorski,T.G. and Olayioye,M.A. (2009) DLC1 activation requires lipid interaction through a polybasic region preceding the RhoGAP domain. Mol Cell Biol. In revision

Fivaz,M. and Meyer,T. (2003) Specific localization and timing in neuronal signal transduction mediated by protein-lipid interactions. Neuron 40 pp319-330

Fugmann,T., Hausser,A., Schöffler,P., Schmid,S., Pfizenmaier,K. and Olayioye,M.A. (2007) Regulation of secretory transport by protein kinase D-mediated phosphorylation of the ceramide transfer protein. J Cell Biol. 178 pp15-22

Hanada,K., Kumangi,K., Yasuda,S., Miura,Y., Kawano,M., Fukasawa,M. and Nishijma,M. (2003) Molecular machinery for non-vesicular trafficking of ceramide. Nature 426 pp803-809

Hausser,A., Storz,P., Märtens,S., Link,G., Toker,A. and Pfizenmaier,K. (2005) Protein kinase D regulates vesicular transport by phosphorylating and activating phosphatidylinositol-4 kinase IIIbeta at the Golgi complex. Nat Cell Biol. 7 pp880-886

Healy,K.D., Hodgson,L., Kim,T.Y., Shutes,A., Maddileti,S., Juliano,R.L., Hahn,K.M., Harden,T.K., Bang,Y.J. and Der,C.J. (2008) DLC-1 suppresses non-small cell lung cancer growth and invasion by RhoGAP-dependent and independent mechanisms. Mol Carcinog. 47 pp326-337

Hatch,G.M., Gu,Y.,. Xu,F.Y., Cizeau,J., Neumann,S., Park,J.S., Loewen,S., Mowat,M.R. (2008) StARD13(Dlc-2) RhoGap mediates ceramide activation of phosphatidylglycerolphosphate synthase and drug response in Chinese hamster ovary cells. Mol Biol Cell 19 pp1083-1092

Heering,J., Erlmann,P. and Olayioye,M.A. (2009) Simultaneous loss of the DLC1 and PTEN tumor suppressors enhances breast cancer cell migration. Exp. Cell Res. In revision

Heo,W.D., Inoue,T., Park,W.S., Kim,M.L. Park,B.O., Wandless,T.J. and Meyer,T. (2006) PI(3,4,5)P3 and PI(4,5)P2 lipids target proteins with polybasic clusters to the membrane. Science 314 pp144-146

Holeiter,G., Heering,J., Erlmann,P., Schmid,S., Jähne,R. and Olayioye,M.A. (2008) Deleted in liver cancer 1 controls cell migration through a Dia1-dependent signaling pathway. Cancer Res. 68 pp8743-8751

Holthuis,J.C.M. and Levine,T.P. (2005) Lipid traffic: Floppy drives and a superhighway. Nature reviews Mol Cell Biol 6 pp209-220

Homma,Y. and Emori,Y. (1995) A dual functional signal mediator showing RhoGAP and phospholipase C-delta stimulating activities. EMBO J. 14 pp286-291

Janmey,P.A. and Lindberg,U. (2004) Cytoskeletal regulation: Rich in lipids. Nature reviews Mol Cell Biol 5 pp658-666

Kaku,U., Kameyama,K., Izawa,M., Yamada,M., Miyamoto,J., Suzuki,T., Sasano,H. and Hasegawa,Y. (2008) Ovarian histological findings in an adult patient with the steroidogenic acute

regulatory protein (StAR) deficiency reveal the impairment of steroidogenesis by lipoid deposition. Endocr J. 55 pp1043-1049

Kanno,K., Wu,M.K., Agate,D.S., Fanelli,B.J., Wagle,N., Scapa,E.F., Ukomandu,C. and Cohen,D.E. (2007) Interacting proteins dictate function of the minimal START domain phosphatidylcholine transfer protein/StarD2. J Biol Chem 282, 19 pp 30728-30736

Kawai,K., Kiyota,M., Seike,J., Deki,Y. and Yagisawa,H. (2007) START-GAP3/DLC3 is a GAP for RhoA and Cdc42 and is localized in focal adhesions regulating cell morphology. Biochem Biophys Res Commun. 364 pp783-789

Kawai,K., Seike,J., Iino,T., Kiyota,M., Iwamae,Y., Nishitani,H. and Yagisawa,H. (2009) START-GAP2/DLC2 is localized in focal adhesions via its N-terminal region. Biochem Biophys Res Commun. 380 pp736-741

Kim,T.Y., Vigil,D., Der,C.J. and Juliano,R.L. (2009) Role of DLC-1, a tumor suppressor protein with RhoGAP activity, in regulation of the cytoskeleton and cell motility. Cancer Metastasis Rev 28 pp77-83

Kumagai,K., Kawano,M., Shinkai-Ouchi,F., Nishijima,M. and Hanada,K. (2007) Interorganelle trafficking of ceramide is regulated by phosphorylation-dependent cooperativity between the PH and START domains of CERT. J Biol Chem. 282, 24 pp17758-17766

Kurokawa,K., Nakamura,T., Aoki,K. and Matsuda,M. (2005) Mechanism and role of localized activation of Rho-family GTPases in growth factor-stimulated fibroblasts and neuronal cells. Biochem Soc Trans. 33 pp631-634

Lemmon,M.A. (2008) Membrane recognition by phospholipid-binding domains. Nature reviews Mol Cell Biol 9 pp99-111

Levine,T. and Loewen,C. (2006) Inter-organelle membrane contact sites: through a glass, darkly. Curr Opin Cell Biol. 18 pp371-378

Li,H., Fung,K.L., Jin,D.Y., Chung,S.S., Ching,Y.P., Ng,I.O., Sze,K.H., Ko,B.C. and Sun,H. (2007) Solution structures, dynamics, and lipid-binding of the sterile alpha-motif domain of the deleted in liver cancer 2. Proteins 67 p1154-1166

Liao,Y.-C., Si,L., deVere White,R.W. and Lo,S.H. (2006) The phosphotyrosine-independent interaction of DLC-1 and the SH2 domain of cten regulates focal adhesion localization and growth suppression activity of DLC-1. JBC 176, 1 pp43-49

Liao,Y.-C., Shih,Y.-P. and Lo,S.H. (2008) Mutation in the focal adhesion targeting region of deleted in liver cancer-1 attenuate their expression and function. Cancer Res 68 pp7718-7722

Litchfield,D.W. (2003) Protein kinase CK2: structure, regulation and role in cellular decisions of life and death. Biochem J. 369 pp1-15

Litvak,V., Shaul,Y.D., Shulewitz,M., Amarilio,R., Carmon,S. and Lev,S. (2002) Targeting of Nir2 to lipid droplets is regulated by a specific threonine residue within its PI-transfer domain. Curr Biol. 12 pp1513-1518

Morgan,C.P., Skippen,A., Segui,B., Ball,A., Allen-Baume,V., Larijani,B., Murray-Rust,J., McDonald,N., Sapkota,G., Morrice,N. and Cockcroft,S. (2004) Phosphorylation of a distinct structural form of phosphatidylinositol transfer protein alpha at Ser166 by protein kinase C disrupts receptor-mediated phospholipase C signaling by inhibiting delivery of phosphatidylinositol to membranes. J Biol Chem. 279, 45 pp47159-47171

Moon,S.Y. and Zheng,Y. (2003) Rho GTPase-activating proteins in cell regulation. Trends Cell Biol. 13 pp13-22

Ng,D.C.-H., Chan,S.-F., Kok,K.H., Yam,J.W.P., Ching,Y.-P., Ng,I.O.-L. and Jin,D.-Y. (2006) Mitochondrial targeting of growth suppressor protein DLC2 through the START domain. FEBS Letters 580 pp191-198

Niggli,V. (2005) Regulation of protein activities by phosphoinositide phosphates. Annu. Rev. Cell Dev. Biol. 21 pp57-79

Olayioye,M.A., Hoffmann,P., Pomorski,T., Armes,J., Simpson,R.J., Kemp,B.E., Lindeman,G.J. and Visvader,J.E. (2004) The phosphoprotein StarD10 is overexpressed in breast cancer and cooperates with ErbB receptors in cellular transformation. Cancer Res. 64 pp3538-3544

Olayioye,M.A., Vehring,S., Müller,P., Herrmann,A., Schiller,J., Thiele,C., Lindeman,G.J., Visvader,J.E. and Pomorski,T. (2005) StarD10, a START domain protein overexpressed in breast cancer, functions as a lipid transfer protein. JBC 280, 29 pp27436-27442

Olayioye,M.A., Buchholz,M., Schmid,S., Schöffler,P., Hoffmann,P. and Pomorski,T. (2007) Phosphorylation of StarD10 on serine 284 by casein kinase II modulates its lipid transfer activity. J Biol Chem. 282, 31 pp22492-22498

Orlando,K., Zhang,J., Zhang,X., Yue,P., Chiang,T., Bi,E. and Guo,W. (2008) Regulation of Gic2 localization and function by phosphatidylinositol 4,5-bisphosphate during the establishment of cell polarity in budding yeast. J Biol Chem. 283, 21 pp14205-20512

Papayannopoulos,V., Co,C., Prehoda,K.E., Snapper,S., Taunton,J. and Lim,W.A. (2005) A polybasic motif allows N-WASP to act as a sensor of PIP(2) density. Mol Cell 17 pp181-191

Resh,M.D. (2004) Membrane targeting of lipid modified signal transduction proteins. Subcell Biochem. 37 p217-32.

Roberts,P.J., Mitin,N., Keller,P.J., Chenette,E.J., Madigan,J.P., Currin,R.O., Cox,A.D., Wilson,O., Kirschmeier,P. and Der,C.J. (2008) Rho family GTPase modification and dependence on CAAX motif-signaled posttranslational modification. JBC 283, 37 pp25150-25163

Saito,S., Matsui,H., Kawano,M., Kumagai,K., Tomishige,N., Hanada,K., Echigo,S., Tamura,S. and Kobayashi,T. (2008) Protein phosphatase 2Cepsilon is an endoplasmic reticulum integral membrane protein that dephosphorylates the ceramide transport protein CERT to enhance its association with organelle membranes. J Biol Chem. 283, 10 pp6584-6593

Sahai,E. and Marshall,C.J. (2002) Rho-GTPases and cancer. Nature reviews cancer 2 pp133-142

Schaaf,G., Ortlund,E.A., Tyeryar,K.R., Mously,C.J., Ile,K.E., Garrett,T.A., Ren,J., Woolls,M.J., Raetz,C.R.H., Redinbo,M.R. and Bankaitis,V.A. (2008) Functional anatomy of phospholipid binding and regulation of phosphoinositide homeostasis by proteins of the Sec14 superfamily. Mol. Cell 29 pp191-206

Scholz,R.P., Regner,J., Theil,A., Erlmann,P., Holeiter,G., Jähne,R., Schmid,S., Hausser,A. and Olayioye,M.A. (2008) DLC1 interacts with 14-3-3 proteins to inhibit RhoGAP activity and block nucleocytoplasmic shuttling. J Cell Sci. 122 pp92-102

Schrick,K., Nguyen,D., Karlowski,W.M. and Mayer,K.F.X. (2004) START lipid/sterol-binding domains are amplified in plants and are predominantly associated with homeodomain transcription factors. Genom Biology 5, 6 R41.1-R41.16

Sechi,A.S. and Wehland,J. (2000) The actin cytoskeleton and the plasma membrane connection: PtdIns(4,5)P2 influences cytoskeletal protein activity at the plasma membrane. JCS 113 pp3685-3695

Shima,T., Nada,S. and Okada,M. (2003) Transmembrane phosphoprotein Cbp senses cell adhesion signaling mediated by Src family kinase in lipid rafts. Proc Natl Acad Sci U S A. 100 pp14897-14902

Stahelin,R.V. (2008) Lipid binding domains: More than simple lipid effectors. JLR S50 ppS299-304

Stahelin,R.V., Subramanian,P., Vora,M., Cho,W. and Chalfant,C.E. (2007) Ceramide 1-phosphate binds group IVA cytosolic phospholipase a2 via a novel site in the C2 domain. JBC 2007 282, 13 pp20467-20474

Takahashi,S. and Pryciak,P.M. (2007) Identification of novel membrane-binding domains in multiple yeast Cdc42 effectors Mol Biol Cell 18 pp4945-4956

Tomishige,N., Kumagai,K., Kusuda,J., Nishijima,M. and Hanada,K. (2008) Casein kinase I{gamma}2 down-regulates trafficking of ceramide in the synthesis of sphingomyelin. Mol Biol Cell 20 pp348-357

Van Meer,G., Voelker,D.R. and Feigenson,G.W. (2008) Membrane lipids: where they are and how they behave. Nature reviews Mol. Cell Biol. 9 pp112-124

Vicinanza,M., D'Angelo,G., Di Campli,A. and De Matteis,M.A. (2008) Function and dysfunction of the PI system in membrane trafficking. EMBO 169 pp1-14

Wang,Q.J. (2006) PKD at the crossroads of DAG and PKC signaling. Trends Pharmacol Sci. 27 pp317-323

Wang,X., Rao,R.P., Kosakowska-Cholody,T., Masood,M.A., Southon,E., Zhang,H., Berthet,C., Nagashim,K., Veenstra,T.K., Tessarollo,L., Acharya,U. and Acharya,J.K. (2009) Mitochondrial degeneration and not apoptosis is the primery cause of embryonic lethality in ceramide transfer protein mutant mice. JBC 184, 12 pp143-158

Wirtz,K.W.A (2006) Phospholipid transfer proteins in perspective. FEBS Letters 580 pp5436-5441

Worth,D.C. and Parsons,M. (2008) Adhesion dynamics: Mechanisms and measurements. Int J Biochem Cell Biol. 40 pp2397-2409

Wymann,M.P. and Schneiter,R. (2008) Lipid signaling in disease. Nature reviews Mol. Cell Biol. 9 pp162-176

Xue,W., Krasnitz,A., Lucito,R., Sordella,R., Vanaelst,L., Cordon-Cardo,C., Singer,S., Kuehnel,F., Wigler,M., Powers,S., Zender,L. and Lowe,S.W. (2008) DLC1 is a chromosome 8p tumor suppressor whose loss promotes hepatocellular carcinoma. Genes Dev. 22 pp1439-1444

Yam,J.W.P., Ko,F.C.F., Chan,C.-Y., Jin,D.-Y. and Ng,I.O.-L. (2006) Interaction of deleted in liver cancer 1 with tensin2 in caveolae and implications in tumor suppression. Cancer Res 66 pp8367-8372

Yang,X.Y., Guan,M., Vigil,D., Der,C.J., Lowy,D.R. and Popescu,N.C. (2009) p120Ras-GAP binds the DLC1 Rho-GAP tumor suppressor protein and inhibits its RhoA GTPase and growth-suppressing activities. Oncogene 28 pp1401-1409

Yeung,T., Gilbert,G.E., Shi,J., Silvius,J., Kapus,A. and Grinstein,S. (2008) Membrane phosphatidylserine regulates surface charge and protein localization. Science 319 p210-213

Yuan,B.Z., Jefferson,A.M., Millecchia,L., Popescu,N.C. and Reynolds,S.H. (2007) Morphological changes and nuclear translocation of DLC1 tumor suppressor protein precede apoptosis in human non-small cell lung carcinoma cells. Exp Cell Res. 313 pp3868-3880

Zhong,D., Zhang,J., Yang,S., Soh,U.J.K., Buschdorf,J.P., Zhou,Y.T., Yang,D. and Low,B.C. (2009) The SAM domain of the RhoGAP DLC1 binds EF1A1 to regulate cell migration. JCS 122 pp414

7. Publication Manuscripts

7.1. Phosphorylation of StarD10 on Serine 284 by Casein Kinase II Modulates Its Lipid Transfer Activity

Monilola A. Olayioye[1], Michael Buchholz[2,3], Simone Schmid[1], Patrik Schöffler[1], Peter Hoffmann[4] and Thomas Pomorski[2]

From the [1] University of Stuttgart, Institute of Cell Biology and Immunology, Allmandring 31, 70569 Stuttgart, Germany and the [2] Humboldt University of Berlin, Institute of Biology, Invalidenstrasse 42, 10115 Berlin, Germany and the [3] Free University of Berlin, Department of Biology, Chemistry, Pharmacy, Takustr.3, 14195 Berlin, Germany and the [4] University of Adelaide, School of Molecular and Biomedical Science, SA 5005, Australia

Address correspondence to: Monilola A. Olayioye, University of Stuttgart, Institute of Cell Biology and Immunology, Allmandring 31, 70569 Stuttgart, Germany, Tel: +49-711-685-69301; Fax: +49-711-685-67484; e-mail: monilola.olayioye@izi.uni-stuttgart.de and Thomas Pomorski, Humboldt University of Berlin, Institute of Biology, Invalidenstrasse 42, 10115 Berlin, Germany, Tel: +49-30-2093-8326; Fax: +49-30-2093-8585; e-mail: thomas.pomorski@rz.hu-berlin.de

StarD10 is a dual specificity lipid transfer protein capable of shuttling phosphatidylcholine and phosphatidylethanolamine between membranes in vitro. We now provide evidence that, in vivo, StarD10 is phosphorylated on serine 284. This novel phosphorylation site was identified by tandem mass spectrometry of immunoaffinity-purified StarD10 from lysates of HEK293T cells transiently expressing the protein. In vitro kinase assays revealed that casein kinase II (CKII) was capable of phosphorylating wild type StarD10 but not a S284A mutant protein. Interestingly, hypotonic extracts prepared from HEK293T cells expressing the serine to alanine mutant exhibited increased lipid transfer activity compared with those from wild type StarD10 expressing cells, suggesting that, in a cellular context, phosphorylation on serine 284 negatively regulates StarD10 activity. Since CKII phosphorylation also inhibited lipid transfer activity of the purified recombinant StarD10 protein, inhibition is not dependent on any cellular cofactors. Instead, our data show that carboxy-terminal StarD10 phosphorylation on serine 284 regulates its association with cellular membranes.

Lipids are essential for the structural and functional integrity of cells. As the predominant constituent of cellular membranes, lipids compartmentalize cellular functions, are critical for protein sorting, and are involved in various aspects of signal transduction. Lipids are differentially distributed both between and within membranes in the cell. This differential distribution of lipids is achieved in part by regulated transport of lipids (1;2). Phospholipids are predominantly synthesized in the endoplasmatic reticulum (ER) and subsequently transported to various destinations by vesicular transport. Lipids can also be delivered to specific cellular organelles by monomeric exchange. This non-vesicular lipid trafficking can be highly efficient and requires desorption of the lipid from the donor membrane, passage through the aqueous phase and subsequent insertion into the acceptor membrane. Spontaneous release from the membrane into the aqueous phase is a rare event for phospholipids carrying two long acyl chains. Several cytosolic proteins with specific lipid binding domains capable of accelerating lipid exchange in vitro have been identified. These proteins include phosphatidylinositol transfer proteins (PITPs), sterol carrier protein 2, and members of the steroidogenic acute regulatory protein (StAR)-related lipid transfer (START) domain family (3).

START domains have been identified in 15 mammalian proteins, which have been assigned the formal names StarD1-15, and are also found in plants, worms, flies, fish, and bacteria (4;5). START domains are approximately 210 amino acids in length and form a hydrophobic tunnel that accommodates a monomeric lipid. The founding member of the START family, StAR/StarD1, is essential for cholesterol transport to the inner mitochondrial membrane, where the conversion of cholesterol to pregnenolone takes place (6). Phosphatidylcholine transfer protein (Pctp/StarD2), on the other hand, is known to bind and transfer phosphatidylcholine (PC) between membranes, but no other phospholipids or sterols. The StarD2 subfamily of START proteins further comprises Cert/StarD11, StarD10 and StarD7. CERT was identified to catalyze the non-vesicular transport of

ceramide from the ER to the Golgi (7). To fulfil its ceramide carrier function CERT contains two membrane-targeting domains: one for ER and another for Golgi targeting (7;8). The protein is thought to either shuttle between the two organelles or act directly between closely opposed donor and acceptor membranes at so-called membrane contact sites (9;10). Opposed to CERT, little is known about the physiological function of Pctp, StarD10, and StarD7. Based on the enrichment of Pctp in liver and the observation that activity in vitro is stimulated by bile salts, it has been postulated that Pctp functions in the delivery of PC from its principal site of synthesis in the ER to hepatocyte canalicular membranes for secretion into bile. However, mice carrying a deletion in the gene encoding Pctp were phenotypically normal (11). This may be due to functional redundancy with StarD10, which is also expressed in liver and possesses lipid transfer activity for PC and, to a lesser extent, phosphatidylethanolamine (PE).

We have previously shown by electron spin resonance measurement of spin-labeled lipids and using fluorescently labeled lipids analogs incorporated into liposomes that recombinant StarD10 interacts with phospholipids in solution and in membranes. Incubation of StarD10 with liposomes prepared with radiolabeled cellular lipids demonstrated that StarD10 also binds endogenous PC and PE. StarD10 was further shown to bind lipids in vivo by crosslinking of protein expressed in transfected HEK293T cells with photoactivable PC (12). The molecular mechanisms, however, that control StarD10 lipid binding and transfer activity are still unknown. Opposed to CERT, StarD10 lacks specific targeting motifs and potential donor and acceptor membranes within the cell still remain elusive. Here we present data that sheds light onto the in vivo regulation of StarD10. StarD10 is phosphorylated by CKII on serine 284, whereby lipid transfer activity and membrane association are inhibited. Carboxyterminal phosphorylation thus appears to represent an efficient means to regulate StarD10 activity.

Experimental procedures

Reagents and antibodies

Porcine brain lipids (total extract) were purchased from Avanti Polar Lipids (Alabaster, AL), pyrene-labeled phospholipids 1-hexadecanoyl-1-(1-pyrenedecanoyl)-sn-glycero-3-phosphocholine (pyrene-PC) and -phosphoethanolamine (pyrene-PE) were from Molecular Probes (Leiden, The Netherlands), 2,4,6-trinitro-phenyl-PE (TNP-PE), kindly provided by P. Somerharju (University of Helsinki), was prepared as described (13). Antibodies used were: mouse anti-Flag and anti-α-tubulin monoclonal antibodies (Sigma-Aldrich), mouse anti-transferrin receptor monoclonal antibody (Invitrogen). Peroxidase-labeled secondary anti-mouse and anti-rabbit IgG antibodies were from Amersham; alkaline phosphatase-labeled secondary anti-mouse IgG antibody was from Sigma.

Cell culture, expression constructs and transfection

HEK293T cells were grown in RPMI supplemented with 10% fetal calf serum (FCS) in a humified atmosphere containing 5% CO_2. Cells were transfected using TransIT293 reagent (Mirus) according to the manufacturer's instructions. The cloning of pEFrPGKpuro-Flag-StarD10 has been described previously (14). The full-length StarD10 cDNA was subcloned into the pEGFPC1 vector (Invitrogen). The cDNA encoding StarD10-Δ8 was generated by PCR amplification and point mutants of StarD10 were generated by Quikchange site-directed PCR mutagenesis following the manufacturer's instructions (Stratagene) and verified by sequencing.

Immunoaffinity purification of StarD10, 2D PAGE and mass spectrometry

HEK293T cells transiently expressing Flag-tagged StarD10 were lysed in NEB [50 mM Tris (pH 7.5), 150 mM NaCl, 1% NP40, 1 mM sodium orthovanadate, 10 mM sodium fluoride, and 20 mM β-glycerophosphate plus Complete protease inhibitors (Roche)] and lysates were clarified by centrifugation before passing over anti-Flag M2 immunoaffinity resin (Sigma). The resin was washed with NEB, followed by washes with phosphate buffered saline (PBS). Flag-StarD10 was eluted with 100 mM glycine, pH 2.5, and fractions were neutralized with 1/10 volume of 1 M Tris, pH 8. Fractions containing StarD10 as determined by Western blotting with anti-Flag antibody were pooled and concentrated by ultrafiltration using Amicon Ultra-4 columns (10000 NMWL, Millipore). The concentrated samples was subjected to two-dimensional SDS-PAGE and stained with Coomassie Phast Blue as described (15). For MS analysis, the protein was subjected to one-dimensional SDS-PAGE and the band corresponding to StarD10 was excised from the gel and destained with 50 mM NH_4HCO_3 /acetonitrile (1:1 by vol.). Cysteines were first reduced with 1,4-dithio-DL-threitol and then alkylated with iodacetamide. The protein was in-gel digested with modified porcine trypsin, the digest was stopped with formic acid and peptides were extracted with 50 µl 25 mM NH_4HCO_3 for 30 min in an ultrasonic bath. The supernatant was recovered and extraction was repeated with 50 µl acteonitrile, followed by 50 µl 5% formic acid and, finally, 50 µl acetonitrile. All supernatants were combined, vacuum-dried and resuspended in 10 µl 5% formic acid. Phosphopeptides were enriched with the SwellGel® Gallium-Chelated Disc (Phosphopeptide Isolation Kit, Pierce, Rockford, IL, USA) according to the manufacturer's recommendations. Eluates were vacuum-concentrated and resuspended in 10 µl 5% formic acid. The sample was then desalted on a Zip Tip® µ-C18 (Millipore, Bedford, MA, USA) and eluted stepwise into nano-spray capillaries (MDS Proteomics, Odense, Denmark) with 20%, 40%, and 60% aqueous methanol containing 5% formic acid. A QSTAR Pulsar *i* quadrupole time of flight (TOF) mass spectrometer (Applied Biosystem, MDS Sciex, Toronto, Canada) equipped with a nano-electrospray ion source (MDS Proteomics, Odense, Denmark) was used. TOF-MS spectra were collected in the "enhance all" modus and charged ions of peptides were chosen manually for product ion analysis. Product ion spectra (tandem MS) were acquired with collision energies optimized for each peptide to obtain an effective fragmentation pattern with 10% intensity of the

residual precursor ion. Argon was used as collision gas at a recorded pressure of 4.3×10^{-5} Torr. Data were searched by the tandem mass spectrum database matching tool Mascot (http://www.matrixscience.com). The NCBInr and SwissProt databases were searched with the variable modifications deamidation, oxidation of methionine, cabarmidomethylation of cysteine and phosphorylation of serine and threonine.

Recombinant protein production

cDNAs encoding StarD10 wild type, StarD10-S284A and StarD10-Δ8 were cloned into pGEX-6P (Amersham, Little Chalfont, UK) and transformed into BL21 bacteria to produce glutathione S-transferase (GST) fusion proteins. Expression was induced with 0.5 mM isopropyl-β-D-1-thiogalactopyranoside for 4 hrs at 30℃. Bacteria were harvested and resuspended in PBS containing 50 μg/ml lysozyme, Complete protease inhibitors, 10 mM sodium fluoride and 20 mM β-glycerophosphate. GST-StarD10 was purified from clarified lysate with glutathione resin and cleaved with PreScission protease according to the manufacturer's instructions (Amersham). The purity of protein preparations was verified by SDS-PAGE and Coomassie staining.

Cell fractionation and Western blotting

Cells were harvested in hypotonic buffer [20 mM Tris, pH 7.4, containing Complete protease inhibitors, 1 mM sodium orthovanadate, 5 mM β-glycerophosphate and 5 mM sodium fluoride] and sheared by passage through a 25G/16mm gauge needle. Nuclei were removed by centrifugation at 500xg and the cytosol (S) and membrane fraction (P) were obtained by 100.000xg centrifugation. 5% of the cytosol and 50% of the membrane fraction were separated by SDS-PAGE and transferred to polyvinylidine difluoride membranes (Roth). Immunodetection of StarD10 was performed by blocking membranes with 0.5% blocking reagent (Roche) in PBS containing 0.1% Tween 20, followed by incubation with Flag-, transferrin receptor- and tubulin-specific antibodies in blocking buffer. Proteins were visualized with peroxidase-coupled secondary antibody using the enhanced chemiluminescence detection system (Pierce).

Immunoprecipitation and kinase assays

Cells were lysed in NEB (see above) and lysates were clarified by centrifugation at 16.000xg for 10 min. Equal amounts of protein were incubated with anti-Flag antibody for 2 h on ice. Immune complexes were collected with protein G-Sepharose (GE Healthcare), washed three times with NEB and twice with kinase buffer [50 mM Tris, pH 7.5, 10 mM $MgCl_2$, 50 mM NaCl] before incubation with five units of calf intestinal phosphatase (Fermentas) for 45 min at 37℃. Dephosphorylated immunoprecipitates were again washed with NEB, followed by two washes with kinase buffer before incubation with 10 ng purified CKII (from B. Lüscher) in the presence of 25 μM cold ATP and 2 μCi $[\gamma\text{-}^{32}P]$-ATP for 30 min at 37 ℃. Samples were resolved by SDS-PAGE, blotted onto membrane and analyzed on a PhosphoImager (Molecular Dynamics), followed by Western

blotting with StarD10-specific antibody In the case of recombinant proteins used for lipid transfer assays, 40 µg protein was incubated with 500 Units CKII (Calbiochem) in kinase buffer [20 mM Tris, pH 7.5, 10 mM $MgCl_2$, 50 mM KCl] in the presence of 200 µM ATP for 2 hours at 30°C.

Lipid transfer assays

HEK293T cells transiently expressing GFP-tagged StarD10 variants were harvested in hypotonic buffer (see above). The cytosol fraction was obtained after 100.000xg centrifugation for 1 h and the amount of expressed protein was quantified by measuring GFP peak emission at 480 - 550 nm (excitation 466 nm). Protein-mediated transfer of PC between SUVs was measured as described previously (12). The transfer assay mixture contained donor vesicles (1 µmol lipid/ml) composed of porcine brain lipids (Avanti Polar Lipids), pyrene-labeled PC and 2,4,6-trinitrophenyl-phosphatidylethanolamine (TNP-PE) (88.6:0.4:11 mol%), and a 10-fold excess of acceptor vesicles composed of porcine brain lipids. Fluorescence intensity was recorded at 395 nm (excitation, 345 nm; slit widths, 4 nm) before and after the addition of 90 µg cytosol from HEK293T cells transiently expressing the individual proteins (see above). Fluorescence intensities were normalized to (i) the maximum intensity obtained after the addition of Triton X-100 (0.5% final concentration) and (ii) the maximum GFP fluorescence, to account for different protein expression levels.

Membrane flotation assays

Multilamellar vesicles (MLVs) (concentration = 1 mM) were generated by resuspension of dried brain lipids in buffer [20 mM Hepes, pH 7.2, 5 mM EDTA, 100 mM NaCl]. MLVs (100 µl) were incubated with 50 µl recombinant StarD10 proteins (20 µg) for 10 min at 37°C. The suspension was adjusted to 30% (w/v) sucrose by addition of 100 µl 75% (w/v) sucrose, overlayed with 200 µl 25% (w/v) sucrose in buffer and 50 µl sucrose-free buffer. Samples were centrifuged at 240.000 x g for 1 h at 4°C in a TLS-55 rotor. The bottom (250 µl) and top (100 µl) fractions were collected and 5 µl aliquots were analyzed by immunoblotting.

Results

Phosphorylation of human StarD10 on serine 284

Phosphorylation of proteins is a common post-translational modification to regulate protein-protein interactions, protein localization or enzymatic activity by inducing conformational changes. We originally identified StarD10 as a phosphoprotein based on its crossreactivity with a phosphospecific antibody and mapped serine 259 to be phosphorylated and provide a specific antibody recognition site (14;16). When we further analyzed StarD10 by 2D-PAGE in lysates from HEK293T cells transiently expressing the protein, we noted three StarD10-specific spots of different pI values (Figure 1A). Such pI shifts are indicative of differential phosphorylation and suggested that at least one additional phosphorylation site existed in StarD10. To map potential phosphorylation sites in StarD10, we affinity-purified the protein and subjected it to analysis by

tandem mass spectrometry. Specific enrichment of phosphopetides was achieved by immobilized metal ion affinity chromatography with gallium(III) ions. The molecular mass of the [M+2H]$^{2+}$-ion shown in Figure 1B corresponds to the singly phosphorylated, methionine-oxidized carboxyterminal tryptic peptide T38. The fragmentation pattern of the [M+2H]$^{2+}$-ion showed y-ion series up to y7, ruling out phosphorylation of threonine 288, serine 289, and threonine 291. The fragmentation spectrum of the [M+2H]$^{2+}$-ion obtained a high score in a Mascot search, and the loss of 49 Dalton from the [M+2H]$^{2+}$-ion further suggested that serine 284 was phosphorylated.

Casein kinase II phosphorylates StarD10 on serine 284

Serine 284 is located within an amino acid stretch containing several negatively charged residues, motifs that are typically recognized by casein kinase II, the minimal consensus sequence being
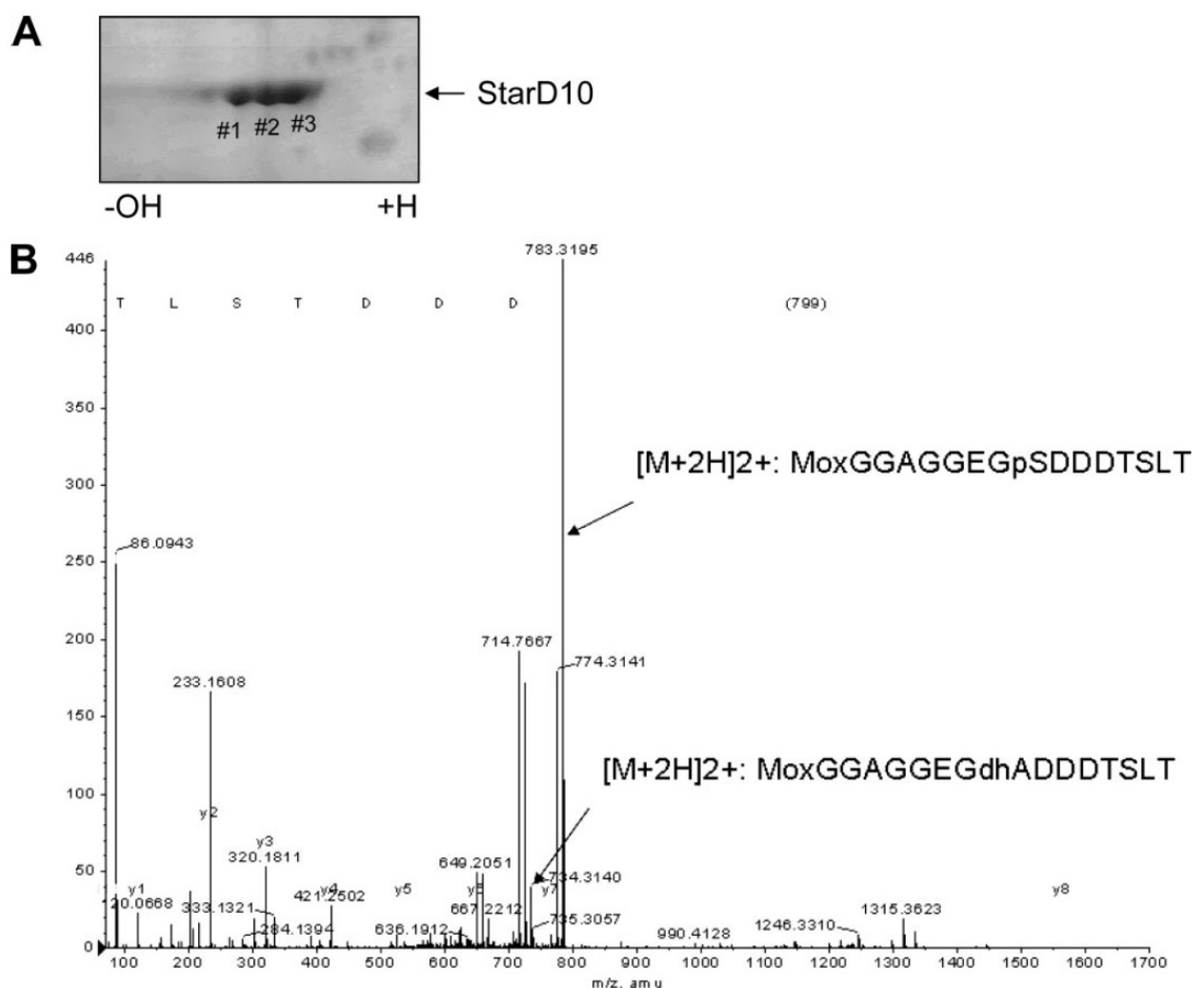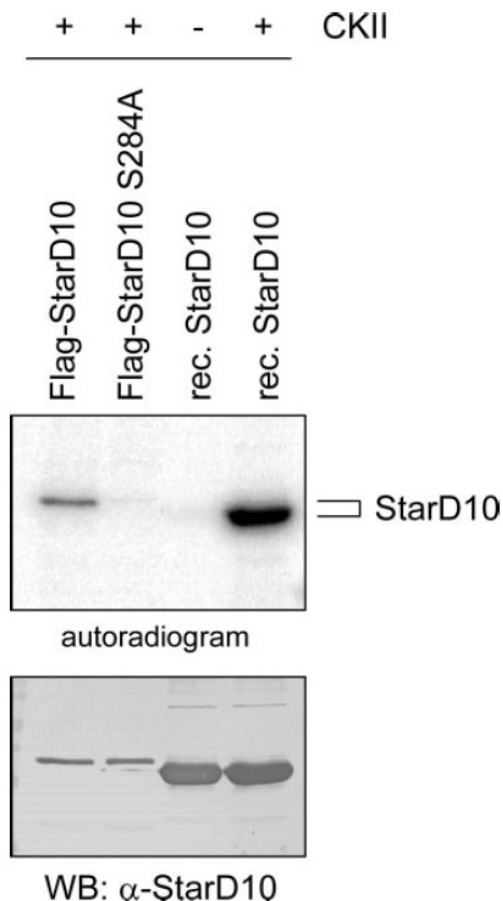

Figure 1: **StarD10 phosphorylation on serine 284.** (A) Affinity-purified Flag-tagged StarD10 from HEK293T cells transiently expressing the protein was subjected to 2-dimensional gel electrophoresis. The gel was stained with Coomassie and StarD10-specific spots are marked (#1-3). (B) Flag-StarD10 was affinity-purified as described in Experimental Procedures, subjected to SDS-PAGE and in-gel digested with trypsin. Phosphopetides were enriched by immobilized metal ion affinity chromatography and analyzed by mass spectrometry. The molecular mass of the [M+2H]$^{2+}$-ion shown corresponds to the singly phosphorylated, methionine-oxidized carboxyterminal tryptic peptide T38. The fragmentation pattern of the [M+2H]$^{2+}$-ion showed y-ion series up to y7, ruling out phosphorylation of threonine 288, serine 289, and threonine 291. The fragmentation spectrum of the [M+2H]$^{2+}$-ion obtained a high score in a Mascot search, and the loss of 49 Dalton from the [M+2H]$^{2+}$-ion further suggested that serine 284 was phosphorylated.

S/T-X-X-D/E (see Figure 3A). To investigate whether CKII was capable of phosphorylating StarD10 we first performed an *in vitro* kinase assay with recombinant StarD10 protein from *E. coli* that is not phosphorylated as determined by mass spetrome try (data not shown). Indeed, addition of purified CKII to the kinase reaction resulted in robust phosphorylation of StarD10 that was not seen in the absence of CKII (Figure 2, lanes 3&4). To analyze whether this phosphorylation occurred on serine 284, the wild type protein and a serine-to-alanine exchange mutant were transiently expressed in HEK293T cells and immunoprecipitated from cell lysates. Incubation with CKII in the presence of radiolabeled ATP led to incorporation phosphate in the case of the wild type protein but was not seen for the mutant (Figure 2, lanes 1&2). This provides evidence that CKII is capable of phosphorylating StarD10 on a single residue, namely serine 284. The fact that CKII phosphorylation of StarD10 immunoprecipitated from cell lysates required prior protein dephosphorylation with alkaline phosphatase indicates a high stoichiometry of phosphorylation on serine 284.

autoradiogram

WB: α-StarD10

Figure 2: *In vitro* **phosphorylation of StarD10 by casein kinase II.** Ectopically expressed Flag-tagged wild type and S284A StarD10 were immunoprecipitated with anti-Flag antibody from HEK293T cell lysates and treated with alkaline phosphatase (lanes 1 & 2). Dephosphorylated immunoprecipitates and, in lanes 3 & 4, recombinant StarD10 were subjected to an *in vitro* kinase assay with purified CKII and radiolabeled γ^{32}P-ATP, followed by SDS-PAGE. Proteins were transferred to membrane and analyzed by PhosphorImager, and then immunoblotted with a StarD10-specific antibody to verify equal loading. WB, Western blot.

Serine 284 phosphorylation regulates StarD10 lipid transfer activity

StarD10 functions as a lipid transfer protein specific for PC and PE. We therefore investigated whether StarD10 phosphorylation on serine 284 affected its phospholipid transfer activity. To this end, GFP fusions of StarD10 wild type and the S284A mutant were transiently expressed in HEK239T cells and the cytosol fraction was analyzed for PC-specific lipid transfer activity using a fluorescence resonance energy-based assay. Small unilamellar vesicles were prepared containing pyrene-labeled PC as a fluorescent donor and quenching amounts of head group-labeled TNP-PE (12;17). When these donor liposomes were mixed with an excess of unlabeled acceptor liposomes, the increase in pyrene fluorescence was negligible, indicating minimal spontaneous transfer (data not shown). Upon addition of StarD10-containing cytosol, a steady increase in fluorescence was noted compared to control cytosol of vector-transfected cells (Figure 3B). Compared to the wild

type protein, cytosol containing StarD10-S284A promoted a more rapid increase in pyrene fluorescence. Interestingly, a truncated variant of StarD10 at residue 283, lacking the last 8 carboxyterminal amino acids (StarD10-Δ8; Figure 3A), displayed even higher lipid transfer activity. Similar results were obtained with pyrene-labeled PE as a fluorescent donor (data not shown). Estimation of initial transfer rates revealed that the phosphorylation defective mutant was two-fold and the truncated protein 3.5-fold more active than the wild type protein (Figure 3C). These data suggest that StarD10 phosphorylation on serine 284 and the carboxyterminus in general inhibits StarD10 lipid transfer activity.
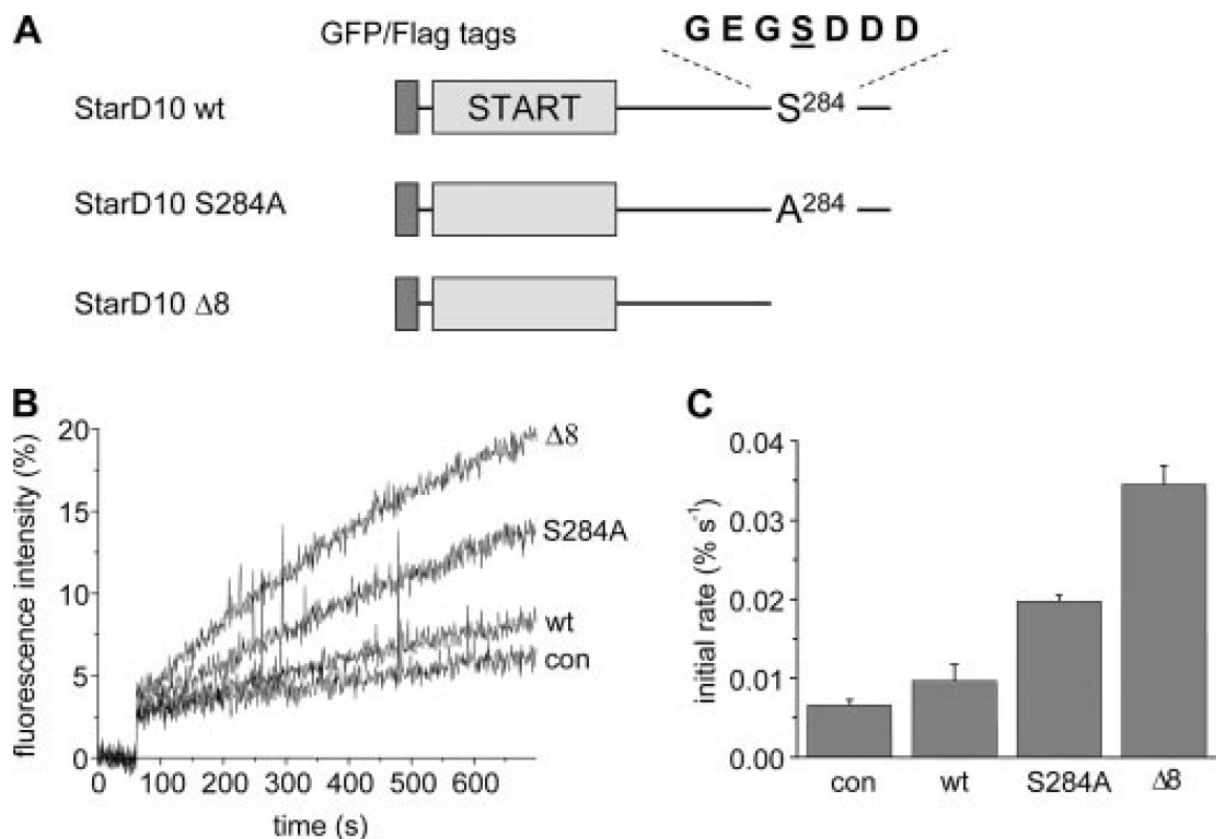

Figure 3. **The StarD10 carboxyterminus regulates in vitro lipid transfer activity.** (A) Schematic representation of the different StarD10 expression constructs containing aminoterminal GFP or Flag tags. StarD10-Δ8 is truncated at amino acid 283. (B) HEK293T cells were transfected with expression plasmids encoding GFP-tagged StarD10 wild type (wt), StarD10-S284A (S284A), StarD10-Δ8 (Δ8), or GFP alone (con). Cells were harvested by hypotonic lysis 48 h post transfection and the cytosol fraction was recovered after centrifugation at 100.000xg. Samples containing equal amounts of GFP fluorescence were used for lipid transfer assays. Donor liposomes containing TNP-PE and pyrene-PC were mixed with a 10-fold excess of unlabeled acceptor liposomes. After 60 sec, cytosol from cells transiently expressing GFP-tagged StarD10 wild type (WT), S284A, Δ8 or GFP alone (con) was added and pyrene fluorescence at 395 nm was recorded (excitation: 340 nm). The fluorescence intensities were normalized to the maximum intensity obtained after the addition of 0.5% Triton X-100. (C) Initial transfer rates were determined by fitting the curves shown in (A) to a single-exponential equation. Values are averages ± SD of two independent experiments.

Regulation of lipid transfer by serine 284 phosphorylation does not require cellular cofactors

Serine/threonine phosphorylation often generates recognition sites for proteins containing specific phosphoserine-/threonine-binding domains and may thus be involved in protein complex formation. To address the question whether inhibition of StarD10 lipid transfer activity in response to CKII phosphorylation may be dependent upon cellular cofactors, we made use of recombinant StarD10 purified from *E. coli,* which is not post-translationally modified. Recombinant StarD10 was incubated in kinase buffer containing ATP in the presence and absence of CKII. Phosphorylation of the protein on serine 284 was found to be highly efficient, as the unphosphorylated tryptic peptide was no longer detected by mass spectrometry (data not shown). When *in vitro* PC transfer of the phosphorylated protein was assessed, its activity was found to be diminished two-fold compared to that of the unphosphorylated protein (Figure 4 A&B). CKII incubation of recombinant StarD10 in which serine 284 was exchanged to an alanine did not alter lipid transfer activity (Figure 4B), proving that inhibition of lipid transfer was indeed due to phosphorylation on this site. In accordance with the data obtained with StarD10 variants expressed in mammalian cells, the recombinant StarD10-Δ8 protein also displayed greater transfer activity. Taken together, these data provide evidence for a protein-intrinsic effect of phosphorylation on StarD10 activity.
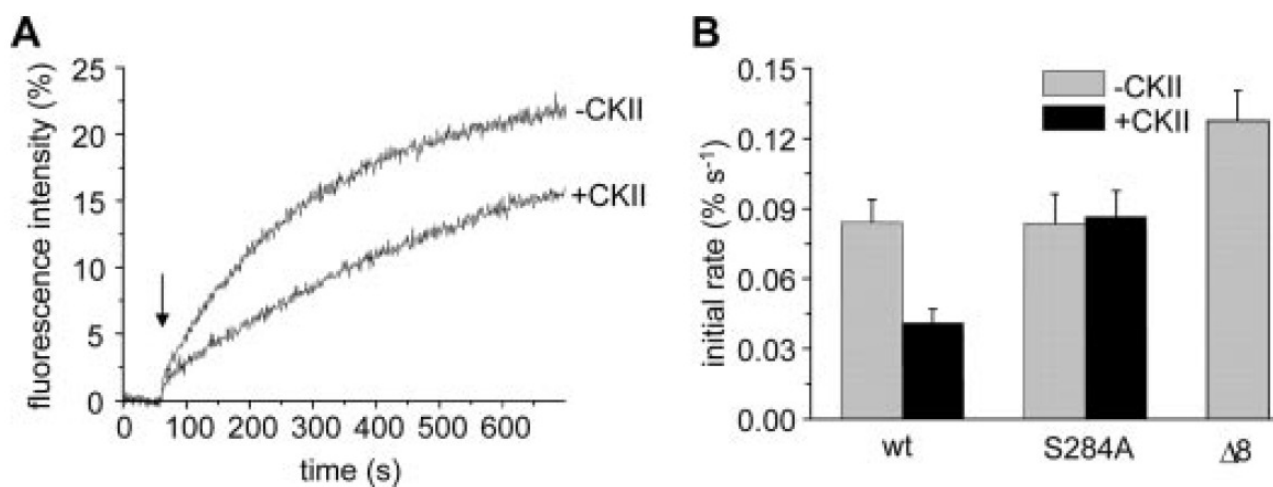

Figure 4: **CKII phosphorylation directly inhibits StarD10 lipid transfer activity.** (A) Transfer of pyrene-labeled PC from donor to acceptor vesicles was performed with recombinant StarD10 phosphorylated with purified CKII (+CKII) or incubated in kinase buffer without addition of CKII (-CKII). The arrow denotes the addition of protein. The fluorescence intensities were normalized to the maximum intensity obtained after addition of 0.5% Triton X-100. (B) Initial transfer rates were determined by fitting the curves shown in (A) to a single-exponential equation. Initial transfer rates obtained with recombinant StarD10-S284A (S284A) and StarD10-Δ8 (Δ8) are also shown. Values are averages ± SD of two independent experiments.

The StarD10 carboxyterminus regulates membrane association

Enhanced lipid transfer activity of StarD10 variants lacking negative charge, either due to dephosphorylation or deletion of carboxyterminal acidic residues, could perhaps affect their affinity for membranes, facilitating lipid uptake from donor and release into acceptor membranes. To analyze whether the carboxyterminus of StarD10 is involved in membrane association, we generated multilamellar vesicles composed of porcine brain lipids and incubated these with recombinant StarD10 wild type and StarD10-Δ8 protein. MLV-associated protein was separated from unbound protein by sucrose gradient centrifugation and analyzed by immunoblotting. Compared to wild type StarD10, relatively more StarD10-Δ8 protein was recovered in the top MLV-containing fraction, suggesting increased affinity for membranes (Figure 5A). This finding was confirmed by fractionation of HEK293T transiently expressing StarD10 wild type, StarD10-S284A and StarD10-Δ8 variants (Figure 5B). Only a small proportion of the wild type protein was
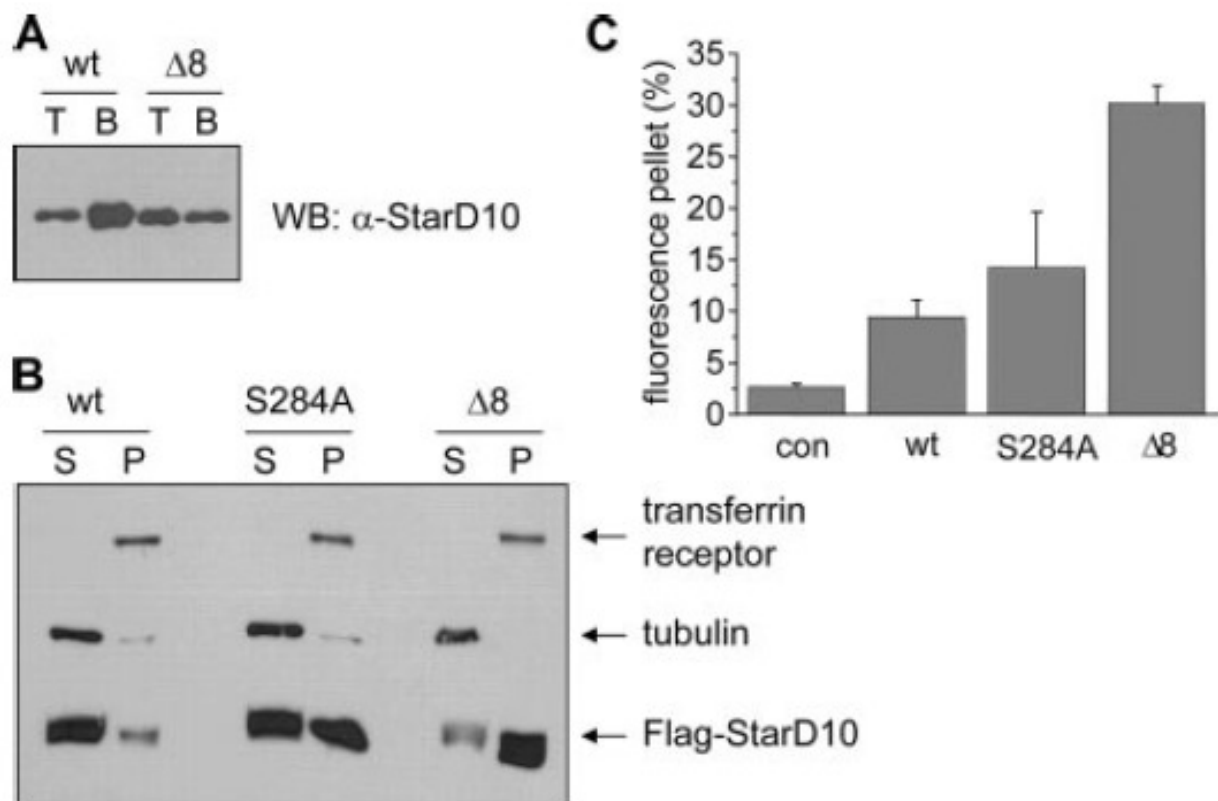

Figure 5: **The StarD10 carboxyterminus regulates membrane association.** (A) Recombinant StarD10 wild type (wt) and StarD10-Δ8 were incubated for 10 min at 37°C with brain lipid MLVs. Subsequently, MLVs were floated on a sucrose step gradient. The top fraction (T) containing MLV-associated protein and the bottom fraction (B) containing unbound protein were analyzed by immunoblotting with StarD10-specific antibody. (B) Cells were lysed in hypotonic buffer and supernatant (S) und pellet (P) fractions were obtained after 100.000xg centrifugation. Proteins were analyzed by immunoblotting with Flag-specific antibody, and transferrin receptor- and tubulin-specific antibodies to control the purity of the fractions. WB, Western blot. (C) HEK293T cells were transfected with expression plasmids encoding GFP-tagged StarD10 wild type (WT), StarD10-S284A and StarD10-Δ8, or GFP alone (con). Cells were lysed in hypotonic buffer and GFP peak fluorescence was determined before and after 100.000xg centrifugation and used to calculate the amount of GFP proteins in pellet fraction. Values are averages ± SD of two independent experiments.

recovered in the pellet fraction whereas S284A and especially the truncated protein were enriched in this fraction. The purity of the individual fractions was confirmed by detection of the transferrin receptor in the membrane and tubulin in the cytosolic fraction (Figure 5B). Association with cellular membranes was further quantified by measuring GFP peak emission before and after 100.000xg centrifugation of cell lysates transiently expressing GFP fusions of StarD10 variants (Figure 5C). Thus, phosphorylation of StarD10 on serine 284 and the acidic carboxyterminus of StarD10 in general provide a mechanism by which membrane association is regulated.

Discussion

Post-translational modification by phosphorylation is a common mechanism by which the activity of proteins can be regulated in a dynamic manner. Here we have mapped by mass spectrometry a novel *in vivo* phosphorylation site on serine 284 in StarD10 and provide evidence that phosphorylation on this site inhibits lipid transfer activity. Phosphorylation increases the local negative charge, eliciting conformational changes or influencing interaction with protein partners, or as shown here, with membranes. Simple exchange of serine 284 with glutamic acid, however, did not appear to mimic the phosphorylated state (data not shown). The carboxyterminus of StarD10 further comprises several acidic residues that apparently contribute to inhibition of membrane association. This is shown by deletion of the last eight carboxyterminal amino acids, which significantly increased membrane binding *in vitro*, association with cellular membranes in intact cells and, finally, *in vitro* lipid transfer activity.

It is conceivable that increased partitioning of StarD10 to membranes allows for fast and efficient lipid transfer by increasing the residence time of the protein at the membrane, thereby increasing the probability of lipid entry into (or exit from) the binding pocket. On the other hand, stable association with membranes could also inhibit lipid transfer, at least *in vitro. In vivo,* however, lipid transfer is thought to occur at membrane contact sites, at which membranes of two organelles come into close apposition (10). Here, dissociation of the protein may not be a prerequisite for efficient lipid transfer.

We previously mapped serine 259 in StarD10 to be phosphorylated by a yet unknown kinase (16). Based on results with a serine to alanine exchange mutant, phosphorylation on this site does not affect StarD10 lipid transfer activity (data not shown), but may rather determine protein stability as a StarD10-S259A mutant was repeatedly found to be expressed at lower levels. Of note, both phosphorylation sites operate independently from one another, since the StarD10-S284A mutant was still phosphorylated on serine 259 as determined by a phosphospecific antibody (data not shown).

Several members of the START family are known to be regulated by phosphorylation, either with regard to their activity or subcellular localization. In StAR, phosphorylation of serine 195 increases

its steroidogenic activity *in vivo* as demonstrated by a phosphorylation site mutant (18), whereas phosphorylation of Pctp regulates its relocation to mitochondria (19). Inhibition of lipid transfer activity due to phosphorylation has been demonstrated for the ceramide transfer protein CERT. Phosphorylation by protein kinase D on serine 132 adjacent to the pleckstrin homology domain negatively regulates CERT interaction with phosphatidylinositol-4-phosphate and inhibits ceramide transfer activity (20).

Although the cellular target membranes have yet to be identified, StarD10 transiently expressed in COS7 cells was found to be mainly cytosolic and it accumulated in a perinuclear region that may represent Golgi and ER membranes (data not shown). Correct localization likely involves association with protein partners and therefore attempts are being made to identify candidate proteins by yeast two hybrid screening.

Studies using truncation mutants and synthetic peptides have provided evidence that the carboxyterminus of Pctp may function as a membrane interaction domain involving an amphipathic α-helix. Removal of the last five residues of Pctp decreased its lipid transfer activity by 50%, whereas deletion of the last 10 residues completely abolished activity and markedly decreased the level of membrane binding (21). Compared with Pctp, StarD10 has a 65 amino acid carboxyterminal extension, thus, deletion of the last eight residues leaves its START domain structurally intact and is not expected to impact on ligand binding. In line with this, lipid transfer activity of the StarD10-Δ8 mutant was found to be enhanced rather than abolished and was independent of cellular cofactors (Figure 4). The carboxyterminal tail thus serves as an intrinsic regulator of StarD10 activity.

It appears that most of the StarD10 protein transiently expressed in HEK293T cells is phosphorylated on serine 284, because *in vitro* CKII phosphorylation required prior dephosphorylation of the protein. Similarly, PKC-mediated phosphorylation of PITPβ isolated from brain could only be observed after dephosphorylation, indicating a high degree of phosphorylation (22). In agreement with serine 284 phosphorylation inhibiting StarD10 membrane association, StarD10 expressed in cells was found to be mainly cytosolic (Figure 5B&C) and its lipid transfer activity was suppressed under normal growth conditions (Figure 3). The challenge remains to identify those conditions that promote dephosphorylation of serine 284, either due to low CKII activity or activation of the phosphatase that dephosphorylates StarD10 on this site.

CKII is a ubiquitously expressed serine/threonine kinase with roles in proliferation, cell survival, differentiation, and transformation. CKII is a tetramer composed of two catalytic (α or α') and two regulatory β subunits. Initially thought to be constitutively active, it is now believed that different cellular CKII pools exist that are regulated locally by differential subunit assembly, phosphorylation, and association with scaffolding proteins (23;24). High CKII levels are found in many proliferating

tumors and in transgenic mice targeted expression of CKIIα in T cells and in the mammary gland induced lymphomagenesis and mammary tumorigenesis, respectively (25;26). The potentiation of NF-κB and Wnt signaling pathways has been suggested to contribute to the oncogenic potential of CKII (25;26). In addition, phoshorylation of proteins such as Bid and Max by CKII protects them from caspase-mediated cleavage, suggesting that CKII further enhances cancer cell survival by inhibiting the action of proteins involved in apoptosis (27;28).

StarD10 was found to be overexpressed in Neu/ErbB2-induced mammary tumors in transgenic mice, in several human breast carcinoma cell lines and in 35% of primary human breast cancers (14). In fibroblasts, StarD10 coexpression with the EGF receptor/ErbB1 augmented growth in soft agar, indicating that the presence of StarD10 may confer a growth advantage and contribute to cellular transformation (14). Whether this is linked to its lipid transfer activity or may be due to an additional function is not known. Due to high CKII levels and/or activity in breast cancer cells, we assume that StarD10 is phosphorylated on serine 284 in these cells, downregulating membrane interaction and lipid transfer activity. In future studies it would thus be of interest to correlate the phosphorylation status of StarD10 with CKII activity in tumor cells.

Acknowledgments

Abbreviations

The abbreviations used are: CKII, casein kinase II; StAR, steroidogenic acute regulatory protein; START, StAR-related lipid transfer; PC, phosphatidylcholine; Pctp, phosphatidylcholine transfer protein; PE, phosphatidylethanolamine; PITP, phosphatidylinositol transfer protein; StarD10, START-domain-containing 10; SUVs, small unilamellar vesicles; MLVs, multilamellar vesicles

References

1.   Sprong, H., van der Sluijs, P., and van Meer, G. (2001) *Nat.Rev.Mol.Cell Biol.* **2,** 504-513

2.   Holthuis, J. C. and Levine, T. P. (2005) *Nat.Rev.Mol.Cell Biol.* **6,** 209-220

3.   Wirtz, K. W. (2006) *FEBS Lett.* **580,** 5436-5441

4.   Soccio, R. E. and Breslow, J. L. (2003) *J.Biol.Chem.* **278,** 22183-22186

5.   Alpy, F. and Tomasetto, C. (2005) *J.Cell Sci.* **118,** 2791-2801

6.   Strauss, J. F., III, Kishida, T., Christenson, L. K., Fujimoto, T., and Hiroi, H. (2003) *Mol.Cell Endocrinol.* **202,** 59-65

7.   Hanada, K., Kumagai, K., Yasuda, S., Miura, Y., Kawano, M., Fukasawa, M., and Nishijima, M. (2003) *Nature* **426,** 803-809

8.   Loewen, C. J., Roy, A., and Levine, T. P. (2003) *EMBO J.* **22,** 2025-2035

9.   Voelker, D. R. (2005) *Trends Biochem.Sci.* **30,** 396-404

10. Levine, T. and Loewen, C. (2006) *Curr.Opin.Cell Biol.* **18,** 371-378

11. van Helvoort, A., de Brouwer, A., Ottenhoff, R., Brouwers, J. F., Wijnholds, J., Beijnen, J. H., Rijneveld, A., van der, P. T., van der Valk, M. A., Majoor, D., Voorhout, W., Wirtz, K. W., Elferink, R. P., and Borst, P. (1999) *Proc.Natl.Acad.Sci.U.S.A* **96,** 11501-11506

12. Olayioye, M. A., Vehring, S., Muller, P., Herrmann, A., Schiller, J., Thiele, C., Lindeman, G. J., Visvader, J. E., and Pomorski, T. (2005) *J.Biol.Chem.* **280,** 27436-27442

13. Gordesky, S. E., Marinetti, G. V., and Segel, G. B. (1973) *J.Membr.Biol.* **14,** 229-242

14. Olayioye, M. A., Hoffmann, P., Pomorski, T., Armes, J., Simpson, R. J., Kemp, B. E., Lindeman, G. J., and Visvader, J. E. (2004) *Cancer Res.* **64,** 3538-3544

15. Verhagen, A. M., Ekert, P. G., Pakusch, M., Silke, J., Connolly, L. M., Reid, G. E., Moritz, R. L., Simpson, R. J., and Vaux, D. L. (2000) *Cell* **102,** 43-53

16. Hoffmann, P., Olayioye, M. A., Moritz, R. L., Lindeman, G. J., Visvader, J. E., Simpson, R. J., and Kemp, B. E. (2005) *Electrophoresis* **26,** 1029-1037

17. Somerharju, P. J., Kasurinen, J., and Wirtz, K. W. (1992) *Methods Enzymol.* **209,** 495-504

18. Arakane, F., King, S. R., Du, Y., Kallen, C. B., Walsh, L. P., Watari, H., Stocco, D. M., and Strauss, J. F., III (1997) *J.Biol.Chem.* **%19;272,** 32656-32662

19. de Brouwer, A. P., Westerman, J., Kleinnijenhuis, A., Bevers, L. E., Roelofsen, B., and Wirtz, K. W. (2002) *Exp.Cell Res.* **274,** 100-111

20. Fugmann, T., Hausser, A., Schoeffler, P., Schmid, S., Pfizenmaier, K., and Olayioye, M. A. *J.Cell Biol.*, in press

21. Feng, L., Chan, W. W., Roderick, S. L., and Cohen, D. E. (2000) *Biochemistry* **39,** 15399-15409

22. Snoek, G. T., van Tiel, C. M., and Egmond, M. R. (2004) *Biochimie* **86,** 857-864

23. Olsten, M. E. and Litchfield, D. W. (2004) *Biochem.Cell Biol.* **82,** 681-693

24. Ahmed, K., Gerber, D. A., and Cochet, C. (2002) *Trends Cell Biol.* **12,** 226-230

25. Landesman-Bollag, E., Romieu-Mourez, R., Song, D. H., Sonenshein, G. E., Cardiff, R. D., and Seldin, D. C. (2001) *Oncogene* **20,** 3247-3257

26. Seldin, D. C. and Leder, P. (1995) *Science* **267,** 894-897

27. Krippner-Heidenreich, A., Talanian, R. V., Sekul, R., Kraft, R., Thole, H., Ottleben, H., and Luscher, B. (2001) *Biochem.J.* **358,** 705-715

28. Desagher, S., Osen-Sand, A., Montessuit, S., Magnenat, E., Vilbois, F., Hochmann, A., Journot, L., Antonsson, B., and Martinou, J. C. (2001) *Mol.Cell* **8,** 601-611

7.2. Regulation of secretory transport by protein kinase D-mediated phosphorylation of the ceramide transfer protein

Tim Fugmann*, Angelika Hausser*, Patrik Schöffler, Simone Schmid, Klaus Pfizenmaier, and Monilola A. Olayioye#

University of Stuttgart, Institute of Cell Biology and Immunology,
Allmandring 31, 70569 Stuttgart, Germany

* Both authors contributed equally to the manuscript

Corresponding author:

Monilola A. Olayioye, Tel: +49 711 685 69301, Fax: + 49 711 685 67484
Email: monilola.olayioye@izi.uni-stuttgart.de

Abstract

Protein kinase D (PKD) has been identified as a crucial regulator of secretory transport at the trans-Golgi-network (TGN). Recruitment and activation of PKD at the TGN is mediated by the lipid diacylglycerol (DAG), a pool of which is generated by sphingomyelin synthase from ceramide and phosphatidylcholine. The non-vesicular transfer of ceramide from the endoplasmic reticulum to the Golgi complex is mediated by the lipid transfer protein CERT. Here we identify CERT as a novel *in vivo* PKD substrate. Phosphorylation on serine 132 by PKD decreases the affinity of CERT towards its lipid target phosphatidylinositol 4-phosphate at Golgi membranes and reduces ceramide transfer activity, identifying PKD as a regulator of lipid homeostasis. We also show that CERT in turn is critical for PKD activation and PKD-dependent protein cargo transport to the plasma membrane. The interdependence of PKD and CERT is thus a key to the maintenance of Golgi membrane integrity and secretory transport.

Introduction

PKD is a family of serine/threonine-specific protein kinases comprising 3 structurally related members: PKD1/PKCμ, PKD2 and PKD3/PKCν. PKD contains 2 zinc finger-like cysteine-rich motifs that bind DAG, a pleckstrin homology (PH) and a kinase domain. PKD localizes to the cytosol, nucleus, Golgi complex and plasma membrane, where it regulates diverse cellular processes including vesicle trafficking (Rykx et al., 2003;Wang, 2006). Thus far, only a few physiological PKD substrates are known, e.g. the neuronal protein Kidins220, the Ras effector RIN1, HDAC5, and PI4KIIIβ (Iglesias et al., 2000;Wang et al., 2002;Vega et al., 2004;Hausser et al., 2005). At the TGN, PKD is critically involved in the fission of transport carriers en route to the cell surface (Liljedahl et al., 2001;Yeaman et al., 2004). PKD is recruited to the TGN by its cysteine-rich regions (Maeda et al., 2001;Hausser et al., 2002;Baron and Malhotra, 2002), where it is activated by PKCη-mediated phosphorylation (Diaz Anel and Malhotra, 2005). PKD-mediated phosphorylation of PI4KIIIβ stimulates its lipid kinase activity, resulting in enhanced phosphatidylinositol 4-phosphate (PI(4)P) production and cargo transport to the plasma membrane (Hausser et al., 2005). Here, we demonstrate that PKD also phosphorylates and regulates the activity of the Golgi-localized ceramide transfer protein CERT (also known as Goodpasture antigen-binding protein), a cytosolic protein essential for the non-vesicular delivery of ceramide from its site of production at the endoplasmic reticulum (ER) to Golgi membranes, where conversion to sphingomyelin (SM) takes place (Hanada et al., 2003). Two CERT isoforms exist: the more abundantly expressed, alternatively spliced form missing a 26 amino acid, serine-rich region and the full-length 624 amino acid protein, designated CERT$_L$ (Raya et al., 2000). Both CERT isoforms possess a steroidogenic acute regulatory (StAR)-related lipid transfer (START) domain that is necessary and sufficient for ceramide binding and transport (Hanada et al., 2003). START domains are ~210 amino acids in length and form a hydrophobic tunnel that

accommodates a monomeric lipid (Soccio and Breslow, 2003;Alpy and Tomasetto, 2005). They are found in 15 mammalian proteins, with CERT being most closely related to Pctp, which binds and shuttles phosphatidylcholine (PC) between membranes, and StarD10, a lipid transfer protein specific for PC and PE (Soccio and Breslow, 2003;Olayioye et al., 2005;Wirtz, 2006). CERT proteins further contain an N-terminal PH domain with specificity for PI(4)P that contributes to Golgi localization (Levine and Munro, 2002;Hanada et al., 2003)} and a FFAT motif (two phenylalanines in an acidic tract) that targets the protein to the ER via interaction with the ER resident transmembrane proteins VAP-A and VAP-B (Loewen et al., 2003;Kawano et al., 2006). Non-vesicular lipid transfer is thought to occur at membrane contact sites (MCS), at which the ER comes into close apposition with other organelles (Levine and Loewen, 2006). CERT may thus shuttle a very short distance between ER and Golgi membranes, or perhaps contact both compartments simultaneously. When overexpressed the START domain of CERT is sufficient for ceramide transfer to the Golgi complex (Kawano et al., 2006). However, under physiological conditions, both Golgi and ER targeting motifs are essential for CERT function. In the CHO cell line LY-A, CERT was identified to contain a mutation within its PH domain (G67E), rendering the protein defective in PI(4)P binding, which resulted in reduced cellular SM levels (Hanada et al., 2003). The PI(4)P requirement for CERT function is further supported by a recent report showing that PI4KIIIβ activity is necessary for efficient ceramide trafficking to the Golgi (Toth et al., 2006). We now provide evidence that PKD phosphorylates CERT on serine 132 adjacent to the PH domain, whereby PI(4)P binding, Golgi targeting and ceramide transfer activity are negatively regulated. Furthermore, by transferring ceramide that is required for DAG production to Golgi membranes, CERT stimulates PKD activity and ensures the maintenance of constitutive secretory transport.

Results and discussion

PKD is a key regulator at the Golgi complex with PI4KIIIβ being the only local substrate identified thus far (Hausser et al., 2005). To test whether the Golgi complex-localized CERT protein may serve as a substrate for PKD, we made use of a phosphospecific substrate antibody, termed pMOTIF, raised against consensus motifs phosphorylated by PKD (Doppler et al., 2005). HEK293T cells were transfected with expression vectors encoding Flag-tagged CERT and $CERT_L$. Immunoprecipitated CERT isoforms were analyzed by Western blotting with the pMOTIF antibody (Fig. 1A). A pMOTIF signal corresponding to the molecular weight of CERT and, more weakly, to that of $CERT_L$ was detected (Fig. 1A). The weaker detection of the $CERT_L$ isoform by approximately 25% compared to CERT may be related to its known behaviour to form aggregates, which may impact phosphosite accessibility to kinases (Raya et al., 2000). To investigate whether recognition of CERT by the pMOTIF antibody was dependent upon PKD, we expressed CERT together with a kinase dead, dominant negative PKD1 variant in HEK293T cells. Coexpression of inactive PKD1 abolished CERT detection by the pMOTIF antibody, suggesting that the signal was

indeed due to PKD-mediated CERT phosphorylation (Fig. 1B). To address the question of which PKD isoform was responsible for CERT phosphorylation, we used an RNA interference approach to downregulate PKD. Silencing of only one isoform did not influence the level of CERT phosphorylation as judged by immunoblotting with the pMOTIF antibody (data not shown). However, simultaneous knockdown of PKD1 and PKD2 greatly reduced CERT phosphorylation (Fig. 1C), suggesting that these 2 isoforms were primarily responsible for phosphorylating CERT,
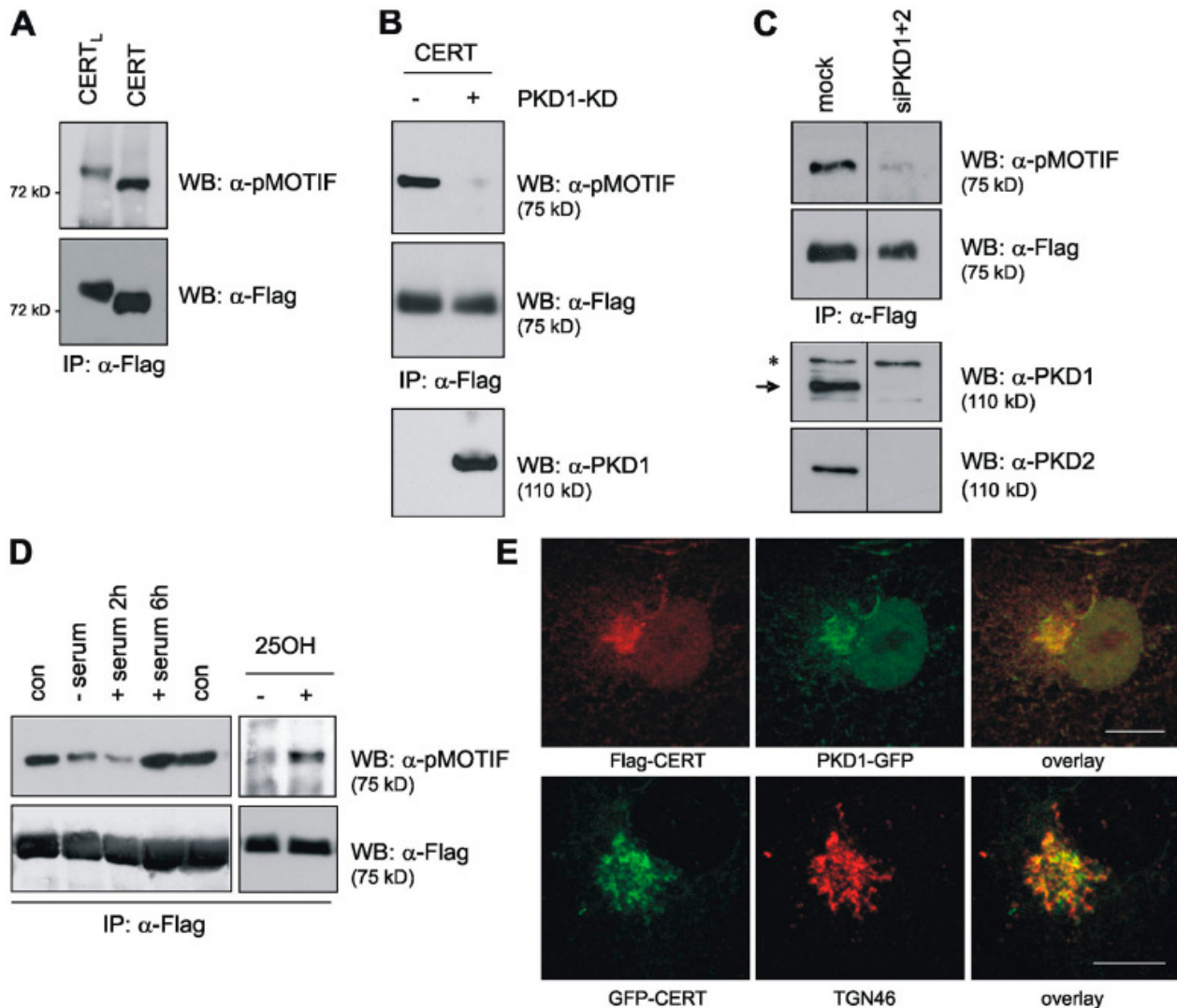

Fig. 1: CERT is detected by a PKD substrate antibody. (A) HEK293T cells were transfected with expression plasmids encoding Flag-tagged CERT$_L$ and CERT. Cells were lysed and CERT isoforms were immunoprecipitated with anti-Flag antibody. Immunoprecipitated proteins were subjected to SDS-PAGE, followed by immunoblotting with PKD substrate antibody (pMOTIF; top) and, after stripping, with anti-Flag antibody (bottom). (B) HEK293T cells were transfected with Flag-CERT expression plasmid, along with GFP-PKD1-KD or empty vector. CERT was analyzed by Western blotting as described in (A). Expression of PKD1-KD was verified by immunoblotting with a PKD1-specific antibody (bottom). (C) HEK293T cells were either mock-transfected or transfected with PKD1- and PKD2-specific siRNAs, followed by transfection with Flag-CERT expression plasmid 48 h later. After 24 h, CERT phosphorylation was analyzed as described in (A) (top). Silencing of PKD1 and PKD2 was verified by immunoblotting of lysates with specific antibodies (bottom). The band marked with an asterisk is due to non-specific binding. (D) HEK293T cells were transfected with Flag-CERT expression plasmid. Cells were left untreated (con) or serum-starved o/n, followed by stimulation with either 10% serum for 2 h and 6 h or 2.5 µg/ml 25OH for 1 h. CERT phosphorylation was analyzed as described in (A). (E) COS7 cells expressing Flag-CERT and PKD1-GFP (top) or GFP-CERT (bottom) were fixed and stained with Flag- and TGN46-specific antibodies (red), respectively. Scale bar, 10 µm.

whereas PKD3 appeared to play a minor role. This is in accordance with previously reported overlapping substrate specificities of PKD1 and PKD2, which both phosphorylate PI4KIIIβ, whereas PKD3 fails to do so (Hausser et al., 2005). The phosphorylation status of CERT was strongly reduced in serum-deprived cells and could be restored by readdition of serum (Fig. 1D), indicating that CERT phosphorylation is dependent on extracellular stimuli. It was recently reported that the oxysterol-binding protein OSBP promotes CERT translocation to the Golgi complex in response to stimulation with its ligand, 25-hydroxycholesterol (25OH), thereby integrating sterol signaling and SM synthesis (Perry and Ridgway, 2006). In line with these studies, 25OH treatment was found to augment CERT phosphorylation (Fig. 1D), possibly by bringing CERT to the Golgi in vicinity of PKD. CERT has been demonstrated to colocalize with the cis/medial-Golgi marker GS28 (Hanada et al., 2003). Immunofluorescence analysis of GFP-tagged CERT expressed in COS7 cells showed that the protein localized to GS28-positive Golgi regions (Fig. S1). However, lipid transfer proteins are thought to act at MCS, which are formed between the ER and TGN (Levine and Loewen, 2006), where PKD is localized. Immunofluorescence staining of Flag-tagged CERT co-expressed with GFP-tagged PKD in COS7 cells revealed that the two proteins colocalize at the Golgi complex. Furthermore, staining of the TGN-specific marker protein TGN46 verified that CERT partially localizes to this compartment (Fig. 1E).

To identify pMOTIF recognition sites in CERT, we searched for potential PKD consensus motifs characterized by a leucine, isoleucine or valine residue in the -5 and arginine in the -3 position relative to a serine or threonine. Two serines at positions 132 and 272 matching the PKD consensus motif (Fig. 2A) were exchanged for alanines by site-directed mutagenesis. Mutants were expressed in HEK293T cells and tested for recognition by the pMOTIF antibody. Interestingly, mutation of serine 132 to alanine abrogated detection of CERT with the pMOTIF antibody and caused an increase in electrophoretic mobility, indicative of loss of phosphorylation, while the S272A mutation did not affect the pMOTIF signal (Fig. 2B). On low percentage gels, the wild type protein migrated as two distinct bands, indicating the presence of a phosphorylated and a nonphosphorylated CERT pool (data not shown). To confirm that PKD was capable of directly phosphorylating serine 132, we performed *in vitro* kinase assays with purified PKD1 and recombinant CERT GST-fusion proteins comprising the first 138 amino acids of the protein. Wild type CERT was efficiently phosphorylated by PKD1 whereas the CERT-S132A protein showed strongly reduced incorporation of radioactivity in this assay (Fig. 2C). Further, *in vitro* PKD phosphorylation of wild type but not CERT-S132A generated a recognition site for the pMOTIF antibody (Fig. 2D). Taken together, these results prove that CERT is a genuine PKD substrate *in vitro* and *in vivo* and identify serine 132 as a specific PKD phosphorylation site in CERT that can be monitored with the pMOTIF antibody.

Serine 132 is in very close proximity to the CERT PH domain (aa 23 - 117), making it possible that phosphorylation on this site affects PI(4)P binding by increasing the local negative charge. We

therefore quantified PI(4)P binding of CERT-WT and CERT-S132A by performing protein-lipid overlay assays. Cytosol from cells transiently expressing the CERT variants was incubated with membranes spotted with a concentration gradient of the different phosphoinositides and bound CERT proteins were detected via their GFP tag. As reported previously, the wild type protein demonstrated weak binding to several phospholipid species, but displayed strong interaction with PI(4)P (Levine and Munro, 2002;Hanada et al., 2003). CERT-S132A binding to PI(4)P was detectable at 2- to 4-fold lower concentrations as compared to that of the wild type protein (Fig. 3A). To corroborate these results, association of CERT with multilamellar vesicles (MLVs) consisting of PC alone or PC plus 5% PI(4)P was measured. While the addition of PI(4)P to PC
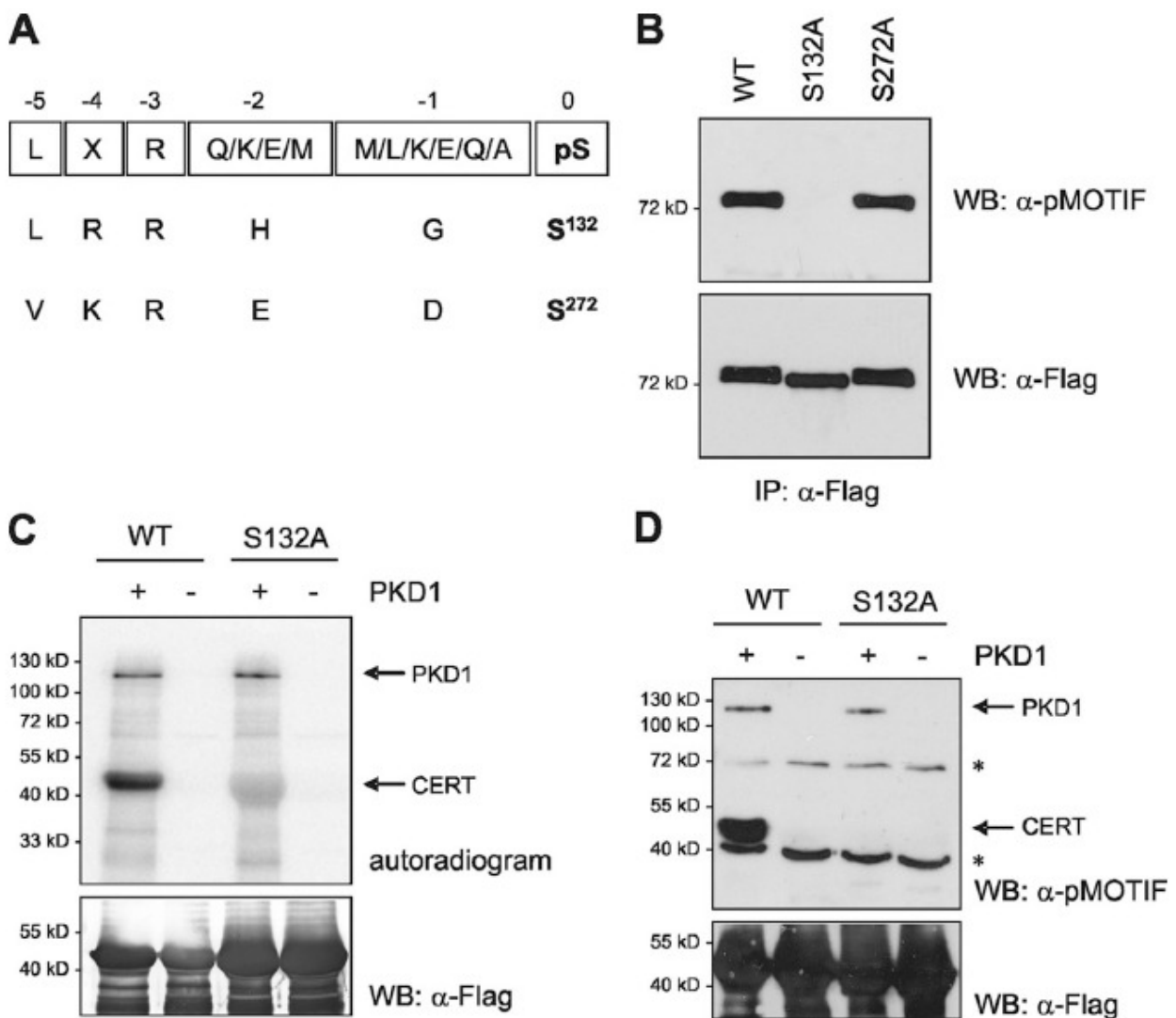

Fig. 2: PKD phosphorylates CERT on serine 132. (A) Alignment of the peptide sequences used to raise the pMotif antibody and 2 potential PKD motifs in CERT. (B) HEK293T cells transiently expressing Flag-tagged CERT-WT, -S132A, and -S272A were lysed and CERT phosphorylation was analyzed as described in Fig. 1A. (C, D) Recombinant GST-Flag-CERT-WT and -S132A proteins were incubated in kinase buffer containing [^{32}P]-γ-ATP (C) or cold ATP (D) in the absence (-) and presence (+) of purified PKD1. Proteins were separated by SDS-PAGE and transferred to membrane. (C) Incorporation of radioactive phosphate was analyzed using a PhosphoImager (top), followed by immunoblotting with Flag-specific antibody to verify equal loading of the CERT proteins. (D) Immunoblotting was performed with the pMOTIF antibody and, after stripping, with Flag-specific antibody to verify equal loading of the CERT proteins. PKD1 and CERT proteins are marked with arrows; the bands with asterisks are due to non-specific binding.

vesicles increased membrane binding of CERT-WT 1.5-fold, binding of CERT-S132A was enhanced 1.9-fold, suggesting increased affinity of the CERT-S132A mutant to PI(4)P (Fig. 3B). To investigate whether this affected association with Golgi membranes in intact cells, we performed fractionation studies with cells expressing CERT-WT and CERT-S132A. To estimate the level of ER binding, we included a CERT mutant (G67E) defective in PI(4)P-binding. Only a small proportion of the wild type and the G67E protein were recovered in the pellet fraction, suggesting that under the experimental conditions used ER binding was negligible and Golgi association of the wild type protein was not maintained (Fig. 3C). The CERT-S132A mutant protein was highly enriched in the pellet fraction confirming that the enhanced affinity for PI(4)P stabilizes membrane association *in vivo.* Together, these data imply that CERT, once bound to the Golgi complex, is phosphorylated by PKD. This then decreases the affinity of CERT to PI(4)P and thereby regulates the interaction of CERT with the Golgi complex. Since PI(4)P is also present at the plasma membrane additional factors must specify CERT targeting to the Golgi complex. One candidate is Arf1, which has been shown to interact with the structurally related proteins OSBP and FAPP1 (Levine and Munro, 2002). Whether CERT phosphorylation influences binding to such additional factors remains to be tested in the future.

The CERT protein has been shown to function as a lipid transfer protein (Hanada et al., 2003). We thus investigated whether CERT phosphorylation on serine 132 influenced its ability to bind and transfer ceramide between membranes. To this end, GFP-tagged versions of CERT-WT and CERT-S132A were transiently expressed in HEK239T cells and the cytosol fraction was analyzed for ceramide-specific lipid transfer activity using a FRET-based assay. In this assay, vesicles containing pyrene-labeled ceramide as a fluorescent donor and quenching amounts of TNP-PE were employed (Somerharju, 2002;Olayioye et al., 2005). The lipid preparation used was total extract from porcine brain, which is likely to contain PI(4)P. Upon addition of cytosol containing CERT-WT, a steady increase in fluorescence was noted, which was not observed when control cytosol of vector-transfected cells was used (Fig. 3D). Compared to the wild type protein, CERT-S132A displayed a higher rate of lipid transfer, evident from a more rapid increase in pyrene fluorescence (Fig. 3D). Similar results were obtained when 0,5% PI(4)P was added to donor liposomes (data not shown). This suggests that CERT phosphorylation on serine 132 downregulates ceramide transfer activity, most likely by decreasing association of the protein with membranes. Previous data have already shown that PKD regulates the level of PI(4)P at the Golgi complex by phosphorylation-mediated activation of PI4KIIIβ (Hausser et al., 2005). Interestingly, PI4KIIIβ is critical for the transport of ceramide between the ER and the Golgi complex (Toth et al., 2006). Accordingly, together with the data presented here, a dual role for PKD in maintaining lipid homeostasis of Golgi membranes becomes apparent by controlling the on-rate (via PI(4)P levels) and the off-rate (via direct phosphorylation) of CERT.

The transfer of ceramide from the ER to the TGN is essential for SM synthesis at this compartment (Hanada et al., 2003). Golgi-localized SM synthase 1 utilizes ceramide and PC to generate SM and DAG (Perry and Ridgway, 2005), the latter being a prerequisite for PKD recruitment and activation. Compounds that block DAG production at the TGN inhibit the binding of PKD to TGN membranes and interfere with secretory transport (Baron and Malhotra, 2002). Therefore, increased ceramide transfer from the ER to the TGN by overexpression of CERT should result in an elevated local
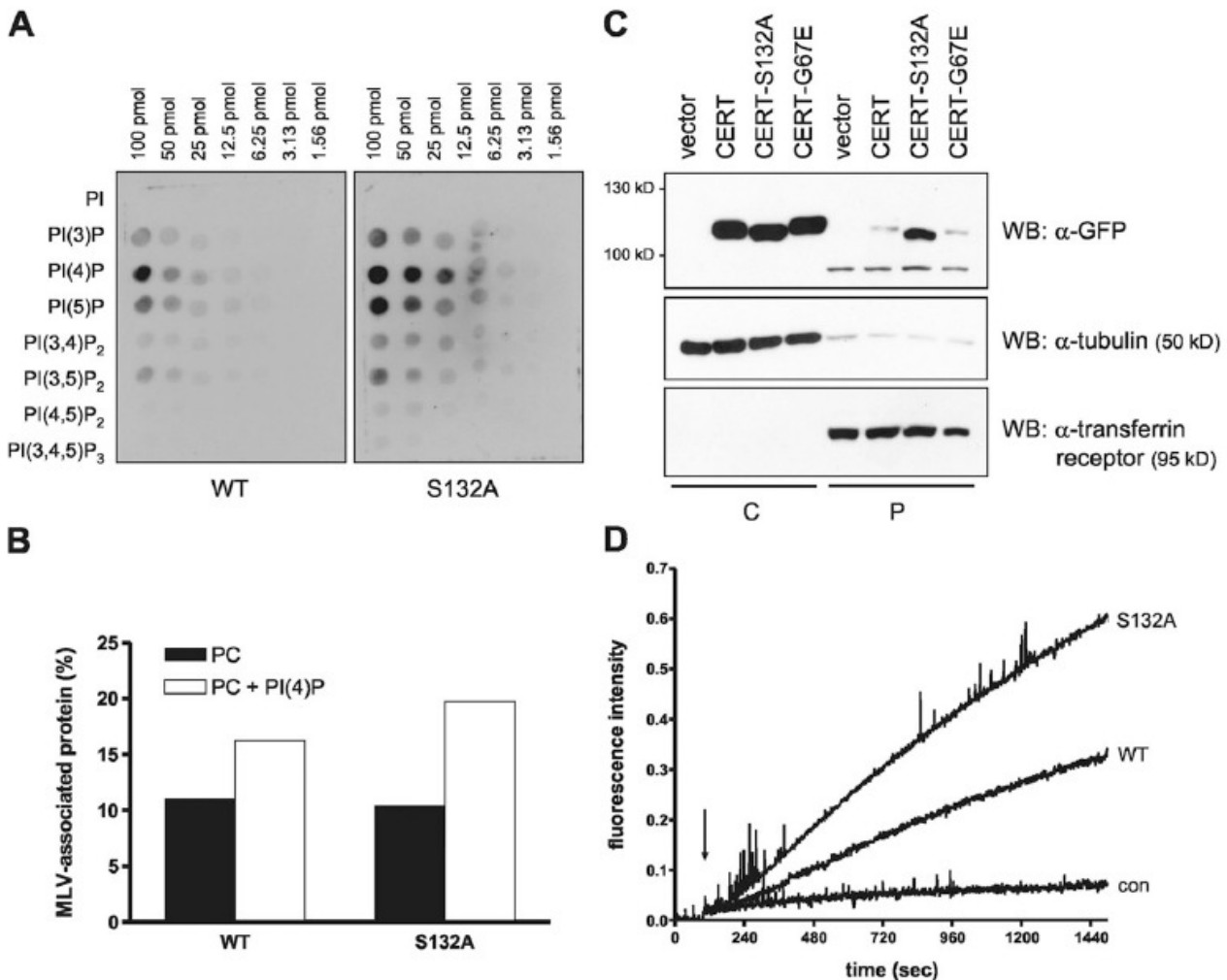

Fig. 3: CERT phosphorylation on serine 132 modulates PI(4)P binding and ceramide transfer activity. HEK293T cells transiently expressing the indicated GFP-tagged CERT variants were harvested by hypotonic lysis and the cytosol fraction was recovered after 100.000 x g centrifugation. Samples containing equal amounts of GFP fluorescence were used for (A) protein-lipid overlay, (B) flotation and (D) *in vitro* ceramide transfer assays. (A) PIP arrays were incubated with cytosol from cells transiently expressing GFP-tagged CERT-WT and -S132A and bound proteins were detected with GFP-specific primary, followed by HRP-labeled secondary antibody. (B) MLVs consisting of PC or PC + 5% PI(4)P were incubated with cytosol and then separated by centrifugation. The amount of CERT protein in top (MLV) and bottom fractions was quantified by measuring GFP fluorescence and set as 100%. Results are plotted as percentages of protein recovered in the MLV fraction. (C) Cytosol (C) and the 100.000 x g pellet (P) containing cellular membranes were analyzed by immunoblotting with GFP-specific antibody. The purity of the individual fractions was confirmed by detection of the transferrin receptor in the membrane and tubulin in the cytosolic fraction. (D) Donor liposomes containing TNP-PE and pyrene-ceramide were mixed with unlabeled acceptor liposomes. After 60 s, cytosol from cells transiently expressing GFP-tagged CERT-WT, -S132A, or GFP alone (con) was added and pyrene fluorescence at 395 nm was recorded.

DAG pool and may consequently stimulate PKD activity and secretory transport. To test this hypothesis, we transiently expressed CERT-WT and CERT-S132A in HEK293T cells and analyzed autophosphorylation of endogenous PKD. Compared to the control, expression of both CERT-WT and CERT-S132A increased PKD activity, as revealed by analyses with a phosphospecific PKD antibody (Fig. 4A). CERT has been reported to possess kinase activity (Raya et al., 2000) making it possible that it activates PKD by direct phosphorylation. However, kinase assays clearly demonstrated that PKD is not phosphorylated by CERT. Moreover, a kinase activity was associated with the CERT protein only under mild detergent conditions (Fig. S1). Our results thus show that PKD activation is regulated by CERT proteins, most likely due to increased ceramide delivery and enforced SM/DAG synthesis. A similar function has recently been described for the lipid transfer protein Nir2 in the maintenance of DAG levels at the Golgi apparatus via regulation of the CDP-choline pathway (Litvak et al., 2005). RNAi-mediated knockdown of Nir2 decreased DAG and PKD levels at the Golgi complex and blocked secretory transport. Interestingly, this effect could be rescued by the addition of exogenous C_6-ceramide (Litvak et al., 2005), indicating a critical role for ceramide in DAG synthesis and PKD recruitment to the Golgi complex.

To address the question of whether CERT-mediated PKD activation indeed translated into enhanced secretory transport, we made use of a plasmid encoding horseradish peroxidase fused to a signal sequence (ss). The fusion protein ssHRP can be used as a reporter for constitutive protein secretion (Bard et al., 2006). In control cells, secretion of ssHRP could be detected within 1 h and increased over time (Fig. 4B). Coexpression of PKD1-KD, which inhibits secretory transport of cargo protein (Liljedahl et al., 2001;Hausser et al., 2005), almost entirely abrogated ssHRP secretion. This confirmed that HRP was secreted in a PKD-dependent manner in our assay. Coexpression of CERT-WT and CERT-S132A strongly augmented the amount of secreted HRP (Fig. 4B). Conversely, knockdown of CERT by RNAi in COS7 cells, inhibited secretion of HRP (Fig. 4C, D), confirming the essential role for CERT in constitutive exocytosis of cargo proteins. We could only detect a slight increase in secretion with the S132A mutant compared to the one observed with the wild type protein. This is in accordance with the comparable activation of PKD by CERT-WT and CERT-S132A (Fig. 4A), but was unexpected in the light of the significantly enhanced *in vitro* lipid transfer activity of the CERT mutant (Fig. 3C). However, increased levels of ceramide may not necessarily translate into equivalent increases in DAG, because DAG synthesis might be limited by the availability of PC and the activity of SM synthase. Accumulation of ceramide is known to affect Golgi membrane stability and induces vesicle fission (Weigert et al., 1999;Fukunaga et al., 2000). We therefore investigated whether overexpression of the CERT-S132A mutant affected its localization and/or caused morphological changes of the Golgi apparatus. In addition to concentrating in GS28-positive regions of the Golgi complex, the CERT-S132A mutant displayed a dispersed, punctate staining (Fig. 5A). However, the distribution of GS28 itself and that of TGN46 was not affected by expression of CERT-S132A, nor were these

proteins present in the vesicular structures observed with the mutant CERT protein (Fig. 5A). This rules out fragmentation of the Golgi apparatus as a consequence of CERT-S132A overexpression. Some of the vesicular structures were found to contain the cargo protein ssHRP, providing evidence that these structures represent Golgi-derived transport carriers (Fig. 5A). It thus appears that the increased membrane affinity of CERT-S132A prevents its dissociation from budding vesicles. Interestingly, when coexpressed with CERT-S132A, the PH domain of OSBP also localized to these vesicles, indicating that these structures are PI(4)P positive (Fig. 5B). The CERT-S132A mutant may therefore inhibit PI(4)P turnover, thus stabilizing the lipid on transport
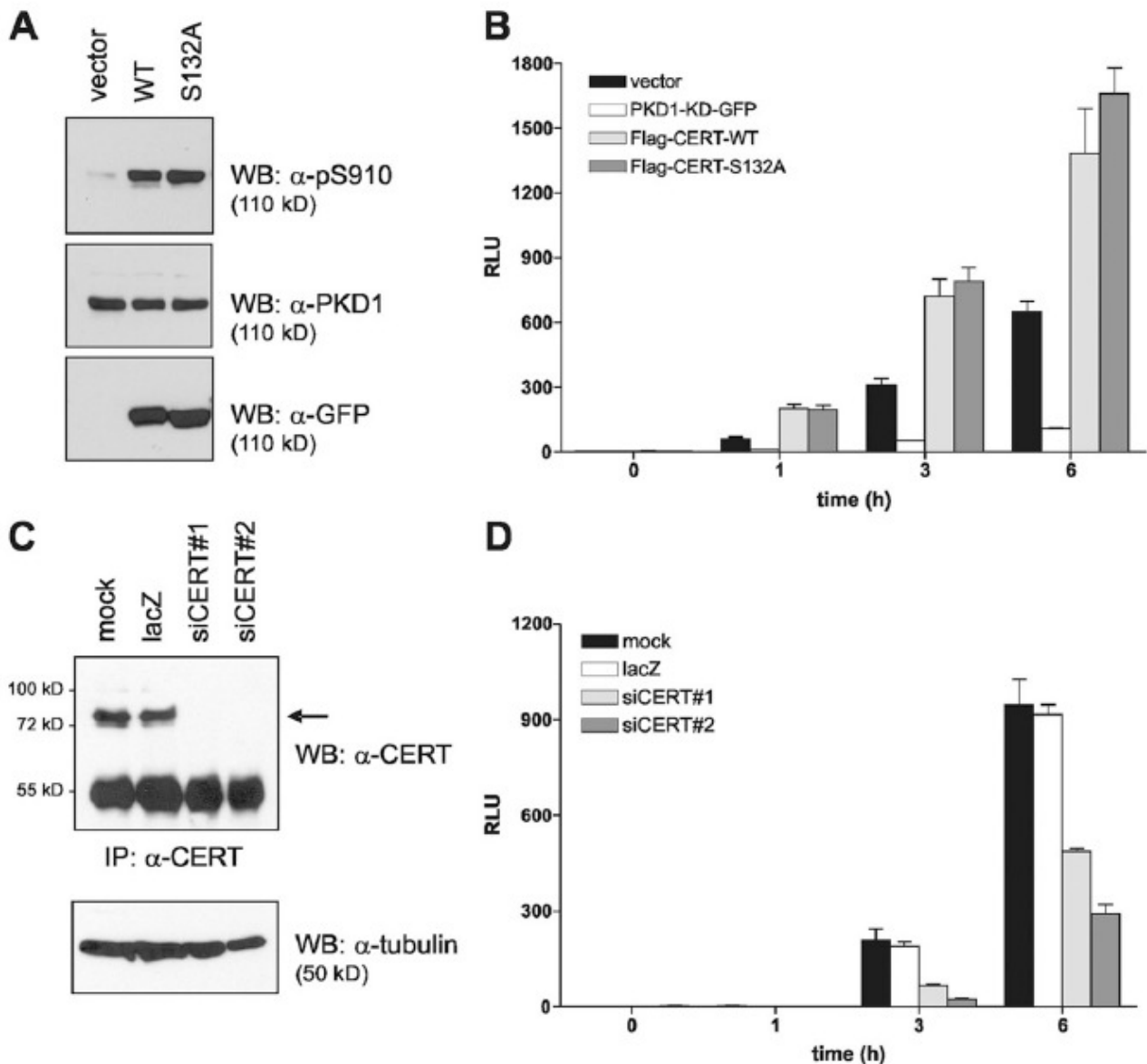

Fig. 4: CERT regulates PKD activation and secretory transport. (A) HEK293T cells were transiently expressing CERT-WT and -S132A were lysed and PKD activation was analyzed by immunoblotting with pS910 PKD antibody (top). Equal loading was verified by reprobing with PKD1-specific antibody (middle). Expression of CERT proteins was verified by immunoblotting with GFP-specific antibody (bottom). (B, D) HEK293T were transfected with indicated expression plasmids (B) and COS7 cells with indicated siRNAs (D) together with ssHRP-Flag plasmid as described in the methods section. The medium was analyzed for HRP activity after 0, 1, 3, and 6 h by chemiluminescence. Values correspond to the mean of triplicate samples and error bars represent SEM. RLU, relative light units. (C) COS7 cells were transfected with the siRNAs indicated and CERT expression was analyzed after 72 h by immunoprecipitaton and Western blotting using a CERT-specific antibody (top). Tubulin levels were not affected (bottom).

carriers. Of note, a CERT-S132E protein was undistinguishable from the alanine mutant in terms of cellular localization and thus could not be used to mimic the phosphorylated state (data not shown).
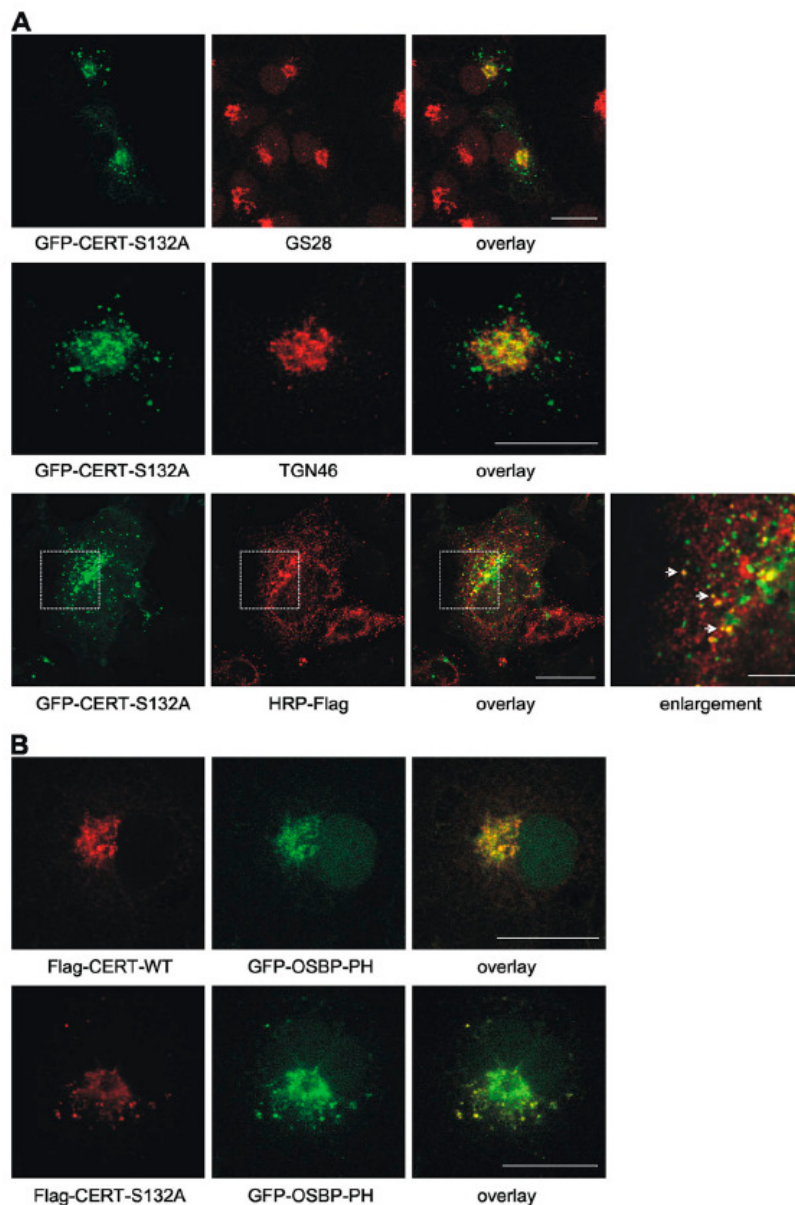

Fig. 5: CERT-S132A localizes to PI(4)P-positive secretory vesicles. (A, B) COS7 cells were transiently transfected with the indicated expression plasmids. Cells were fixed and stained with GS28- (red) (A, top), TGN46- (red) (A, middle), and Flag-specific antibodies (red) (A, bottom and B). Scale bar, 20 µm and 5 µm (enlargement).

Taken together, our data support the following working model: PKD is recruited to the TGN by a local DAG pool that can be generated via different metabolic pathways. PKD then activates PI4KIIIβ, increasing PI(4)P levels at the TGN. This, in turn, recruits the CERT protein to the Golgi complex where it contributes to PKD activation and vesicular transport processes by providing ceramide as a precursor for further DAG production. The system is tightly regulated by a negative feedback loop: Active PKD phosphorylates CERT at serine 132, thus decreasing the affinity of CERT towards its lipid target PI(4)P to ensure continuous rounds of lipid transfer from the ER to the Golgi compartment. In conclusion, we have identified CERT as a PKD substrate and provide evidence for a novel relationship between membrane lipid biogenesis and protein secretion.

Materials and methods

Antibodies and reagents, DNA constructs, and cell culture and transfection

see Supplementary Information.

Immunofluorescence microscopy

Cells were fixed in 4% PFA for 10 min, washed and incubated with PBS containing 0.1 M glycine for 15 min. Cells were permeabilized with PBS containing 0.1% Triton for 5 min and blocked with 5% goat serum in PBS containing 0.1% Tween-20 for 30 min. Cells were then incubated with primary antibody diluted in blocking buffer for 2 h, followed by incubation with secondary antibodies diluted in blocking buffer for 1 h. Coverslips were mounted in Fluoromount G (Southern Biotechnology) and analyzed on a confocal laser scanning microscope (TCS SL, Leica) using 488 and 543 nm excitation and a 40.0/1.25 HCX PL APO objective lens. Images were processed with Adobe Photoshop. All images shown are stacks of several confocal sections.

Protein extraction, immunoprecipitation and Western blotting

Whole cell extracts were obtained by solubilizing cells in NP40 extraction buffer (NEB) [50 mM Tris (pH 7.5), 150 mM NaCl, 1% NP40, 1 mM sodium orthovanadate, 10 mM sodium fluoride, and 20 mM β-glycerophosphate plus Complete protease inhibitors (Roche)]. Lysates were clarified by centrifugation at 16,000 x g for 10 min. For immunoprecipitations, equal amounts of protein were incubated with specific antibodies for 2 h on ice. Immune complexes were collected with protein G-Sepharose (GE Healthcare) and washed 3x with NEB. Whole cell extracts or immunoprecipitated proteins were subjected to SDS-PAGE and proteins were blotted onto PVDF membranes (Roth). After blocking with 0.5% blocking reagent (Roche) in PBS containing 0.1% Tween 20, filters were probed with specific antibodies. Proteins were visualized with HRP-coupled secondary antibody using the ECL system (Pierce). Stripping of membranes was performed in 62.5 mM Tris (pH 6.8), 2% SDS, and 100 mM β-mercaptoethanol for 30 min at 60°C. Membranes were then reprobed with the indicated antibodies.

Recombinant protein purification and *in vitro* kinase assays

BL21 bacteria were transformed with pGEX6P-Flag-CERT-WT(1-138) and -S132A(1-138) vectors. Expression was induced with 0.5 mM IPTG for 4 h at 30°C. Bacteria were harvested and resuspended in PBS containing 50 µg/ml lysozyme, Complete protease inhibitors, 10 mM sodium fluoride and 20 mM β-glycerophosphate. Triton X-100 was added to a final concentration of 1% prior to sonication. GST-CERT fusions were purified from clarified lysate with glutathione resin (GE Healthcare). Recombinant proteins were incubated with purified PKD1 from insect cells in kinase buffer [50 mM Tris, pH 7.5, 10 mM MgCl$_2$ and 1 mM DTT] in the presence of either 2 µCi [γ-^{32}P]-ATP or 75 µM cold ATP for 30 min. Samples were resolved by SDS-PAGE, blotted onto

membrane and analyzed on a PhosphoImager (Molecular Dynamics) and detected with the indicated antibodies.

Cellular fractionation

Cells were harvested in hypotonic buffer [50 mM Tris, pH 7.4, containing Complete protease inhibitors, 1 mM PMSF, 5 mM β-glycerophosphate and 5 mM sodium fluoride] and sheared by passage through a 25G/16 mm gauge needle. Nuclei were removed by centrifugation at 500 x g and cytosol (C) and membrane fractions (P) were obtained by 100.000 x g centrifugation.

PIP arrays, flotation and ceramide transfer assays

The amount of expressed CERT protein in the cytosolic fraction was quantified by GFP peak emission at 480 - 550 nm (excitation 466 nm). PIP arrays (Echelon) were blocked in TBS-T [10 mM Tris, pH 8, 150 mM NaCl, 0.1 % Tween-20] containing 3 % fatty acid-free BSA (Roth), followed by incubation with 500 µg cytosol containing equal amounts of GFP proteins in 5 ml blocking buffer for 1 h. Bound proteins were detected with anti-GFP antibody, followed by HRP-conjugated secondary antibody. Flotation assays were performed by incubating 50 µl cytosol containing equal amounts of GFP-tagged CERT proteins with 100 µl MLVs in 50 mM Tris, pH 7.5 and 50 mM NaCl buffer for 10 min at RT. The suspension was adjusted to 30% sucrose by addition of 100 µl 75% sucrose, overlayed with 200 µl 25% sucrose in buffer and 50 µl sucrose-free buffer. Samples were centrifuged at 240.000 x g for 1 h. The bottom (250 µl) and top (100 µl) fractions were collected and analyzed by fluorescence spectrometry. Protein-mediated transfer of ceramide between SUVs was measured as described previously (Olayioye et al., 2005). The transfer assay mixture contained donor vesicles (2 nmol lipid/ml) composed of brain lipids, pyrene-labeled C_{16}-ceramide, 2,4,6-trinitrophenyl-phosphatidylethanolamine (TNP-PE) (provided by Pentti Somerharju, University of Helsinki, Finland) (88.6:0.4:11 mol %), and a 10-fold excess of acceptor vesicles composed of brain lipids. Fluorescence intensity was recorded at 395 nm (excitation, 345 nm; slit widths, 4 nm) before and after the addition of 75 µg cytosol from HEK293T cells transiently expressing GFP-tagged CERT-WT and -S132A. Fluorescence intensities were normalized to the maximum intensity obtained after addition of 0.5 % Triton X-100 and the maximum GFP fluorescence, to account for different protein expression levels.

Secretion assay

HEK293T cells were cotransfected with ssHRP-Flag plasmid and empty vector, pEGFPN1-PKD1-KD, pcDNA3-Flag-CERT-WT and -S132A at a ratio of 1:6.5, respectively. For CERT RNAi, COS7 cells were transfected with ssHRP-Flag plasmid, harvested after 8 hrs, replated and transfected with siRNAs. HEK293T and COS7 cells were washed with serum-free medium 24 and 48 h post-transfection, respectively, and HRP secretion was quantified by incubation of clarified cell

supernatant with ECL reagent. Measurements were done with a luminometer (Lucy2, Anthos) at 450 nm.

Online supplemental material

Fig. S1 shows that CERT does not phosphorylate PKD directly. Fig. S2 shows colocalization of CERT-WT and GS28.

Acknowledgments

Abbreviations

PH, pleckstrin homology
START, steroidogenic acute regulatory lipid transfer
TGN, trans-Golgi network
PI(4)P, phosphatidylinositol 4-phosphate
SM, sphingomyelin
DAG, diacylglycerol
PKD, protein kinase D
PC, phosphatidylcholine
ER, endoplasmic reticulum

References

1.   Alpy, F. and C.Tomasetto. 2005. Give lipids a START: the StAR-related lipid transfer (START) domain in mammals. *J. Cell Sci.* 118:2791-2801.

2.   Bard, F., L.Casano, A.Mallabiabarrena, E.Wallace, K.Saito, H.Kitayama, G.Guizzunti, Y.Hu, F.Wendler, R.Dasgupta, N.Perrimon, and V.Malhotra. 2006. Functional genomics reveals genes involved in protein secretion and Golgi organization. *Nature* 439:604-607.

3.   Baron, C.L. and V.Malhotra. 2002. Role of diacylglycerol in PKD recruitment to the TGN and protein transport to the plasma membrane. *Science* 295:325-328.

4.   Diaz Anel, A.M. and V.Malhotra. 2005. PKCeta is required for beta1gamma2/beta3gamma2- and PKD-mediated transport to the cell surface and the organization of the Golgi apparatus. *J. Cell Biol.* 169:83-91.

5.   Doppler, H., P.Storz, J.Li, M.J.Comb, and A.Toker. 2005. A phosphorylation state-specific antibody recognizes Hsp27, a novel substrate of protein kinase D. *J. Biol. Chem.* 280:15013-15019.

6.   Fukunaga, T., M.Nagahama, K.Hatsuzawa, K.Tani, A.Yamamoto, and M.Tagaya. 2000. Implication of sphingolipid metabolism in the stability of the Golgi apparatus. *J. Cell Sci.* 113 (Pt 18):3299-3307.

7.   Hanada, K., K.Kumagai, S.Yasuda, Y.Miura, M.Kawano, M.Fukasawa, and M.Nishijima. 2003. Molecular machinery for non-vesicular trafficking of ceramide. *Nature* 426:803-809.

8.   Hausser, A., G.Link, L.Bamberg, A.Burzlaff, S.Lutz, K.Pfizenmaier, and F.J.Johannes. 2002. Structural requirements for localization and activation of protein kinase C mu (PKC mu) at the Golgi compartment. *J. Cell Biol.* 156:65-74.

9.   Hausser, A., P.Storz, S.Martens, G.Link, A.Toker, and K.Pfizenmaier. 2005. Protein kinase D regulates vesicular transport by phosphorylating and activating phosphatidylinositol-4 kinase IIIbeta at the Golgi complex. *Nat. Cell Biol.* 7:880-886.

10.   Iglesias, T., N.Cabrera-Poch, M.P.Mitchell, T.J.Naven, E.Rozengurt, and G.Schiavo. 2000. Identification and cloning of Kidins220, a novel neuronal substrate of protein kinase D. *J. Biol. Chem.* 275:40048-40056.

11.   Kawano, M., K.Kumagai, M.Nishijima, and K.Hanada. 2006. Efficient trafficking of ceramide from the endoplasmic reticulum to the Golgi apparatus requires a VAMP-associated protein-interacting FFAT motif of CERT. *J. Biol. Chem.* 281:30279-30288.

12.   Levine, T. and C.Loewen. 2006. Inter-organelle membrane contact sites: through a glass, darkly. *Curr. Opin. Cell Biol.* 18:371-378.

13.   Levine, T.P. and S.Munro. 2002. Targeting of Golgi-specific pleckstrin homology domains involves both PtdIns 4-kinase-dependent and -independent components. *Curr. Biol.* 12:695-704.

14.   Liljedahl, M., Y.Maeda, A.Colanzi, I.Ayala, J.Van Lint, and V.Malhotra. 2001. Protein kinase D regulates the fission of cell surface destined transport carriers from the trans-Golgi network. *Cell* 104:409-420.

15.   Litvak, V., N.Dahan, S.Ramachandran, H.Sabanay, and S.Lev. 2005. Maintenance of the diacylglycerol level in the Golgi apparatus by the Nir2 protein is critical for Golgi secretory function. *Nat. Cell Biol.* 7:225-234.

16.   Loewen, C.J., A.Roy, and T.P.Levine. 2003. A conserved ER targeting motif in three families of lipid binding proteins and in Opi1p binds VAP. *EMBO J.* 22:2025-2035.

17.   Maeda, Y., G.V.Beznoussenko, J.Van Lint, A.A.Mironov, and V.Malhotra. 2001. Recruitment of protein kinase D to the trans-Golgi network via the first cysteine-rich domain. *EMBO J.* 20:5982-5990.

18.   Olayioye, M.A., S.Vehring, P.Muller, A.Herrmann, J.Schiller, C.Thiele, G.J.Lindeman, J.E.Visvader, and T.Pomorski. 2005. StarD10, a START domain protein overexpressed in breast cancer, functions as a phospholipid transfer protein. *J. Biol. Chem.* 280:27436-27442.

19.   Perry, R.J. and N.D.Ridgway. 2005. Molecular mechanisms and regulation of ceramide transport. *Biochim. Biophys. Acta* 1734:220-234.

20.   Perry, R.J. and N.D.Ridgway. 2006. Oxysterol-binding protein and vesicle-associated membrane protein-associated protein are required for sterol-dependent activation of the ceramide transport protein. *Mol. Biol. Cell* 17:2604-2616.

21.   Raya, A., F.Revert-Ros, P.Martinez-Martinez, S.Navarro, E.Rosello, B.Vieites, F.Granero, J.Forteza, and J.Saus. 2000. Goodpasture antigen-binding protein, the kinase that phosphorylates the goodpasture antigen, is an alternatively spliced variant implicated in autoimmune pathogenesis. *J. Biol. Chem.* 275:40392-40399.

22.   Rykx, A., L.De Kimpe, S.Mikhalap, T.Vantus, T.Seufferlein, J.R.Vandenheede, and J.Van Lint. 2003. Protein kinase D: a family affair. *FEBS Lett.* 546:81-86.

23.   Soccio, R.E. and J.L.Breslow. 2003. StAR-related lipid transfer (START) proteins: mediators of intracellular lipid metabolism. *J. Biol. Chem.* 278:22183-22186.

24.   Somerharju, P. 2002. Pyrene-labeled lipids as tools in membrane biophysics and cell biology. *Chem. Phys. Lipids* 116:57-74.

25.   Toth, B., A.Balla, H.Ma, Z.A.Knight, K.M.Shokat, and T.Balla. 2006. Phosphatidylinositol 4-kinase IIIbeta regulates the transport of ceramide between the endoplasmic reticulum and Golgi. *J. Biol. Chem.*

26.   Vega, R.B., B.C.Harrison, E.Meadows, C.R.Roberts, P.J.Papst, E.N.Olson, and T.A.McKinsey. 2004. Protein kinases C and D mediate agonist-dependent cardiac hypertrophy through nuclear export of histone deacetylase 5. *Mol. Cell Biol.* 24:8374-8385.

27.   Wang, Q.J. 2006. PKD at the crossroads of DAG and PKC signaling. *Trends Pharmacol. Sci.* 27:317-323.

28.   Wang, Y., R.T.Waldron, A.Dhaka, A.Patel, M.M.Riley, E.Rozengurt, and J.Colicelli. 2002. The RAS effector RIN1 directly competes with RAF and is regulated by 14-3-3 proteins. *Mol. Cell Biol.* 22:916-926.

29.   Weigert, R., M.G.Silletta, S.Spano, G.Turacchio, C.Cericola, A.Colanzi, S.Senatore, R.Mancini, E.V.Polishchuk, M.Salmona, F.Facchiano, K.N.Burger, A.Mironov, A.Luini, and D.Corda. 1999. CtBP/BARS induces fission of Golgi membranes by acylating lysophosphatidic acid. *Nature* 402:429-433.

30.   Wirtz, K.W. 2006. Phospholipid transfer proteins in perspective. *FEBS Lett.* 580:5436-5441.

31.   Yeaman, C., M.I.Ayala, J.R.Wright, F.Bard, C.Bossard, A.Ang, Y.Maeda, T.Seufferlein, I.Mellman, W.J.Nelson, and V.Malhotra. 2004. Protein kinase D regulates basolateral membrane protein exit from trans-Golgi network. *Nat. Cell Biol.* 6:106-112.

7.3. Deleted in Liver Cancer 1 controls cell migration through a Dia1-dependent signaling pathway

Gerlinde Holeiter, Johanna Heering, Patrik Erlmann, Simone Schmid, Ruth Jähne, and Monilola A. Olayioye#

University of Stuttgart, Institute of Cell Biology and Immunology,

Allmandring 31, 70569 Stuttgart, Germany

Corresponding author:

Monilola A. Olayioye, Tel: +49 711 685 69301, Fax: + 49 711 685 67484

Email: monilola.olayioye@izi.uni-stuttgart.de

Abstract

Deleted in Liver Cancer (DLC) 1 and 2 are Rho GTPase activating proteins that are frequently downregulated in various types of cancer. Ectopic expression in carcinoma cell lines lacking these proteins has been shown to inhibit cell migration and invasion. However, whether the loss of DLC1 or DLC2 is the cause of aberrant Rho signaling in transformed cells has not been investigated. Here we have downregulated DLC1 and DLC2 expression in breast cancer cells using an RNA interference approach. Silencing of DLC1 led to the stabilization of stress fibers and focal adhesions and enhanced cell motility in wound healing as well as chemotactic transwell assays. We provide evidence that enhanced migration of cells lacking DLC1 is dependent upon the Rho effector protein Dia1 but does not require the activity of Rho kinase. By contrast, DLC2 knock-down failed to affect the migratory behavior of cells, suggesting that the two proteins have distinct functions. This is most likely due to their differential subcellular localizations, with DLC1 found in focal adhesions and DLC2 being mainly cytosolic. Collectively, our data demonstrate that DLC1 is critically involved in the control of Rho signaling and actin cytoskeleton remodeling and that its cellular loss is sufficient for the acquisition of a more migratory phenotype of breast cancer cells.

Introduction

Cell migration is a biological process involved in development, inflammation, wound healing, and tumor metastasis. The migration of cells is a multi-step cycle starting with the formation of membrane protrusions driven by actin polymerization at the cell front. These protrusions are anchored to the extracellular matrix by integrin receptors forming focal adhesions. The migratory cycle is continued by actomyosin-driven contraction of the cell body at the back and is completed by the subsequent detachment of the cell rear. Therefore, cell migration requires coordinated changes in cytoskeletal dynamics (1). The Rho GTPases Rho, Rac and Cdc42 are key players in the control of cell migration and have defined functions with regard to cytoskeletal remodeling. Active Rho is known to induce the assembly of stress fibers and focal adhesions, whereas Rac and Cdc42 promote the formation of specialized membrane protrusions called lamellipodia and filopodia, respectively (2,3).

Rho proteins cycle between an inactive GDP- and an active GTP-bound state. When bound to GTP, they interact with effector proteins, modulating their activity and localization. Signaling of growth factor receptors and integrins can induce exchange of GDP for GTP on Rho proteins. This activation of Rho proteins is controlled by the guanine nucleotide exchange factors (GEFs), which promote the release of bound GDP and facilitate GTP binding, and the GAP proteins, which increase the intrinsic GTPase activity of Rho GTPases to accelerate the return to the inactive state (2). The structurally related proteins DLC1 and DLC2 belong to the GAP family and display *in vitro* specificity for Rho and to a lesser extent for Cdc42 (4-6). In addition to their GAP domain, DLC1

and DLC2 further contain a sterile alpha motif (SAM) and a StAR-related lipid transfer (START) domain, which may have regulatory roles that remain to be defined.

The DLC1 gene was originally isolated as a candidate tumor suppressor gene in primary human hepatocellular carcinoma located on chromosome 8p22 (7). Loss of expression due to chromosomal deletion or promoter hypermethylation has subsequently been shown in other tumor types, including breast, colon, prostate, and lung (8). Transfection of the DLC1 cDNA into carcinoma cell lines lacking DLC1 expression inhibited cell growth and tumorigenicity in nude mice (9-12). Microinjection of rat DLC1 suppressed the formation of LPA-induced stress fibers and focal adhesions (13). Furthermore, stable expression of human DLC1 in hepatocellular and breast carcinoma cell lines was shown to reduce cell motility and invasiveness, consistent with the inhibition of Rho signaling (14,15). The DLC2 gene whose expression is similarly downregulated in various tumor types is located on chromosome 13q13 and encodes a protein that is approximately 60% identical to DLC1 (5). Reminiscent of DLC1, cellular re-expression disrupted the actin cytoskeleton and inhibited cell proliferation and migration (16). It thus appears that DLC1 and DLC2 may be functionally redundant in suppressing Rho signaling and Rho-mediated cellular processes.

Rho is known to be required for Ras-mediated oncogenic transformation and activated mutants were shown to be weakly transforming in murine fibroblasts (17,18). However, no constitutively active Rho mutants have been identified in human tumors, instead Rho proteins are rather found to be overexpressed. In mammalian cells, there are three structurally related Rho proteins, RhoA, B and C. In breast cancer and testicular germ-cell tumors, RhoA expression levels correlated positively with the tumor stage (19,20), and overexpression of RhoC was shown to be causally linked to inflammatory breast cancers (21). In *in vivo* models of tumor dissemination, RhoC has been identified to enhance the metastatic potential of melanoma cells (22).

An alternative mechanism by which Rho activation can be achieved is the deregulation of GEFs or the loss of its GAPs. In this study we analyzed the consequences of DLC1 and DLC2 knock-down at the molecular and cellular level. We show that silencing of DLC1 in breast cancer cells augments cellular RhoA levels and enhances cell motility, whereas downregulation of DLC2 had no effect on the migratory behavior of cells. Our results further shed light onto the underlying molecular mechanisms by identifying Dia1 as the Rho effector involved in DLC1-mediated control of breast cancer cell migration.

Material and methods

Antibodies and reagents

Antibodies used were: mouse anti-DLC1, mouse anti-Dia1 and mouse anti-paxillin mAbs (BD), mouse anti-RhoA mAb, rabbit anti-RhoA (119) pAb, rabbit anti-Cdc42 pAb and goat anti-Dia1 pAb

(Santa Cruz Biotechnology), and mouse anti-tubulin mAb (Sigma). The anti-DLC2 antiserum was raised by immunizing rabbits with DLC2-peptide (C-[373]TALPDAGDQSRMHEFH[388]) coupled to keyhole limpet hemocyanin (Pineda, Germany). Antibodies were affinity purified with the Sulfolink Immobilization Kit for Peptides (Pierce). Elution was with 100 mM glycine buffer, pH 2.7, and neutralized antibody fractions were pooled and dialyzed against PBS. HRP-labeled secondary anti-mouse and anti-rabbit IgG antibodies were from GE Healthcare; HRP-labeled secondary anti-goat IgG antibody was from Santa Cruz Biotechnology; Alexa Fluor 488- and 546-labeled secondary anti-mouse IgG antibodies, Alexa Fluor 546-labeled phalloidin were from Molecular Probes. The ROCK inhibitors Y27632 and H1152 were from Calbiochem.

DNA cloning

pCS2+MT-DLC1 and pEGFPC1-DLC2α were kindly provided by I. Ng (University of Hongkong). The full-length DLC1 cDNA was amplified by PCR using pCS2+MT-DLC1 as a template with primers containing BamHI restriction sites (DLC1-minusATG-F: 5'-CGC GGA TCC TGC AGA AAG AAG CCG GAC CC-3' and DLC1-STOP-R: 5'- CGC GGA TCC TCA CCT AGA TTT GGT GTC TTT GG-3') and (DLC1-ATG-F: 5'-CGC GGA TCC ACC ATG TGC AGA AAG AAG CCG GAC ACC-3' and DLC1-minusSTOP-R: 5'-CGC GGA TCC CTA GAT TTG GTG TCT TTG GTT TC -3′), and cloned into pEGFPC1 and pEGFPN1 vectors, respectively (Clontech). Full-length DLC cDNAs were subcloned by BamHI restriction (for DLC1) into the pmCherryN1 vector and by HindIII restriction (for DLC2) into the pmCherryC1 vector (Clontech). DLC1-K714E was generated by QuikChange site-directed PCR mutagenesis (Stratagene). The forward primer used was: DLC1-K714E-for (5'-CGT GGC AGA CAT GCT GGA GCA GTA TTT TCG AG-3'). All amplified cDNAs were verified by sequencing. Oligonucleotides were purchased from MWG Biotech.

Cell culture and transfection

Cell lines used were cultured in DMEM or RPMI media (Invitrogen) supplemented with 10% FCS (PAA) in a humidified atmosphere of 5% CO_2 at 37°C. HEK293T cells were transfected with TransIT (Mirus) and MCF7 cells with Lipofectamine 2000 and, for RNAi, with Oligofectamine (Invitrogen). The siRNAs used were: 5'-GGA CAC GGU GUU CUA CAU C dTdT-3' (siDLC1); 5'-CCA AGG CAC UUU CUA UUG A dTdT-3' (siDLC2); 5'-GCU GGU CAG AGC CAU GGA U dTdT-3' (siDia1); 5'-GCG GCU GCC GGA AUU UAC C dTdT-3' (siLacZ). Independent control siRNAs used were: 5'-UUA AGA ACC UGG AGG ACU A dTdT-3' (siDLC1#2); 5'-GCU CUC CAC GAG UCA UAC A dTdT-3' (siDLC2#2); 5'-GAA GUU GUC UGU UGA AGA A dTdT-3' (siDia1#2). RhoA-, RhoC- and Cdc42-specific siRNAs have been described previously (23,24). All siRNAs were obtained from MWG Biotech.

Semi-quantitative RT-PCR

RNA was extracted using the PureLink™ Micro-to-Midi™ Total RNA Purification System (Invitrogen) and reverse transcribed into cDNA using a First Strand cDNA Synthesis Kit with random hexamer primers (Fermentas). The cDNA was then used as a template for PCR analysis with REDTaq PCR Master Mix (Sigma). Primers used were: DLC1-137F (5'-TGG TCA AGA GAG AGC ATG AT-3') and DLC1-643R (5'-TGA AGC TGA AGC TGG ACA GT-3'); DLC2-376F (5'-CAA AGG AAA AAG GGT GAC GA-3') and DLC2-1282R (5'-TCC TCC AAT TAA CCC CAT TG-3') or DLC2-2021F (5'-AGC CCC TGC CTC AAA GTA TT-3') and DLC2-2423R (5'-ATG GGC GTC ATC TGA TTC TC-3'); GAPDH-F (5'-CCC CTT CAT TGA CCT CAA CTA-3') and GAPDH-R (5'-CGC TCC TGG AAG ATG GTG AT-3').

Cell lysis, SDS-PAGE and Western Blotting

Cells were lysed in RIPA buffer [50 mM Tris (pH 7.5), 150 mM NaCl, 1% NP-40, 0.5% sodium deoxycholate, 0.1% SDS, 1 mM sodium orthovanadate, 10 mM sodium fluoride, and 20 mM β-glycerophosphate plus Complete protease inhibitors (Roche)]. Lysates were clarified by centrifugation at 16,000 x g for 10 min. Equal amounts of protein were separated by SDS-PAGE and transferred to PVDF membrane (Roth). The membrane was blocked with 0,5% blocking reagent (Roche) in PBS containing 0.1% Tween-20 and then incubated with primary antibodies, followed by HRP-conjugated secondary antibodies. Visualization was with the ECL detection system (Pierce).

RBD pulldowns

BL21 bacteria were transformed with a pGEX vector encoding the RBD of rhotekin and expression was induced with 0.1 mM isopropyl-β-D-1-thiogalactopyranoside for 4 h at 37°C. Bacteria were harvested, resuspended in PBS containing Complete protease inhibitors and sonicated. Triton X-100 was added (1% final) and the lysate centrifuged for 10 min at 8,000 x g. GST-RBD was purified with glutathione resin (GE Healthcare). For pulldowns, cells were lysed in RBD extraction buffer [50 mM Tris (pH 7.5), 500 mM NaCl, 10 mM MgCl$_2$, 1% Triton X-100, 1 mM sodium orthovanadate, 10 mM sodium fluoride, 20 mM β-glycerophosphate, 0,5 mM PMSF plus Complete protease inhibitors without EDTA (Roche)]. Equal amounts of cleared lysates were incubated with GST-RBD beads for 45 min at 4 °C. Beads were washed with RBD extraction buffer, bound proteins were separated by SDS–PAGE and RhoA was analyzed by immunoblotting.

Immunofluorescence microscopy

Cells grown on glass coverslips coated with 25 μg/ml collagen (Serva) were fixed with 4% PFA for 10 min, permeabilized with PBS containing 0.1% Triton X-100 for 5 min and blocked with 5% goat serum in PBS containing 0.1% Tween-20 for 30 min. Cells were incubated with primary antibody in blocking buffer for 2 h, followed by incubation with secondary antibody in blocking buffer for 1 h. To

analyze cytoskeletal structures in cells lacking DLC1 or DLC2 (Fig. 3A), cells were simultaneously fixed and permeabilized with 4% PFA in PBS containing 0.1% Triton X-100 for 10 min. Paxillin staining was done as described above. F-actin was stained with Alexa Fluor 546-conjugated phalloidin for 20 min prior to mounting of coverslips in Fluoromount G (Southern Biotechnology). Cells were analyzed on a confocal laser scanning microscope (TCS SL, Leica) using 488, 543 and 561 nm excitation and a 40.0/1.25 HCX PL APO oil objective lens. Images were processed with Adobe Photoshop.

Cell migration assays

Transwells (8.0-µm; Costar) were coated with 2,5 µg/ml collagen and 10^5 cells in 100 µl medium with 0,5% FCS were added to the top chamber and allowed to migrate over night (MCF7) or for 4 h (MDA-MB 436). The bottom chamber was supplemented with 10% FCS. Cells on the upper side of the membranes were removed using a cotton swab and cells on the underside were fixed in 4% PFA and stained with 0.1% crystal violet. Cells were counted in 5 independent microscopic fields at a 20-fold magnification. Experiments were performed in duplicate and repeated at least three times. In the case of Rho kinase inhibition, 10 µM Y-27632 or 1 µM H-1152 were added to cells in the top chamber.

Wound healing assays

MCF7 cells (6 x 10^5) were seeded into collagen-coated (25 µg/ml) 12-well dishes. The next day, confluent cell monolayers were wounded with a micropipette tip and plates were returned to the tissue culture incubator. For quantification, images at the beginning and after 14 h and 24 h were captured and the wound width of three defined positions was determined.

Rho biosensor assays

HEK293T cells transiently expressing the Raichu-RhoA biosensor and pmCherry-DLC constructs were lysed in 50 mM Tris pH 7.5, 5 mM β-glycerophosphate, 5 mM sodium fluoride and 0.5% Triton X-100 and debris was removed by centrifugation at 16,000 x g for 10 min. Emission ratios (FRET/CFP) were determined by measuring CFP and YFP fluorescence after background subtraction at 475 and 530 nm, respectively, using a Tecan Infinite 200M plate reader (excitation = 433 nm). Expression of the DLC proteins was controlled by measuring mCherry emission at 615 nm (excitation 575 nm).

Luciferase reporter assays

HEK293T cells were grown on collagen-coated 24-well dishes (2.5 µg/ml) and transfected with 50 ng 3DA-Luc firefly luciferase reporter containing three SRF binding elements, 50 ng Renilla luciferase plasmid and 25 ng of the respective DLC plasmids. After serum starvation over night, cells were stimulated with 15% serum for 6 h. Cells were lysed with 300 µl passive lysis buffer (Promega) and luciferase activities in 10 µl lysate were measured by addition of 50 µl firefly

substrate [470 µM D-luciferin, 530 µM ATP, 270 µM coenzyme A, 33 mM DTT, 20 mM Tricine, 2,67 mM $MgSO_4$, 01 mM EDTA, pH 7,8], followed by addition of 100 µl Renilla substrate [0,7 µM coelenterazine, 2,2 mM Na_2EDTA, 0,44 mg/ml bovine serum albumin, 1,1 M NaCl, 1,3 mM NaN_3, 0.22 M potassium phosphate buffer, pH 5,0]. Luminescence was measured with a Tecan Infinite 200M plate reader. DLC protein expression was verified by measuring GFP fluorescence of the lysates.

Results

DLC1 and DLC2 inhibit Rho signaling in intact cells

DLC1 and DLC2 have been reported to possess the same substrate selectivity *in vitro*, with GAP activity being most pronounced for RhoA and lower activity towards Cdc42 (5,6). In intact cells, substrate specificity of these GAP proteins may depend on additional factors and has not been compared thus far. To do so, we made use of a genetically encoded fluorescence resonance energy transfer (FRET)-based RhoA biosensor, termed Raichu-RhoA (25). This sensor consists of RhoA, the Rho binding domain (RBD) of the effector PKN and the fluorescence donor-acceptor pair CFP and YFP. Upon activation by GTP loading, the RBD binds RhoA, modifying the orientation of the fusion protein and allowing FRET to occur. Since RhoA activation is approximated to be proportional to the ratio of FRET/CFP emission, the activity of GAP proteins
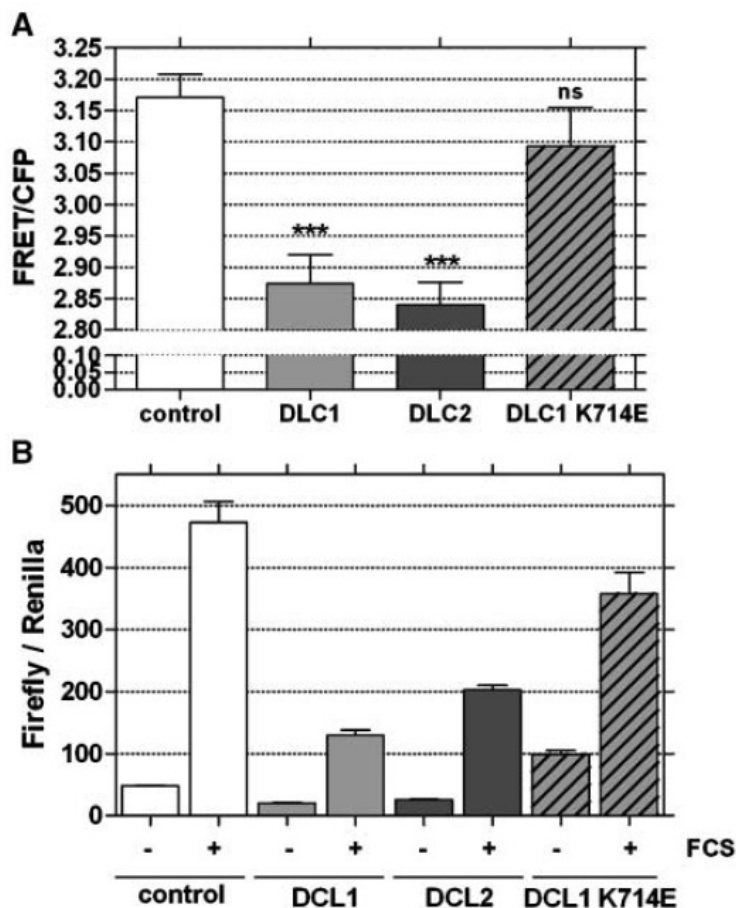

Figure 1: DLC1 and DLC2 inhibit Rho signaling in intact cells. (A) HEK293T cells were cotransfected with plasmids encoding the Raichu-RhoA biosensor and Cherry-DLC1, -DLC1-K714E, -DLC2 or empty vector (control). The next day, the emission ratio of Raichu-RhoA was determined by measuring YFP (FRET) and CFP fluorescence (excitation 433 nm) in cell lysates. The mean of four independent experiments performed with triplicate samples is shown; error bars represent SEM. Values for DLC1 and DLC2 versus the control were statistically significant (two-tailed unpaired t-test, p < 0.0001), whereas those for DLC1 K714E were not significantly different (ns, p = 0,287). (B) HEK293T cells were transfected with the SRF-responsive 3DA.Luc firefly luciferase reporter along with plasmids encoding Renilla luciferase and GFP-DLC1, -DLC1-K714E, -DLC2 or empty vector (control), starved over night and then either left unstimulated (-) or stimulated with FCS (+) for 6 hrs. Firefly luciferase activity in cell lysates of triplicate samples was determined and normalized by Renilla luciferase activity. The data correspond to one representative experiment out of three.

expressed along with the biosensor can be measured. As shown in Figure 1A, cotransfection of Raichu-RhoA with expression plasmids encoding DLC1 and DLC2 into HEK293T cells led to a decrease in the emission ratio, indicating that both proteins increase RhoA-GTP hydrolysis *in vivo* (Fig. 1A). This can be attributed to the GAP activity of the proteins because an inactive DLC1 variant harboring a point mutation in its GAP domain (DLC1 K714E) only had a minimal effect on the emission ratio of the biosensor (Fig. 1A), as did a DLC2 GAP-inactive mutant (data not shown). Although DLC1 and DLC2 displayed activity for Cdc42 *in vitro,* we did not observe an effect on the emission ratio of a Raichu-Cdc42 biosensor coexpressed in HEK293T cells (Supplementary Fig. 4C).

To address the question how the two DLC proteins modulate endogenous Rho signaling we further analyzed their ability to block serum response factor (SRF)-dependent transcription, which is known to require functional Rho (26). HEK293T cells were transfected with a SRF-responsive luciferase reporter along with DLC1 or DLC2 expression plasmids, starved over night and then restimulated with serum. As shown in Figure 1B, both DLC1 and DLC2 wild type proteins suppressed SRF-dependent transcription in a similar fashion, whereas DLC1 K714E only slightly reduced serum-induced luciferase reporter levels. These results are in accordance with those obtained with the RhoA biosensor and demonstrate that both DLC1 and DLC2 target Rho in intact cells.

DLC1 and DLC2 knock-down increases cellular RhoA-GTP levels

DLC1 and DLC2 are thought to act as tumor suppressors by antagonizing Rho signaling based on the fact that ectopic expression in carcinoma cell lines lacking these proteins reduces Rho-GTP levels and Rho-mediated cellular processes, such as cell migration and invasion (5,14). However, whether the absence of DLC1 and DLC2 really impacts on Rho activity and associated cellular events has not been investigated, nor is it clear whether these GAP proteins have redundant functions. To mimic the loss of DLC1 and DLC2 we therefore used an RNAi approach in cancer cells that express both genes and compared the molecular and cellular consequences. To first select appropriate cell lines, we examined expression of the DLC1 and DLC2 genes in a panel of breast cancer cell lines by semi-quantitative RT-PCR (Fig. 2A). In most of the cell lines, transcripts specific for both DLC genes could be detected. While DLC1 was absent in a subset of the cell lines, DLC2 was more uniformly expressed. The MCF7 cell line was chosen for further studies, since these cells express both genes and can be transfected at high efficiency with siRNAs as tested with a fluorescently labeled control siRNA (data not shown). Specific siRNAs were designed for DLC1 and DLC2 and silencing efficiency was verified by semi-quantitative RT-PCR (Fig. 2B). Downregulation of the individual transcripts was observed by 48 h post transfection and persisted for at least 96 h. The siRNAs were found to be selective as knock-down of DLC1 did not effect DLC2 transcript levels and vice versa, in comparison to the siLacZ control (Fig. 2B). Specific downregulation of the DLC1 protein was further verified by immunoblotting (Fig. 2C). Due to the

lack of a commercially available antibody for DLC2, we raised a polyclonal DLC2 peptide antibody, which specifically detected the overexpressed protein in Western blots (data not shown). Due to the presence of non-specific bands, the DLC2 protein could not be visualized in MCF7 cells, but specific siRNA-mediated DLC2 downregulation could be observed in MDA-MB 436 cells (see Fig. 5D).
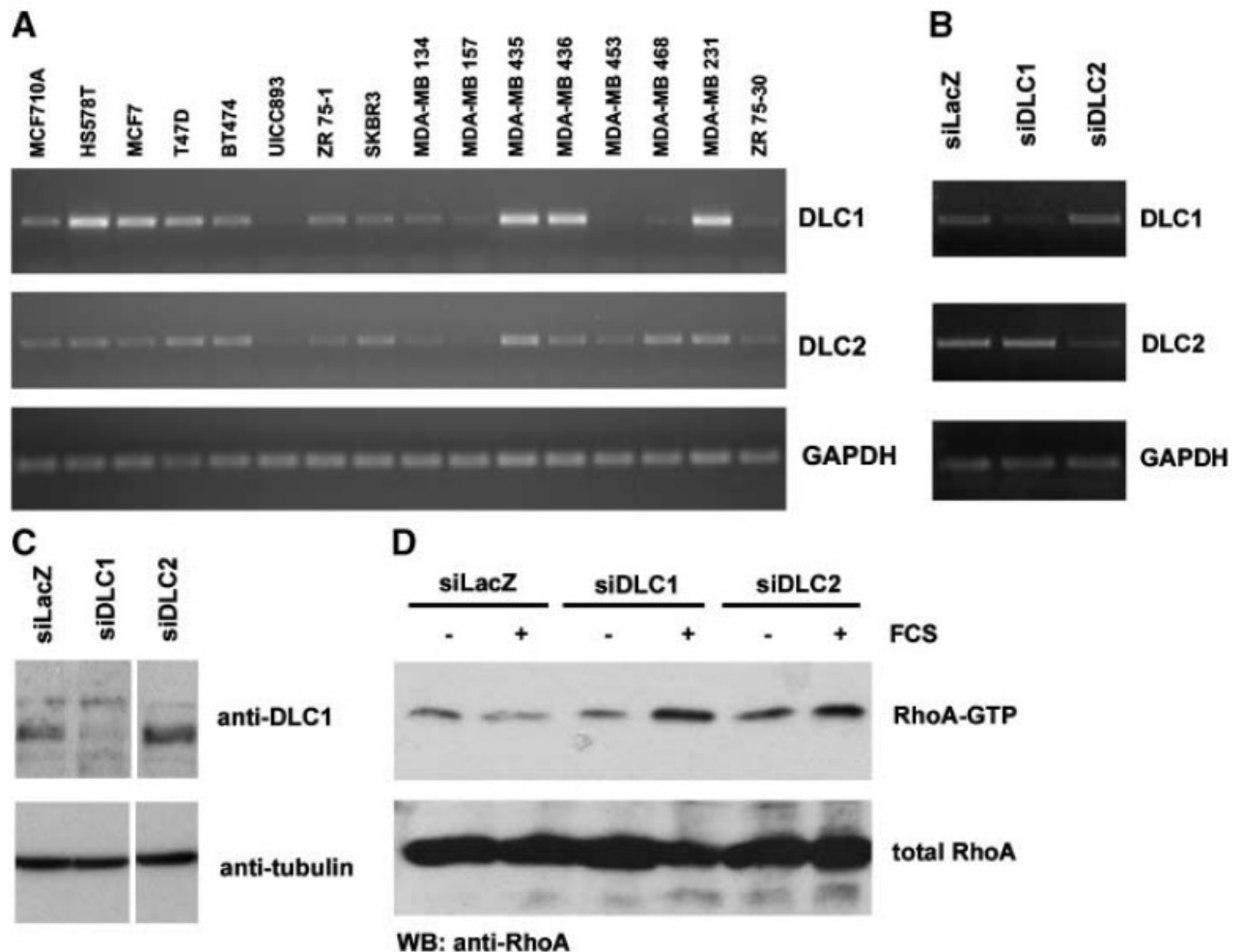

Figure 2: DLC1 and DLC2 knock-down increases cellular RhoA-GTP levels. (A) Semi-quantitative RT-PCR analysis of DLC1 and DLC2 genes. cDNA from the breast epithelial cell lines indicated was amplified using specific primers that span introns in the genomic sequence. GAPDH was amplified as a loading control. (B, C) MCF7 cells were transiently transfected with DLC1- or DLC2-specific siRNAs and, three days post transfection, DLC expression was evaluated by semi-quantitative RT-PCR (B) or by Western blotting (C). Cells transfected with a LacZ-specific siRNA were used as a negative control. (C) Equal amounts of total cell lysates were subjected to SDS-PAGE, transferred to membrane and DLC1 expression was analyzed by immunoblotting using a DLC1-specific antibody (top panel). Equal loading was verified by reprobing the membrane with tubulin-specific antibody (bottom panel). The lanes shown are from the same membrane. (D) MCF7 cells were transiently transfected with siRNAs specific for DLC1 and DLC2, or with LacZ-specific control siRNA. Three days post transfection, cells were starved in serum-free media for 24h and then either left untreated (-) or restimulated with 20% FCS for 5 min (+). RhoA-GTP was precipitated by incubation of total cell lysates with GST-RBD coupled to glutathione beads. Bound proteins were separated by SDS-PAGE and analyzed by Western blotting with RhoA-specific monoclonal antibody (top panel). Total RhoA levels were determined by immunoblotting of cell lysates with RhoA-specific antibody (bottom panel).

We then analyzed RhoA-GTP levels in MCF7 cells lacking DLC1 or DLC2 by GST pulldown assays with the RBD of rhotekin. Cells were transfected with DLC1- and DLC2-specific siRNAs, respectively, starved and then restimulated with serum for 5 min (Fig. 2D). Downregulation of both DLC1 and DLC2 enhanced serum-induced RhoA-GTP levels compared to the control, suggesting that both proteins indeed reduce the amount of active RhoA. This is consistent with the fact that overexpression of both DLC1 and DLC2 target RhoA in intact cells (see Fig. 1).

DLC1 depletion enhances stress fiber formation and focal adhesion assembly

Overexpression of DLC1 and DLC2 has been shown to cause cell detachment associated with the disassembly of stress fibers and focal adhesions (13,14). To investigate whether the loss of endogenous DLC proteins influences the architecture of the actin cytoskeleton, we analyzed the structure of focal adhesions and stress fibers in siRNA-transfected MCF7 cells. To this end, MCF7 cells lacking DLC1 and DLC2 were stained with a paxillin-specific antibody and phalloidin to visualize focal adhesions and F-actin structures, respectively. Analysis by confocal microscopy revealed that silencing of DLC1 stabilized actin stress fibers and promoted an accumulation of focal adhesions located at the tips of these actin-myosin bundles (Fig. 3A). This was verified with a second independent siRNA for DLC1, proving that the effect was specific (Supplementary Fig. 1). Surprisingly, cells lacking DLC2 demonstrated no obvious morphological changes and could not be distinguished from siLacZ control cells (Fig. 3A).
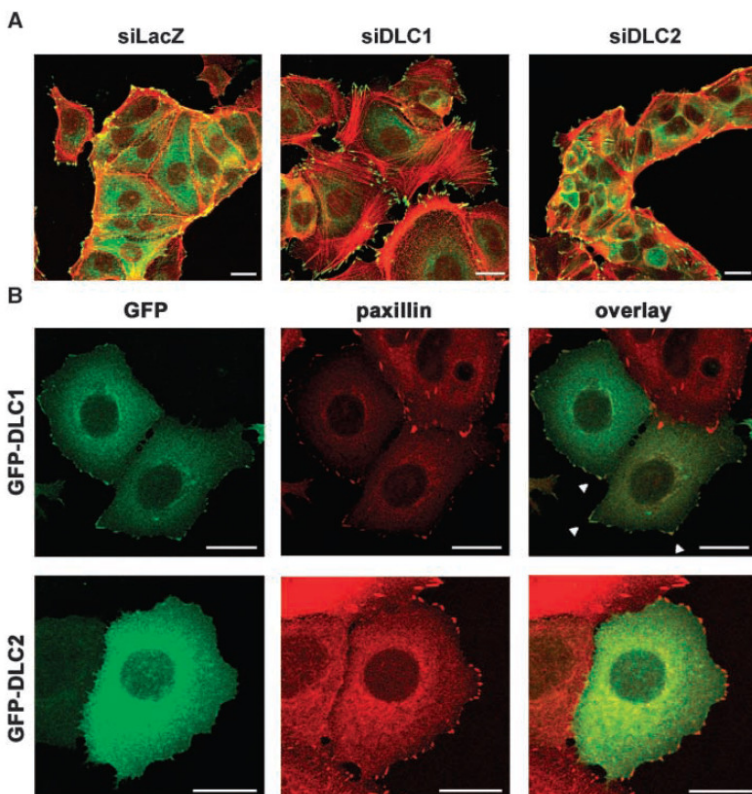

Figure 3: Loss of DLC1 enhances stress fiber formation and focal contact assembly. (A) MCF7 cells were transiently transfected with siRNAs specific for DLC1 and DLC2, or with LacZ-specific control siRNA and replated onto collagen-coated glass coverslips three days post transfection. The next day, cells were fixed and stained with paxillin-specific primary and Alexa Fluor 488-labeled secondary antibody (green). F-actin was visualized by co-staining with Alexa Fluor 546-phalloidin (red). (B) For subcellular localization studies, MCF7 cells were transiently transfected with expression vectors encoding GFP-DLC1 or GFP-DLC2. The next day, cells were fixed and stained with paxillin-specific primary and Alexa Fluor 546-labeled secondary antibody (red). DLC1-positive focal adhesions are marked with arrowheads in the overlay. The confocal images shown are stacks of 3-4 sections taken from the bottom of the cell. Scale bars = 20 μm.

DLC1 has been reported to localize to focal adhesions, as shown by colocalization with the focal adhesion protein vinculin (27). Recently, yeast two hybrid screenings identified DLC1 as a binding partner for members of the tensin family of focal adhesion proteins and this interaction has been proposed to be associated with biological activity (28-30). We thus examined the subcellular localization of DLC1 and DLC2 in MCF7 cells by transiently expressing GFP-tagged variants of the two proteins since low expression levels and/or the quality of specific antibodies precluded visualization of the endogenous proteins. Indirect immunostaining revealed that DLC1 colocalized with paxillin, whereas DLC2 failed to do so (Fig. 3B). These distinct subcellular localizations are likely to provide an explanation for the effect of DLC1 silencing, and not that of DLC2, on stress fiber formation and focal adhesion assembly.

Downregulation of DLC1 enhances cell migration

Rho proteins are important players in the regulation of cell motility. To study the effect of DLC1 and DLC2 downregulation on directed cell migration we performed scratch assays by wounding confluent monolayers of siRNA-transfected MCF7 cells. Compared to the siLacZ control, cells lacking DLC1 closed the wound more rapidly, whereas silencing of DLC2 had a slight inhibitory on the speed of wound closure (Fig. 4A). This is quantified in Figure 4B: Cells lacking DLC1 closed 53% of the gap after 14 h and 67% after 24 h, compared to 27% and 38%, respectively, in the case of the siLacZ control. To address the question how DLC proteins affect chemotaxis in the presence of a serum gradient we measured cell motility in transwell assays with 0.5% serum in the upper and 10% serum in the lower chamber. In MCF7 cells, the loss of DLC1 typically stimulated
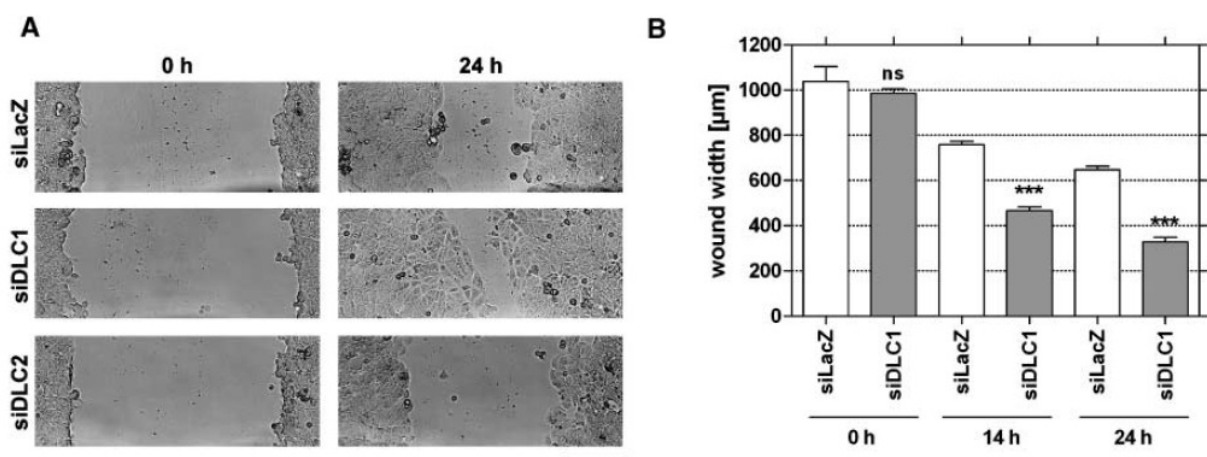

Figure 4: Loss of DLC1 enhances wound closure. (A) MCF7 cells were transiently transfected with siRNAs specific for DLC1 and DLC2, or with LacZ-specific control siRNA and replated onto collagen-coated dishes two days post transfection. The next day, confluent monolayers were scratched with a white pipette tip. Pictures were taken at a 10-fold magnification to document the scratch at time point zero and after incubation for 24 h. Scale bar = 200 μm. (B) Quantification of wound closure in MCF7 cells transfected with DLC1- and LacZ-specific siRNAs. Three independent positions of the wounded cell monolayers were photographed at 0, 14 and 24h and the width of the scratch was determined. The mean of 10 independent measurements per photograph is plotted, error bars represent SEM. Results for siDLC1- versus siLacZ-transfected cells at 14h and 24h were statistically significant (two-tailed unpaired t-test, p = 0.0002), while the difference of the initial wound width at 0h was not significant (ns, p = 0.4877).

migration 3-fold compared to the siLacZ control (Fig. 5A). A second DLC1-specific siRNA equally enhanced cell migration, confirming that the effect was due to the knock-down of DLC1 (Supplementary Fig. 1). In line with the wounding experiments, silencing of DLC2 had no effect on serum-induced chemotaxis (Fig. 5A). The failure of DLC2 knock-down to enhance cell motility in wounding and transwell assays was confirmed with an independent siRNA (Supplementary Fig. 2). In the absence of a serum gradient, transwell migration of MCF7 cells was very poor but also stimulated by the loss of DLC1, indicating that DLC1 is involved in the regulation of both directed and random cell migration (data not shown).
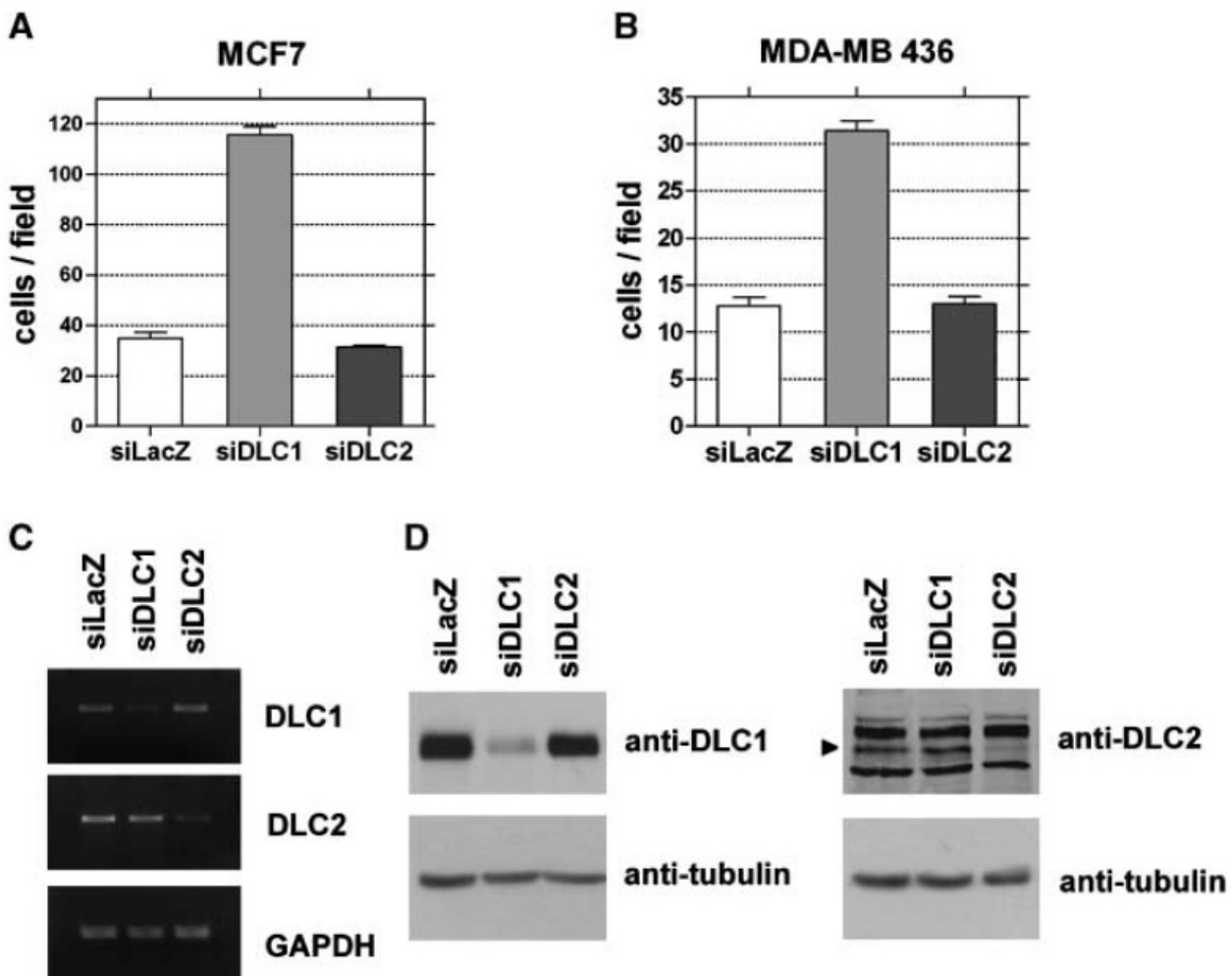

Figure 5: Downregulation of DLC1 but not DLC2 stimulates migration of MCF7 and MDA-MB 436 cells. MCF7 (A) and MD-MB 436 cells (B) were transiently transfected with siRNAs specific for DLC1 and DLC2, or with LacZ-specific control siRNA. Three days post transfection, 10^5 cells were seeded in medium containing 0,5% FCS into the upper chamber of a transwell. The lower well contained medium supplemented with 10% FCS. Cells that had migrated across the filter after over night incubation (MCF7 cells) and after 4 h (MDA-MB 436 cells) were fixed and stained. The number of migrated cells was determined by counting five independent microscopic fields (20-fold magnification). Data shown are the mean of duplicate wells and are representative of at least three independent experiments. Error bars represent SEM. (C, D) Silencing efficiency in siRNA-transfected MDA-MB 436 cells was verified three days post transfection by (C) semi-quantative RT-PCR as described in Figure 2 and (D) immunoblotting of cell lysates using DLC1- and DLC2-specific antibodies (top panels). Equal loading was verified by reprobing the membranes with tubulin-specific antibody (bottom panels).

To verify these results with a second cell line, we performed transwell assays with MDA-MB 436 cells that also express both DLC genes (Fig. 2A). Consistent with the results in MCF7 cells, downregulation of DLC1 enhanced cell migration, whereas depletion of DLC2 had no effect on the migratory behavior of the cells (Fig. 5B). Efficient silencing of the DLC proteins in MDA-MB 436 cells is demonstrated by semi-quantitative RT-PCR and by Western blotting (Fig. 5C, D).

DLC1 controls cell migration by modulation of Dia1 signaling

The multiple functions of Rho are mediated by its downstream effectors, the major ones being the Rho kinase (ROCK) and Dia1, the mammalian ortholog of Drosophila Diaphanous 1. Rho stimulates actin polymerization through activation of Dia1, which promotes addition of actin
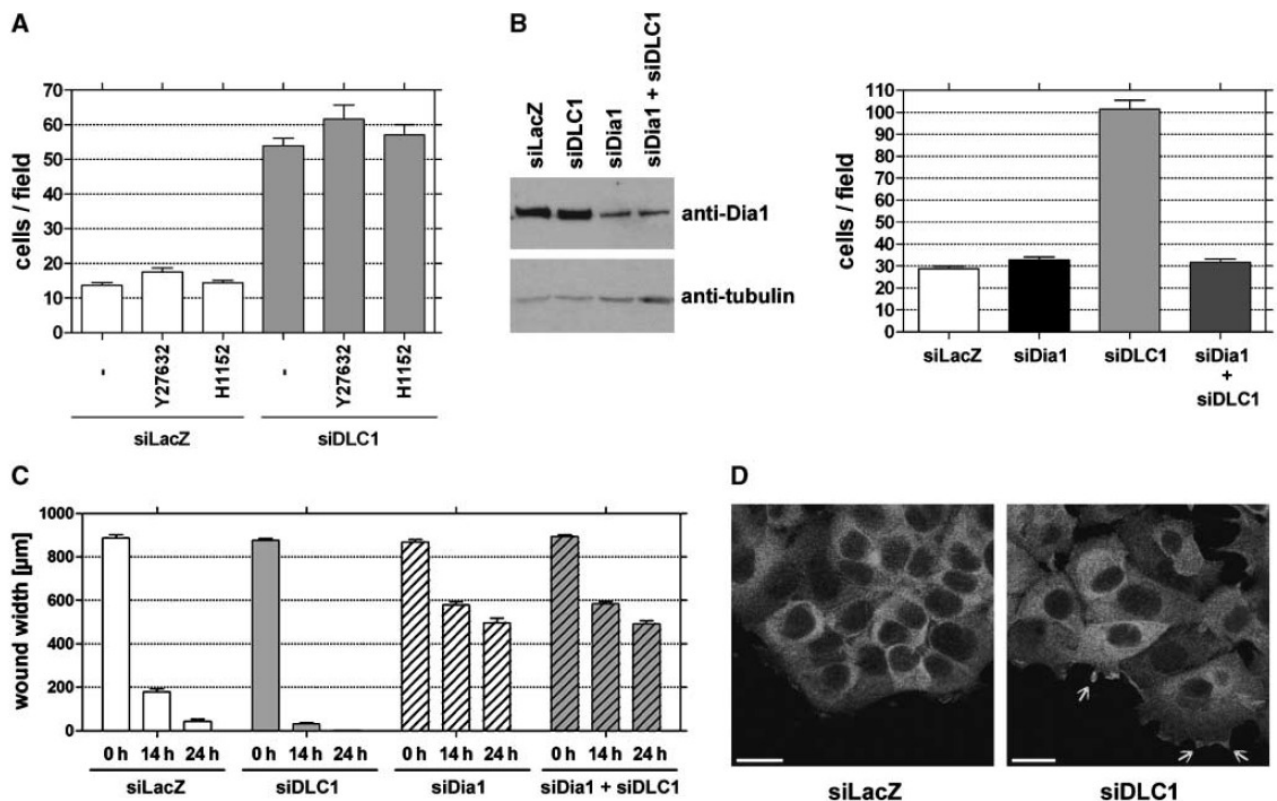

Figure 6: Migration of DLC1-depleted cells requires Dia1. (A) MCF7 cells were transiently transfected with siRNAs specific for DLC1 or LacZ. Three days post transfection, 10^5 cells were seeded into the upper chamber of a transwell in medium containing 0.5% FCS (-), plus 10 µM Y-27632 or 1 µM H-1152, respectively. The lower well contained medium supplemented with 10% FCS. The number of migrated cells after over night incubation was determined by counting five independent microscopic fields (20-fold magnification). Data shown are the mean of duplicate wells. Error bars represent SEM. (B & C) MCF7 cells were transiently transfected with siRNAs specific for LacZ, DLC1, Dia1 and DLC1 plus Dia1 at a 1:1 ratio. The siRNA amount in each transfection mix was adjusted with LacZ siRNA. (B) Silencing efficiency of Dia1 in MCF7 cells was verified three days post transfection by immunoblotting of cell lysates using Dia1-specific polyclonal antibody (left panels, top). Equal loading was verified by reprobing the membrane with tubulin-specific antibody (left panels, bottom). MCF7 cells were harvested three days post transfection and subjected to migration assays as described in Figure 5 (right panel). A representative experiment out of three is shown. (C) MCF7 cells were harvested two days post transfection and wounding assays were performed and quantified as described in Figure 4. (D) MCF7 cells transfected with siLacZ and siDLC1 were replated onto collagen-coated coverslips and confluent monolayers were wounded with a pipet tip. Cells were fixed 6 h later and stained with a Dia1-specific monoclonal antibody and Alexa Fluor 488-conjugated secondary antibody. Dia1-positive membrane protrusions are marked with arrows. Images are stacks of several confocal sections. Scale bar, 20 µm.

monomers to the barbed end of actin filaments. Dia1 acts together with ROCK to mediate Rho-induced stress fiber formation. ROCK phosphorylates and activates LIM kinase, leading to the inhibition of the actin-depolymerizing factor cofilin. In addition, ROCK induces actomyosin-based contractility through phosphorylation-induced inactivation of myosin light chain phosphatase (2,3).

To identify the molecular pathway underlying DLC1 inhibition of cell migration, we utilized the pharmacological inhibitors Y27632 and H-1152 to specifically inactivate ROCK. These inhibitors were added to siRNA-transfected MCF7 cells in the upper chamber of the transwells and the number of migrated cells was then quantified. As shown in Figure 6A, migration of cells lacking DLC1 was not affected by the presence of either ROCK inhibitor. We next depleted Dia1 using a siRNA that was used previously to show that Dia1 is crucial for stroma cell-derived factor 1α-induced migration of rat glioma cells (31). Efficient silencing of Dia1 in MCF7 cells was confirmed by Western analysis (Fig. 6B, left panel). Interestingly, simultaneous downregulation of Dia1 and DLC1 completely abrogated cell migration resulting from DLC1 knock-down, while knock-down of Dia1 alone did not affect basal cell migration (Fig. 6B, right panel). A second Dia1-specific siRNA confirmed these results (Supplementary Fig. 3). We also tested whether silencing of Dia1 prevents the increased migration of cells lacking DLC1 in wounding assays. Dia1 knock-down reduced basal cell motility under these conditions, and in line with the transwell migration assays, completely blocked increased motility of DLC1-depleted cells (Fig. 6C). Immunostaining revealed that Dia1 accumulated in membrane protrusions of migratory cells at the wound edge, which were especially prominent in cells lacking DLC1 (Fig. 6D). Accordingly, our data indicate a dominant role of Dia1 rather than ROCK in promoting migration of breast carcinoma cells.

Discussion

Rho GTPases are proteins with pleiotropic cellular functions that include the regulation of actin cytoskeletal dynamics, proliferation, migration, and invasion, which necessitates precise spatiotemporal control of their activity. Deregulation of Rho activity is known to be involved in oncogenic transformation of cells. DLC1 and DLC2 are structurally related RhoGAP proteins that have been proposed to act as tumor suppressors by antagonizing Rho signaling. Here we show that both proteins are capable of inactivating Rho when expressed in intact cells, based on results obtained with a RhoA biosensor and SRF luciferase assays. To investigate the cellular consequences of DLC1 and DLC2 loss, we knocked down expression in MCF7 breast carcinoma cells. In accordance with their GAP specificity for Rho, RNAi-mediated silencing of DLC1 and DLC2 enhanced cellular RhoA-GTP levels. These observations initially suggested that the two proteins may have redundant cellular functions. However, wound healing and chemotactic transwell assays revealed that only cells lacking DLC1, but not DLC2, acquired a more migratory phenotype, providing evidence that this oncosuppressive property is specific to DLC1.

It is becoming apparent that the DLC proteins require precise localization to fulfill their function. In MCF7 cells, GFP-tagged DLC1 was associated with focal adhesions, whereas DLC2 was mainly cytosolic. Recently, DLC1 recruitment to focal adhesions was shown to be mediated by interaction with tensin proteins (28-30). The four tensin members bind to the cytoplasmic tails of β integrins, and tensins 1-3 also interact with actin (32). DLC1 mutants deficient in tensin binding were compromised in their ability to inhibit cell growth, suggesting that tensin association is required for biological activity (28,29). Interaction with tensins has also been demonstrated for the less characterized DLC3 protein (28), but not for DLC2, making it tempting to speculate that DLC3 may perhaps have functions that overlap with those of DLC1. The exclusion of DLC2 from focal adhesions thus appears to provide an explanation for its inability to regulate actin remodeling in our experimental model. Nevertheless DLC2 knock-down led to enhanced total RhoA-GTP levels, indicating that it is active as a GAP protein, although its precise biological function still remains to be defined.

In Huh-7 hepatoma cells, DLC2 was reported to target to mitochondria via its START domain (33). However, we did not observe mitochondrial localization of DLC2 in MCF7 cells labeled with Mitotracker (data not shown). It is therefore possible that in addition to the START domain cell type-specific cofactors assist in DLC2 mitochondrial targeting. In addition to RhoA, DLC1 was recently shown to possess *in vitro* GAP activity for RhoB and RhoC (34), which may also be the case for DLC2. Since the Rho proteins present with different subcellular localizations, with RhoA and RhoC found in the cytoplasm and at the plasma membrane and RhoB predominantly at late endosomes (35), DLC2 substrate selection and function will also depend on the spatial distribution of its Rho targets.

The fact that DLC2 depletion did not facilitate migration of MCF7 and MDA-MB 436 cells conflicts with a previous study demonstrating enhanced motility of HepG2 cells in which DLC2 was silenced with a set of four siRNA duplexes (16). It is important to note that in our hands such a commercially available siRNA pool for DLC2 also downregulated DLC1 transcript levels. It thus cannot be ruled out that the reported enhanced migratory potential of HepG2 cells, which also express DLC1 (7,12), was in fact due to an off-target effect involving the knock-down of DLC1. Alternatively, the cellular consequences of DLC gene silencing may be cell type specific, possibly depending on Rho expression levels and/or on the balance of GEFs and other GAPs proteins that keep Rho in check.

Active Rho is known to stabilize focal adhesions and promote stress fiber formation, which is in line with the morphological changes observed in MCF7 cells lacking DLC1. We further show that ablation of DLC1 favors directed migration of MCF7 and MDA-MB 436 cells. The contribution of Rho to cell migration has been discussed controversially. Elevated levels of active RhoA were shown to negatively modulate cell migration due to excessive stress fiber formation and adhesion forces (36,37). In addition, RhoA has always been assumed to act at the back of migrating cells to

induce tail retraction via activation of ROCK. More recent studies using biosensors combined with live cell microscopy have provided proof that RhoA activity is detectable throughout cell migration and is not restricted to the rear but also present at the leading edge of cells (38-40). A role for DLC1 at sites of membrane protrusion was proposed by Healy et al., 2007, who observed local inactivation of a RhoA biosensor in MEFs ectopically expressing DLC1 (41).

To investigate the contribution of the different Rho proteins to migration of DLC1-depleted cells, we downregulated RhoA and RhoC by RNAi. Surprisingly, knock-down of both RhoA and RhoC increased cell migration and did not prevent migration of cells lacking DLC1, suggesting that these Rho isoforms are not the main mediators of cell migration in the absence of DLC1. However, silencing of RhoA/C also reduced DLC1 expression levels, making interpretation of results difficult (Supplementary Figure 4). Because it is unlikely that both siRNAs have the same non-specific effect, this observation may indicate that DLC1 protein levels are regulated by RhoA/C expression in a feedback manner. Interestingly, downregulation of Cdc42 partially inhibited migration of cells lacking DLC1 (Supplementary Fig. 4). Although ectopic DLC1 expression did not lead to measurable GTP hydrolysis of the Raichu-Cdc42 biosensor, negative regulation of endogenous Cdc42 by DLC1 cannot be ruled out. It is also possible that the effect of Cdc42 downregulation on migration of cells lacking DLC1 is indirect, as Dia1 has been reported to contribute to localization of Cdc42 to the leading edge of migrating cells (31). Unlike Dia2 and Dia3, Dia1 is not a characterized Cdc42 effector, making future studies necessary to address which Rho protein is responsible for promoting cell migration in DLC1-depleted cells.

The Rho effectors ROCK and Dia1 have both been implicated in negative and positive regulation of cell migration depending on the cell type and condition. Elongated protrusive cell movement in 3D matrices, for example, does not require ROCK, as opposed to movement involving a rounded blebbing morphology for which ROCK is essential (42). In MCF7 cells lacking DLC1, pharmacological suppression of ROCK activity did not impede cell migration. In contrast to this, Dia1 depletion completely abrogated increased migration in the absence of DLC1. This is in accordance with two recent studies, in which Dia1 was identified as a critical component in directed migration of MEFs and glioma cells, respectively (31,39). Together, our data provide evidence that despite their overlapping substrate specificity towards RhoA, DLC1 and DLC2 have non-redundant cellular functions most likely due to distinct spatial distributions. DLC1 thus appears to be involved in the remodeling of the actin cytoskeleton by local suppression of active Rho proteins and controls directed cell migration through a Dia1-dependent pathway.

Acknowledgments

References

1.   Ridley AJ, Schwartz MA, Burridge K, et al. Cell migration: integrating signals from front to back. Science 2003;302:1704-9.

2.   Jaffe AB, Hall A. Rho GTPases: biochemistry and biology. Annu Rev Cell Dev Biol 2005;21:247-69.

3.   Ridley AJ. Rho GTPases and actin dynamics in membrane protrusions and vesicle trafficking. Trends Cell Biol 2006;16:522-9.

4.   Homma Y, Emori Y. A dual functional signal mediator showing RhoGAP and phospholipase C-delta stimulating activities. EMBO J 1995;14:286-91.

5.   Ching YP, Wong CM, Chan SF, et al. Deleted in liver cancer (DLC) 2 encodes a RhoGAP protein with growth suppressor function and is underexpressed in hepatocellular carcinoma. J Biol Chem 2003;278:10824-30.

6.   Wong CM, Lee JM, Ching YP, et al. Genetic and epigenetic alterations of DLC-1 gene in hepatocellular carcinoma. Cancer Res 2003;63:7646-51.

7.   Yuan BZ, Miller MJ, Keck CL, et al. Cloning, characterization, and chromosomal localization of a gene frequently deleted in human liver cancer (DLC-1) homologous to rat RhoGAP. Cancer Res 1998;58:2196-9.

8.   Durkin ME, Yuan BZ, Zhou X, et al. DLC-1:a Rho GTPase-activating protein and tumour suppressor. J Cell Mol Med 2007;11:1185-207.

9.   Yuan BZ, Zhou X, Durkin ME, et al. DLC-1 gene inhibits human breast cancer cell growth and in vivo tumorigenicity. Oncogene 2003;22:445-50.

10.   Yuan BZ, Jefferson AM, Baldwin KT, et al. DLC-1 operates as a tumor suppressor gene in human non-small cell lung carcinomas. Oncogene 2004;23:1405-11.

11.   Zhou X, Thorgeirsson SS, Popescu NC. Restoration of DLC-1 gene expression induces apoptosis and inhibits both cell growth and tumorigenicity in human hepatocellular carcinoma cells. Oncogene 2004;23:1308-13.

12.   Ng IO, Liang ZD, Cao L, Lee TK. DLC-1 is deleted in primary hepatocellular carcinoma and exerts inhibitory effects on the proliferation of hepatoma cell lines with deleted DLC-1. Cancer Res 2000;60:6581-4.

13. Sekimata M, Kabuyama Y, Emori Y, Homma Y. Morphological changes and detachment of adherent cells induced by p122, a GTPase-activating protein for Rho. J Biol Chem 1999;274:17757-62.

14. Wong CM, Yam JW, Ching YP, et al. Rho GTPase-activating protein deleted in liver cancer suppresses cell proliferation and invasion in hepatocellular carcinoma. Cancer Res 2005;65:8861-8.

15. Goodison S, Yuan J, Sloan D, et al. The RhoGAP protein DLC-1 functions as a metastasis suppressor in breast cancer cells. Cancer Res 2005;65:6042-53.

16. Leung TH, Ching YP, Yam JW, et al. Deleted in liver cancer 2 (DLC2) suppresses cell transformation by means of inhibition of RhoA activity. Proc Natl Acad Sci U S A 2005;102:15207-12.

17. Malliri A, Collard JG. Role of Rho-family proteins in cell adhesion and cancer. Curr Opin Cell Biol 2003;15:583-9.

18. Sahai E, Marshall CJ. RHO-GTPases and cancer. Nat Rev Cancer 2002;2:133-42.

19. Fritz G, Brachetti C, Bahlmann F, et al. Rho GTPases in human breast tumours: expression and mutation analyses and correlation with clinical parameters. Br J Cancer 2002;87:635-44.

20. Kamai T, Arai K, Tsujii T, et al. Overexpression of RhoA mRNA is associated with advanced stage in testicular germ cell tumour. BJU Int 2001;87:227-31.

21. van Golen KL, Wu ZF, Qiao XT, et al. RhoC GTPase, a novel transforming oncogene for human mammary epithelial cells that partially recapitulates the inflammatory breast cancer phenotype. Cancer Res 2000;60:5832-8.

22. Clark EA, Golub TR, Lander ES, Hynes RO. Genomic analysis of metastasis reveals an essential role for RhoC. Nature 2000;406:532-5.

23. Yamaguchi H, Lorenz M, Kempiak S, et al. Molecular mechanisms of invadopodium formation: the role of the N-WASP-Arp2/3 complex pathway and cofilin. J Cell Biol 2005;168:441-52.

24. Simpson KJ, Dugan AS, Mercurio AM. Functional analysis of the contribution of RhoA and RhoC GTPases to invasive breast carcinoma. Cancer Res 2004;64:8694-701.

25.   Yoshizaki H, Ohba Y, Kurokawa K, et al. Activity of Rho-family GTPases during cell division as visualized with FRET-based probes. J Cell Biol 2003;162:223-32.

26.   Posern G, Treisman R. Actin' together: serum response factor, its cofactors and the link to signal transduction. Trends Cell Biol 2006;16:588-96.

27.   Kawai K, Yamaga M, Iwamae Y, et al. A PLCdelta(1)-binding protein, p122RhoGAP, is localized in focal adhesions. Biochem Soc Trans 2004;32:1107-9.

28.   Qian X, Li G, Asmussen HK, et al. Oncogenic inhibition by a deleted in liver cancer gene requires cooperation between tensin binding and Rho-specific GTPase-activating protein activities. Proc Natl Acad Sci U S A 2007;104:9012-7.

29.   Liao YC, Si L, deVere White RW, Lo SH. The phosphotyrosine-independent interaction of DLC-1 and the SH2 domain of cten regulates focal adhesion localization and growth suppression activity of DLC-1. J Cell Biol 2007;176:43-9.

30.   Yam JW, Ko FC, Chan CY, et al. Interaction of deleted in liver cancer 1 with tensin2 in caveolae and implications in tumor suppression. Cancer Res 2006;66:8367-72.

31.   Yamana N, Arakawa Y, Nishino T, et al. The Rho-mDia1 pathway regulates cell polarity and focal adhesion turnover in migrating cells through mobilizing Apc and c-Src. Mol Cell Biol 2006;26:6844-58.

32.   Lo SH. Tensin. Int J Biochem Cell Biol 2004;36:31-4.

33.   Ng DC, Chan SF, Kok KH, et al. Mitochondrial targeting of growth suppressor protein DLC2 through the START domain. FEBS Lett 2006;580:191-8.

34.   Healy KD, Hodgson L, Kim TY, et al. DLC-1 suppresses non-small cell lung cancer growth and invasion by RhoGAP-dependent and independent mechanisms. Mol Carcinog 2007.

35.   Wheeler AP, Ridley AJ. Why three Rho proteins? RhoA, RhoB, RhoC, and cell motility. Exp Cell Res 2004;301:43-9.

36.   Besson A, Gurian-West M, Schmidt A, et al. p27Kip1 modulates cell migration through the regulation of RhoA activation. Genes Dev 2004;18:862-76.

37.   Sahai E, Olson MF, Marshall CJ. Cross-talk between Ras and Rho signalling pathways in transformation favours proliferation and increased motility. EMBO J 2001;20:755-66.

38.   Pertz O, Hodgson L, Klemke RL, Hahn KM. Spatiotemporal dynamics of RhoA activity in migrating cells. Nature 2006;440:1069-72.

39.   Goulimari P, Kitzing TM, Knieling H, et al. Galpha12/13 is essential for directed cell migration and localized Rho-Dia1 function. J Biol Chem 2005;280:42242-51.

40.   Kurokawa K, Matsuda M. Localized RhoA activation as a requirement for the induction of membrane ruffling. Mol Biol Cell 2005;16:4294-303.

41.   Healy KD, Hodgson L, Kim TY, et al. DLC-1 suppresses non-small cell lung cancer growth and invasion by RhoGAP-dependent and independent mechanisms. Mol Carcinog 2007.

42.   Sahai E, Marshall CJ. Differing modes of tumour cell invasion have distinct requirements for Rho/ROCK signalling and extracellular proteolysis. Nat Cell Biol 2003;5:711-9.

7.4. DLC1 interaction with 14-3-3 proteins inhibits RhoGAP activity and blocks nucleocytoplasmic shuttling

Rolf-Peter Scholz*, Jennifer Regner*[1], Anke Theil, Patrik Erlmann, Gerlinde Holeiter, Ruth Jähne, Simone Schmid, Angelika Hausser and Monilola A. Olayioye

University of Stuttgart, Institute of Cell Biology and Immunology,

Allmandring 31, 70569 Stuttgart, Germany

[1] current address: Orthopaedic University Hospital of Heidelberg, Schlierbacher Landstrasse 200a, 69118 Heidelberg, Germany

* both authors contributed equally to the manuscript

Address correspondence to: Monilola A. Olayioye, Tel: +49 711 685 69301, Fax: + 49 711 685 67484, Email: monilola.olayioye@izi.uni-stuttgart.de

Summary

Deleted in Liver Cancer 1 (DLC1) is a Rho GTPase activating protein (GAP) that is downregulated in various tumor types. Via its GAP domain DLC1 specifically inactivates the small GTPases RhoA, B and C in vitro and this appears to contribute to its tumor suppressor function in vivo. Thus far, molecular mechanisms that control DLC1 activity have not been investigated. Here we show that phorbol ester-induced activation of protein kinases C and D stimulates DLC1 association with the phosphoserine/-threonine-binding 14-3-3 adaptor proteins via recognition motifs that involve serines 327 and 431. Association with 14-3-3 proteins is shown to inhibit DLC1 GAP activity, facilitating signaling by active Rho. We further provide evidence that treatment of cells with phorbol ester or 14-3-3 coexpression block DLC1 nucleocytoplasmic shuttling, most likely by masking a previously unrecognized nuclear localization sequence. 14-3-3 binding thus provides a novel mechanism by which DLC1 activity is regulated and compartmentalized.

Introduction

The DLC1 gene was first isolated as a candidate tumor suppressor gene in primary human hepatocellular carcinoma and loss of expression has subsequently been shown in other tumor types, including colon, breast, prostate and lung (Durkin et al. 2007b). Transfection of the DLC1 cDNA into different carcinoma cell lines lacking DLC1 expression inhibited cell growth and tumorigenicity in nude mice (Ng et al. 2000;Yuan et al. 2003;Yuan et al. 2004;Zhou et al. 2004). Recently, the structurally related proteins DLC2 and DLC3 were found to be downregulated in various tumor types and their re-expression in cancer cells similarly inhibited proliferation, colony formation and growth in soft agar (Ching et al. 2003;Durkin et al. 2007a).

DLC1 contains a GAP domain specific for the small GTPases RhoA, B and C, and to a lesser extent Cdc42 (Healy et al. 2008;Wong et al. 2003). It further contains an aminoterminal sterile alpha motif (SAM) and a StAR-related lipid transfer (START) domain at its carboxyterminus, whose function remain to be characterized. The Rho family of GTPases are important regulators of diverse biological responses, including actin cytoskeletal rearrangements, gene transcription, cell cycle regulation, apoptosis and membrane trafficking (Jaffe and Hall 2005;Ridley 2006). Rho proteins cycle between a GTP-bound active state to interact with effector proteins, modulating their activity and localization, and an inactive GDP-bound state. Signaling of growth factor receptors and integrins can induce exchange of GDP for GTP on Rho proteins. This activation of Rho proteins is controlled by the guanine nucleotide exchange factors (GEFs), which promote the release of bound GDP and facilitate GTP binding, and the GAP proteins, which increase the intrinsic GTPase activity of Rho GTPases to accelerate the return to the inactive state. Activation of Rho is known to induce the assembly of actin stress fibers and focal adhesions, whereas Cdc42 promotes the formation of specialized membranes protrusions called filopodia (Jaffe and Hall 2005;Ridley 2006).

Indeed, microinjection of p122, the rat homolog of DLC1, suppressed the formation of LPA-induced stress fibers and focal adhesions (Sekimata et al. 1999). Furthermore, stable expression of human DLC1 in hepatocellular and breast carcinoma cell lines was shown to reduce cell motility and invasiveness, consistent with the inhibition of Rho signaling (Goodison et al. 2005;Wong et al. 2005). Interestingly, an inactive form of DLC1 expressed in a non-small cell lung cancer cell line was recently found to partially suppress anchorage independent growth and invasion in vitro, suggesting that the anti-tumor function of DLC1 may also be determined by GAP-independent activities (Healy et al. 2008).

The human genome is estimated to encode for up to 80 RhoGAPs, implicating a necessity for very tight temporal and spatial regulation of the 20 known Rho GTPase substrates (Moon and Zheng 2003). Regulation of RhoGAP proteins is achieved by several mechanisms such as protein or lipid interactions, and post-translational modification (Bernards and Settleman 2005). Although DLC1 expression has been studied at the transcriptional level, little is known about its regulation at the protein level. Rat DLC1 was recently shown to be phosphorylated by PKB/Akt and Rsk kinases on serine 322, corresponding to serine 329 in the human protein, however, the significance of this phosphorylation remains to be elucidated (Hers et al. 2006).

Scansite analysis of the DLC1 protein sequence at high stringency revealed the presence of a putative 14-3-3 binding motif conserved amongst different species (TRTRS^{327}LS in human DLC1). Members of the 14-3-3 family are ubiquitously expressed small acidic proteins with a molecular weight of approximately 30 kDa. Seven highly conserved 14-3-3 isoforms exist in mammals (β, γ, ζ, σ, τ, ε, η), which form homo- and heterodimers (Bridges and Moorhead 2004;Dougherty and Morrison 2004). Generally, 14-3-3 proteins function as adaptors that bind to their target proteins in a phosphorylation dependent manner. Consensus motifs for binding are RSXpSXP and RXXXpSXP, with phosphothreonine being able to replace phosphoserine (Yaffe et al. 1997). Many target proteins do not contain sequences that conform precisely to these motifs, and in some cases interaction has been shown to be independent of phosphorylation. The crystal structure of 14-3-3 dimers revealed that each subunit can independently bind one discrete phosphoserine- or phosphothreonine-containing ligand. Each dimer therefore contains two binding pockets and as a result can interact with two motifs simultaneously, located either on a single target or on separate binding partners. Binding of 14-3-3 proteins often sequesters the target protein in a particular subcellular compartment and the release of 14-3-3 then allows the target to relocate. This relocation is often due to the exposure of an intrinsic subcellular targeting sequence masked by the 14-3-3 dimer. 14-3-3 binding can also induce conformational changes of the target protein or may have a scaffolding function (Bridges and Moorhead 2004;Dougherty and Morrison 2004).

Here we show that DLC1 interacts with 14-3-3 proteins in a phosphorylation dependent manner, requiring phosphorylation of serines 327 and 431. These serines lie within consensus motifs for the

protein kinase D (PKD) family of serine/threonine kinases. Activation of PKD requires the recruitment to membranes through diacylglycerol (DAG) binding and involves phosphorylation of its activation loop by novel PKCs (Rykx et al. 2003;Wang 2006). Thus, treatment of cells with phorbol ester, a DAG analog, stimulated DLC1 phosphorylation and association with 14-3-3 proteins. This interaction was found to suppress DLC1 GAP activity, preventing DLC1-mediated stimulation of Rho-GTP hydrolysis as determined with a RhoA biosensor, and enabling downstream signaling, as shown with serum response factor (SRF)-dependent reporter assays. Accordingly, a DLC1 S327/431A mutant was more active than the wild type protein in inhibiting cell growth. DLC1 is further revealed to undergo rapid nucleocytoplasmic shuttling, which was inhibited by phorbol ester-induced phosphorylation and 14-3-3 binding, most likely by masking a novel NLS located adjacent to the serine 431 phosphorylation site.

Results

DLC1 specifically interacts with 14-3-3 proteins

To investigate DLC1 interaction with 14-3-3 proteins, all 7 mammalian isoforms were purified as GST fusions from *E. coli* and used in pulldown assays with whole cell extracts of HEK293T cells transiently expressing myc-tagged DLC1. Figure 1A shows that DLC1 associates with all 14-3-3 isoforms with varying affinity except 14-3-3σ, and does not interact with GST alone. 14-3-3 proteins commonly bind target proteins via a conserved amphipathic groove comprising a cluster of basic amino acids. To test whether the interaction with DLC1 was mediated by this region, we made use of a R56/60A 14-3-3τ mutant protein previously shown to be deficient in target protein binding (Hausser et al. 2006;Xing et al. 2000). DLC1 did not bind to the R56/60A mutant in a pulldown assay (Fig. 1B), confirming that association involved the 14-3-3 binding groove. To identify the region in DLC1 responsible for 14-3-3 binding, truncation mutants were generated, in which the aminoterminal SAM (ΔSAM) or the carboxyterminal START domain (ΔSTART) were deleted (Fig. 1C). Deletion of neither domain affected 14-3-3 binding (Fig. 1D). However, the carboxyterminus of the protein comprising the RhoGAP and START domains (Fig. 1C; ΔN) failed to interact with GST-14-3-3β, suggesting that DLC1 interaction with 14-3-3 proteins is mediated by the linker region (aa 79-625) connecting the SAM and RhoGAP domains.

The interaction of DLC1 with 14-3-3 proteins was further analyzed by coimmunoprecipitation experiments. Myc-tagged DLC1 was coexpressed with either Glu-Glu (EE)-tagged 14-3-3ζ or γ, or HA-tagged 14-3-3τ in HEK293T cells. 14-3-3 proteins were then immunoprecipitated from whole cell extracts using the respective HA- or EE-specific antibodies. DLC1 was found to coprecipitate with 14-3-3τ and γ, but did not interact with 14-3-3ζ under these conditions (Fig. 2A), which correlates with the weak interaction seen with the ζ isoform in the pulldown assay. The same results were obtained by first precipitating myc-DLC1 and subsequent detection of 14-3-3 isoforms (Fig. 2B). Thus, DLC1 also interacts with 14-3-3 proteins expressed in eukaryotic cells, confirming

the results obtained in the pulldown assays. Finally, the association of DLC1 with endogenous 14-3-3 proteins was investigated. HEK293T cells were transiently transfected with myc-tagged DLC1 and whole cell extracts were incubated with either 14-3-3-specific antibody that recognizes all 14-3-3 isoforms or a control IgG. DLC1 was detected in the 14-3-3 immunoprecipitate (Fig. 2C), proving that DLC1 also associates with endogenous 14-3-3 isoforms.
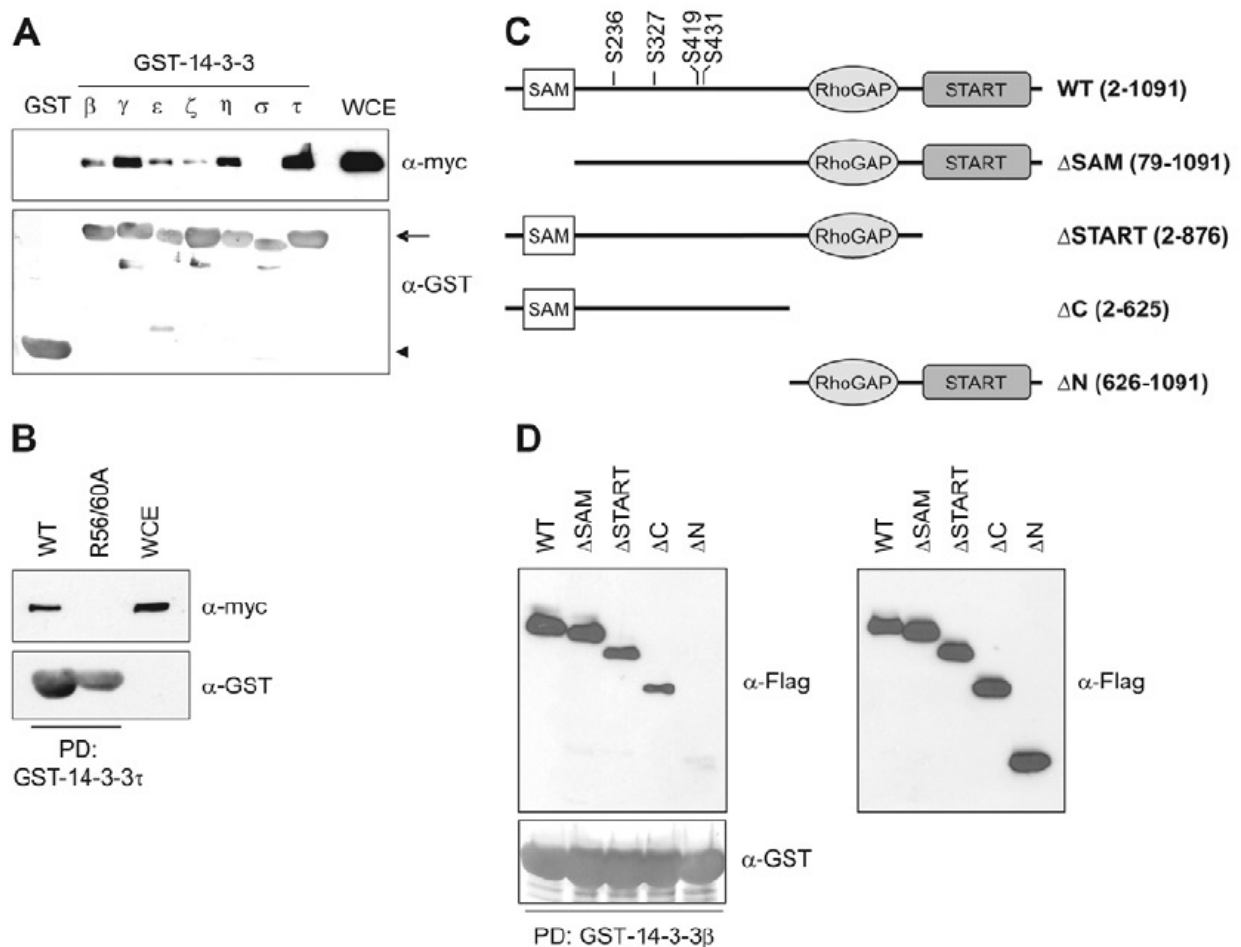

Fig. 1: Interaction of DLC1 with recombinant GST-14-3-3 proteins. (A) HEK293T cells were transiently transfected with a plasmid encoding myc-tagged DLC1. WCE were incubated with glutathione beads coupled to the indicated GST-14-3-3 isoforms, or GST alone, and bound proteins were separated by SDS-PAGE. DLC1 was detected by Western blotting with a myc-specific antibody (top panel). The integrity of GST (marked with an arrowhead) and GST-14-3-3 isoforms (marked with an arrow) was verified by probing the membrane with GST-specific antibody. (B) WCE of HEK293T cells transiently expressing myc-DLC1 were subjected to a pulldown (PD) with wild type (WT) or R56/60A GST-14-3-3τ and bound proteins were analyzed as described in A. (C) Schematic representation of DLC1 truncation mutants and putative PKD phosphorylation sites. (D) WCE of HEK293T cells transiently expressing the indicated Flag-tagged DLC1 mutants were subjected to a pulldown with GST-14-3-3β and bound proteins were analyzed with Flag-specific antibody as described in A. Expression of the different DLC1 variants was verified by immunoblotting of WCE with Flag-specific antibody (right panel).

Phorbol ester stimulation enhances DLC1 association with 14-3-3 proteins

In most cases, 14-3-3 recognition of target proteins is phosphorylation dependent and thus controlled by the kinases and phosphatases that modulate the phosphorylation state of the target protein. To first analyze whether the interaction of DLC1 with 14-3-3 proteins was dependent upon phosphorylation, we treated HEK293T cells transiently expressing myc-DLC1 with the serine/threonine phosphatase inhibitor okadaic acid (OA). Cells were lysed and subjected to pulldown assays with GST-14-3-3τ. Compared to the DMSO control, OA treatment of cells strongly
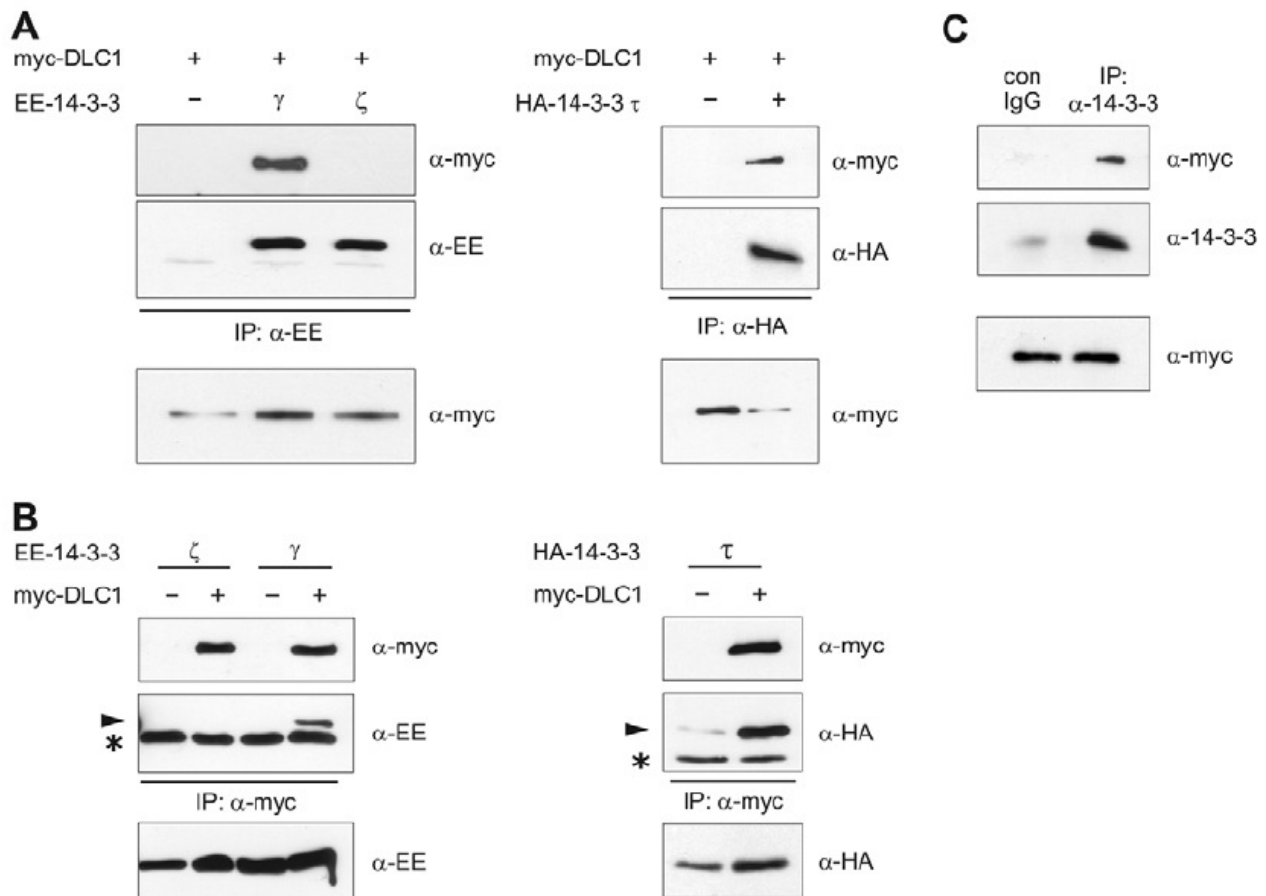

Fig. 2: Coimmunoprecipitation of DLC1 with 14-3-3 proteins. (A) HEK293T cells were transiently transfected with myc-tagged DLC1 and empty vector (-), EE-tagged 14-3-3γ or 14-3-3ζ or HA-tagged 14-3-3τ expression vectors. 14-3-3 isoforms were immunoprecipitated from WCE with EE- and HA-specific antibodies, respectively, and immune complexes were separated by SDS-PAGE. Coprecipitated DLC1 was detected by Western blotting with myc-specific antibody (top panels). Immunoprecipitation of 14-3-3 isoforms was verified by probing the membrane with EE- and HA-specific antibodies, respectively (middle panels), and expression of DLC1 was verified by immunoblotting of WCE with myc-specific antibody (bottom panels). (B) HEK293T cells were transiently transfected with expression vectors encoding EE-tagged 14-3-3γ or ζ, or HA-tagged 14-3-3τ, and empty vector or myc-tagged DLC1. DLC1 was immunoprecipitated from WCE with myc-specific antibody and immune complexes were separated by SDS-PAGE. Coprecipitated 14-3-3 isoforms were detected by Western blotting with EE- and HA-specific antibodies, respectively (middle panels, indicated with arrowheads). IgG chains are marked with asterisks. Immunoprecipitation of DLC1 was verified with myc-specific antibody (top panels), and expression of 14-3-3 isoforms was verified by immunoblotting of WCE with EE- and HA-specific antibodies (bottom panels). (C) HEK293T cells transiently expressing myc-tagged DLC1 were lysed and 14-3-3 proteins were immunoprecipitated from WCE with 14-3-3-specific rabbit pAb. An unrelated rabbit pAb was used as a control (con IgG). Immune complexes were separated by SDS-PAGE. Coprecipitated DLC1 was detected by Western blotting with myc-specific antibody (top panel). Immunoprecipitation of 14-3-3 proteins were verified by probing the membrane with 14-3-3-specific mouse mAb (middle panel). Expression of DLC1 was verified by immunoblotting of WCE with myc-specific antibody (bottom panel).

enhanced 14-3-3τ binding to DLC1 after 2 and 4 h (Fig. 3A, top panel). Additionally, the DLC1 protein displayed lower electrophoretic mobility after OA treatment (Fig. 3A, bottom panel), suggestive of increased phosphorylation. This substantial phosphoshift indicates that DLC1 is a phosphoprotein that may be phosphorylated on multiple sites. OA is an effective inhibitor of protein phosphatase 2A (PP2A) and the less abundant protein phosphatases 4 and 5, but has no detectable inhibitory effect on protein phosphatase 1 or other major serine/threonine phosphatases (Favre et al. 1997). Because DLC1 phosphorylation increased after OA treatment, it is thus likely that DLC1 is a target for PP2A.

To further characterize the interaction of DLC1 with 14-3-3 proteins, we aimed to identify the signaling pathways involved in the regulation of this interaction. Phorbol-12,13-dibutyrate (PDBu), an analog of DAG, was found to increase association of DLC1 with GST-14-3-3τ as early as 15 min after stimulation of cells, with elevated binding observed for up to 2 h (Fig. 3B). The main cellular kinases that directly bind and are activated by phorbol esters are the classical PKCs (α, β, γ), the novel PKCs (δ, η, ε, θ) and the PKD family members PKD1/PKCμ, PKD2 and PKD3/PKCν (Griner and Kazanietz 2007). To investigate the potential involvement of these kinases in DLC1 phosphorylation and 14-3-3 binding, we tested the ability of different pharmacological inhibitors to block PDBu-induced 14-3-3 binding to DLC1. Staurosporine is a non-specific kinase inhibitor that inhibits PKCs and PKD, the more selective compound Gö6983 inhibits classical and novel PKCs, and Gö6976 inhibits both classical PKCs and PKD. Pretreatment of cells with these inhibitors blocked PDBu-induced 14-3-3τ binding to DLC1 (Fig. 3C), whereas pharmacological inhibition of
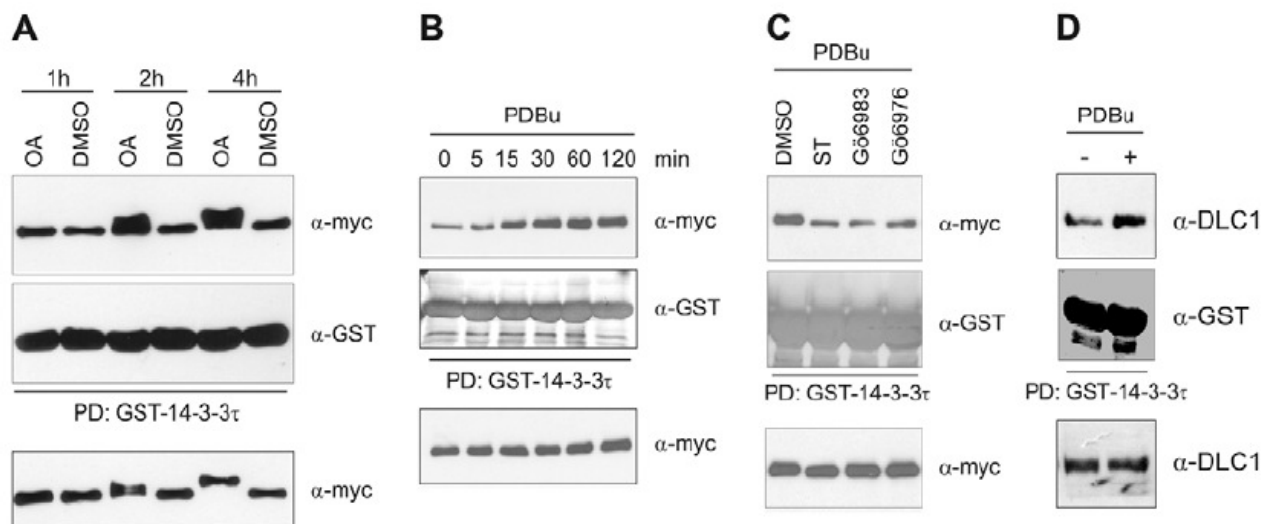

Fig. 3: Phosphorylation-dependent interaction of DLC1 with 14-3-3 proteins. HEK293T cells were transiently transfected with a myc-DLC1 expression vector and treated with (A) 100 nM OA or solvent (DMSO), or (B) 100 nM PDBu for the indicated times prior to lysis. In C, cells were incubated with 1 µM staurosporine (ST), 5 µM Gö6983, 5 µM Gö6976 or solvent (DMSO) for 90 min before stimulation with 1 µM PDBu for 15 min. In D, MDAMB231 cells were left untreated or treated with 1 µM PDBu for 15 min prior to lysis. WCE were subjected to a pulldown with GST-14-3-3τ beads and bound proteins were separated by SDS-PAGE. DLC1 was detected with myc-specific antibody in A-C and DLC1-specific antibody in D (top panels). The integrity of recombinant GST-14-3-3τ was verified by probing the membrane with GST-specific antibody (middle panels), and expression of DLC1 was verified by immunoblotting of WCE with myc-specific antibody in A-C and DLC1-specific antibody in D (bottom panels).

other AGC kinases like PKA (with H89) and PKB/Akt (by blocking PI3K with LY294002) had no effect (data not shown). Since novel PKC-mediated phosphorylation of the PKD activation loop is required for PKD kinase activity, inhibition of novel PKCs is expected to impinge on PKD substrate phosphorylation. Finally, we verified that endogenous DLC1 also associates with 14-3-3 proteins in response to phorbol ester stimulation by performing a GST-14-3-3τ pulldown of DLC1 from lysates of MDAMB231 breast cancer cells (Fig. 3D). Together, these results suggest that activation of phorbol ester-responsive PKCs and/or PKD regulate DLC1 association with 14-3-3 proteins.

DLC1 phosphorylation on serines 327 and 431 is required for 14-3-3 interaction

In silico analysis of DLC1 with Motif Scan predicted several potential 14-3-3 binding sites, with serine 327 fulfilling high stringency criteria (Obenauer et al. 2003). Interestingly, serine 327 lies within an optimal consensus sequence for PKD kinases (L/I/VxRxxS/T), determined by an arginine in the -3 and a leucine, isoleucine or valine in the -5 position relative to the serine or threonine to be phosphorylated (Nishikawa et al. 1997). Intriguingly, PKD-mediated phosphorylation of substrates such as phosphatidylinositol 4-kinase IIIβ, histone deacetylase 5 and the Ras effector RIN1 has been described to generate 14-3-3 recognition motifs (Hausser et al. 2006;Vega et al. 2004;Wang et al. 2002). We therefore coexpressed GFP-tagged PKD1 with Flag-DLC1 in HEK293T cells and analyzed DLC1 binding to GST-14-3-3τ with pulldown assays. Coexpression of PKD1 was indeed found to enhance DLC1 interaction with 14-3-3τ (Fig. 4C, lanes 1-2). To test whether serine 327 in DLC1 was essential for 14-3-3 association, we exchanged this serine for an alanine by site-directed mutagenesis. However, no obvious difference in the interaction with GST-14-3-3τ was observed between wild type DLC1 and the S327A mutant protein (Fig. 4A, lanes 1-2). The linker region of DLC1 identified to mediate 14-3-3 binding contains three additional serines at positions 236, 419 and 431 that match PKD substrate site criteria (see Fig. 1C). Due to the dimeric nature of 14-3-3 proteins, target protein binding often involves more than one phosphorylation site. We therefore generated combinatorial DLC1 phosphorylation site mutants, since individual mutation of these sites failed to abolish DLC1 binding to 14-3-3 proteins. Interestingly, a DLC1 double mutant, in whom serines 327 and 431 were mutated to alanines, displayed reduced 14-3-3 binding in both pulldown assays and coimmunoprecipitations (Fig. 4A and 4B). Additional mutation of serines 236 and 419 did not reduce 14-3-3 binding any further (Fig. 4F), suggesting that serines 327 and 431 in DLC1 are the only sites that confer 14-3-3 binding downstream of PKD. This is supported by the finding that PKD1 coexpression with the DLC1 S327/431A mutant no longer enhanced 14-3-3 binding as it did when coexpressed with wild type DLC1 (Fig. 4C). The residual 14-3-3 binding to the DLC1 S327/431A mutant (observed in longer exposures) and higher order mutants could still be enhanced by OA or PDBu treatment, suggesting at least one additional PKD-independent phosphorylation site that contributes to 14-3-3 binding (Fig. 4D & F). We attempted to generate a DLC1 variant that constitutively binds 14-3-3 proteins by exchanging serines 327 and 431 to glutamic acid. However, this DLC1 S327/431D mutant was indistinguishable from the serine
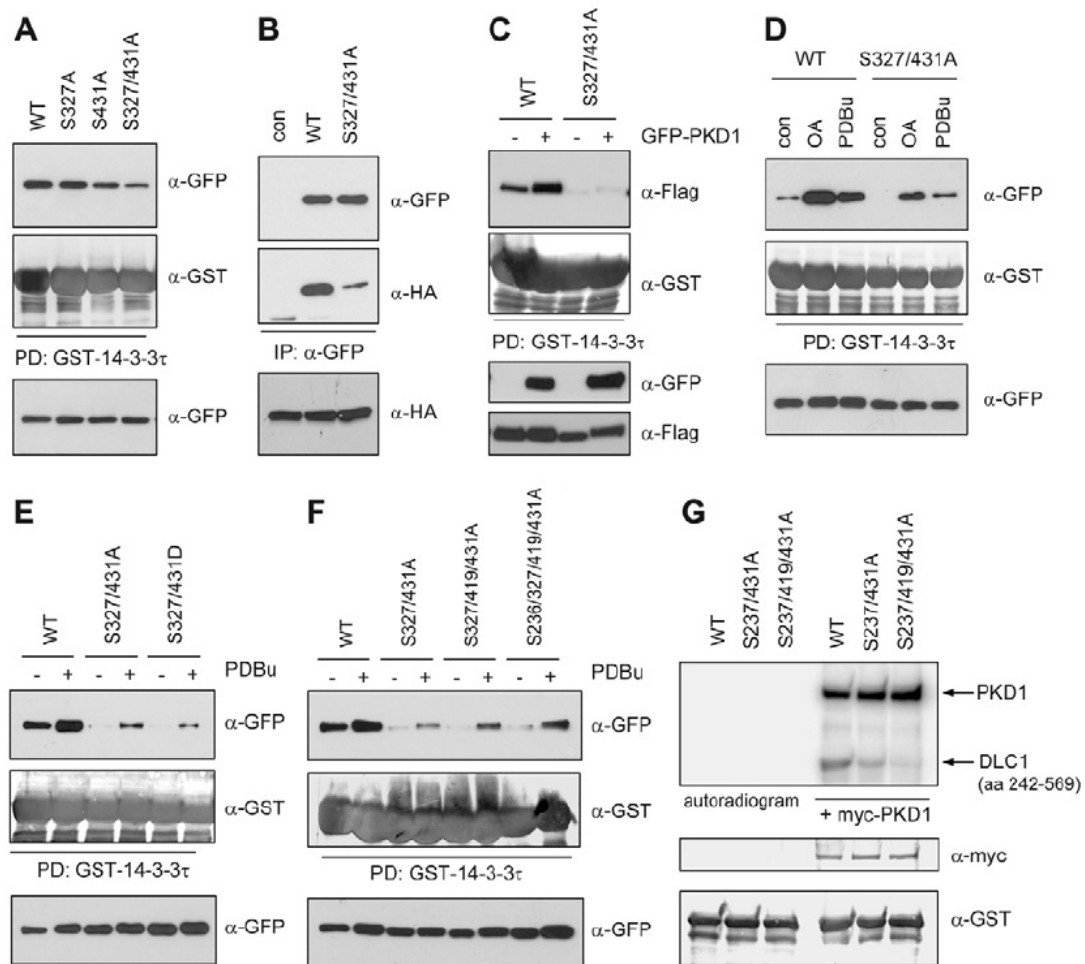
Fig. 4: DLC1 interaction with 14-3-3 proteins requires phosphorylation of serines 327 and 431.
HEK293T cells were transiently transfected with GFP-tagged DLC1 WT, S327A, S431A, or S327/431A expression vectors. WCE were subjected to a pulldown with GST-14-3-3τ beads and bound proteins were separated by SDS-PAGE. DLC1 variants were detected with a GFP-specific antibody (top panel). The integrity of recombinant GST-14-3-3τ was verified by probing the membrane with GST-specific antibody (middle panel), and expression of DLC1 variants was verified by immunoblotting of WCE with GFP-specific antibody (bottom panel). (B) An HA-tagged 14-3-3τ expression vector was transiently transfected into HEK293T cells along with DLC1 WT, S327/431A or empty vector (con). DLC1 variants were immunoprecipitated from WCE with GFP-specific antibody and immune complexes were separated by SDS-PAGE. Coprecipitated 14-3-3τ was detected by Western blotting with HA-specific antibody (middle panel). Immunoprecipitation of DLC1 variants was verified by probing the membrane with GFP-specific antibody (top panel). Equal expression of 14-3-3τ was verified by immunoblotting of WCE with HA-specific antibody (bottom panel). (C) HEK293T cells were transiently transfected with expression plasmids encoding Flag-tagged DLC1 WT or S327/431 and empty vector (-) or GFP-tagged PKD1 (+), respectively. WCE were subjected to GST-14-3-3τ pulldowns and analyzed as described in A. Expression of PKD1 and DLC1 variants was verified by immunoblotting of WCE with GFP- and Flag-specific antibodies, respectively (bottom panels). (D) HEK293T transiently expressing GFP-DLC1 WT or S327/431A were treated left untreated or treated with 100 nM OA for 2 h or 1 µM PDBu for 15 min. WCE were subjected to GST-14-3-3τ pulldowns and analyzed as described in A. (E) HEK293T cells transiently expressing GFP-tagged DLC1 WT, S327/431A or S327/431D were left untreated (-) or treated with 1 µM PDBu (+) for 15 min. WCE were subjected to GST-14-3-3τ pulldowns and analyzed as described in A. (F) HEK293T cells transiently expressing GFP-tagged DLC1 WT, S327/431A, S327/419/431A, or S236/327/419/431A were left untreated (-) or treated with 1 µM PDBu (+) for 15 min. WCE were subjected to GST-14-3-3τ pulldowns and analyzed as described in A. (G) Recombinant GST-DLC1(aa242-569) proteins were incubated in kinase buffer containing [^{32}P]-γ-ATP in the absence (left lanes) or presence of purified myc-tagged PKD1 (right lanes). Proteins were separated by SDS-PAGE and transferred to membrane. Incorporation of radioactive phosphate was analyzed using a PhosphoImager (top panel), followed by immunoblotting with GST- and myc-specific antibodies to verify equal loading (bottom panels). The GST-DLC1 fusion proteins and myc-PKD1 are marked with arrows in the autoradiogram.

to alanine double exchange mutant in terms of 14-3-3 binding (Fig. 4E), indicating that introduction of negative charge is not sufficient to mimic a phosphorylated 14-3-3 recognition motif.

To provide direct evidence that PKD is capable of phosphorylating serines 327 and 431 in DLC1 we fused a fragment spanning these sites (amino acids 242-569) to GST and subjected the recombinant fusion protein to an in vitro kinase assay with purified PKD1. This fusion protein was phosphorylated only in the presence of PKD1 (Fig. 4G). A fusion protein in which serines 327 and 431 were mutated to alanines incorporated significantly lower amounts of radiolabeled phosphate, proving that these serines are genuine PKD phosphorylation sites (Fig. 4G). No phosphorylation was observed when serine 419, which also matches a PKD consensus sequence, was additionally mutated (Fig. 4G). However, as shown in Figure 4F, this site does not contribute to 14-3-3 binding.

14-3-3 binding blocks DLC1 RhoGAP function

We next sought to address the functional consequences of 14-3-3 binding to DLC1. DLC1 is a GAP protein reported to enhance GTP hydrolysis rates of RhoA, B and C (Healy et al. 2008;Wong et al. 2003). To study how 14-3-3 binding may affect DLC1-mediated Rho inactivation we made use of a genetically encoded fluorescence resonance energy transfer (FRET)-based RhoA biosensor, termed Raichu-RhoA (Yoshizaki et al. 2003). This sensor consists of full-length RhoA, the Rho binding domain (RBD) of the effector PKN, which specifically binds Rho-GTP, and the fluorescence donor-acceptor pair CFP and YFP. Upon activation by GTP loading, the RBD binds RhoA, modifying the orientation of the fusion protein and allowing FRET to occur. RhoA activation is approximated to be proportional to the ratio of FRET/CFP emission. As expected, transient expression of Raichu-RhoA together with DLC1 in HEK293T cells led to a decreased emission ratio measured in cellular lysates, indicating stimulation of RhoA-GTP hydrolysis (Fig. 5A). This was partially reversed upon coexpression of 14-3-3τ, suggesting that association with 14-3-3 proteins inactivates DLC1 GAP function. By contrast, coexpression of 14-3-3τ had no significant effect on the GAP activity of DLC1 S327/431A in this assay (Fig. 5A).

To address how 14-3-3 binding to DLC1 impacts on endogenous Rho signaling we analyzed the ability of DLC1 to block SRF-dependent transcription, which is known to require functional Rho (Posern and Treisman 2006). Here we used Flp-In T-Rex 293 cells that stably express the Tet repressor and contain a single genomic Flp recombination target site to generate an inducible DLC1-expressing line by Flp recombinase-mediated integration of a GFP-tagged DLC1 cDNA under the control of tetracycline-regulatable promoter. In these stable 293 Flp-In-DLC1 cells, GFP-DLC1 expression was tightly controlled, with no expression observed in the absence of doxycycline (Fig. 5B, top panel). Cellular RhoA levels were not affected by doxycycline-induced DLC1 expression (Fig. 5B, bottom panel). These cells were transfected with a SRF-responsive luciferase reporter along with empty vector or a 14-3-3τ expression plasmid, serum-starved and doxycycline was added to induce DLC1 expression. Cells were then stimulated with PDBu, which activates
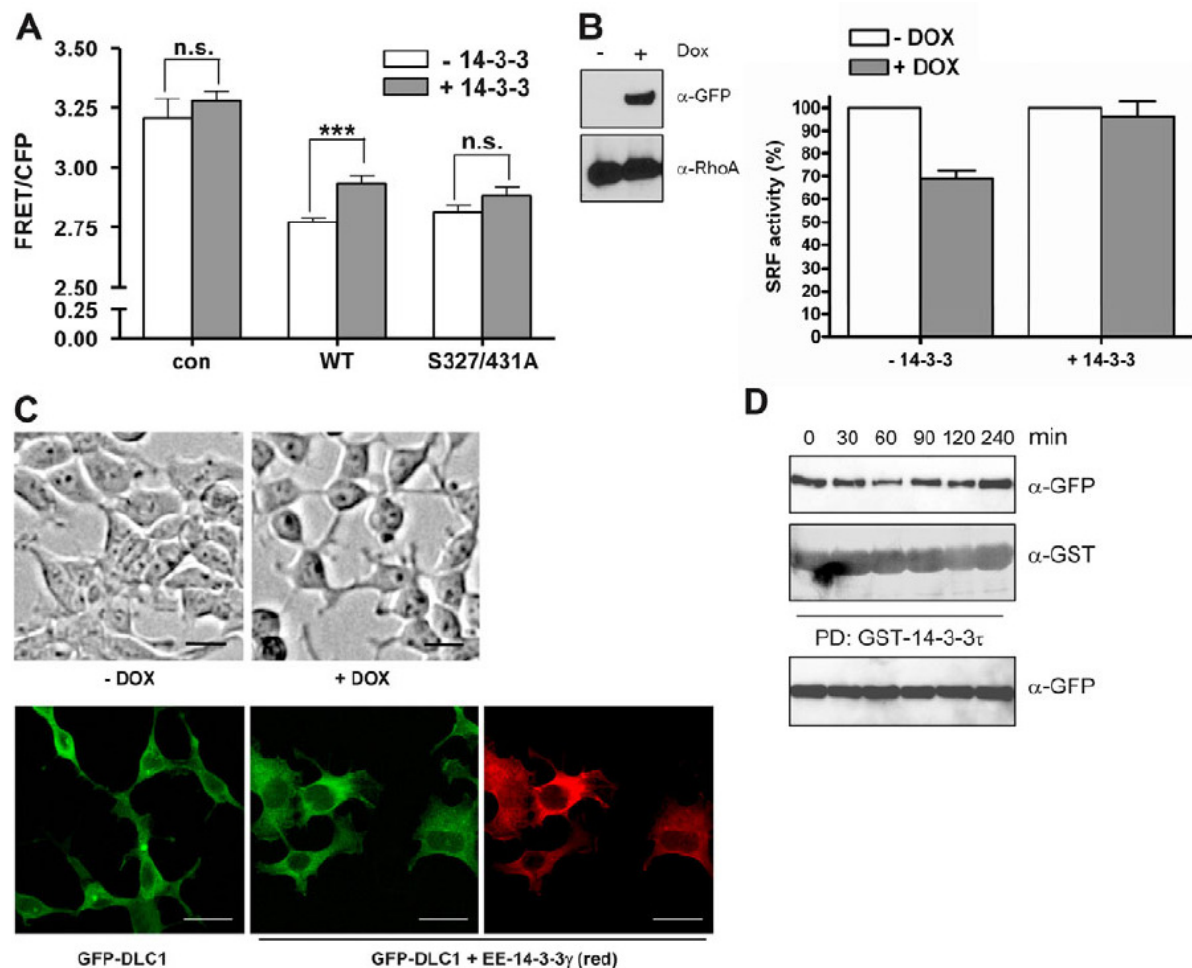
Fig. 5: 14-3-3 binding inhbits DLC1 RhoGAP activity. (A) HEK293T cells were transiently transfected with expression vectors encoding Raichu-RhoA (con) along with Flag-DLC1 WT or S327/431A, and HA-14-3-3τ where indicated. The emission ratio of Raichu-RhoA was determined by measuring YFP (FRET) and CFP fluorescence (excitation 433 nm) in cell lysates. Equal expression of 14-3-3τ and DLC1 proteins was verified by immunoblotting of lysates with HA- and Flag-specific antibodies, respectively (not shown). The mean of 3 independent experiments performed with triplicate samples is shown; error bars represent SEM. Results were statistically significant for the wild type protein (two-tailed unpaired t-test, $p = 0.0006$); no significant difference was observed for the control and the S327/431A mutant protein (n.s., $p > 0.05$). (B) 293 Flp-In-DLC1 cells were left untreated (-) or treated with 10 ng/ml doxycycline (+) over night to induce GFP-DLC1 expression. WCE were separated by SDS-PAGE and analyzed by Western blotting with GFP- (top panel) and RhoA-specific antibodies (bottom panel). For SRF reporter assays, Flp-In-DLC1 cells were transiently transfected with the 3DA.Luc reporter, pTK-Renilla and HA-14-3-3τ or empty vector. Cells were left untreated (- DOX) or treated with 10 ng/ml doxycycline (+ DOX) for 4 h, followed by PDBu stimulation (100 nM) for additional 4 h. Firefly luciferase activity in cell lysates was determined and normalized by Renilla luciferase activity. Fold inductions after PDBu stimulation were calculated and values for uninduced cells (-DOX) were set to 100%. Expression of DLC1 and 14-3-3 proteins was verified by immunoblotting of lysates with GFP- and HA-specific antibodies, respectively (not shown). The mean of 3 independent experiments performed with triplicate samples is shown, error bars represent SEM. (C) Flp-In-DLC1 cells were left untreated or treated with 10 ng/ml doxycycline over night and photographed with a Leitz DM IRB microscope equipped with a NPLAN 10/0.25 PH1 objective (Leica) and an AxioCam MRc camera (Zeiss) (left panels). Flp-In-DLC1 cells were transiently transfected with empty vector or EE-14-3-3γ expression plasmid, followed by induction of GFP-DLC1 expression with 10 ng/ml doxycycline over night. Cells were fixed and stained with EE-specific antibody (red) (right panels). Stacks of several confocal sections are shown. Scale bars, 20 μm. (D) Flp-In-DLC1 cells were treated with 10 ng/ml doxycycline over night, trypsinized and kept in suspension for 1 h. Cells were then plated onto collagen-coated dishes for the indicated times and lysed. WCE were subjected to a pulldown with GST-14-3-3τ beads and bound proteins were separated by SDS-PAGE. DLC1 was detected with GFP-specific antibody (top panel). The integrity of recombinant GST-14-3-3τ was verified by probing the membrane with GST-specific antibody (middle panel), and expression of DLC1 was verified by immunoblotting of WCE with GFP-specific antibody (bottom panel).

SRF-mediated transcription and simultaneously induces DLC1 phosphorylation. DLC1 expression was found to inhibit PDBu-induced SRF-dependent transcription by approximately 30% compared to the uninduced control (Fig. 5B). Coexpression of 14-3-3τ almost completely abrogated the inhibitory effect of DLC1 on SRF-mediated gene expression (Fig. 5B), confirming the results obtained with the exogenous RhoA biosensor.
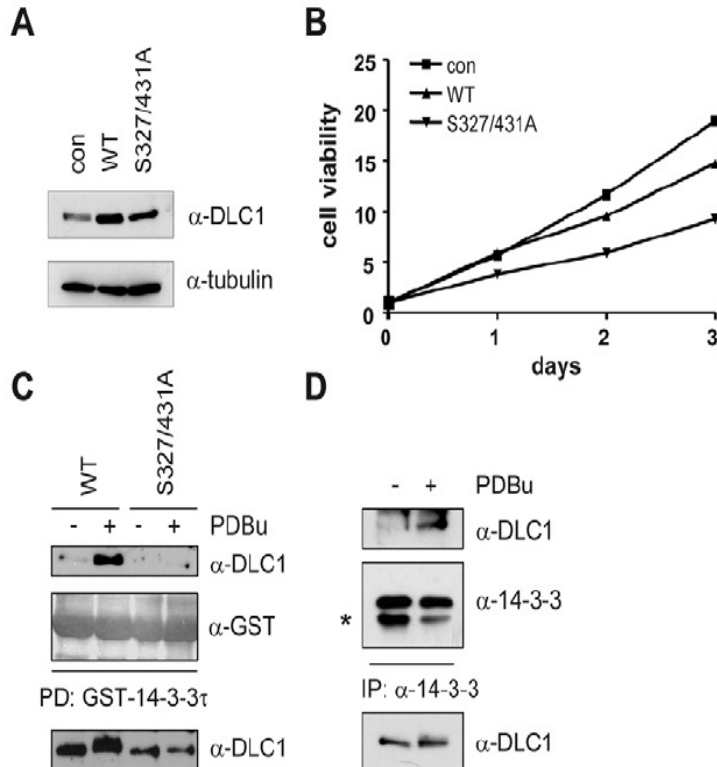

Fig. 6: Stable expression of DLC1 variants in MCF7 cells inhibits proliferation. (A) Stable expression of DLC1 variants in MCF7 cells was verified by immunoblotting of WCE using a DLC1-specific antibody (top panel). Equal loading was confirmed by probing the membrane with tubulin-specific antibody (bottom panel). (B) Proliferation of MCF7 cells stably overexpressing DLC1 WT and S327/431A, respectively, and vector control cells was measured by MTT assay. Data are normalized to absorbance at day 0. (C) MCF7 DLC1 WT and S327/431A cells were left untreated or treated with 1 μM PDBu for 15 min prior to lysis. WCE were subjected to a pulldown with GST-14-3-3τ beads and bound proteins were separated by SDS-PAGE. DLC1 was detected with DLC1-specific antibody (top panel). The integrity of recombinant GST-14-3-3τ was verified by probing the membrane with GST-specific antibody (middle panel), and expression of DLC1 was verified by immunoblotting of WCE with DLC1-specific antibody (bottom panel). (D) MCF7 DLC1 WT cells were left untreated or treated with 1 μM PDBu prior to lysis. 14-3-3 proteins were immunoprecipitated from WCE with 14-3-3-specific rabbit pAb. Immune complexes were separated by SDS-PAGE. Coprecipitated DLC1 was detected by Western blotting with DLC1-specific antibody (top panel). Immunoprecipitation of 14-3-3 proteins were verified by probing the membrane with 14-3-3-specific rabbit pAb (middle panel; IgG chains are marked with an asterisk). Expression of DLC1 was verified by immunoblotting of WCE with DLC1-specific antibody (bottom panel).

Overexpression of DLC1 has been shown to cause cell detachment associated with the disassembly of stress fibers and focal adhesions, whose establishment and maintenance require active Rho (Sekimata et al. 1999;Wong et al. 2005). In line with these observations, 293 Flp-In cells lost their spread appearance and presented with a rounded cell body and long spindle-shaped extensions when DLC1 expression was induced (Fig. 5C). Transfection of cells with an expression plasmid encoding 14-3-3γ prior to DLC1 induction rescued this phenotype (Fig. 5C). RhoA activity is transiently inhibited during the course of cell adhesion and spreading (Arthur et al. 2000;Ren et al. 1999). To investigate the potential dynamic regulation of DLC1 by integrin engagement, we performed GST-14-3-3τ pulldown assays with lysates from 293 Flp-In cells induced to express DLC1 and plated onto collagen-coated dishes for different periods of time (Fig. 5D). In suspended cells, DLC1 was found to associate with 14-3-3τ. Upon plating, DLC1 interaction with GST-14-3-3τ initially decreased and then increased

again at later times (Fig. 5D), indicating an inverse relationship between DLC1 and RhoA activation kinetics in adhering cells.

Ectopic expression of DLC1 has been shown to inhibit cell proliferation (Ng et al. 2000;Yuan et al. 2003;Yuan et al. 2004;Zhou et al. 2004). We therefore stably expressed DLC1 wild type and the S327/431A mutant in MCF7 cells, which express low levels of endogenous DLC1 (Fig. 6A), and analyzed their impact on cell proliferation. Compared to the wild type protein, the DLC1 mutant was more active in inhibiting cell growth as assessed by MTT assays (Fig. 6B). To verify that DLC1 was subject to the same molecular regulation in these cells, we performed pulldown assays with GST-14-3-3τ. As seen in HEK293 cells, the wild type protein was readily precipitated from MCF7 cell lysates in a PDBu-inducible fashion, whereas interaction was barely visible in the case of the S327/431A mutant protein (Fig. 6C). Ectopically expressed Flag-DLC1 further coimmunoprecipitated with endogenous 14-3-3 proteins upon PDBu stimulation of MCF7-DLC1 cells (Fig. 6D). Taken together, these data suggest that the phosphorylation-dependent interaction with 14-3-3 proteins negatively regulates DLC1 function, by preventing inactivation of Rho signaling.

14-3-3 binding inhibits DLC1 nuclear import by masking a novel NLS

14-3-3 binding often affects cellular localization of protein partners by sequestration. We noted that serine 431 in DLC1 lies in close proximity to a potential NLS that follows the 'pat7' rule: This pattern starts with a proline and is followed within 3 residues by a basic segment containing 3 arginines or lysine residues out of 4 (Fig. 7A, aa 423-429, underlined). The basic cluster at this position may also be part of a bipartite NLS, which is characterized by 2 basic residues, a 10-residue spacer, and another basic region consisting of at least 3 basic residues out of 5 (Fig. 7A, highlighted in bold) (Nakai and Horton 1999). These basic residues are recognized by importin α proteins that bind cargo to be transported to the nucleus. To first investigate whether DLC1 shuttles through the nucleus, we expressed GFP-tagged DLC1 in MCF7 cells, followed by treatment of cells with leptomycin B (LMB), an antifungal antibiotic that inhibits Crm1-dependent nuclear export. In untreated cells, DLC1 was evenly distributed in the cytoplasm, without any nuclear localization detectable under these steady-state conditions (Fig. 7B, left panel). However, after treatment of cells with LMB for 2 h DLC1 was predominantly found in the nucleus (Fig. 7B, right panel), indicating that DLC1 molecules undergo continuous nuclear import and export. To determine whether the potential mono- or bipartite NLS neighboring serine 431 was responsible for DLC1 nuclear import, we exchanged the arginines 428 and 429 with glycine residues and analyzed protein localization before and after LMB treatment. In the absence of LMB, the DLC1 R428/429 mutant was indistinguishable from the wild type protein (data not shown). However, after 2 h of LMB treatment, the DLC1 R428/429 mutant was homogenously distributed in both compartments (Fig. 7C, left panel). Less than 20% of cells displayed accumulation of the DLC1 R428/429 mutant

protein in the nucleus, as compared to approximately 80% of cells expressing the wild type protein (Fig. 7D). Mutation of arginines 415 and 416 had a negligible effect on LMB-induced DLC1 nuclear accumulation, indicating that these residues are unlikely to be part of a bipartite NLS (Fig. 7D). To rule out any contribution of this first basic cluster, we generated a quadruple DLC1 R415/416/428/429G mutant. This mutant demonstrated nuclear import kinetics identical to the R428/429G mutant (Fig. 7D), suggesting that the second basic cluster is sufficient for the generation a functional NLS. Since the R428/429G mutant displayed slower import kinetics but was not excluded from the nucleus completely, other motifs that contribute to DLC1 nuclear import are likely to exist. In the DLC1 aminoterminus three additional potential NLS were found using the Psort prediction program, however, mutation of none of these basic clusters affected LMB-induced
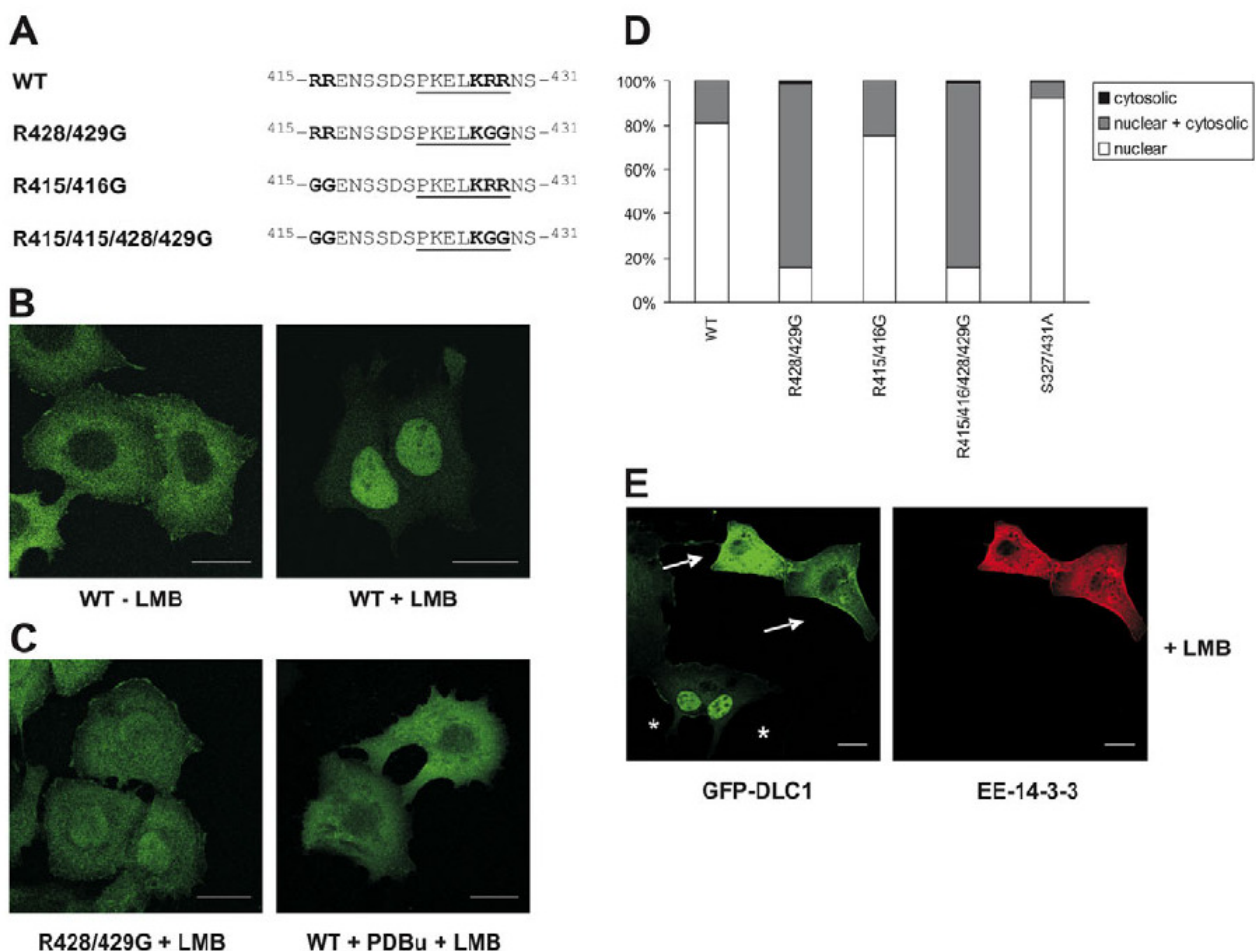

Fig. 7: 14-3-3 binding inhibits DLC1 nuclear transport mediated by an NLS spanning amino acids 423-429. (A) Schematic representation of DLC1 WT and arginine to glycine exchange mutants. The putative bipartite NLS is highlighted in bold, the pat7 NLS is underlined. (B, C) MCF7 cells were transiently transfected with GFP-tagged DLC1 WT or R428/429G and treated with LMB for 2 h prior to fixation. In C (right panel), cells were stimulated with 100 nM PDBu prior to LMB addition. (D) MCF7 cells transiently expressing the indicated GFP-tagged DLC1 variants were treated with LMB for 2 h and fixed. The number of cells displaying mainly cytosolic, homogenous (nuclear + cytosolic) or mainly nuclear protein distribution was determined by counting 100 cells each in random microscopic fields. Values correspond to the mean of 2 independent experiments. (E) COS7 cells were transiently transfected with both GFP-tagged DLC1 and EE-14-3-3γ expression vectors and treated with 10 ng/ml LMB for 1 h prior to fixation and staining with EE-specific antibody. Cells expressing only DLC1 are marked with asterisks, cells expressing DLC1 and 14-3-3γ are marked with arrows. All images are single confocal sections. Scale bars, 20 µm.

nuclear accumulation of DLC1. It is possible that these sequences assist in nuclear entry and only when mutated simultaneously will the protein escape recognition and be trapped in the cytoplasm.

We next tested whether the phosphorylation status was involved in the regulation of DLC1 nucleocytoplasmic shuttling. To this end, cells expressing GFP-DLC1 were treated with PDBu for 15 min prior to LMB administration for 2 h. As shown in Figure 7C (right panel), phorbol ester stimulation prevented LMB-induced nuclear accumulation of DLC1, raising the possibility that DLC1 phosphorylation and 14-3-3 binding may interfere with NLS function. In agreement with this hypothesis, the DLC1 S327/431A mutant identif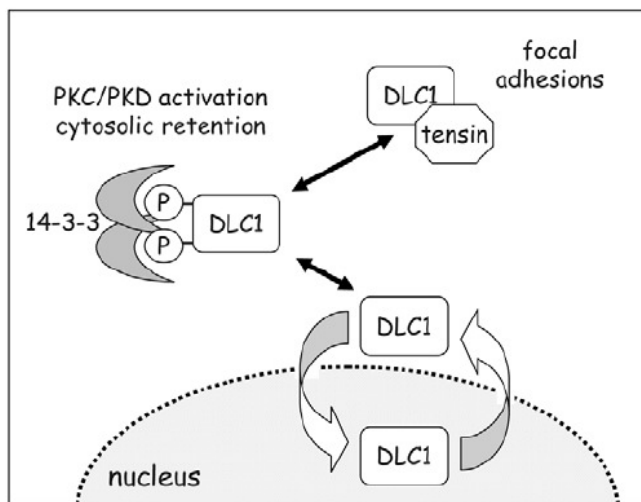ied to be severely impaired in 14-3-3 binding accumulated more rapidly in the nucleus, with more than 90% of the cells presenting with nuclear DLC1 localization after 2 h of LMB treatment (Fig. 7D). Finally, we examined whether 14-3-3γ coexpression was capable of preventing DLC1 nucleocytoplasmic shuttling. Cells that only expressed DLC1 demonstrated LMB-induced nuclear accumulation as expected, whereas DLC1 was retained in the cytoplasm in cells expressing both proteins (Fig. 7E). Phorbol ester-induced activation of PKC and PKD kinases thus leads to DLC1 phosphorylation on multiple sites, which include serines 327 and 431. This promotes 14-3-3 adaptor protein binding, whereby DLC1 RhoGAP activity is inhibited and the protein sequestered in the cytoplasm by masking of a novel NLS (see Fig. 8 for a model).

Fig. 8: Regulation of DLC1 by 14-3-3 binding. Activation of PKC/PKD kinases leads to DLC1 phosphorylation on sites that include serines 327 and 431. This creates binding sites for 14-3-3 adaptor proteins, whereby DLC1 RhoGAP activity is inhibited, most likely by cytosolic sequestration. 14-3-3 binding furthermore masks a nuclear localization signal spanning amino acids 423 – 429, thus preventing DLC1 nucleocytoplasmic shuttling.

Discussion

Here we report a novel phosphorylation dependent interaction between the RhoGAP protein DLC1 and 14-3-3 adaptors. In GST pulldown assays DLC1 interacted with all 14-3-3 isoforms except 14-3-3σ. The latter isoform is unique in that it is primarily expressed in epithelial tissues and appears to be involved in cellular responses to DNA damage and in human oncogenesis. Structural analysis revealed that 14-3-3σ preferentially homodimerizes and that residues specific to this isoform determine substrate selection (Wilker et al. 2005). The other 14-3-3 members are ubiquitously expressed, readily form homo- and heterodimers and could therefore potentially participate in the regulation of DLC1 function. Recent global 14-3-3 interaction screens identified many proteins involved in cytoskeletal regulation, including several GEFs and GAPs, implicating a

general role for 14-3-3 proteins in cellular architecture (Angrand et al. 2006;Jin et al. 2004;Rubio et al. 2004). The RhoGEF AKAP-Lbc, for example, is phosphorylated by PKA, which recruits 14-3-3 proteins and suppresses its GEF activity (Diviani et al. 2004;Jin et al. 2004). DLC1 was not isolated in any of these screens, possibly due to low expression levels and/or low basal phosphorylation.

Inhibition of cellular protein phosphatase activity with OA stabilized DLC1 in a hyperphosphorylated form, as deduced from the dramatic shift in electrophoretic mobility, which suggests phosphorylation on multiple sites. We provide evidence that phorbol ester stimulation promotes DLC1 phosphorylation on serines 327 and 431 and at least one additional site to generate cooperating 14-3-3 binding motifs. Mutation of both serines 327 and 431 in DLC1 was necessary to impair 14-3-3 binding. Due to dimeric nature of 14-3-3, protein contact through multiple sites is a common theme. In fact, a phosphopeptide with two 14-3-3 binding motifs binds 14-3-3 with a 30-fold greater affinity than a phosphopetide containing a single motif (Yaffe et al. 1997). DLC1 association with 14-3-3 proteins was blocked by pharmacological inhibition of the phorbol ester-responsive kinases PKC and PKD. Based on our in vitro kinase assay results, serines 327 and 431 are most likely phosphorylated by PKD directly. The additional phorbol ester-induced 14-3-3 binding site that remains to be identified appears to be phosphorylated independently of PKD. It is possible that this site is phosphorylated by PKC but it could also be a substrate of a kinase activated indirectly by phorbol ester stimulation. Serine 322 in rat DLC1 is phosphorylated in response to insulin (Hers et al. 2006) and according to Scansite could generate a 14-3-3 binding site. However, insulin treatment of HEK293T cells expressing human DLC1 did not enhance 14-3-3 binding as judged by GST pulldowns. Moreover, alanine mutation of the equivalent serine in the human protein had no influence on DLC1 interaction with 14-3-3 proteins (data not shown), making it unlikely that this site is involved in 14-3-3 binding.

14-3-3 proteins often regulate cellular processes by modulating target protein localization. Here we provide evidence for a pat7 NLS spanning amino acids 423-429 that appears to be masked by phorbol ester-induced DLC1 phosphorylation and 14-3-3 binding. Inactivation of this NLS by exchange of criticial arginine residues impaired but did not prevent nuclear import. This suggests that at least one additional NLS exists that contributes to DLC1 nuclear shuttling. The function of DLC1 in the nucleus remains to be defined. The carboxyterminal polybasic region of Rac1 was shown to function as a NLS. In RhoA, this region does not have functional NLS activity, but other Rho GTPases that are transported to the nucleus via their polybasic region may serve as substrates for DLC1 (Williams 2003). Alternatively, DLC1 may have non-GTPase substrates in this compartment. Rat DLC1 was originally reported to bind and activate phospholipase C δ1 (PLC-δ1) (Homma and Emori 1995), an enzyme that translocates to the nucleus during specific phases of the cell cycle (Stallings et al. 2005). However, in overexpression studies human DLC1 did not stimulate phospholipid hydrolysis activity of PLC-δ1 (Healy et al. 2008). The nucleus may alternatively restrict the amount of DLC1 available in the cytoplasm to control cellular Rho-GTP

levels. In a recent publication nuclear translocation of DLC1 was proposed to be associated with apoptosis by a yet unknown mechanism (Yuan et al. 2007). The authors further claimed that nuclear entry was mediated by a bipartite NLS involving arginines 415 and 416. This contrasts with our data that rule out contribution of these residues to nuclear transport. The different results may be explained by the substitution of arginines 415/416 with bulky tryptophan residues (as opposed to glycines used in our study), which may alter conformation and functionality of the pat7 NLS located further downstream.

It has now become apparent that 14-3-3 mediated compartmentalization is not restricted to nuclear proteins but is a regulatory mechanism that also applies to proteins that shuttle from the cytoplasm to the plasma membrane. Ras is a membrane-bound small GTPase, with many of its effectors and regulators being cytosolic. To exert their function, these molecules must translocate to the cell surface. Interestingly, PKD has been implicated in the regulation of such a translocation process by direct phosphorylation of the Ras effector RIN1 on serine 351, which creates a 14-3-3 binding site (Wang et al. 2002). When 14-3-3 binding is disrupted, RIN1 exhibits increased association with the plasma membrane and competes with Raf for Ras binding. We observed that DLC1 expressed in MCF7 cells was associated with focal adhesions and the plasma membrane, in line with previous reports. Coexpression of 14-3-3 proteins had no obvious influence on DLC1 targeting to these subcellular compartments, as judged by indirect immunofluorescence and cell fractionations (data not shown). However, since 14-3-3 binding requires DLC1 phosphorylation, a low stoichiometry of phosphorylation may impede visualization of location changes. A DLC1 variant that constitutively binds 14-3-3 proteins would be required to address this issue, but the attempt to generate such a mutant by introducing negatively charged amino acids was not successful. In cells treated with phorbol ester DLC1 was mainly cytosolic, suggesting exclusion of the phosphorylated protein from focal adhesions. However, phorbol ester treatment appeared to generally affect cellular cytoskeletal architecture as judged by immunostaining of the focal adhesion protein paxillin (Fig. S1). 14-3-3γ and τ expressed in MCF7 cells colocalized with DLC1 in the cytosol and at the plasma membrane, but were excluded from focal adhesions, suggesting that 14-3-3 interaction occurs with the soluble and membrane-bound DLC1 pool. If 14-3-3 association does not relocate DLC1 from the plasma membrane, it is also possible that inhibition of DLC1 function is due to a conformational change elicited by 14-3-3 binding that blocks its GAP activity.

DLC1 is directed to focal adhesions by interacting with tensin proteins and this localization has been proposed to be associated with biological activity (Liao et al. 2007;Qian et al. 2007;Yam et al. 2006). Although still active with respect to GAP function, DLC1 mutants deficient in tensin binding were no longer able to suppress cell growth. The 4 tensin members have a phosphotyrosine binding domain that mediates interaction with the cytoplasmic tails of β integrins (Lo 2004). Tensins 1-3 also interact with actin at multiple sites in their aminoterminal region, as opposed to the shorter tensin 4 (also known as cten) that lacks the actin binding sites. Interaction with tensins

was mapped to amino acids 440-445 in DLC1 and occurs via the tensin Src homology 2 (SH2) domain (Liao et al. 2007;Qian et al. 2007). This tensin binding sequence in DLC1 is adjacent to the 14-3-3 binding site harboring serine 431, prompting the idea that 14-3-3 proteins may compete with tensin interaction. However, phorbol ester-induced phosphorylation of DLC1 did not suppress interaction with the cten SH2 domain in GST pulldown assays (data not shown). Since the tensin phosphotyrosine binding domain has also been implicated in interacting with the DLC1 aminoterminus (Qian et al. 2007;Yam et al. 2006), it remains to be tested with full-length proteins whether 14-3-3 and tensin binding are mutually exclusive.

Complex formation with 14-3-3 proteins, at least downstream of phorbol ester-induced intracellular signaling, appears to be a regulatory mechanism restricted to DLC1. GST pulldown assays did not reveal any PDBu-induced 14-3-3 binding to the structurally related DLC2 or DLC3 proteins. This agrees with the fact that serines 327 and 431 are not conserved in DLC2 and DLC3, nor is the NLS identified in this study, suggesting distinct modes of regulation provided by the non-conserved linker regions, despite their overlapping in vitro substrate specificities. PKD participates in the regulation of diverse cellular processes, including cell migration, proliferation and secretory transport from the trans-Golgi compartment to the plasma membrane. To accomplish these diverse functions, depending on the cell type and external stimulus, PKD localizes to the Golgi complex, the plasma membrane and is also found in the nucleus (Rykx et al. 2003;Wang 2006). In future studies, it will be of particular interest to define the compartment in which PKD phosphorylates DLC1 and extend our investigations on physiological conditions that trigger inhibitory DLC1 phosphorylation and 14-3-3 association, with a special focus on cell adhesion processes, to maintain local Rho signaling.

Material and Methods

Antibodies and reagents

Antibodies used were: mouse anti-Flag mAb (Sigma-Aldrich), mouse anti-GFP mAb (Roche), goat anti-GST pAb (GE Healthcare), mouse anti-GluGlu mAb (Hiss Diagnostics), rabbit anti-14-3-3 pAb (K19), mouse anti-14-3-3 mAb (H8), rabbit anti-GFP pAb (FL) and mouse anti-Rho mAb (26C4) (Santa Cruz Biotechnology), mouse anti-DLC1 mAb (BD), mouse anti-α-tubulin mAb (Sigma). Mouse anti-myc mAb, clone 9E10, and mouse anti-HA mAb, clone 12CA5, were kindly provided by H. Böttinger (University of Stuttgart, Germany). HRP-labeled secondary anti-mouse and anti-rabbit IgG antibodies were from Amersham, HRP-labeled secondary anti-goat IgG antibody was from Santa Cruz Biotechnology; alkaline phosphatase-labeled secondary anti-goat IgG antibody was from Sigma; Alexa Fluor 546-labeled secondary anti-mouse IgG antibody was from Molecular Probes. Staurosporine and okadaic acid were from Alexis; Gö6983, Gö6976, PDBu and doxycycline were from Calbiochem, and LMB was from Biomol.

DNA constructs

pCS2+MT-DLC1 encoding myc-tagged DLC1 was kindly provided by I. Ng. Full-length DLC1 cDNA was amplified by PCR using pCS2+MT-DLC1 as a template with primers containing BamHI restriction sites (DLC1-for: 5'-cgcggatcctgcagaaagaagccggaccc-3' and DLC1-rev: 5'-cgcggatcctcac ctagatttggtgtctttgg-3') and cloned into Flag-pEFrPGKpuro, pEGFPC1, and pcDNA5/FRT/TO-GFP (see below) vectors. Truncated DLC1 variants were generated by PCR amplification using the following primers: DLC1-ΔSAM (5'-cgcggatccatt agtcctcatcggaaacgaag-3' and DLC1-rev); DLC1-ΔStart (DLC1-for and 5'-cgcggatcctcacagg tgcccgagtgcttc-3'); DLC1-ΔC (DLC1-for and 5'-cgcggatc ctcacatgaacttgggcacggcc-3'); DLC-ΔN (5'-cgcggatccaagaggatcaaggttccagac-3' and DLC1-rev). DLC1 point mutants were generated by Quikchange site-directed PCR mutagenesis according to the manufacturer's instructions (Stratagene). The forward primers used were: S236A-for (5'-gctgaa acggatggaggccctgaagctcaagagc-3'); S327A-for (5'-gttacgaggacccgggccctcagtgcgtgc-3'); S419A-for (5'-cctcaggagggaaaacgctagcgacagccccaagg-3'); S431A-for (5'-ctgaagagacgcaatgcttccagctccatga gc-3'); R415/416G-for (5'-gccacatcagcctcggggggggaaaacagtagcg-3'); R428/429G-for (5'-cccaaggaa ctgaagggaggcaattcttccagctcc-3'). To generate the inducible DLC1 expression vector pcDNA5/FRT/TO-GFP-DLC1, the enhanced GFP cDNA was excised from the pEGFPC1 vector with Eco47III and KspA1 and ligated with pcDNA5/FRT/TO digested with MssI. The DLC1 cDNA was then inserted in frame as a BamHI fragment. All amplified cDNAs were verified by sequencing. Oligonucleotides were purchased from MWG Biotech. pEGFPN1-PKD1, pGEX-14-3-3τ WT and R56/60, HA-tagged 14-3-3τ and EE-tagged 14-3-3γ and ζ in pEF vectors have been described previously (Hausser et al. 2005;Hausser et al. 2006;Olayioye et al. 2003). pGEX-DLC1(aa242-569)-WT, -S327/431A and -S327/419/431A constructs were generated by subcloning of Ecl136II fragments from the respective full length constructs into the pGEX6P1 vector linearized with SmaI.

Cell culture and transfection

HEK293T, COS7, MCF7 and MDAMB231 cells were grown in RPMI containing 10% FCS in a humified atmosphere containing 5% CO_2. HEK293T cells were transfected using TransIT293 reagent (Mirus). For immunofluorescence, MCF7 and COS7 cells were grown on glass coverslips and transfected with Lipofectamine 2000 (Invitrogen). Flp-In T-Rex 293 cells (Invitrogen) were grown in DMEM containing 10% FCS, 100 µg/ml zeocin and 15 µg/ml blasticidin. These cells stably express the Tet repressor and contain a single Flp Recombination Target (FRT) site and were used to generate the Flp-In-DLC1 line. Cells were cotransfected with pcDNA5/FRT/TO-GFP-DLC1 and the Flp recombinase expression plasmid pOG44 at a ratio of 1:10 and then selected with 100 µg/ml hygromycin. Stable MCF7 lines were generated by transfection of vectors encoding Flag-tagged DLC1 wild type and S327/431, or empty vector as a control, followed by selection with 1,5 µg/ml puromycin for 10 days.

Immunofluorescence microscopy

Cells were fixed in 4% PFA for 10 min, washed and incubated with PBS containing 0.1 M glycine for 15 min. Cells were permeabilized with PBS containing 0.1% Triton for 5 min and blocked with 5% goat serum in PBS containing 0.1% Tween-20 for 30 min. Cells were then incubated with primary antibody diluted in blocking buffer for 2 h, followed by incubation with secondary antibody diluted in blocking buffer for 1 h. Coverslips were mounted in Fluoromount G (Southern Biotechnology) and analyzed on a confocal laser scanning microscope (TCS SL, Leica) using 488 and 543 nm excitation and a 40.0/1.25 HCX PL APO objective lens.

Bacterial expression of GST proteins

E. coli were transformed with pGEX vectors encoding GST-14-3-3 proteins, DLC1(aa242-569) variants or GST alone and expression was induced with 0.1 mM IPTG for 4 h at 37°C. The bacterial cultures were harvested and pellets were resuspended in PBS containing Complete protease inhibitors (Roche). The suspension was then sonicated 3x for 10 s on ice, Triton X-100 was added to a final concentration of 1% and the lysate centrifuged for 10 min at 8,000 x g. Purification of GST-tagged proteins was performed with glutathione resin (GE Healthcare). The resin was washed with PBS and the purity and amount of bound GST proteins was then determined by SDS-PAGE and Coomassie staining.

Pulldowns, immunoprecipitations, and Western Blotting

Whole cell extracts (WCE) were obtained by solubilizing cells in Triton extraction buffer (TEB) [50 mM Tris (pH 7.5), 150 mM NaCl, 1% Triton X-100, 1 mM sodium orthovanadate, 10 mM sodium fluoride, and 20 mM β-glycerophosphate plus Complete protease inhibitors]. Lysates were clarified by centrifugation at 16,000 x g for 10 min. Pulldowns were performed by incubating WCE with immobilized GST proteins for 2 h. Beads were washed 3x with TEB. For immunoprecipitations, equal amounts of protein were incubated with specific antibodies for 2 h on ice. Immune complexes were collected with protein G-Sepharose (GE Healthcare) and washed 3x with TEB. In the case of stably expressed Flag-DLC1 precipitation was over night and washes were with TEB containing 0.5% Triton X-100. Precipitated proteins were released by boiling in sample buffer, subjected to SDS-PAGE and blotted onto PVDF membranes (Roth). After blocking with 0.5% blocking reagent (Roche) in PBS containing 0.1% Tween 20, filters were probed with specific antibodies. Proteins were visualized with HRP-coupled secondary antibody using the ECL detection system (Pierce) or alkaline phosphatase-coupled secondary antibody and NBT/BCIP as a substrate.

Kinase assays

Equal amounts of the purified GST-DLC1(aa242-569) proteins were mixed with kinase buffer (50mM Tris pH 7.4, 10mM $MgCl_2$, 1mM DTT) containing 2 µCi [γ-^{32}P]-ATP and incubated for 5min

at 37°C in presence or absence of 50 ng purified myc-PKD1 (Dieterich et al. 1996). Samples were then resolved by SDS-PAGE, transferred to membrane and analyzed on a PhosphoImager (Molecular Dynamics), followed by immunoblotting.

Luciferase reporter assays

293 Flp-In-DLC1 cells were grown on collagen-coated 24-well dishes and transfected with 50 ng each of the 3DA.Luc firefly luciferase reporter containing 3 SRF binding elements, pRL-TK, a Renilla luciferase plasmid under the control of the thymidine kinase promoter, and pEF-HA-14-3-3τ. After serum starvation over night, DLC1 expression was switched on by addition of 10 ng/ml doxycycline and, 4 h later, cells were stimulated with 100 nM PDBu for 4 h. Cells were lysed with 300 µl passive lysis buffer (Promega) and luciferase activities in 10 µl lysate were measured by addition of 50 µl firefly substrate [470 µM D-luciferin, 530 µM ATP, 270 µM coenzyme A, 33 mM DTT, 20 mM Tricine, 2,67 mM $MgSO_4$, 01 mM EDTA, pH 7,8], followed by addition of 100 µl Renilla substrate [0,7 µM coelenterazine, 2,2 mM Na_2EDTA, 0,44 mg/ml bovine serum albumin, 1,1 M NaCl, 1,3 mM NaN_3, 0.22 M potassium phosphate buffer, pH 5,0]. Luminescence was measured with a Tecan Infinite 200M plate reader.

Rho activity measurements

HEK293T cells transiently expressing the Raichu-RhoA biosensor were lysed in 50 mM Tris pH 7.5, 5 mM β-glycerophosphate, 5 mM sodium fluoride and 0.5% Triton X-100 and debris was removed by centrifugation at 16,000 x g for 10 min. Emission ratios (FRET/CFP) were determined by measuring CFP and YFP fluorescence after background subtraction at 475 and 530 nm, respectively, using a Tecan Infinite 200M plate reader (excitation = 433 nm).

MTT assays

2000 cells in 150 µl medium were plated into 96 well plates (n = 5) and incubated with 15 µl of 3-(4,5-dimethylthiazol-2yl-)2,5-diphenyl tetrazolium bromide (MTT) solution (5 mg/ml) for 2 h. Cells were lysed in 100 µl 50 % dimethylformamide containing 10 % SDS and absorbance at 595 nm was determined with background subtraction at 655 nm and absorbance of medium alone using a SpectraMax 340PC[384] reader (Molecular Devices).

Acknowledgments

References

Angrand, P. O., Segura, I., Volkel, P., Ghidelli, S., Terry, R., Brajenovic, M., Vintersten, K., Klein, R., Superti-Furga, G., Drewes, G., Kuster, B., Bouwmeester, T., and Acker-Palmer, A. (2006). Transgenic mouse proteomics identifies new 14-3-3-associated proteins involved in cytoskeletal rearrangements and cell signaling. *Mol.Cell Proteomics.* 5, 2211-2227.

Arthur, W. T., Petch, L. A., and Burridge, K. (2000). Integrin engagement suppresses RhoA activity via a c-Src-dependent mechanism. *Curr.Biol.* 10, 719-722.

Bernards, A. and Settleman, J. (2005). GAPs in growth factor signalling. *Growth Factors* 23, 143-149.

Bridges, D. and Moorhead, G. B. (2004). 14-3-3 proteins: a number of functions for a numbered protein. *Sci.STKE.* 2004, re10.

Ching, Y. P., Wong, C. M., Chan, S. F., Leung, T. H., Ng, D. C., Jin, D. Y., and Ng, I. O. (2003). Deleted in liver cancer (DLC) 2 encodes a RhoGAP protein with growth suppressor function and is underexpressed in hepatocellular carcinoma. *J.Biol.Chem.* 278, 10824-10830.

Dieterich, S., Herget, T., Link, G., Bottinger, H., Pfizenmaier, K., and Johannes, F. J. (1996). In vitro activation and substrates of recombinant, baculovirus expressed human protein kinase C mu. *FEBS Lett.* 381, 183-187.

Diviani, D., Abuin, L., Cotecchia, S., and Pansier, L. (2004). Anchoring of both PKA and 14-3-3 inhibits the Rho-GEF activity of the AKAP-Lbc signaling complex. *EMBO J.* 23, 2811-2820.

Dougherty, M. K. and Morrison, D. K. (2004). Unlocking the code of 14-3-3. *J.Cell Sci.* 117, 1875-1884.

Durkin, M. E., Ullmannova, V., Guan, M., and Popescu, N. C. (2007a). Deleted in liver cancer 3 (DLC-3), a novel Rho GTPase-activating protein, is downregulated in cancer and inhibits tumor cell growth. *Oncogene* 26, 4580-4589.

Durkin, M. E., Yuan, B. Z., Zhou, X., Zimonjic, D. B., Lowy, D. R., Thorgeirsson, S. S., and Popescu, N. C. (2007b). DLC-1:a Rho GTPase-activating protein and tumour suppressor. *J.Cell Mol.Med.* 11, 1185-1207.

Favre, B., Turowski, P., and Hemmings, B. A. (1997). Differential inhibition and posttranslational modification of protein phosphatase 1 and 2A in MCF7 cells treated with calyculin-A, okadaic acid, and tautomycin. *J.Biol.Chem.* 272, 13856-13863.

Goodison, S., Yuan, J., Sloan, D., Kim, R., Li, C., Popescu, N. C., and Urquidi, V. (2005). The RhoGAP protein DLC-1 functions as a metastasis suppressor in breast cancer cells. *Cancer Res.* 65, 6042-6053.

Griner, E. M. and Kazanietz, M. G. (2007). Protein kinase C and other diacylglycerol effectors in cancer. *Nat.Rev.Cancer* 7, 281-294.

Hausser, A., Link, G., Hoene, M., Russo, C., Selchow, O., and Pfizenmaier, K. (2006). Phospho-specific binding of 14-3-3 proteins to phosphatidylinositol 4-kinase III beta protects from dephosphorylation and stabilizes lipid kinase activity. *J.Cell Sci.* 119, 3613-3621.

Hausser, A., Storz, P., Martens, S., Link, G., Toker, A., and Pfizenmaier, K. (2005). Protein kinase D regulates vesicular transport by phosphorylating and activating phosphatidylinositol-4 kinase IIIbeta at the Golgi complex. *Nat.Cell Biol.* 7, 880-886.

Healy, K. D., Hodgson, L., Kim, T. Y., Shutes, A., Maddileti, S., Juliano, R. L., Hahn, K. M., Harden, T. K., Bang, Y. J., and Der, C. J. (2008). DLC-1 suppresses non-small cell lung cancer growth and invasion by RhoGAP-dependent and independent mechanisms. *Mol.Carcinog.* 47, 326-337.

Hers, I., Wherlock, M., Homma, Y., Yagisawa, H., and Tavare, J. M. (2006). Identification of p122RhoGAP (deleted in liver cancer-1) Serine 322 as a substrate for protein kinase B and ribosomal S6 kinase in insulin-stimulated cells. *J.Biol.Chem.* 281, 4762-4770.

Homma, Y. and Emori, Y. (1995). A dual functional signal mediator showing RhoGAP and phospholipase C-delta stimulating activities. *EMBO J.* 14, 286-291.

Jaffe, A. B. and Hall, A. (2005). Rho GTPases: biochemistry and biology. *Annu.Rev.Cell Dev.Biol.* 21, 247-269.

Jin, J., Smith, F. D., Stark, C., Wells, C. D., Fawcett, J. P., Kulkarni, S., Metalnikov, P., O'Donnell, P., Taylor, P., Taylor, L., Zougman, A., Woodgett, J. R., Langeberg, L. K., Scott, J. D., and Pawson, T. (2004). Proteomic, functional, and domain-based analysis of in vivo 14-3-3 binding proteins involved in cytoskeletal regulation and cellular organization. *Curr.Biol.* 14, 1436-1450.

Liao, Y. C., Si, L., deVere White, R. W., and Lo, S. H. (2007). The phosphotyrosine-independent interaction of DLC-1 and the SH2 domain of cten regulates focal adhesion localization and growth suppression activity of DLC-1. *J.Cell Biol.* 176, 43-49.

Lo, S. H. (2004). Tensin. *Int.J.Biochem.Cell Biol.* 36, 31-34.

Moon, S. Y. and Zheng, Y. (2003). Rho GTPase-activating proteins in cell regulation. *Trends Cell Biol.* 13, 13-22.

Nakai, K. and Horton, P. (1999). PSORT: a program for detecting sorting signals in proteins and predicting their subcellular localization. *Trends Biochem.Sci.* 24, 34-36.

Ng, I. O., Liang, Z. D., Cao, L., and Lee, T. K. (2000). DLC-1 is deleted in primary hepatocellular carcinoma and exerts inhibitory effects on the proliferation of hepatoma cell lines with deleted DLC-1. *Cancer Res.* 60, 6581-6584.

Nishikawa, K., Toker, A., Johannes, F. J., Songyang, Z., and Cantley, L. C. (1997). Determination of the specific substrate sequence motifs of protein kinase C isozymes. *J.Biol.Chem.* 272, 952-960.

Obenauer, J. C., Cantley, L. C., and Yaffe, M. B. (2003). Scansite 2.0: Proteome-wide prediction of cell signaling interactions using short sequence motifs. *Nucleic Acids Res.* 31, 3635-3641.

Olayioye, M. A., Guthridge, M. A., Stomski, F. C., Lopez, A. F., Visvader, J. E., and Lindeman, G. J. (2003). Threonine 391 phosphorylation of the human prolactin receptor mediates a novel interaction with 14-3-3 proteins. *J.Biol.Chem.* 278, 32929-32935.

Posern, G. and Treisman, R. (2006). Actin' together: serum response factor, its cofactors and the link to signal transduction. *Trends Cell Biol.* 16, 588-596.

Qian, X., Li, G., Asmussen, H. K., Asnaghi, L., Vass, W. C., Braverman, R., Yamada, K. M., Popescu, N. C., Papageorge, A. G., and Lowy, D. R. (2007). Oncogenic inhibition by a deleted in liver cancer gene requires cooperation between tensin binding and Rho-specific GTPase-activating protein activities. *Proc.Natl.Acad.Sci.U.S.A* 104, 9012-9017.

Ren, X. D., Kiosses, W. B., and Schwartz, M. A. (1999). Regulation of the small GTP-binding protein Rho by cell adhesion and the cytoskeleton. *EMBO J.* 18, 578-585.

Ridley, A. J. (2006). Rho GTPases and actin dynamics in membrane protrusions and vesicle trafficking. *Trends Cell Biol.* 16, 522-529.

Rubio, M. P., Geraghty, K. M., Wong, B. H., Wood, N. T., Campbell, D. G., Morrice, N., and Mackintosh, C. (2004). 14-3-3-affinity purification of over 200 human phosphoproteins reveals new links to regulation of cellular metabolism, proliferation and trafficking. *Biochem.J.* 379, 395-408.

Rykx, A., De Kimpe, L., Mikhalap, S., Vantus, T., Seufferlein, T., Vandenheede, J. R., and Van Lint, J. (2003). Protein kinase D: a family affair. *FEBS Lett.* 546, 81-86.

Sekimata, M., Kabuyama, Y., Emori, Y., and Homma, Y. (1999). Morphological changes and detachment of adherent cells induced by p122, a GTPase-activating protein for Rho. *J.Biol.Chem.* 274, 17757-17762.

Stallings, J. D., Tall, E. G., Pentyala, S., and Rebecchi, M. J. (2005). Nuclear translocation of phospholipase C-delta1 is linked to the cell cycle and nuclear phosphatidylinositol 4,5-bisphosphate. *J.Biol.Chem.* 280, 22060-22069.

Vega, R. B., Harrison, B. C., Meadows, E., Roberts, C. R., Papst, P. J., Olson, E. N., and McKinsey, T. A. (2004). Protein kinases C and D mediate agonist-dependent cardiac hypertrophy through nuclear export of histone deacetylase 5. *Mol.Cell Biol.* 24, 8374-8385.

Wang, Q. J. (2006). PKD at the crossroads of DAG and PKC signaling. *Trends Pharmacol.Sci.* 27, 317-323.

Wang, Y., Waldron, R. T., Dhaka, A., Patel, A., Riley, M. M., Rozengurt, E., and Colicelli, J. (2002). The RAS effector RIN1 directly competes with RAF and is regulated by 14-3-3 proteins. *Mol.Cell Biol.* 22, 916-926.

Wilker, E. W., Grant, R. A., Artim, S. C., and Yaffe, M. B. (2005). A structural basis for 14-3-3sigma functional specificity. *J.Biol.Chem.* 280, 18891-18898.

Williams, C. L. (2003). The polybasic region of Ras and Rho family small GTPases: a regulator of protein interactions and membrane association and a site of nuclear localization signal sequences. *Cell Signal.* 15, 1071-1080.

Wong, C. M., Lee, J. M., Ching, Y. P., Jin, D. Y., and Ng, I. O. (2003). Genetic and epigenetic alterations of DLC-1 gene in hepatocellular carcinoma. *Cancer Res.* 63, 7646-7651.

Wong, C. M., Yam, J. W., Ching, Y. P., Yau, T. O., Leung, T. H., Jin, D. Y., and Ng, I. O. (2005). Rho GTPase-activating protein deleted in liver cancer suppresses cell proliferation and invasion in hepatocellular carcinoma. *Cancer Res.* 65, 8861-8868.

Xing, H., Zhang, S., Weinheimer, C., Kovacs, A., and Muslin, A. J. (2000). 14-3-3 proteins block apoptosis and differentially regulate MAPK cascades. *EMBO J.* 19, 349-358.

Yaffe, M. B., Rittinger, K., Volinia, S., Caron, P. R., Aitken, A., Leffers, H., Gamblin, S. J., Smerdon, S. J., and Cantley, L. C. (1997). The structural basis for 14-3-3:phosphopeptide binding specificity. *Cell* 91, 961-971.

Yam, J. W., Ko, F. C., Chan, C. Y., Jin, D. Y., and Ng, I. O. (2006). Interaction of deleted in liver cancer 1 with tensin2 in caveolae and implications in tumor suppression. *Cancer Res.* 66, 8367-8372.

Yoshizaki, H., Ohba, Y., Kurokawa, K., Itoh, R. E., Nakamura, T., Mochizuki, N., Nagashima, K., and Matsuda, M. (2003). Activity of Rho-family GTPases during cell division as visualized with FRET-based probes. *J.Cell Biol.* 162, 223-232.

Yuan, B. Z., Jefferson, A. M., Baldwin, K. T., Thorgeirsson, S. S., Popescu, N. C., and Reynolds, S. H. (2004). DLC-1 operates as a tumor suppressor gene in human non-small cell lung carcinomas. *Oncogene* 23, 1405-1411.

Yuan, B. Z., Jefferson, A. M., Millecchia, L., Popescu, N. C., and Reynolds, S. H. (2007). Morphological changes and nuclear translocation of DLC1 tumor suppressor protein precede apoptosis in human non-small cell lung carcinoma cells. *Exp.Cell Res.* 313, 3868-3880.

Yuan, B. Z., Zhou, X., Durkin, M. E., Zimonjic, D. B., Gumundsdottir, K., Eyfjord, J. E., Thorgeirsson, S. S., and Popescu, N. C. (2003). DLC-1 gene inhibits human breast cancer cell growth and in vivo tumorigenicity. *Oncogene* 22, 445-450.

Zhou, X., Thorgeirsson, S. S., and Popescu, N. C. (2004). Restoration of DLC-1 gene expression induces apoptosis and inhibits both cell growth and tumorigenicity in human hepatocellular carcinoma cells. *Oncogene* 23, 1308-1313.

7.5. Simultaneous loss of the DLC1 and PTEN tumor suppressors enhances breast cancer cell migration

Johanna Heering, Patrik Erlmann and Monilola A. Olayioye[#]

University of Stuttgart, Institute of Cell Biology and Immunology,

Allmandring 31, 70569 Stuttgart, Germany

Corresponding author:

Monilola A. Olayioye, Tel: +49 711 685 69301, Fax: + 49 711 685 67484

Email: monilola.olayioye@izi.uni-stuttgart.de

Abstract

The phosphatase and tensin homolog (PTEN) gene is a tumor suppressor frequently deleted or mutated in sporadic tumors of the breast, prostate, endometrium and brain. The protein acts as a dual specificity phosphatase for lipids and proteins. PTEN loss confers a growth advantage to cells, protects from apoptosis and favors cell migration. The deleted in liver cancer 1 (DLC1) gene has emerged as a novel tumor suppressor downregulated in a variety of tumor types including those of the breast. DLC1 contains a Rho GTPase activating domain that is involved in the inhibition of cell proliferation, migration and invasion. To investigate how simultaneous loss of PTEN and DLC1 contributes to cell transformation, we downregulated both proteins by RNA interference in the non-invasive MCF7 breast carcinoma cell line. Joint depletion of PTEN and DLC1 resulted in enhanced cell migration in wounding and chemotactic transwell assays. Interestingly, both proteins were found to colocalize at the plasma membrane and interacted physically in biochemical pulldowns and coimmunoprecipitations. We therefore postulate that the concerted local inactivation of signaling pathways downstream of PTEN and DLC1, respectively, is required for the tight control of cell migration.

Introduction

Cancer is a multistep process arising from the cellular accumulation of gain of function mutations that target oncogenes and/or loss of function mutations of so-called tumor suppressors. Germline mutations of the PTEN gene located on chromosome 10q23 are the cause of Cowden disease, which is characterized by the development of hamartomas and other benign tumors, and a higher risk of developing breast and thyroid cancers later in their life. Genetic alteration of both PTEN alleles occurs in nearly all types of human cancers examined, with inactivation usually due to mutation accompanied by loss of heterozygosity (LOH) [1;2]. In breast tumorigenesis, loss of PTEN is associated with a poor outcome of cancer patients. Although somatic PTEN mutations are detected only in a smaller fraction of breast cancer cases, LOH at the PTEN locus is frequently found [3;4]. Immunohistochemical studies, however, revealed that loss of PTEN protein expression is a common event in breast cancer [5-7], indicating that epigenetic mechanisms might be responsible for a number of cases in which PTEN levels are downregulated or even totally ablated in the absence of a detectable mutation.

Complete loss of PTEN in mice is lethal early in development [8-10]. Heterozygous mice are viable, however, and adults eventually develop LOH of the remaining PTEN allele, leading to the appearance of tumors in the endometrium, liver, prostate, gastrointestinal tract, thyroid and thymus, including breast cancer [8-12]. Conditional deletion of the Pten gene in the mammary gland caused excessive ductal branching, precocious lobuloalveolar development and delayed involution. By 10 months of age, 50% of these mice (n=37) developed breast tumors [13].

PTEN contains an aminoterminal phosphatase domain that acts on both protein and lipid substrates, a carboxyterminal C2 domain that interacts in a Ca2+-independent manner with phospholipid substrates to mediate recruitment to the membrane and a carboxyterminal PDZ binding motif. PTEN specifically dephosphorylates phosphatidylinositol 3,4,5-trisphosphate (PIP3), thereby antagonizing the phosphatidylinositol 3-kinase (PI3K) signaling pathway [14]. PIP3 levels are very low in resting cells and increase upon activation of cell surface receptors that recruit PI3K. PIP3 binds pleckstrin homology domain containing proteins, the most important ones being Akt/PKB and their regulator PDK1 [15]. Cells lacking PTEN have elevated levels of PIP3 and consequently a constitutively active PI3K signaling pathway. These cells display elevated rates of proliferation, growth and motility and resistance to apoptosis [15].

The DLC1 gene was originally isolated as a candidate tumor suppressor gene in primary human hepatocellular carcinoma located on chromosome 8p22 [16]. Loss of expression due to chromosomal deletion or promoter hypermethylation has subsequently been shown in other tumor types, including breast, colon, prostate, and lung [17;18]. DLC1 contains a GAP domain specific for the small GTPases RhoA, B and C, and to a lesser extent Cdc42 [19;20]. It further contains an aminoterminal sterile alpha motif (SAM) and a StAR-related lipid transfer (START) domain at its carboxyterminus, whose function remain to be characterized. The Rho family of GTPases regulate diverse biological processes that include actin cytoskeletal rearrangements, gene transcription, cell cycle regulation, apoptosis and membrane trafficking [21;22]. Rho proteins cycle between a GTP-bound active state to interact with effector proteins, modulating their activity and localization, and an inactive GDP-bound state. Signaling of growth factor receptors and integrins can induce exchange of GDP for GTP on Rho proteins. This activation of Rho proteins is controlled by the guanine nucleotide exchange factors (GEFs), which promote the release of bound GDP and facilitate GTP binding, and the GAP proteins, which increase the intrinsic GTPase activity of Rho GTPases to accelerate the return to the inactive state [21;22].

Initial studies towards understanding the function of DLC1 were based on overexpression of the protein in different carcinoma cell lines, demonstrating inhibition of cell proliferation, migration and invasion [17]. The consequences of DLC1 loss have only recently been investigated. First evidence supporting a bona fide tumor suppressive function of DLC1 was provided by Xue et al., who showed that shRNA-mediated knock-down of DLC1 promoted carcinogenesis of liver cells in an in vivo model [23]. Work from our own laboratory revealed that DLC1 loss is sufficient to promote a more migratory behavior of breast cancer cells [24]. Cell migration relies on a complex series of events that include the formation of membrane protrusions driven by actin polymerization at the cell front and actomyosin-driven contraction of the cell body at the back. The coordination of these events requires a multi-molecular network of proteins that fulfill diverse functions [25]. Here we provide evidence that DLC1 and PTEN are part of such a protein complex involved in the regulation of cell migration.

Material and Methods

Antibodies and reagents

Antibodies used were: mouse anti-DLC1, mouse anti-Dia1 and mouse anti-FAK (pY397) mAbs (BD), rabbit anti-PTEN mAb and rabbit anti-phospho-T308-Akt pAb (Cell Signalling), and mouse anti-tubulin mAb (Sigma). The HA-specific mouse mAb 9E10 was provided by H. Böttinger (University of Stuttgart) HRP-labeled secondary anti-mouse and anti-rabbit IgG antibodies were from GE Healthcare; Alexa Fluor 488- and 546-conjugated secondary anti-mouse and anti-rabbit IgGs were from Invitrogen. PDGF-BB was purchased from R&D.

Plasmids

A plasmid encoding myc-tagged PTEN was kindly provided by B. Lüscher (University Aachen). The PTEN cDNA was amplified by PCR using 5´-CGC GGA TCC ACA GCC ATC ATC AAA GAG ATC-3´ (PTEN-F) and 5´-CGC GGA TCC TCA GAC TTT TGT AAT TTG TGT ATG CTG-3´ (PTEN-R) primers and subcloned into the pEGFPC1 vector (Clontech) as a BamHI fragment. PTEN deletion mutants were generated by PCR using the following primers: pEGFPC1-PTEN-ΔCAT (5´-CGC GGA TCC GTG TAT TAT TAT AGC TAC CTG TTA AAG-3´ and PTEN-R), pEGFPC1-PTEN-ΔPDZ (PTEN-F and 5´-CGC GGA TCC TCA ATC TTC ATC AAA AGG TTC ATT TCT-3´) and pEGFPC1-PTEN-ΔTail (PTEN-F and 5´-CGC GGA TCC TCA CTC CTC TAC TGT TTT TGT GAA G-3´). pEGFPC1-PTEN-S385A and -C124S were generated by Quikchange mutagenesis using the forward primers 5´-CTG ACA CCA CTG ACG CTG ATC CAG AGA ATG-3´ and 5´-GTT GCA GCA ATT CAC AGT AAA GCT GGA AAG GGA CG-3´, respectively, according to the manufacturers instructions (Stratagene). The PTEN-C124S cDNA was then subcloned into the pEFrPuro-HA vector as a BamHI fragment. pEGFPC1-DLC1 WT, K714E and ΔSAM have been described previously [24;26]. The SAM domain of DLC1 was amplified by PCR using the forward 5´-CGC GGA TCC TGC AGA AAG AAG CCG GAC ACC-3´ and reverse primers 5´-CGC CTC GAG TCA ACT TCG TTT CCG ATG AGG ACT-3´ and pEGFPC1-DLC1 as a template and subcloned as a BamHI/XhoI fragment into the pGEX6P3 vector. All constructs were validated by sequencing.

Cell culture and transfection

Cells were cultured in RPMI media (Invitrogen) supplemented with 10% FCS (PAA) in a humidified atmosphere of 5% CO_2 at 37℃. HEK293T cells were transfected with TransIT (Mirus) and MCF7 cells with Lipofectamine 2000 (Invitrogen) according to the manufacturers' instructions. For RNAi, cells were transfected with siRNAs using Oligofectamine reagent according to the manufacturer's instructions (Invitrogen). The siRNAs used were: siDLC1 5'-GGA CAC GGU GUU CUA CAU C dTdT-3' and siDLC1#2 5´-UUA AGA ACC UGG AGG ACU A dTdT-3´; siPTEN 5´-AAC AGU AGA GGA GCC GUC AAA dTdT-3´ and siPTEN#2 5´-CGU UAG CAG AAA CAA AAG GAG dTdT-3´ ;

siLacZ 5'-GCG GCU GCC GGA AUU UAC C dTdT-3'. All siRNAs were obtained from MWG Biotech.

Bacterial expression of GST proteins

E. coli were transformed with pGEX6P3-SAM (aa 2-86) or GST alone and expression was induced with 0.1 mM IPTG for 4 h at 37°C. The bacterial cultures were harvested and pellets were resuspended in PBS containing Complete protease inhibitors (Roche). The suspension was then sonicated 3x for 10 s on ice, Triton X-100 was added to a final concentration of 1% and the lysate centrifuged for 10 min at 8,000 x g. Purification of GST-tagged proteins was performed with glutathione resin (GE Healthcare). The resin was washed with PBS and the purity and amount of bound GST proteins was then determined by SDS-PAGE and Coomassie staining.

Pulldowns, immunoprecipitations, and Western Blotting

Whole cell extracts (WCE) were obtained by solubilizing cells in RIPA buffer [50 mM Tris (pH 7.5), 150 mM NaCl, 1% NP-40, 0.5% sodium deoxycholate, 0.1% SDS, 1 mM sodium orthovanadate, 10 mM sodium fluoride, and 20 mM β-glycerophosphate plus Complete protease inhibitors (Roche)] or in NP40 extraction buffer (NEB) [50 mM Tris (pH 7.5), 150 mM NaCl, 0.5% NP40, 1 mM sodium orthovanadate, 10 mM sodium fluoride, and 20 mM β-glycerophosphate plus Complete protease inhibitors] for pulldowns and coimmunoprecipitations. Lysates were clarified by centrifugation at 16,000 x g for 10 min. Pulldowns were performed by incubating WCE with GST-SAM beads for 2 h. Beads were washed 3x with NEB. For immunoprecipitations, equal amounts of protein were incubated with specific antibodies for 4 h on ice. Immune complexes were collected with protein G-Sepharose (GE Healthcare) and washed 3x with NEB. Precipitated proteins were released by boiling in sample buffer, subjected to SDS-PAGE and blotted onto PVDF membranes (Roth). After blocking with 0.5% blocking reagent (Roche) in PBS containing 0.1% Tween 20, filters were probed with specific antibodies. Proteins were visualized with HRP-coupled secondary antibody using the ECL detection system (Pierce) or alkaline phosphatase-coupled secondary antibody and NBT/BCIP as a substrate.

Immunofluorescence microscopy

Cells grown on glass coverslips coated with 25 µg/ml collagen (Serva) were fixed with 4% PFA in PBS and blocked with PBS-T (PBS with 0.1% Tween-20) supplemented with 5% goat serum (Invitrogen) for 30 min at RT. Cells were then incubated with primary antibody in blocking buffer for 2 h, washed four times for 5 min with PBS-T, and then incubated with secondary antibody in blocking buffer for 1 h at RT. Cells were again washed four times with PBS-T before mounting in Fluoromount G (Southern Biotechnology). Confocal analysis was performed with a Leica TCS SL microscope using 488, 543 and 561 nm excitation and a 40X / 1.25 HCX PL APO oil objective lens. Images were processed with Adobe Photoshop.

Cell migration assays

Transwells (8.0-µm membrane pores; Costar) were coated with 2.5 µg/ml collagen over night at 4°C. 10^5 cells in 100 µl medium with 0.5% FCS were added to the top chamber and allowed to migrate for 8h in the case of serum and over night in the case of PDGF as a chemoattractant. The bottom chamber was supplemented with 10% FCS or 30 ng/ml PDGF in medium containing 0.5% FCS. Cells on the top surface of the membranes were removed using a cotton swab and cells on the underside were fixed in 4% PFA and stained with 0.1% crystal violet. Quantification was done by counting the number of cells in 5 independent microscopic fields at a 20-fold magnification. Experiments were performed in duplicate and repeated at least three times with consistent results.

Wound healing assays

MCF7 cells (6×10^5) were seeded into 12-well dishes. The next day, confluent cell monolayers were wounded with a sterile white micropipette tip and plates were returned to the tissue culture incubator. Images were captured at the beginning and 24 h later.

Cell proliferation assays

MCF7 cells were plated at a density of 5×10^4 cells/ well in 100 µl medium into 96 well plates (n = 3), and cell proliferation was determined by a colorimetic MTT assay for 5 days. Cells were incubated with 10 µl of 3-(4,5-dimethylthiazol-2yl-)2,5-diphenyl tetrazolium bromide (MTT; Sigma) solution (5mg/ml) for 3 h. Cells were lysed with 100 µl solubilization solution (10% SDS, 50% N,N-dimethylformamide) and the absorbance at 595 nm was determined after background subtraction at 655 nm using a Tecan Infinite 200M plate reader.

Results

Simultaneous downregulation of PTEN and DLC1 in MCF7 cells does not confer a growth advantage

To address the question how simultaneous loss of the tumor suppressor proteins PTEN and DLC1 contributes to oncogenic transformation of breast cancer cells, we silenced these genes individually and in combination in MCF7 cells which express both wild type PTEN and DLC1. To first verify silencing efficiency and specificity, cells were transfected with PTEN- and DLC1-specific siRNAs, respectively, and a siRNA targeting β-galactosidase (siLacZ) as a control. Whole cell lysates were prepared three days post transfection and analyzed by immunoblotting. As shown in Figure 1A, PTEN and DLC1 proteins were almost completely downregulated by the respective siRNAs. Consistent with its role as negative regulator of the PI3K signaling pathway, downregulation of PTEN led to increased levels of phosphorylated Akt (Fig. 1A). Interestingly, downregulation of DLC1 also slightly enhanced phosphorylated Akt levels (Fig. 1A). No changes in the total level of phosphorylated focal adhesion kinase (FAK) were observed (Fig. 1A). To analyze the impact of PTEN and DLC1 loss on cell viability, MCF7 cells lacking DLC1 or PTEN, or both,

were subjected to an MTT assay. While silencing of PTEN led to an increased growth rate of cells compared to the siLacZ control, knockdown of DLC1 did not favor cell proliferation (Fig. 1B). Accordingly the combined knock-down of both genes did not confer a growth advantage to cells over those lacking only PTEN.
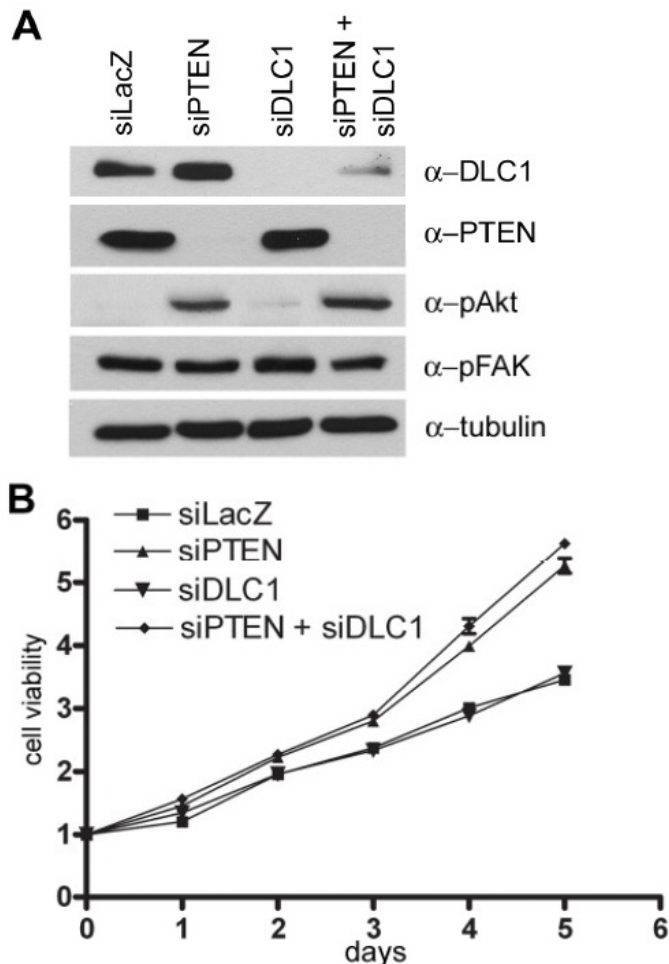

Figure 1: Simultaneous downregulation of PTEN and DLC1 in MCF7 cells does not enhance cell proliferation. (A & B) MCF7 cells were transiently transfected with siRNAs specific for PTEN, DLC1 or PTEN plus DLC1. A LacZ-specific siRNA was used as a negative control and to adjust the siRNA amount in each transfection mix. (A) Three days post transfection, cells were lysed, and equal amounts of total protein were subjected to SDS-PAGE and transferred to membrane. PTEN and DLC1 expression was analyzed by immunoblotting using PTEN- and DLC1-specific antibodies (top panels). The amount of phosphorylated Akt and FAK were analyzed with pAkt(T308)- and pFAK(Y397)-specific antibodies, respectively (panels 3 & 4). Equal loading was verified by reprobing the membrane with tubulin-specific antibody (bottom panel). (B) For analysis of cell proliferation, cells were harvested three days post transfection and replated into 96 well plates in triplicates. Cell proliferation was determined on five consecutive days by performing a colorimetic MTT assay as described in the Material and Methods section.

Simultaneous knock-down of DLC1 and PTEN enhances cell migration

PTEN plays a key role in regulating migration of different mammalian cell types [27;28]. In addition, we have recently shown that silencing of DLC1 enhances breast cancer cell migration [24]. We therefore investigated how the simultaneous loss of PTEN and DLC1 influences the migratory behavior of MCF7 cells by performing wound healing assays. Confluent cell monolayers were wounded with a pipet tip and wound closure was monitored after 24 h. Consistent with their role as negative regulators of cell migration, cells lacking PTEN closed the wound faster than the siLacZ control, as did cells lacking DLC1 (Fig. 2A). Interestingly, joint depletion of PTEN and DLC1 enabled cells to completely close the wound by 24 h (Fig. 2A). The same results were obtained with cells treated with mitomycin C, ruling out a proliferative effect in this assay (data not shown). To further analyze cell motility, we employed transwell filter assays, in which cells were seeded in medium containing 0.5% serum into the top chambers and allowed to migrate across the filter

towards a 10% serum gradient in the bottom chambers. Again, cells lacking PTEN and DLC1, respectively, demonstrated increased cell migration (Fig. 2B, top panel). In the absence of both proteins, cell migration was enhanced even further (Fig. 2B, top panel), which was confirmed with independent siRNAs for both PTEN and DLC1 (siPTEN#2 and siDLC1#2; Fig. 2C). These results are in accordance with those obtained in wound healing assays and suggest that the simultaneous loss of PTEN and DLC1 has an additive effect on cell migration.
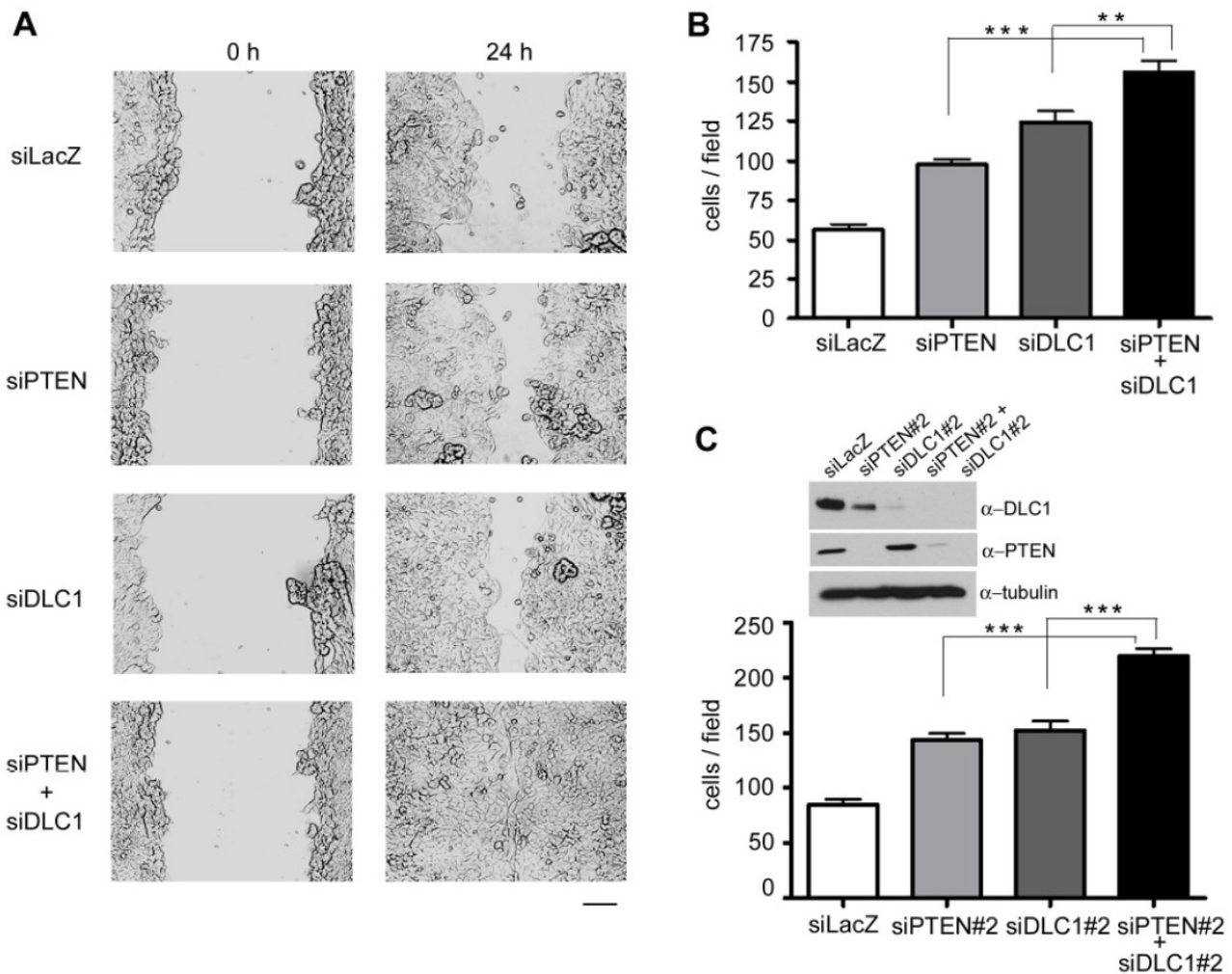

Figure 2: Simultaneous knock-down of DLC1 and PTEN enhances cell migration. (A-C) MCF7 cells were transiently transfected with the indicated siRNAs and harvested three days post transfection. (A) Cells were replated at high density and, the next day, confluent monolayers were scratched with a white pipette tip. Pictures were taken at a 10-fold magnification to document the scratch at time point zero and after incubation for 24 h. Scale bar = 200 µm. (B, C) 10^5 cells were seeded in medium containing 0.5% FCS into the upper chamber of a transwell; the lower well contained medium supplemented with 10% FCS. Cells that had migrated across the filter after 8 h were fixed and stained. The number of migrated cells was determined by counting five independent microscopic fields (20-fold magnification). Data shown are the mean of duplicate wells and error bars represent SEM. A representative experiment out of four is shown. Results for single- versus double-transfected cells were statistically significant (two-tailed unpaired t-test, $p < 0.001$ (***), $p < 0.01$ (**)). (C) Efficient silencing of DLC1 and PTEN using independent siRNAs was verified by immunoblotting as described in Figure 1A.

Colocalization of DLC1 and PTEN at the plasma membrane

Ectopic expression of both DLC1 and PTEN have been reported to lead to dissolution of focal adhesions and actin stress fibers [29;30]. To visualize where DLC1 and PTEN act while conserving cellular morphology, we transiently expressed inactive variants of the two proteins in MCF7 cells (DLC1-K714E and PTEN-C124S) and analyzed their subcellular localization by confocal microscopy. Localization of PTEN is known to be cell type dependent and was seen mainly in the cytosol and in the nucleus as previously described for MCF7 cells [31]. A small proportion of the protein also resided at the plasma membrane. Interestingly, we observed partial colocalization with DLC1 at the cell periphery (Fig. 3).
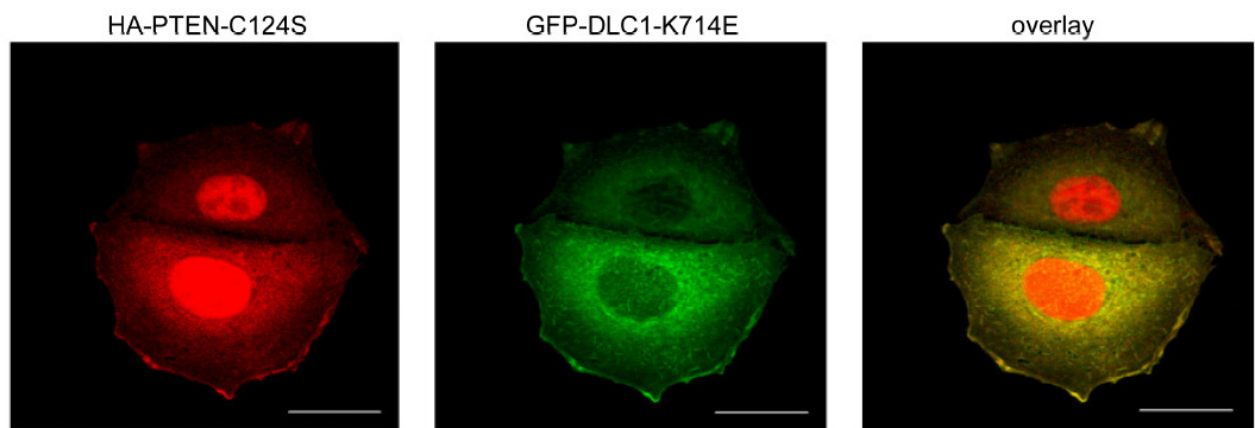

Figure 3: DLC1 and PTEN colocalize at the plasma membrane. MCF7 cells were transiently transfected with expression vectors encoding GFP-DLC1-K714E and HA-PTEN-C124S. The next day, cells were fixed and stained with HA-specific primary and Alexa Fluor 546-labeled secondary antibody (red). Colocalization areas are marked with arrowheads in the overlay. The images shown are stacks of several confocal sections. Scale bars = 20 µm.

The DLC1 SAM domain mediates association with PTEN

The intriguing colocalization of DLC1 and PTEN at the plasma membrane prompted us to investigate whether both proteins are part of a protein signaling complex. To this end, we transiently transfected HEK293T cells with plasmids encoding Flag-DLC1 and GFP-PTEN and immunoprecipitated DLC1 with Flag-specific antibody from cell lysates. By immunoblotting with a GFP-specific antibody, PTEN was readily detected in the immunoprecipitate (Fig. 4A). A DLC1 mutant protein lacking the aminoterminal SAM domain failed to precipitate PTEN, indicating that the interaction was specific and mediated by the SAM domain of DLC1 (Fig. 4A). Further support for this interaction is provided by a pulldown assay with the isolated SAM domain of DLC1 coupled to GST. Here endogenous PTEN could be precipitated from MCF7 cell lysates with GST-SAM but not GST alone (Fig. 4B). We next sought to identify the region in PTEN mediating association with DLC1 and generated various PTEN deletion mutants that lacked the aminoterminal catalytic domain (PTEN-ΔCAT), the carboxyterminal PDZ domain (PTEN-ΔPDZ) or the entire carboxyterminus (PTEN-ΔC). All deletion mutants were still able to interact with the SAM domain of DLC1 (Fig. 4C), suggesting that the C2 domain is involved in mediating interaction with DLC1.

DLC1 preferentially interacts with activated PTEN

We noticed that the PTEN mutant lacking the carboxyterminal tail interacted particularly well with DLC1 (Fig. 4C). The carboxyterminal tail contains several phosphorylation sites which are known to keep the protein in an inactive state [32]. Upon activation, PTEN is dephosphorylated, leading to its recruitment to the plasma membrane where it is turned over rapidly. Serine 385 has been
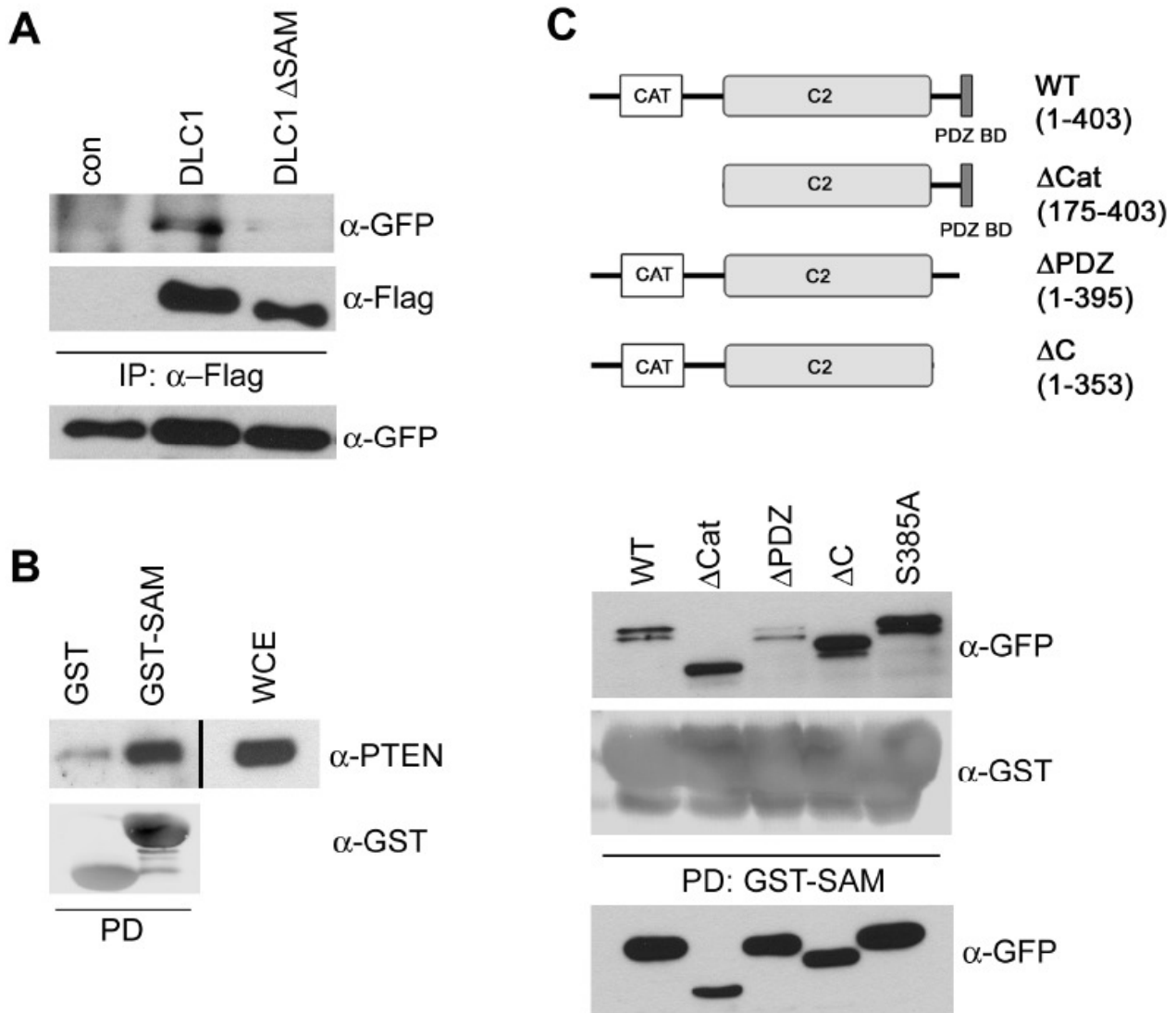

Figure 4: DLC1 and PTEN physically interact via the DLC1 SAM domain. (A) HEK293T cells were transiently transfected with GFP-tagged PTEN and empty vector (con), Flag-tagged full-length DLC1 or DLC1-ΔSAM expression vectors, respectively. Full-length DLC1 and DLC1-ΔSAM were immunoprecipitated from WCE with Flag-specific antibody and immune complexes were separated by SDS-PAGE. Coprecipitated PTEN was detected by Western blotting with GFP-specific antibody (top panel). Immunoprecipitation of full length DLC1 and DLC1-ΔSAM was verified by probing the membrane with Flag-specific antibody (middle panel), and expression of PTEN was verified by immunoblotting of WCE with GFP-specific antibody (bottom panel). (B) WCE of MCF7 cells were incubated with glutathione beads coupled to GST-SAM, or GST alone, and bound proteins were separated by SDS-PAGE. Endogenous PTEN was detected by Western blotting with a PTEN-specific antibody (top panel). The integrity of the GST proteins was verified by probing the membrane with GST-specific antibody (bottom panel). (C) HEK293T cells were transiently transfected with full-length and the different schematically represented GFP-tagged PTEN deletion mutants. WCE were subjected to a pulldown with GST-SAM beads, bound proteins were separated by SDS-PAGE and detected by immunoblotting with GFP-specific antibody. The integrity of GST-SAM was verified by probing the membrane with GST-specific antibody (middle panel) and the expression of the different PTEN variants was verified by immunoblotting of WCE with GFP-specific antibody (bottom panel).

characterized as a priming phosphorylation site and a PTEN-S385A mutant possesses increased activity and membrane binding properties [33]. Similar to PTEN-ΔC, this mutant also demonstrated increased association with DLC1 (Fig. 4C), suggesting that DLC1 preferentially interacts with active, dephosphorylated PTEN. This is in accordance with the colocalization of both proteins observed at the plasma membrane (Fig. 3).

PTEN is known to attenuate PI3K signalling downstream of the platelet-derived growth factor (PDGF) receptor. We therefore investigated the potential regulation of DLC1-PTEN complex formation in response to PDGF treatment of cells. HEK293T cells transiently expressing Flag-DLC1 and GFP-PTEN were serum-starved over night and then stimulated with PDGF for different periods of time (Fig. 5A). Notably, the amount of PTEN detected in DLC1 immunoprecipitates underwent a transient increase, peaking after 15 min of PDGF stimulation (Fig. 5A). To confirm that the endogenous proteins also interact in response to PDGF stimulation, we immunoprecipitated PTEN from lysates of the breast carcinoma cell line MDAMB231, which expresses relatively high levels of DLC1. Indeed, endogenous DLC1 was detected in PTEN immunoprecipitates of PDGF-stimulated MDAMB231 cells (Fig. 5B). To investigate whether migration of MCF7 cells lacking PTEN and DLC1 was also enhanced in response to growth factor
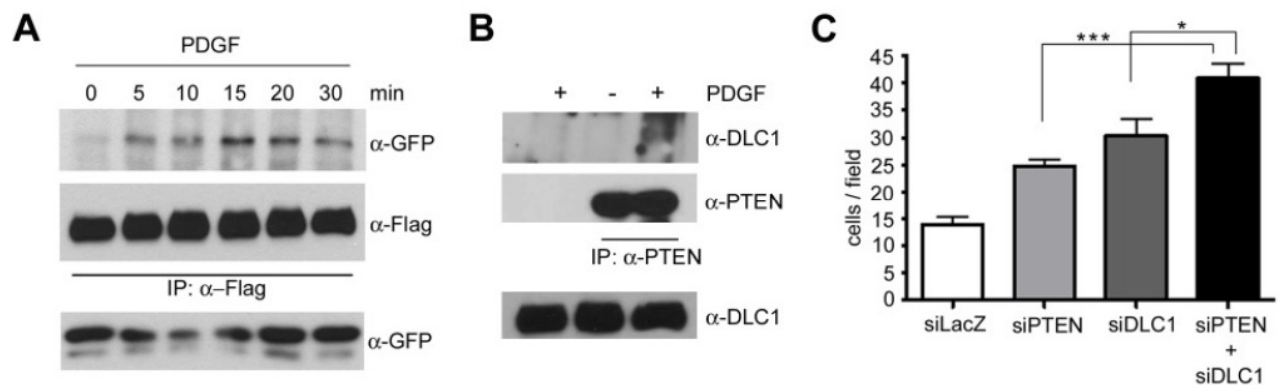

Figure 5: PDGF stimulates association of DLC1 and PTEN. (A) HEK293T cells were transiently transfected with expression vectors encoding Flag-DLC1 and GFP-PTEN. The next day, cells were starved over night and then treated with 30 ng/ml PDGF for the indicated times prior to lysis. DLC1 was immunoprecipitated from WCE with Flag-specific antibody and immune complexes were separated by SDS-PAGE. Coprecipitated PTEN was detected by immunoblotting with GFP-specific antibody (top panel). Immunoprecipitation of DLC1 was verified by reprobing the membrane with Flag-specific antibody (middle panel), and expression of PTEN was verified by immunoblotting of WCE with GFP-specific antibody (bottom panel). (B) MDAMB231 cells were starved over night and left untreated (-) or treated with 30 ng/ml PDGF for 15 min (+) prior to lysis. PTEN was immunoprecipitated from WCE with a PTEN-specific antibody and immune complexes were separated by SDS-PAGE. Coprecipitated DLC1 was detected by immunoblotting with a DLC1-specific antibody (top panel); the left lane shows an IP control without antibody. Immunoprecipitation of PTEN was verified by reprobing the membrane with PTEN-specific antibody (middle panel), and DLC1 expression by immunoblotting of WCE with DLC1-specific antibody (bottom panel). (C) MCF7 cells were transiently transfected with the indicated siRNAs. Three days post transfection, 10^5 cells were seeded in medium containing 0.5% FCS into the upper chamber of a transwell. The lower well contained medium supplemented with 0.5% FCS plus 30 ng/ml PDGF. Cells that had migrated across the filter after over night incubation were fixed and stained. The number of migrated cells was determined by counting five independent microscopic fields (20-fold magnification). Data shown are the mean of duplicate wells and error bars represent SEM. One representative experiment out of three is shown. Results for single- versus double-transfected cells were statistically significant (two-tailed unpaired t-test, $p < 0.001$ (***), $p < 0.05$ (*)).

treatment, we used PDGF as a chemoattractant in the transwell assays. Again, cells in which both DLC1 and PTEN were depleted displayed enhanced migration compared to cells lacking only one of the proteins (Fig. 5C). Of note, in control experiments, haptotaxis (without PDGF) and chemokinesis (PDGF in both chambers) were also increased in the absence of PTEN and DLC1, suggesting a general influence on cell motility (data not shown). However, under these conditions the number of migrated cells was relatively low, whereas robust migration was seen when using a chemotactic set-up.

Activation of FAK and Dia1 in PTEN/DLC1 negative cells

We have recently demonstrated that the Rho effector protein Dia1 is required for enhanced migration of MCF7 cells lacking DLC1 [24]. Several reports suggest that PTEN regulates cell migration independently of its lipid phosphatase activity, potentially by direct dephosphorylation of FAK. To investigate how these molecular targets are influenced in PTEN/DLC1 negative cells, we immunostained cells transfected with the respective siRNAs and subjected to a wounding assay with antibodies specific for autophosphorylated, active FAK (Y397) and Dia1, respectively. In accordance with our previous observations, Dia1 was enriched in membrane protrusions of DLC1-depleted cells at the wound edge compared to the siLacZ control, whereas PTEN loss did not affect Dia1 localization (Fig. 6). In cells lacking PTEN, we noted enhanced pFAK staining in cells migrating to close the wound, which was not the case in siLacZ control and DLC1-negative cells
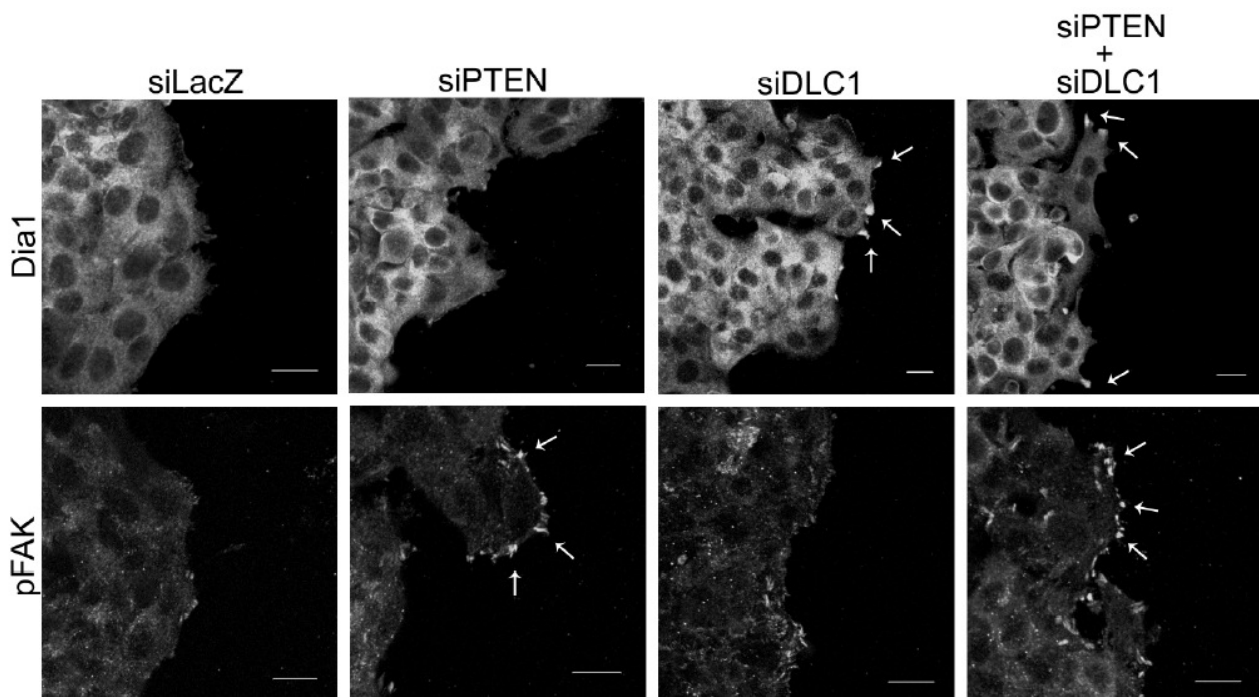

Figure 6: Dia1 and pFAK localization in PTEN/DLC1 negative cells. MCF7 cells were transfected with the indicated siRNAs and plated onto collagen-coated coverslips two days post transfection. Confluent cell monolayers were wounded with a pipet tip, fixed 6 h later and stained with Dia1- and pFAK-specific monoclonal antibodies, followed by Alexa Fluor 488-conjugated secondary antibody. Cells with elevated pFAK- and Dia1 staining are marked with arrows. Images are stacks of several confocal sections. Scale bar, 20 µm.

(Fig. 6). When cells were cotransfected with siRNAs specific for both PTEN and DLC1, pFAK and Dia1 staining, respectively, was similar to that seen in cells lacking the individual proteins (Fig. 6). Therefore, we conclude that PTEN and DLC1 both locally inactivate their respective signaling pathways to ensure tight control of cell migration processes.

Discussion

The development of cancer requires a variety of different mutations to oncogenes and tumor suppressor genes, finally leading to the transformed phenotype. The importance of PTEN as a tumor suppressor in mammary carcinogenesis is implicated by several studies describing the frequent loss of PTEN protein expression in breast tumors [5;6]. However, the long latency observed in different mouse models suggests that PTEN loss is not sufficient for breast tumor formation and requires additional mutations for tumor progression. The absence of PTEN, for example, collaborated with Wnt1 to accelerate the induction of ductal carcinoma in the mammary gland [34]. Similarly, mammary specific deletion of PTEN alleles accelerated mammary tumor progression induced by an activated ErbB2 and increased the frequency of lung metastases [35].

DLC1 expression is also commonly downregulated in breast cancer due to chromosomal deletions and promoter hypermethylation and a recent study reported the occurrence of mutations leading to reduced RhoGAP activity of the protein [36]. Determination of the frequency of simultaneous functional inactivation of PTEN and DLC1 in different cancer types will thus require analysis at the protein level. Here we investigated the cellular consequences of the joint depletion of PTEN and DLC1 in the non-invasive MCF7 breast cancer cell line. Using RNAi, we were able to almost completely downregulate PTEN, correlating with an increase in phosphorylated Akt levels. In line with PTEN overexpression studies in MCF7 cells, which suppressed cell growth due to reduced phospho-Akt levels [37], our results show that PTEN depletion confers a growth advantage to the cells. However, although overexpression of DLC1 in breast cancer cell lines similarly resulted in inhibition of cell growth [38], siRNA-mediated depletion of DLC1 did not augment proliferation of MCF7 cells in comparison to siLacZ-transfected control cells. DLC1 knockdown modestly but reproducibly increased phospho-Akt levels, but these low levels of active Akt do not appear to be sufficient to promote cell proliferation. Accordingly, simultaneous knockdown of both PTEN and DLC1 did not favor cell proliferation compared to cells lacking PTEN alone.

PI3K signaling plays an important role in the regulation of cell migration and particularly in controlling the directionality of chemotaxis. Initial studies in Dictyostelium revealed an accumulation of PIP3 at the leading edge while PTEN localized to the back of the cell [39;40]. Cells lacking PTEN often generate inappropriate pseudopodia at the sides and rear and are thus impaired in the speed and directionality of chemotaxis [41]. In mammalian cells, introduction of PTEN into fibroblast and glioblastoma cell lines was shown to impair cell spreading on fibronectin and inhibit cell migration in wounding assays, which was associated with a reduction of focal adhesions and stress fibers

[29]. Regulation of cell migration by PTEN has been confirmed in other cell types, such as murine B cells and Jurkat T cells [42-44]. However, PTEN appears to be dispensable for chemotactic responses of primary murine neutrophils [45].

The molecular mechanisms underlying PTEN regulation of cell motility in mammalian cells are not fully understood. Initial studies suggested that cell migration occurs independently of the lipid phosphatase domain, but requires the protein phosphatase activity, via direct dephosphorylation of FAK [29]. More recent studies narrowed down the C2 domain to mediate the negative control of cell migration. In the full-length protein the C2 domain appears to be attenuated due to inhibitory phosphorylation of the carboxyterminal tail [46]. PTEN autodephosphorylation thus appears to be a prerequisite to relieve inhibition of the C2 domain and block cell migration. An alternative mechanism by which PTEN may regulate cell migration was proposed by Lilienthal who showed that PTEN-deficient murine fibroblasts migrate faster due to elevated levels of active Rac1 and Cdc42. Alterations in the amount of phosphorylated FAK were not observed, and, in this case, control of cell motility by PTEN was dependent upon its lipid phosphatase activity [42]. It thus appears that the dominant molecular pathway triggered by PTEN to control cell motility may depend on the cell type and/or experimental setup. Although silencing of PTEN in MCF7 cells did not lead to an increase in total cellular pFAK levels (Fig. 1), cells migrating to close a wound displayed enhanced pFAK staining (Fig. 6).

Only a few DLC1 interacting proteins have been described thus far. Localization of DLC1 to focal adhesions is mediated by interaction with tensins [47;48] whereas cytosolic retention and thus inhibition of GAP function is controlled by interaction with 14-3-3 adaptors [26]. DLC1 interaction with PTEN is mediated by the aminoterminal SAM domain, a module of approximately 70 amino acids found in diverse proteins whose function range from signal transduction to transcriptional repression. Structural analysis of the TEL transcriptional repressor SAM domain revealed a mechanism for self-association, but SAM domains also undergo heterotypic interactions with non-SAM domain containing proteins [49]. Physical interaction of PTEN and DLC1 is shown by coimmunoprecipitation of ectopically expressed proteins in HEK293T cells and by association of endogenous PTEN with the DLC1 SAM domain in GST pulldowns.

PTEN carboxyterminal tail phosphorylation is known to affect membrane localization and phosphatase activity of the protein [32]. Phosphorylation on serine 385 is thought to be the priming event for phosphorylation of a cluster of carboxyterminal serines and threonines [33]. When phosphorylated, this cluster interacts with the internal C2 domain leading to an autoinhibition [33;46]. The strong binding of the PTEN S385A mutant to the DLC1 SAM domain in our pulldowns suggests that DLC1 preferentially interacts with active, dephosphorylated PTEN. In agreement with this result, deletion of the PTEN carboxyterminus also led to an increased interaction with DLC1. We furthermore demonstrate that the physical interaction of DLC1 and PTEN is stimulated in

response to PDGF, which activates PI3K signaling and PTEN. Together with the fact that the two proteins colocalize at the membrane, we conclude that a PTEN-DLC1 protein complex is formed to negatively regulate Rho GTPase and PTEN-dependent signaling pathways during cell migration. RhoA was reported to stimulate PTEN activity via Rho kinase mediated phosphorylation, leading to reduction of phospho-Akt levels [50]. It is thus possible that DLC1 either directly or indirectly through Rho inactivation alters PTEN function. Vice versa, PTEN could also influence DLC1 activity. In overexpression experiments we did not observe any synergistic effects of the two proteins with regard to downstream signaling, suggesting that their activities are not interdependent. However, because a PTEN/DLC1 complex is likely to act locally, its activity may only be revealed at the single cell level by imaging of complex formation and signaling events at the plasma membrane in migrating cells. From our data we conclude that the local concerted action of PTEN, targeting FAK, and that of DLC1, impinging on Dia1, is necessary for the synchronization of signaling processes during cell migration and propose that loss of both proteins in cancer cells leads to a more transformed phenotype with an increased metastatic potential.

Acknowledgments

Abbreviations

DLC1, deleted in liver cancer 1; GAP, GTPase activating protein; GEF, guanine nucleotide exchange factor; LOH, loss of heterozygosity; PI3K, phosphatidylinositol 3-kinase; PIP3, phosphatidylinositol 3,4,5-trisphosphate; PTEN, phosphatase and tensin homolog; SAM, sterile alpha motif; START, StAR-related lipid transfer

References

[1]   L.Salmena, A.Carracedo, P.P.Pandolfi. Tenets of PTEN tumor suppression, Cell, 133, (2008) 403-414.

[2]   R.H.Kim, T.W.Mak. Tumours and tremors: how PTEN regulation underlies both, Br.J.Cancer, 94, (2006) 620-624.

[3]   H.E.Feilotter, V.Coulon, J.L.McVeigh, A.H.Boag, F.Dorion-Bonnet, B.Duboue, W.C.Latham, C.Eng, L.M.Mulligan, M.Longy. Analysis of the 10q23 chromosomal region and the PTEN gene in human sporadic breast carcinoma, Br.J.Cancer, 79, (1999) 718-723.

[4]   J.M.Garcia, J.M.Silva, G.Dominguez, R.Gonzalez, A.Navarro, L.Carretero, M.Provencio, P.Espana, F.Bonilla. Allelic loss of the PTEN region (10q23) in breast carcinomas of poor pathophenotype, Breast Cancer Res.Treat., 57, (1999) 237-243.

[5]   P.L.Depowski, S.I.Rosenthal, J.S.Ross. Loss of expression of the PTEN gene protein product is associated with poor outcome in breast cancer, Mod.Pathol., 14, (2001) 672-676.

[6]   A.Perren, L.P.Weng, A.H.Boag, U.Ziebold, K.Thakore, P.L.Dahia, P.Komminoth, J.A.Lees, L.M.Mulligan, G.L.Mutter, C.Eng. Immunohistochemical evidence of loss of PTEN expression in primary ductal adenocarcinomas of the breast, Am.J.Pathol., 155, (1999) 1253-1260.

[7]   L.H.Saal, K.Holm, M.Maurer, L.Memeo, T.Su, X.Wang, J.S.Yu, P.O.Malmstrom, M.Mansukhani, J.Enoksson, H.Hibshoosh, A.Borg, R.Parsons. PIK3CA mutations correlate with hormone receptors, node metastasis, and ERBB2, and are mutually exclusive with PTEN loss in human breast carcinoma, Cancer Res., 65, (2005) 2554-2559.

[8]   A.Suzuki, J.L.de la Pompa, V.Stambolic, A.J.Elia, T.Sasaki, B.B.del, I, A.Ho, A.Wakeham, A.Itie, W.Khoo, M.Fukumoto, T.W.Mak. High cancer susceptibility and embryonic lethality associated with mutation of the PTEN tumor suppressor gene in mice, Curr.Biol., 8, (1998) 1169-1178.

[9]   V.Stambolic, A.Suzuki, J.L.de la Pompa, G.M.Brothers, C.Mirtsos, T.Sasaki, J.Ruland, J.M.Penninger, D.P.Siderovski, T.W.Mak. Negative regulation of PKB/Akt-dependent cell survival by the tumor suppressor PTEN, Cell, 95, (1998) 29-39.

[10]   A.Di Cristofano, B.Pesce, C.Cordon-Cardo, P.P.Pandolfi. Pten is essential for embryonic development and tumour suppression, Nat.Genet., 19, (1998) 348-355.

[11]   V.Stambolic, M.S.Tsao, D.Macpherson, A.Suzuki, W.B.Chapman, T.W.Mak.   High incidence of breast and endometrial neoplasia resembling human Cowden syndrome in pten+/- mice, Cancer Res., 60, (2000) 3605-3611.

[12]   K.Podsypanina, L.H.Ellenson, A.Nemes, J.Gu, M.Tamura, K.M.Yamada, C.Cordon-Cardo, G.Catoretti, P.E.Fisher, R.Parsons. Mutation of Pten/Mmac1 in mice causes neoplasia in multiple organ systems, Proc.Natl.Acad.Sci.U.S.A, 96, (1999) 1563-1568.

[13]   G.Li, G.W.Robinson, R.Lesche, H.Martinez-Diaz, Z.Jiang, N.Rozengurt, K.U.Wagner, D.C.Wu, T.F.Lane, X.Liu, L.Hennighausen, H.Wu. Conditional loss of PTEN leads to precocious development and neoplasia in the mammary gland, Development, 129, (2002) 4159-4170.

[14]   T.Maehama, G.S.Taylor, J.E.Dixon. PTEN and myotubularin: novel phosphoinositide phosphatases, Annu.Rev.Biochem., 70, (2001) 247-279.

[15]   B.D.Manning, L.C.Cantley. AKT/PKB signaling: navigating downstream, Cell, 129, (2007) 1261-1274.

[16]   B.Z.Yuan, M.J.Miller, C.L.Keck, D.B.Zimonjic, S.S.Thorgeirsson, N.C.Popescu. Cloning, characterization, and chromosomal localization of a gene frequently deleted in human liver cancer (DLC-1) homologous to rat RhoGAP, Cancer Res., 58, (1998) 2196-2199.

[17]   M.E.Durkin, B.Z.Yuan, X.Zhou, D.B.Zimonjic, D.R.Lowy, S.S.Thorgeirsson, N.C.Popescu. DLC-1:a Rho GTPase-activating protein and tumour suppressor, J.Cell Mol.Med., 11, (2007) 1185-1207.

[18]   A.Lahoz, A.Hall. DLC1: a significant GAP in the cancer genome, Genes Dev., 22, (2008) 1724-1730.

[19]   K.D.Healy, L.Hodgson, T.Y.Kim, A.Shutes, S.Maddileti, R.L.Juliano, K.M.Hahn, T.K.Harden, Y.J.Bang, C.J.Der. DLC-1 suppresses non-small cell lung cancer growth and invasion by RhoGAP-dependent and independent mechanisms, Mol.Carcinog., 47, (2008) 326-337.

[20]   C.M.Wong, J.M.Lee, Y.P.Ching, D.Y.Jin, I.O.Ng. Genetic and epigenetic alterations of DLC-1 gene in hepatocellular carcinoma, Cancer Res., 63, (2003) 7646-7651.

[21]   A.B.Jaffe, A.Hall. Rho GTPases: biochemistry and biology, Annu.Rev.Cell Dev.Biol., 21, (2005) 247-269.

[22] A.J.Ridley. Rho GTPases and actin dynamics in membrane protrusions and vesicle trafficking, Trends Cell Biol., 16, (2006) 522-529.

[23] W.Xue, A.Krasnitz, R.Lucito, R.Sordella, L.Vanaelst, C.Cordon-Cardo, S.Singer, F.Kuehnel, M.Wigler, S.Powers, L.Zender, S.W.Lowe. DLC1 is a chromosome 8p tumor suppressor whose loss promotes hepatocellular carcinoma, Genes Dev., 22, (2008) 1439-1444.

[24] G.Holeiter, J.Heering, P.Erlmann, S.Schmid, R.Jahne, M.A.Olayioye. Deleted in liver cancer 1 controls cell migration through a Dia1-dependent signaling pathway, Cancer Res., 68, (2008) 8743-8751.

[25] A.J.Ridley, M.A.Schwartz, K.Burridge, R.A.Firtel, M.H.Ginsberg, G.Borisy, J.T.Parsons, A.R.Horwitz. Cell migration: integrating signals from front to back, Science, 302, (2003) 1704-1709.

[26] R.P.Scholz, J.Regner, A.Theil, P.Erlmann, G.Holeiter, R.Jahne, S.Schmid, A.Hausser, M.A.Olayioye. DLC1 interacts with 14-3-3 proteins to inhibit RhoGAP activity and block nucleocytoplasmic shuttling, J.Cell Sci., 122, (2009) 92-102.

[27] V.Kolsch, P.G.Charest, R.A.Firtel. The regulation of cell motility and chemotaxis by phospholipid signaling, J.Cell Sci., 121, (2008) 551-559.

[28] N.R.Leslie, X.Yang, C.P.Downes, C.J.Weijer. The regulation of cell migration by PTEN, Biochem.Soc.Trans., 33, (2005) 1507-1508.

[29] M.Tamura, J.Gu, K.Matsumoto, S.Aota, R.Parsons, K.M.Yamada. Inhibition of cell migration, spreading, and focal adhesions by tumor suppressor PTEN, Science, 280, (1998) 1614-1617.

[30] M.Sekimata, Y.Kabuyama, Y.Emori, Y.Homma. Morphological changes and detachment of adherent cells induced by p122, a GTPase-activating protein for Rho, J.Biol.Chem., 274, (1999) 17757-17762.

[31] M.E.Ginn-Pease, C.Eng. Increased nuclear phosphatase and tensin homologue deleted on chromosome 10 is associated with G0-G1 in MCF-7 cells, Cancer Res., 63, (2003) 282-286.

[32] F.Vazquez, P.Devreotes. Regulation of PTEN function as a PIP3 gatekeeper through membrane interaction, Cell Cycle, 5, (2006) 1523-1527.

[33] L.Odriozola, G.Singh, T.Hoang, A.M.Chan. Regulation of PTEN activity by its carboxyl-terminal autoinhibitory domain, J.Biol.Chem., 282, (2007) 23306-23315.

[34] Y.Li, K.Podsypanina, X.Liu, A.Crane, L.K.Tan, R.Parsons, H.E.Varmus. Deficiency of Pten accelerates mammary oncogenesis in MMTV-Wnt-1 transgenic mice, BMC.Mol.Biol., 2, (2001) 2.

[35] N.Dourdin, B.Schade, R.Lesurf, M.Hallett, R.J.Munn, R.D.Cardiff, W.J.Muller. Phosphatase and tensin homologue deleted on chromosome 10 deficiency accelerates tumor induction in a mouse model of ErbB-2 mammary tumorigenesis, Cancer Res., 68, (2008) 2122-2131.

[36] Y.C.Liao, Y.P.Shih, S.H.Lo. Mutations in the focal adhesion targeting region of deleted in liver cancer-1 attenuate their expression and function, Cancer Res., 68, (2008) 7718-7722.

[37] L.P.Weng, W.M.Smith, P.L.Dahia, U.Ziebold, E.Gil, J.A.Lees, C.Eng. PTEN suppresses breast cancer cell growth by phosphatase activity-dependent G1 arrest followed by cell death, Cancer Res., 59, (1999) 5808-5814.

[38] B.Z.Yuan, X.Zhou, M.E.Durkin, D.B.Zimonjic, K.Gumundsdottir, J.E.Eyfjord, S.S.Thorgeirsson, N.C.Popescu. DLC-1 gene inhibits human breast cancer cell growth and in vivo tumorigenicity, Oncogene, 22, (2003) 445-450.

[39] S.Funamoto, R.Meili, S.Lee, L.Parry, R.A.Firtel. Spatial and temporal regulation of 3-phosphoinositides by PI 3-kinase and PTEN mediates chemotaxis, Cell, 109, (2002) 611-623.

[40] M.Iijima, P.Devreotes. Tumor suppressor PTEN mediates sensing of chemoattractant gradients, Cell, 109, (2002) 599-610.

[41] D.Wessels, D.F.Lusche, S.Kuhl, P.Heid, D.R.Soll. PTEN plays a role in the suppression of lateral pseudopod formation during Dictyostelium motility and chemotaxis, J.Cell Sci., 120, (2007) 2517-2531.

[42] J.Liliental, S.Y.Moon, R.Lesche, R.Mamillapalli, D.Li, Y.Zheng, H.Sun, H.Wu. Genetic deletion of the Pten tumor suppressor gene promotes cell motility by activation of Rac1 and Cdc42 GTPases, Curr.Biol., 10, (2000) 401-404.

[43] A.Suzuki, T.Kaisho, M.Ohishi, M.Tsukio-Yamaguchi, T.Tsubata, P.A.Koni, T.Sasaki, T.W.Mak, T.Nakano. Critical roles of Pten in B cell homeostasis and immunoglobulin class switch recombination, J.Exp.Med., 197, (2003) 657-667.

[44] R.A.Lacalle, C.Gomez-Mouton, D.F.Barber, S.Jimenez-Baranda, E.Mira, A.Martinez, A.C.Carrera, S.Manes. PTEN regulates motility but not directionality during leukocyte chemotaxis, J.Cell Sci., 117, (2004) 6207-6215.

[45] M.Nishio, K.Watanabe, J.Sasaki, C.Taya, S.Takasuga, R.Iizuka, T.Balla, M.Yamazaki, H.Watanabe, R.Itoh, S.Kuroda, Y.Horie, I.Forster, T.W.Mak, H.Yonekawa, J.M.Penninger, Y.Kanaho, A.Suzuki, T.Sasaki. Control of cell polarity and motility by the PtdIns(3,4,5)P3 phosphatase SHIP1, Nat.Cell Biol., 9, (2007) 36-44.

[46] M.Raftopoulou, S.Etienne-Manneville, A.Self, S.Nicholls, A.Hall. Regulation of cell migration by the C2 domain of the tumor suppressor PTEN, Science, 303, (2004) 1179-1181.

[47] J.W.Yam, F.C.Ko, C.Y.Chan, D.Y.Jin, I.O.Ng. Interaction of deleted in liver cancer 1 with tensin2 in caveolae and implications in tumor suppression, Cancer Res., 66, (2006) 8367-8372.

[48] X.Qian, G.Li, H.K.Asmussen, L.Asnaghi, W.C.Vass, R.Braverman, K.M.Yamada, N.C.Popescu, A.G.Papageorge, D.R.Lowy. Oncogenic inhibition by a deleted in liver cancer gene requires cooperation between tensin binding and Rho-specific GTPase-activating protein activities, Proc.Natl.Acad.Sci.U.S.A, 104, (2007) 9012-9017.

[49] C.A.Kim, J.U.Bowie. SAM domains: uniform structure, diversity of function, Trends Biochem.Sci., 28, (2003) 625-628.

[50] Z.Li, X.Dong, Z.Wang, W.Liu, N.Deng, Y.Ding, L.Tang, T.Hla, R.Zeng, L.Li, D.Wu. Regulation of PTEN by Rho small GTPases, Nat.Cell Biol., 7, (2005) 399-404.

7.6. DLC1 activation requires lipid interaction through a polybasic region preceding the RhoGAP domain

Patrik Erlmann[1], Simone Schmid[1], Florian A. Horenkamp[2], Matthias Geyer[2], Thomas G. Pomorski[3], and Monilola A. Olayioye[1]

[1] The University of Stuttgart, Institute of Cell Biology and Immunology, Allmandring 31, 70569 Stuttgart, Germany

[2] Max-Planck-Institute of Molecular Physiology, Dept. of Physical Biochemistry, Otto-Hahn-Strasse 11, 44227 Dortmund, Germany

[3] The University of Copenhagen, Dept. Plant Biology and Biotechnology, Thorvaldsensvej 40, 1871 Frederiksberg C, Denmark

To whom correspondence should be addressed: Dr. Monilola A. Olayioye, phone: +49 711 685 69301, fax: +49 711 685 67484, email: monilola.olayioye@izi.uni-stuttgart.de

Abstract

Deleted in Liver Cancer 1 (DLC1) is a GTPase activating protein (GAP) with specificity for RhoA, RhoB and RhoC that is frequently deleted in various tumor types. By inactivating these small GTPases, DLC1 controls actin cytoskeletal remodeling and biological processes such as cell migration and proliferation. Here we provide evidence that DLC1 binds to phosphatidylinositol-4,5-bisphosphate ($PI(4,5)P_2$) through a previously unrecognized polybasic region (PBR) adjacent to its RhoGAP domain. Importantly, $PI(4,5)P_2$-containing membranes are shown to stimulate DLC1 GAP activity *in vitro.* In living cells, a DLC1 mutant lacking an intact PBR inactivated Rho signaling less efficiently and was severely compromised in suppressing cell spreading, directed migration and proliferation. We therefore propose that $PI(4,5)P_2$ is an important cofactor in DLC1 regulation *in vivo* and that the PBR is essential for the tumor suppressive functions of the protein.

Introduction

DLC1 was first isolated as a candidate tumor suppressor gene in primary human hepatocellular carcinoma and loss of expression has subsequently been shown in other tumor types, including colon, breast, prostate and lung (Durkin et al., 2007b;Lahoz and Hall, 2008). Transfection of the DLC1 cDNA into different carcinoma cell lines lacking DLC1 expression was then demonstrated to inhibit cell growth and tumorigenicity in nude mice (Ng et al., 2000;Yuan et al., 2003;Yuan et al., 2004;Zhou et al., 2004). Comparison of breast cancer sublines by transcriptional profiling revealed that DLC1 expression is linked to their metastatic potential, with downregulation favoring the formation of pulmonary metastases in athymic mice (Goodison et al., 2005). Recent studies using RNA interference-based approaches provide further proof for a tumor suppressor function of DLC1. Its downregulation in the breast carcinoma cell lines MCF7 and MDAMB436 promoted enhanced wound closure and Transwell migration via a Dia1-dependent pathway, demonstrating that DLC1 loss is sufficient for the acquisition of a more migratory phenotype (Holeiter et al., 2008). A tumor suppressor function of DLC1 was moreover confirmed in vivo, where DLC1 downregulation was shown to cooperate with myc overexpression in p53 null cells to promote liver tumorigenesis in mice (Xue et al., 2008). The structurally related proteins DLC2 and DLC3 are thought to serve a similar tumor suppressive function, as they are also frequently lost in various tumor types and their re-expression in cancer cells was shown to inhibit proliferation, colony formation and growth in soft agar (Ching et al., 2003;Durkin et al., 2007a).

DLC1 is a GAP protein with *in vitro* activity for the small GTPases RhoA, RhoB and RhoC, and to a lesser extent Cdc42 (Wong et al., 2003;Healy et al., 2008). The Rho family of GTPases are important regulators of diverse biological responses, including actin cytoskeletal rearrangements, gene transcription, cell cycle regulation, apoptosis and membrane trafficking (Jaffe and Hall, 2005;Ridley, 2006). Rho proteins cycle between a GTP-bound active state to interact with effector

proteins, modulating their activity and localization, and an inactive GDP-bound state. Activation of Rho proteins is controlled by the guanine nucleotide exchange factors (GEFs), which promote the release of bound GDP and facilitate GTP binding. GAP proteins, on the other hand, are negative regulators that increase the intrinsic GTPase activity of Rho GTPases to accelerate the return to the inactive state (Jaffe and Hall, 2005;Ridley, 2006;Bos *et al.*, 2007). RhoA, RhoB and RhoC are post-translationally modified by prenylation of a conserved carboxy-terminal cysteine. The prenyl group anchors the GTPase into membranes and this modification is essential for activity. While RhoA and RhoC are geranylgeranylated, RhoB is also farnesylated, which accounts for differences in localization (Wheeler and Ridley, 2004). Another layer of complexity is added by the guanine nucleotide dissociation inhibitors which sequester Rho GTPases in the cytoplasm by binding to the prenyl group (Jaffe and Hall, 2005;Ridley, 2006).

Active RhoA, RhoB and RhoC promote the formation of actin stress fibers and focal adhesions (Wheeler and Ridley, 2004). In accordance with its RhoGAP function, microinjection of p122, the rat homolog of DLC1, suppressed the formation of lysophosphatidic acid-induced stress fibers and focal adhesions (Sekimata et al., 1999). Furthermore, stable expression of human DLC1 in hepatocellular and breast carcinoma cell lines was shown to reduce cell motility and invasiveness, consistent with the inhibition of Rho signaling (Wong et al., 2005;Goodison *et al.*, 2005). Regulation of GAP proteins is achieved by several mechanisms such as protein or lipid interactions, and post-translational modification (Bernards and Settleman, 2005). However, little is known about the molecular regulation of DLC1. Recent reports have provided evidence that interaction with tensin proteins is important for the recruitment of DLC1 to focal adhesions (Yam et al., 2006;Qian et al., 2007;Liao et al., 2007). DLC1 mutants deficient in tensin binding and thus focal adhesion localization lose their ability to suppress colony formation, indicating that DLC1 location to these sites is linked to biological activity (Qian *et al.*, 2007;Liao *et al.*, 2007). On the other hand, the phosphorylation-dependent interaction with 14-3-3 adaptor proteins retains DLC1 in the cytoplasm and inhibits its cellular functions (Scholz et al., 2009). Negative regulation is also achieved by direct binding of p120RasGAP to the GAP domain of DLC1, which was shown to impair the growth suppressing properties of DLC1 (Yang et al., 2009).

DLC1 is a multidomain protein that contains an amino-terminal sterile alpha motif (SAM) and a StAR-related lipid transfer (START) domain at its carboxy-terminus. SAM domains mediate homo- and heterotypic interactions with other SAM domains, but they were also shown to interact with other proteins, lipids and RNA (Kim and Bowie, 2003). START domains are typically found in lipid transfer proteins and form a hydrophobic pocket to accommodate a single lipid molecule that is shuttled between membranes (Alpy and Tomasetto, 2005). Protein and/or lipid interactions via SAM and START domains are thus potential mechanisms by which DLC localization and/or activity may be regulated. Because the active forms of Rho GTPases are associated with cellular membranes, it is here where the DLC proteins are expected to exert their function. Therefore, we

argued that DLC1 may be recruited to and activated at membrane proximal sites not only by protein but also by lipid interaction to inactivate target Rho GTPases. Here we identify a novel interaction of DLC1 with negatively charged phospholipids, with highest affinity observed for $PI(4,5)P_2$, that is independent of SAM and START domains. Instead, the interaction is mediated by a polybasic region (PBR) directly preceding the GAP domain that is conserved within the DLC protein family. *In vitro* assays with prenylated RhoA show that the presence of $PI(4,5)P_2$-containing membranes stimulate DLC1's GAP activity. We further demonstrate that, in a cellular context, an intact PBR is essential for DLC1 inhibition of Rho signaling and, accordingly, suppression of cell proliferation and directed migration.

Materials and Methods

Antibodies and reagents

Antibodies used were: mouse anti-GFP mAb (Roche Applied Science), mouse anti-paxillin mAb (BD), mouse anti-tubulin mAb (Sigma Aldrich), goat anti-GST pAb (GE Healthcare). HRP-labeled anti-mouse IgG antibody was from Amersham, HRP-labeled anti-goat IgG antibody was from Santa Cruz Biotechnology, Alexa Fluor 546-labeled anti-mouse IgG antibody, Alexa Fluor 546-labeled phalloidin and 1-hexadecanoyl-2-(1-pyrenedecanoyl)-sn-glycero-3-phosphocholine (pyrene-PC) were from Molecular Probes. PS, PA, PC, and $PI(4,5)P_2$ were purchased from Sigma Aldrich, PI(4)P and $PI(3,4,5)P_3$ was from Biomol, PI and porcine brain lipids were from Avanti Polar Lipids. All chemicals, if not stated otherwise, were purchased from Roth.

DNA cloning

The plasmids encoding full length human DLC1 (Genbank accession no. AAK07501.1) pEGFPC1-DLC1 and pEFrPGKpuroFlag-DLC1 and the truncated variants pEGFPC1-DLC1 ΔSAM and pEGFPC1-DLC1 ΔSTART were described previously (Holeiter *et al.*, 2008;Scholz *et al.*, 2009). DLC1 ΔN_{long} (aa 596-1091) and DLC1 ΔN_{short} (aa 637-1091) were amplified by PCR using pEGFPC1-DLC1 as a template with primers containing *Bam*HI restriction sites. Forward primers used were 5'-CGC GGA TCC AAA TAC TCA CTC CTA AAG CTA ACG G-3' for DLC1 ΔN_{long} and 5'-CGC GGA TCC AGT GTG TTT GGG GTC CCA C-3' for DLC1 ΔN_{short}. The reverse primer used was 5'-CGC GGA TCC TCA CCT AGA TTT GGT GTC TTT GG-3'. DLC1 K626A/R627G and ΔPBR (Δ623-631) mutants were generated by QuikChange site-directed PCR mutagenesis using pEGFPC1-DLC1 as a template according to the manufacturer's instructions (Stratagene). The forward primers used were: DLC1 K626A/R627G 5'-CGT GCC CAA GTT CAT GGC GGG GAT CAA GGT TCC AGA C-3'and DLC1 ΔPBR 5'-GCT GGG CCG TGC CCG ACT ACA AGG ACC GG-3'. DLC1 constructs were subcloned into pEFrPGKpuro-Flag and pGEX6-P3 vectors by *Bam*HI restriction. The DLC1 ΔPBR cDNA was also subcloned into the pcDNA5/FRT/TO-GFP vector, which we described recently (Scholz *et al.*, 2009). The human DLC3β cDNA, a shorter form lacking

the SAM domain, was amplified by PCR using clone IRATp970E0455D (ImaGenes, Germany) as a template with forward primer 5'-CCG GAA TTC TAC CTT GAA TAA TTG TGC CTC GAT G-3' and reverse primer 5'-CCG GAA TTC TTC ACA GCT TTG TCT CAG GGC-3' and cloned into the pEGFPC1 vector as an *Eco*RI fragment. The 5' region encoding the SAM domain present in DLC3α was amplified by PCR using cDNA derived from HeLa cells as a template with the forward primer 5'-CCG GAA TTC TCC TCT GCT GGA CGT TTT CTG-3' and reverse primer 5'-TTC TGA GTC TTC ATT CTG CTT GC-3'. The PCR product and pEGFPC1-DLC3β were digested with *Eco*RI and *Bpi*I, and the DLC3 fragments were ligated with *Eco*RI-digested pEGFPC1, generating pEGFPC1-DLC3α used in this study. All amplified cDNAs were confirmed by sequencing. Oligonucleotides were purchased from MWG Biotech.

Cell culture and transfection

All cell lines used were cultured in RPMI media (Invitrogen) supplemented with 10% FCS (PAA) in a humidified atmosphere of 5% CO_2 at 37°C. Flp-In T-Rex HEK293 cells (Invitrogen) were grown in RPMI containing 10% FCS, 100 µg/ml zeocin and 15 µg/ml blasticidin. These cells stably express the Tet repressor and contain a single Flp Recombination Target (FRT) site and were used to generate the HEK293 Flp-In DLC1 lines. Cells were cotransfected with pcDNA5/FRT/TO-GFP-DLC1 WT and ΔPBR and the Flp recombinase expression plasmid pOG44 at a ratio of 1:10 and then selected with 100 µg/ml hygromycin. HEK293 cells were transfected using TransIt reagent (Mirus), MCF7 cells were transfected using Lipofectamine 2000 (Invitrogen) or by nucleofection (Amaxa).

Purification of recombinant proteins from *E. coli*

pGEX6-P3 DLC1 ΔN_{long} and ΔN_{short} vectors were transformed into BL21 bacteria. Production cultures were inoculated from overnight cultures (1/25) and grown for 3 h at 37°C. Cultures were then shifted to 30°C, induced with 0.5 mM IPTG (Fermentas) and protein production continued for 3-4 h. Bacteria were harvested by centrifugation and resuspended in PBS with PMSF and Complete protease inhibitors (Roche). Bacteria were lysed by sonification (2 x 10 cycles, 50% duty cycle), debris was removed by centrifugation and the supernatant was incubated with glutathione beads (Roche) for 2 h at 4°C. Beads were washed with PBS and protein was eluted with 30 mM glutathione in 50 mM Tris, pH 7.4 and 100 mM NaCl buffer. Purity and concentration of the protein was determined by SDS-PAGE and Coomassie staining. Purified proteins were stored at -80°C. GST-RhoA was purified in the same fashion, but all buffers were supplemented with 5 mM $MgCl_2$ and 1 µM GDP. *In vitro* prenylation of GST-RhoA was performed in a buffer containing 50 mM TrisHCl, pH 8.0, 100 mM NaCl, 20 mM KCl, 5 mM $MgCl_2$, 1 mM DTE, 50 µM GDP, 5 µM $ZnCl_2$, 0.5% NP40. A reaction mixture of 20 µM GST-RhoA, 25 µM yeast GST-GGTaseI and 50 µM of geranylgeranyl pyrophosphate (Sigma Aldrich) was incubated at 4°C for 14 h. Completeness of GST-RhoA prenylation was verified by mass spectrometry.

Hypotonic cell lysis

HEK293T cells transiently expressing the different GFP-tagged DLC1 variants were lysed in 50 mM TrisHCl, pH 7.4, containing Complete protease inhibitors, 1 mM PMSF, 5 mM ß-glycerophosphate, and 5 mM sodium fluoride. Lysates were passed through a 0.45 mm needle, and nuclei and debris were removed by centrifugation (16,000g, 4°C, 10 min). The total protein concentration and the amount of GFP-tagged proteins were determined by Bradford assay (BioRad) and measurement of GFP fluorescence (excitation 466 nm, emission 512 nm), respectively, using a Tecan Infinite 200M reader

Lipid ELISA

Phospholipids dissolved in ethanol were spotted onto polystyrol 96 well plates (2 µg per well; Greiner) and left to dry. The wells were blocked with PBS containing 0.05% Tween-20 (PBS-T) and 5% lipid-free BSA for 1 h, incubated with hypotonic cell lysate (150 µg total protein) containing equal amounts of GFP-tagged proteins for 40 min and then washed 3 times with PBS-T. The wells were then incubated with anti-GFP antibody in PBS-T for 2 h, followed by HRP-conjugated secondary antibody in PBS-T for 1 h. ABTS (2,2'-azino-di (3-ethylbenzthiazoline-6-sulfonate) peroxidase substrate at 1 mg/ml in ABTS buffer (Roche) was added and absorption at 405 nm was recorded with a Tecan Infinite 200M plate reader after 30 min.

Lipid vesicle preparation

The indicated amount of lipid in chloroform was dried under a nitrogen stream. For SUV preparations, buffer containing 20 mM Hepes, pH 7.2, 5 mM EDTA, and 100 mM NaCl was added and lipids were rehydrated by sonification (10 min, 20% duty cycle) on ice. For membrane interaction assays, SUVs were prepared in the presence of pyrene-PC (10 mol%). For MLV preparations, buffer containing 20 mM TrisHCl, pH 7.5, 25 mM NaCl, and 4 mM EDTA was added, and after incubation for 1 h on ice, lipids were rehydrated by vigorous vortexing.

Membrane interaction assay

Protein binding to vesicles was evaluated by measuring FRET from tryptophan residues to the pyrene fluorophore of pyrene-PC as follows. Emission scans were recorded in the absence of protein (wavelength, 310 to 500 nm; excitation, 290 nm; slit widths, 4 nm) at 20°C for samples containing 30 µl pyrene-PC-containing SUVs (16 µM lipid) in 1,8 ml buffer (20 mM Hepes, pH 7.2, 5 mM EDTA, 100 mM NaCl) using an Aminco Bowman series 2 spectrofluorometer (SLM Instruments, Rochester, NY). Then, equal amounts of recombinant GST-tagged DLC1 ΔN_{long} or ΔN_{short} were added and the emission spectrum was recorded again. FRET/tryptophan ratios were calculated using the mean peak values (FRET: 376 to 379 nm; tryptophan: 336 to 338 nm) after subtraction of values in the absence of protein.

In vitro RhoGAP activity assay

GST-RhoA (~10 µg) was preloaded with γ^{32}P-GTP (Hartmann Analytic) in 60 µl loading buffer (20 mM TrisHCl, pH 7.5, 25 mM NaCl, 4 mM EDTA, 0.1 mM DTT, 0.125 µCi γ^{32}P-GTP) at 30°C for 5 min. Preloading of GST-RhoA$_{GG}$ (~10 µg) was performed in the presence of 20 µg MLVs. Preloading was stopped by adding 10 mM MgCl$_2$. 10 µl of the loading mix was added to 40 µl reaction mix (20 mM TrisHCl, pH 7.5, 0.1 mM DTT, 1 mM GTP, 1 mg/ml BSA) on ice, with or without DLC1 ΔN_{long} or ΔN_{short} (~1 µg) and shifted to 20°C to start the reaction. At 0 and 10 min, 10 µl of the reaction mix was added to 1 ml of ice-cold wash buffer (20 mM TrisHCl, pH 7.5, 5 mM MgCl$_2$) and samples were filtered through nitrocellulose membranes (Millipore), retaining RhoA-bound γ^{32}P-GTP. After washing, membranes were measured by scintillation counting (Cherenkov radiation, Packard 1600TR scintillation analyzer).

Raichu-RhoA biosensor measurements

HEK293T cells were transiently transfected with plasmids encoding the Raichu-RhoA biosensor (Yoshizaki *et al.*, 2003) and Flag-DLC1 WT, K626A/R627G and ΔPBR. Cells were lysed in 50 mM Tris, pH 7.5, 100 mM NaCl and 0.5% Triton X-100 and debris was removed by centrifugation at 16,000g for 5 min. Lysates were transferred to white Nunc 96-well plates and emission ratios (FRET/CFP) were determined by measuring CFP and YFP fluorescence after background subtraction at 475 and 530 nm, respectively, using a Tecan Infinite 200M plate reader (excitation, 433 nm). Equal expression of the DLC1 variants was confirmed by immunoblotting of lysates.

Luciferase assays

HEK293T cells were grown on collagen-coated 24-well plates (Greiner) and transfected with 50 ng each of the 3DA.Luc firefly luciferase reporter containing three SRF binding elements, pRL-TK, a Renilla luciferase plasmid under the control of the thymidine kinase promoter, and pEGFPC1-DLC1 WT, K626A/R627G and ΔPBR, respectively. After serum starvation over night, cells were stimulated with 15% FCS for 6 h. Cells were lysed with 300 µl passive lysis buffer (Promega) and luciferase activities in 10 µl lysate were measured by addition of 50 µl firefly substrate [470 µM D-luciferin, 530 µM ATP, 270 µM coenzyme A, 33 mM DTT, 20 mM Tricine, 2.67 mM MgSO4, 0.1 mM EDTA, pH 7,8], followed by addition of 100 µl Renilla substrate [0.7 µM coelenterazine, 2.2 mM Na$_2$EDTA, 0.44 mg/ml bovine serum albumin, 1.1 M NaCl, 1.3 mM NaN$_3$, 0.22 M potassium phosphate buffer, pH 5,0]. Luminescence was measured with a Tecan Infinite 200M plate reader.

Immunofluorescence microscopy

Cells grown on collagen-coated glass coverslips were transfected with the indicated expression plasmids and after 24 h, cells were fixed in 4% PFA for 10 min, washed and incubated with PBS containing 0.1 M glycine for 15 min. Cells were permeabilized with PBS containing 0.1% Triton for 5 min and blocked with 5% goat serum (Invitrogen) in PBS containing 0.1% Tween-20 for 30 min.

Cells were then incubated with paxillin-specific antibody diluted in blocking buffer for 2 h, followed by incubation with secondary Alexa Fluor 546-coupled antibody diluted in blocking buffer for 1 h. F-actin staining was done by incubating fixed cells with Alexa Fluor 546-coupled phalloidin diluted in blocking buffer for 1 h. Coverslips were mounted in Fluoromount G (Southern Biotechnology) and optical sections were acquired using a Zeiss Axiovision system equipped with an Apotome using a Plan-Apochromat 63x/1.40 Oil DIC M27 objective and the Axiovision Software.

Live cell imaging

Non-induced HEK293 FlpIn cells and cells induced to express DLC1 WT and ΔPBR (100 ng/ml doxycycline for 24 h) were harvested and resuspended in phenol red-free RPMI (Invitrogen) containing 10% FCS and plated onto collagen-coated glass bottom dishes (World Precision Instruments). After 5 min, recording was started by acquiring bright field images every 30 seconds with a Zeiss Axiovision system equipped with a heated incubation chamber using a Plan-Apochromat 20x/0.8 M27 objective and the Axiovision software.

Migration assays

HEK293T Flp-In cells were induced with 100 ng/ml doxycycline for 24 h prior to the experiment, non-induced cells were used as controls. Transwells (8.0 μm; Costar) were coated with 2.5 μg/ml collagen on the underside and $5x10^4$ cells in 100 μl medium containing 0.5% FCS were added to the top chamber. The bottom chamber was supplemented with 10% FCS. Cells were allowed to migrate for 4 h. Cells on the upper side of the membranes were removed using a cotton swab and cells on the underside were fixed in 4% PFA and stained with 0.1% crystal violet. Cells were counted in five independent microscopic fields at a 20-fold magnification.

MTT assays

MCF7 cells were transfected with GFP-DLC1 WT and ΔPBR or with empty vector using the Amaxa nucleofector (Kit V; program P-020). 1000 cells were plated into 96 well cell culture plates. At each time point, 10 μl 3-(4,5-dimethylthiazol-2yl-)2,5-diphenyl tetrazolium bromide (MTT) solution (5 mg/ml) was added and the cells were incubated for 2 h. The medium was aspirated and the cells were lysed in 100 μl 50% dimethylformamide containing 10% SDS. Absorbance at 570 nm was determined with background subtraction at 630 nm using a Tecan Infinite 200M plate reader.

Results

DLC1 interacts with negatively charged phospholipids independently of its SAM and START domains

To investigate the ability of DLC1 to bind to different lipid species we performed lipid ELISA assays. Here, lipids spotted onto 96-well plates were incubated with hypotonic lysates of HEK293T cells transiently expressing GFP-tagged DLC1. Bound DLC1 was then detected with a GFP-specific primary and HRP-labeled secondary antibody, followed by incubation with ABTS peroxidase substrate (Figure 1A). Using this assay, DLC1 was found to strongly bind to $PI(4,5)P_2$, and modestly to phosphatidic acid (PA), and phosphatidylinositol-3,4,5-trisphosphate ($PI(3,4,5)P_3$), while binding to phosphatidylcholine (PC), phosphatidylinositol (PI), phosphatidylserine (PS) and phosphatidylinositol-4-phosphate (PI(4)P) was negligible (Figure 1A). Interestingly, $PI(4,5)P_2$-binding of DLC1 variants lacking the amino-terminal SAM (DLC1 ΔSAM) and carboxy-terminal START domains (DLC1 ΔSTART) were identical to that of the wild type protein (Figure 1B), indicating that the interaction was independent of these domains. Of note, lipid ligands of the START domain are unlikely to be identified in this assay, since lipid uptake into the hydrophobic pocket requires administration in solution.
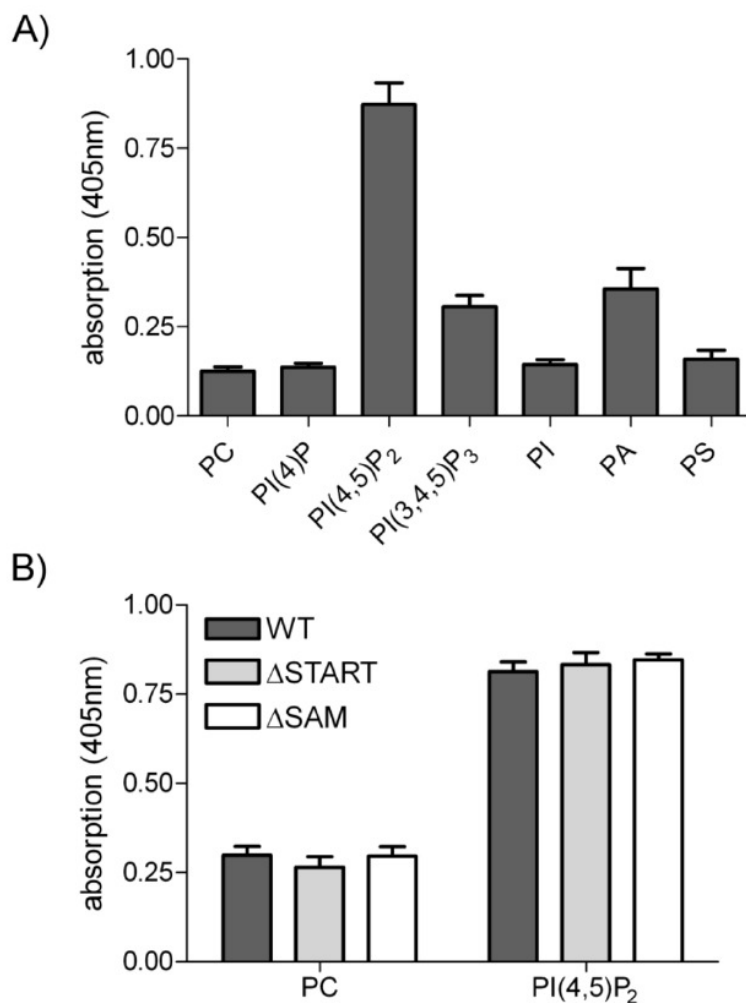

Fig. 1: DLC1 binding to phospholipids. (A) 96-well plates containing immobilized egg PC plus 15 mol% of the indicated lipids were incubated with hypotonic lysate from HEK293T cells transiently expressing GFP-tagged DLC1. Bound DLC1 was detected with GFP-specific antibody, followed by HRP-conjugated secondary antibody and visualized with ABTS peroxidise substrate. Absorption was measured after 30 min at 405 nm. The mean of two independent experiments performed with triplicate samples is shown; error bars represent SEM. (B) Immobilized $PI(4,5)P_2$ (15 mol% in PC) was incubated with hypotonic lysate from HEK293T cells transiently expressing GFP-tagged DLC1 wild type (WT), ΔSAM and ΔSTART proteins. Detection of bound proteins was done as described in panel A. A representative experiment with triplicate samples is shown. Error bars represent SEM.

DLC proteins possess a highly conserved polybasic region adjacent to the GAP domain

Binding of negatively charged phospholipids such as $PI(4,5)P_2$ can be mediated by short sequences enriched in basic amino acids (Fivaz and Meyer, 2003). A ScanProsite motif search identified such a polybasic region (PBR) in close proximity of the DLC1 RhoGAP domain. Sequence comparison of human, mouse and rat DLC1 proteins including the Drosophila and Xenopus homologs revealed conservation of this region amongst the different species. In addition, the PBR was present in DLC2 and DLC3 (Figure 2A). Lipid ELISA analysis showed that DLC2 and DLC3 were also able to interact with $PI(4,5)P_2$ (Figure 2B), raising the possibility that lipid binding is a general mechanism of the DLC protein family mediated by a conserved PBR.
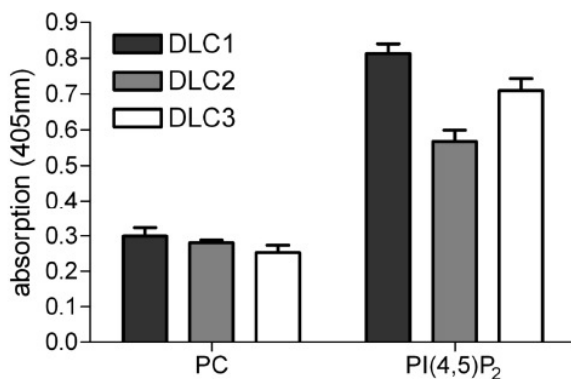

A)

```
DLC1 human           614-KHGFSWAVPKFMKRIKVPDYKDR
DLC1 rat             615-KHGFSWAVPKFMKRIKVPDYKDR
DLC1 mouse           615-KHGFSWAVPKFMKRIKVPDYKDR
DLC2 human           636-KHGWTWSVPKFMKRMKVPDYKDK
DLC3 human           545-KQGWVWSMPKFMRRNKTPDYRGQ
Shirin Xenopus       625-KHGWTWSVPKFMKRMKGPDYKDK
RhoGAP88C Drosophila 538-RSGWNWELPKFIKKIKMPDYKDK
consensus               :-G:-W-:PKF:::-K-PDY:.:
```

B)

Fig. 2: The DLC protein family contains a conserved polybasic region and interacts with $PI(4,5)P_2$. (A) Sequence comparison of DLC1 from different species and human DLC2 and DLC3. Basic amino acids are highlighted in bold. (B) GFP-tagged DLC1, DLC2 and DLC3 were tested for their ability to bind to immobilized $PI(4,5)P_2$ as described in Figure 1. A representative experiment with triplicate samples is shown. Error bars represent SEM.

DLC1 interaction with $PI(4,5)P_2$ is mediated by the polybasic amino acid cluster

To investigate the importance of the identified PBR for DLC1 interaction with negatively charged phospholipids we generated carboxy-terminal constructs containing the GAP and START domains, either comprising the PBR (DLC1 ΔN_{long}) or lacking this region (DLC1 ΔN_{short}) (Figure 3A). Lipid ELISA analysis showed that the PBR was indeed responsible for mediating the interaction with $PI(4,5)P_2$ (Figure 3B). The amount of DLC1 ΔN_{long} bound by immobilized $PI(4,5)P_2$ was significantly higher than that bound by PC alone, while binding of DLC1 ΔN_{short} was not enhanced by $PI(4,5)P_2$. To assess if the PBR also recognizes $PI(4,5)P_2$ when incorporated into membranes, we employed a fluorescence resonance energy transfer (FRET)-based assay, in which the aromatic amino acid tryptophan served as the FRET donor and pyrene-labeled PC as the FRET acceptor. Pyrene-PC was incorporated into small unilamellar vesicles (SUVs) made of porcine brain lipids (BL), with or without the addition of 10 mol% $PI(4,5)P_2$. These vesicles were then incubated with recombinant GST-tagged DLC1 ΔN_{long} and ΔN_{short} purified from *E. coli.* In the case of DLC1 ΔN_{long}, a clear FRET peak was visible in the presence of vesicles comprised of BL and $PI(4,5)P_2$, indicating the close
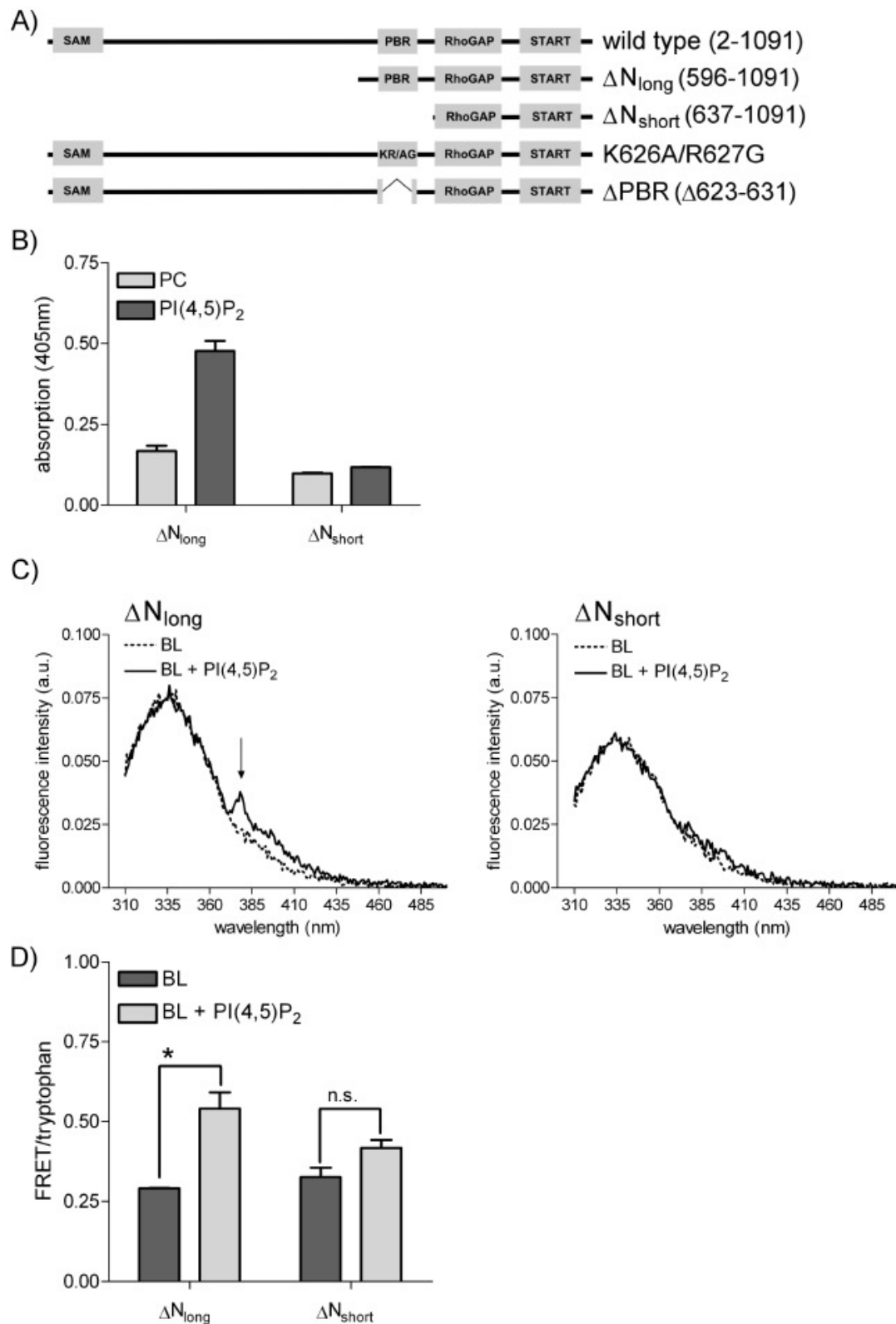
Fig. 3: The DLC1 polybasic region mediates PI(4,5)P$_2$ interaction. (A) Schematic representation of DLC1 WT, ΔN_{long}, ΔN_{short}, K626A/R627G and ΔPBR. (B) GFP-DLC1 ΔN_{long} and ΔN_{short} were tested for their ability to bind to immobilized PI(4,5)P$_2$ as described in Figure 1. (C) Recombinant GST-DLC1 ΔN_{long} (upper panel) or ΔN_{short} proteins (lower panel) were incubated with SUVs comprised of porcine brain lipids (BL) and pyrene-PC, with or without the addition of 10 mol% PI(4,5)P$_2$. The samples were excited at 290 nm and emission scans were recorded from 310 to 500 nm (a. u., arbritary units). Background spectra were recorded before protein addition. The arrow indicates pyrene fluorescence emission (376 to 379 nm) caused by FRET. (D) FRET/tryptophan ratios were calculated as described in the Methods section. Data shown are the mean of two experiments in the case of BL and three experiments in the case of BL + PI(4,5)P$_2$; error bars represent SEM. P values were determined by unpaired two-sided student's t test; * P$\leq$ 0.05; n.s. P>0.05.

proximity of the donor and acceptor (Figure 3C, left, FRET marked with an arrow). When DLC1 ΔN_{short} was incubated with PI(4,5)P$_2$-containing vesicles no FRET peak was observed (Figure 3C, right). FRET/tryptophan ratios are quantified in Figure 3D. In the case of DLC1 ΔN_{short} there was only a small non-significant difference between the FRET/tryptophan ratios for vesicles with and without PI(4,5)P$_2$ (Figure 3D). Collectively, our results provide evidence that DLC1 interacts with PI(4,5)P$_2$-containing membranes via a region rich in basic amino acids that directly precedes its GAP domain.

DLC1 activity is stimulated by PI(4,5)P$_2$-containing membranes

Due to the close proximity of the PI(4,5)P$_2$-binding motif to the DLC1 GAP domain, we speculated that lipid binding may modulate DLC1 GAP activity. We first determined *in vitro* GAP activities of GST-tagged DLC1 ΔN_{long} and ΔN_{short} in the absence of membranes using recombinant GTP-loaded RhoA as a substrate. As shown in Figure 4A, both DLC1 ΔN_{long} and ΔN_{short} displayed similar *in vitro* GAP activity for RhoA, proving that the deletion of the PBR *per se* does not impact on the DLC1 GAP domain. Of note, the addition of PI(4,5)P$_2$-containing vesicles did not affect the rate of RhoA-GTP hydrolysis in this assay (data not shown). In the cell, RhoA is post-translationally modified by geranylgeranylation, which targets it to membranes. Importantly, prenylation has been previously shown to alter the susceptibility of Rho GTPases towards GAP proteins (Ligeti et al., 2004). Thus, to investigate the impact of membranes on DLC1 GAP activity and the role of PI(4,5)P$_2$-binding, we set up an *in vitro* assay with prenylated recombinant RhoA (RhoA$_{GG}$) that mimics more closely the cellular environment. In order to compare for the different Rho preparations, we normalized the results for RhoA and RhoA$_{GG}$ to their intrinsic GTPase activity (Figure 4A+B). Interestingly, the presence of multilamellar vesicles (MLVs) composed of brain lipids (BL) strongly increased the GAP activity of DLC1 ΔN_{long} for Rho$_{GG}$ (from 80% to 48% remaining GTP), compared to nonprenylated RhoA (Figure 4A+B). Addition of PI(4,5)P$_2$ to these MLVs stimulated GAP activity even further (approximately twofold; Figure 4B, left). In contrast to DLC1 ΔN_{long}, DLC1 ΔN_{short} activity towards RhoA$_{GG}$ in a membrane environment was comparable to that observed for unprenylated RhoA and was not stimulated by incorporation of PI(4,5)P$_2$ into vesicles (Figure 4B, right).

To confirm these activity differences in intact cells, we ectopically expressed GFP-tagged variants of DLC1 ΔN_{long} and ΔN_{short} in MCF7 breast epithelial cells. DLC1 overexpression has been shown to induce cell rounding and leads to the development of neurite-like extensions, associated with a reduced stress fiber content due to decreased Rho-GTP levels (Sekimata *et al.*, 1999;Wong *et al.*, 2005). Expression of an isolated GAP domain is known to be sufficient for the induction of such effects. Indeed, MCF7 cells expressing DLC1 ΔN_{long} showed the typical 'neurite-like' morphology and a strong reduction of the number of stress fibers as determined by phalloidin staining (Figure 4C, upper panels). By contrast, cells expressing DLC1 ΔN_{short} displayed a normal flat morphology

and stress fibers appeared unchanged (Figure 4C, lower panels). Taken together, these results strongly suggest that the PBR-mediated lipid interaction is important for DLC1 RhoGAP function *in vitro* and *in vivo*.
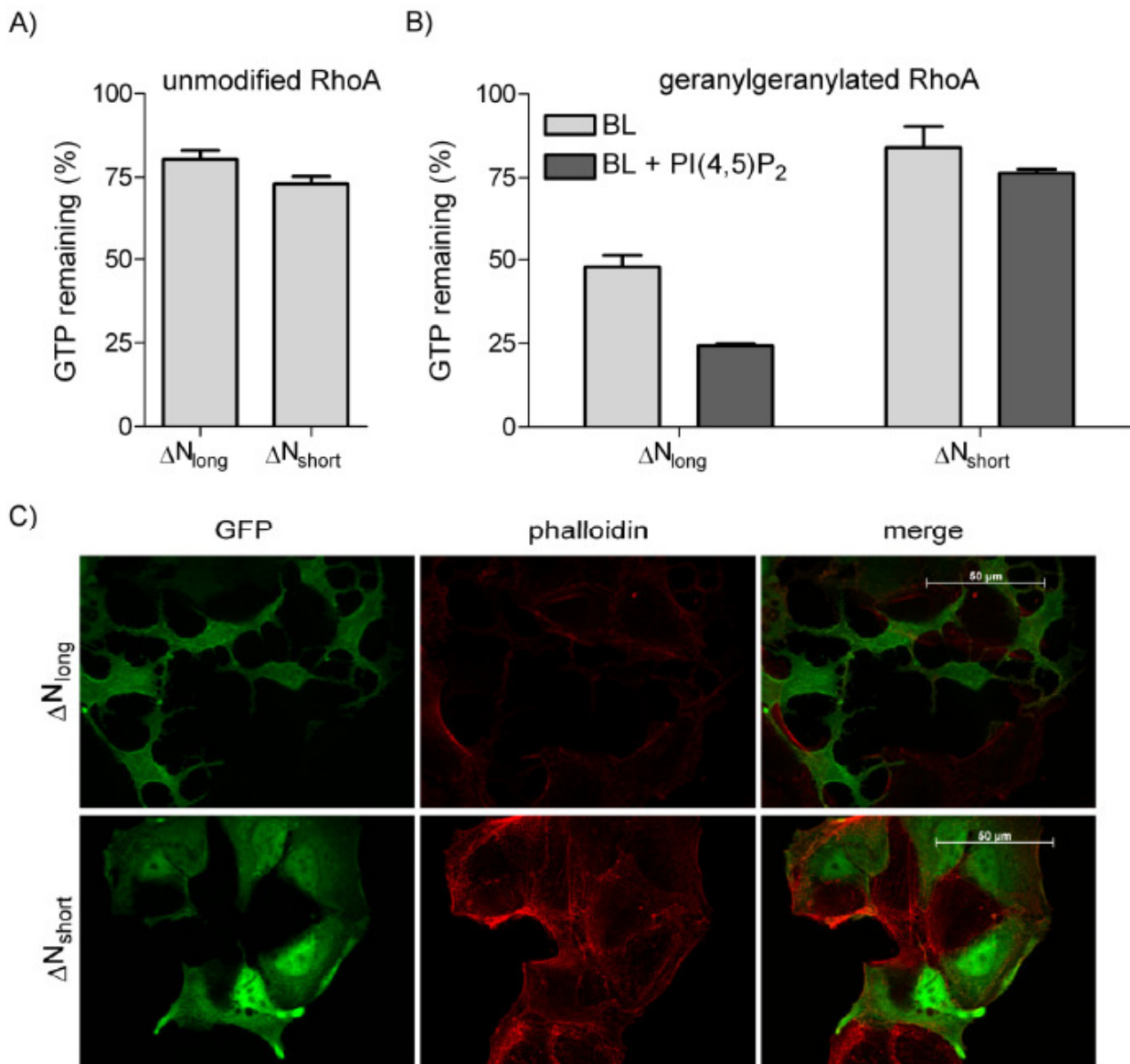

Fig. 4: Lipid interaction stimulates *in vitro* DLC1 RhoGAP activity. (A) GST-RhoA (10 µg) was loaded with γ^{32}P-GTP and incubated with equal amounts of GST-DLC1 ΔN_{long} and ΔN_{short} at 20°C. GTP hydrolysis was determined after 0 and 10 min by measuring protein-bound γ^{32}P-GTP. The intrinsic RhoA GTPase activity was set to 100%. The graph shows a representative experiment performed with triplicate samples; error bars represent SEM. (B) GST-RhoA was geranylgeranylated *in vitro* as described in the methods section. 10 µg GST-RhoA$_{GG}$ was loaded with γ^{32}P-GTP in the presence of 10 µg MLVs and incubated with equal amounts of GST-DLC1 ΔN_{long} and ΔN_{short} at 20°C. GTP hydrolysis was determined after 0 and 10 min by measuring protein-bound γ^{32}P-GTP. The intrinsic RhoA GTPase activity was set to 100%. The graph shows a representative experiment performed with triplicate samples; error bars represent SEM. (C) MCF7 cells were grown on collagen-coated cover slips and transfected with expression plasmids encoding GFP-DLC1 ΔN_{long} and ΔN_{short}. After 24 h cells were fixed and actin stress fibers were stained with Alexa Fluor 546-conjugated phalloidin (red). The images shown are stacks of 3-4 optical sections taken at 0.5 µm intervals; The scale bar corresponds to 50 µm.

The PBR in DLC1 is required for inactivation of Rho signaling

To study the role of the identified lipid binding region in the context of full length DLC1, we generated mutants deficient in $PI(4,5)P_2$-binding by (i) exchanging two basic amino acids in the core of the PBR (K626A/R627G) and (ii) deleting nine amino acids (623-631), generating a DLC1
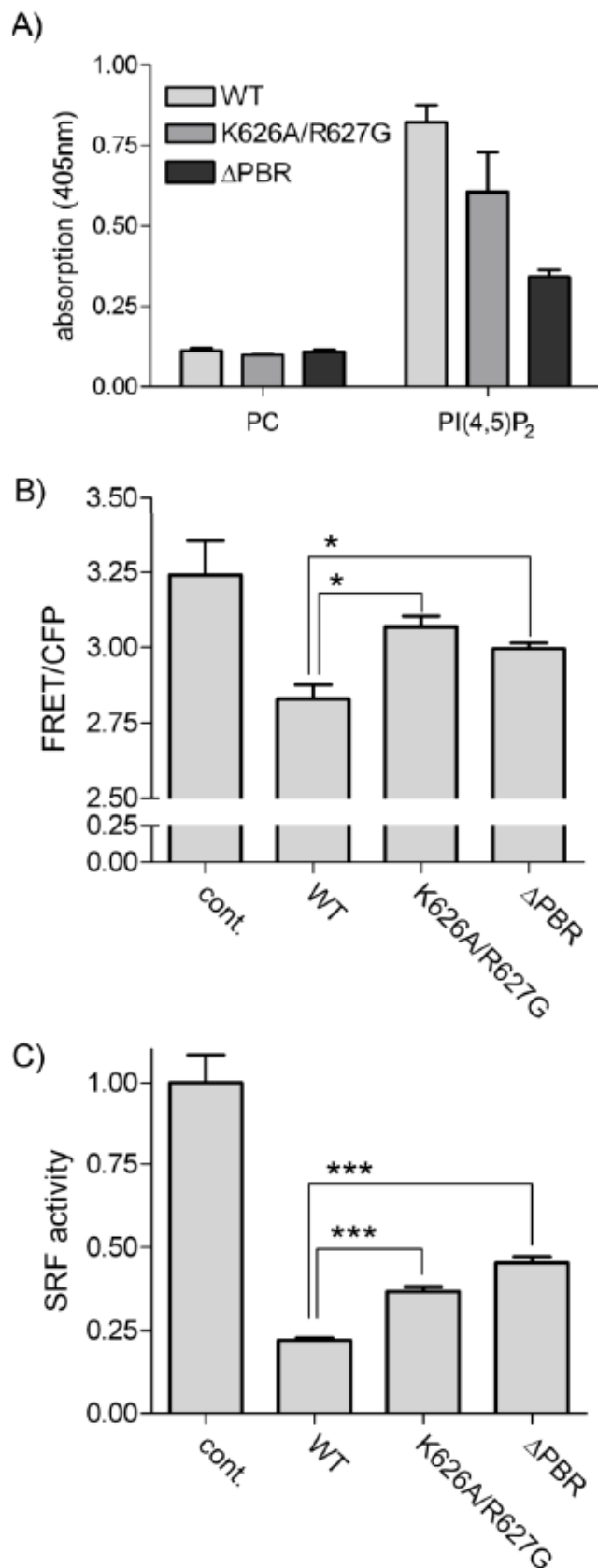
ΔPBR mutant (see Figure 2A). These mutations are expected to have a minimal impact on the overall structure of the protein. Lipid ELISA analysis confirmed that both mutations decreased $PI(4,5)P_2$-binding, with the ΔPBR deletion being more potent (Figure 5A). To determine the effects of these DLC1 variants on cellular Rho activity, we made use of a previously described Raichu-RhoA biosensor, whose FRET/CFP emission ratios reflect endogenous Rho-GTP levels (Yoshizaki et al., 2003). Compared to the wild type, DLC1 K626A/R627G and ΔPBR were less efficient at reducing the emission ratio of Raichu-RhoA (Figure 5B), indicating reduced GAP activities of the mutant proteins. To

Fig. 5: The DLC1 PBR is required for RhoGAP activity in intact cells. (A) GFP-tagged DLC1 WT, K626A/R627G and ΔPBR were tested for their ability to bind immobilized $PI(4,5)P_2$ as described in Figure 1. (B) HEK293T cells were cotransfected with plasmids encoding the Raichu-RhoA biosensor and Flag-DLC1 WT, K626A/R627G, ΔPBR or empty vector (cont.). The next day, the emission ratio of Raichu-RhoA was determined by measuring YFP (FRET) and CFP fluorescence (excitation 433 nm) in cell lysates. One representative experiment out of three is shown; error bars represent SEM. P values were determined by unpaired two-sided student's t test; * ≤ 0.05. (C) HEK293T cells were transiently transfected with the 3DA.Luc reporter, a plasmid encoding for Renilla luciferase and empty vector (cont.), pEGFPC1 DLC1 WT, K626A/R627G or ΔPBR, respectively. Cells were serum-starved overnight and then restimulated with 15% serum for 6 h. Firefly luciferase activity was determined and normalized by Renilla luciferase activity. The control was set to 1. Equal expression of the DLC1 variants was verified by measuring GFP fluorescence in the lysates with a fluorescence spectrometer. One representative experiment out of three is shown, each performed with triplicate samples; error bars represent SEM. P values were determined by unpaired two-sided student's t test; *** ≤ 0.005.

independently determine the contribution of the PBR to DLC1 RhoGAP function, we performed serum response factor (SRF) luciferase reporter assays, which are responsive to signaling by active Rho. Here, cells were transfected with an SRF reporter, serum-starved over night and then restimulated with serum. Compared to the wild type protein, which suppressed SRF-dependent transcription by 75%, the DLC1 K626A/R627G and ΔPBR mutants were less potent at inhibiting transcription (Figure 5C).
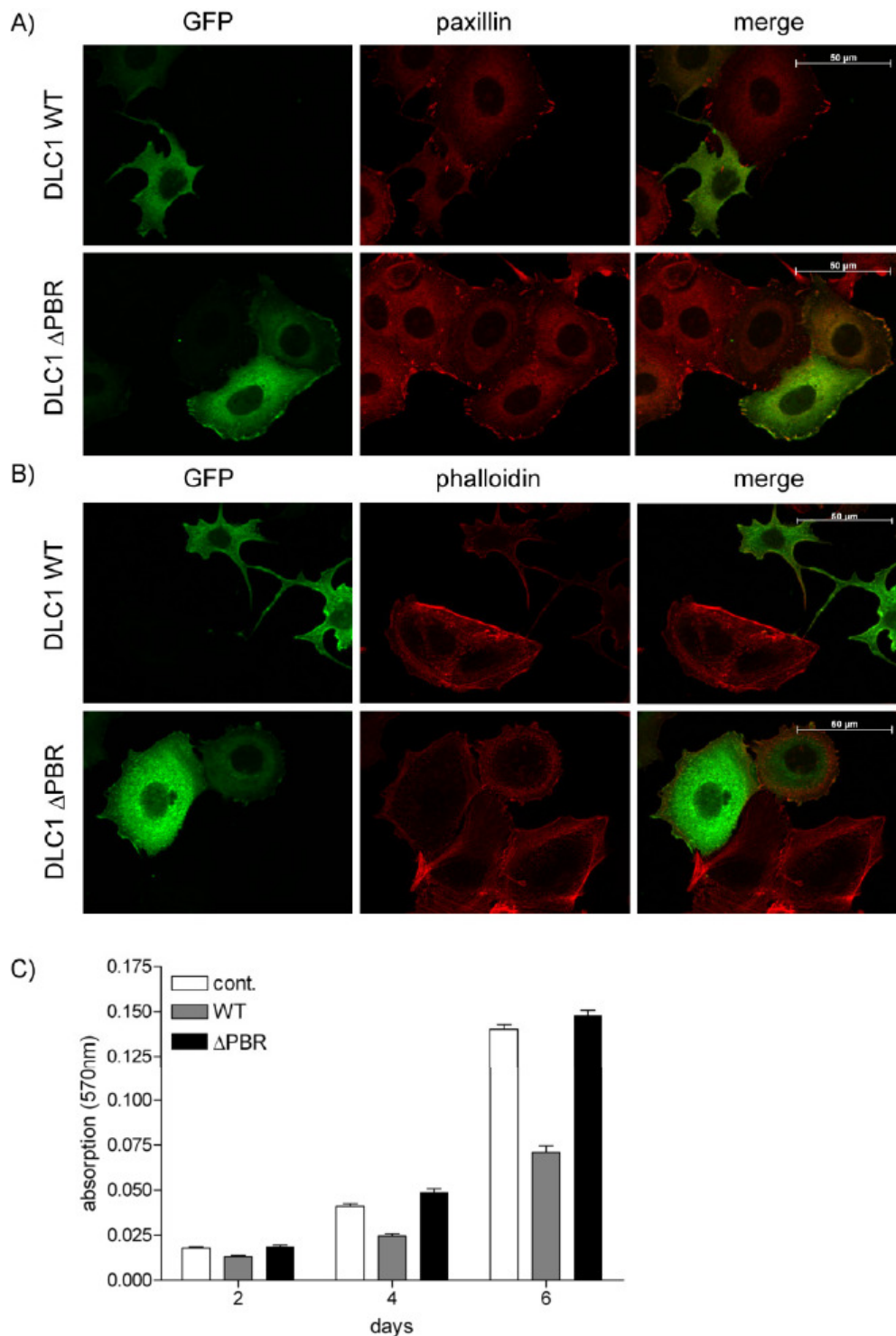

Fig. 6: The PBR is required for DLC1-mediated actin cytoskeletal changes and suppression of cell proliferation. (A) MCF7 cells grown on collagen-coated cover slips were transfected with expression plasmids encoding GFP-DLC1 WT or ΔPBR and fixed after 24 h. Focal adhesions were visualized with a paxillin-specific primary and Alexa Fluor 546-coupled secondary antibody (red). (B) Actin stress fibers were stained with Alexa Fluor 546-conjugated phalloidin (red). The images shown are stack of 3-4 optical sections taken at 0.5 µm intervals. The scale bar corresponds to 50 µm. (C) MCF7 cells were transfected by nucleofection with GFP-DLC1 WT, GFP-DLC1 ΔPBR and vector alone as a control (cont.). Proliferation of the cells was measured by MTT assay. A representative experiment is shown. Data are the mean of 9 wells, normalized to absorbance at day 0; error bars represent SEM.
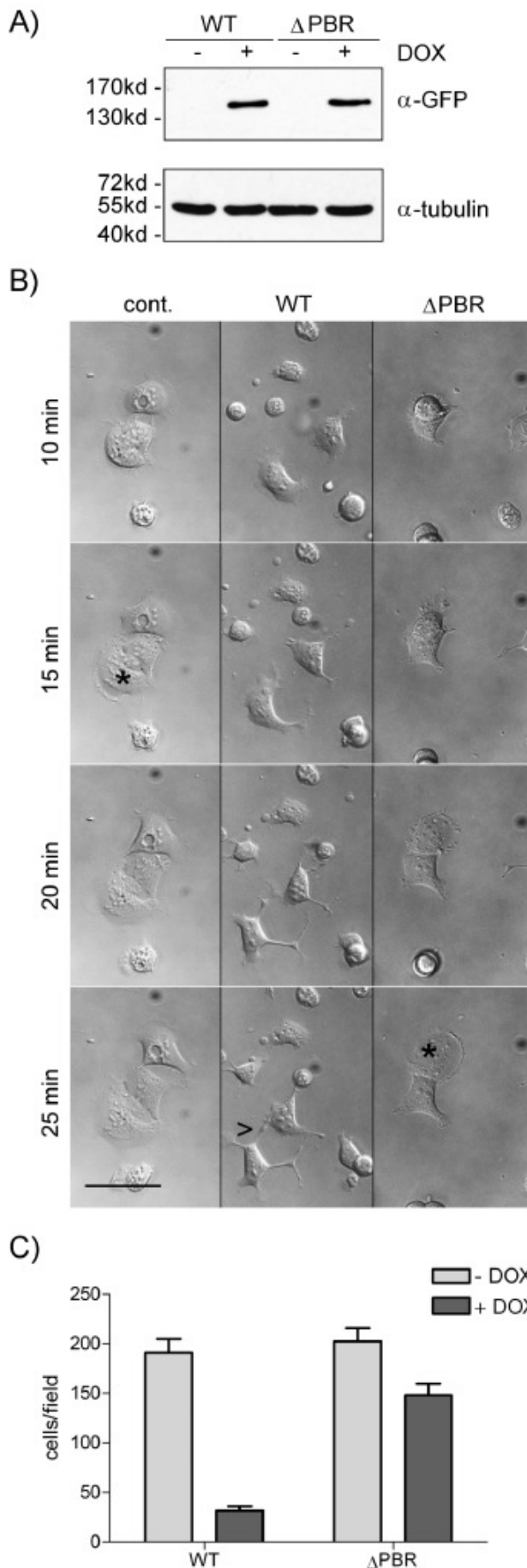
PBR deletion does not alter DLC1 localization but activity in MCF7 cells

To investigate whether the PBR may be involved in DLC1 subcellular localization, we ectopically expressed DLC1 WT and ΔPBR in MCF7 cells. Consistent with previous observations (Holeiter *et al.*, 2008), full length DLC1 localized to focal adhesions in these cells as determined by paxillin co-staining. DLC1 ΔPBR was also recruited to these sites but failed to lead to their dissolution (Figure 6A). Phalloidin staining further confirmed the reduced capacity of DLC1 ΔPBR to inhibit stress fiber formation compared to the wild type protein (Figure 6B), correlating with the results obtained with the truncated DLC1 variants. DLC1 has also been reported to localize to the leading edge of migrating cells (Healy *et al.*, 2008). However, membrane localization of DLC1 wild type and ΔPBR proteins were comparable as judged microscopically and by fractionation assays (data not shown), suggesting that deletion of the PBR does not alter DLC1 subcellular localization. We previously showed that DLC1 expression inhibits growth of MCF7 cells (Scholz *et al.*, 2009), but expression of DLC1 ΔPBR failed to do so as measured by an MTT assay (Figure 6C). Taken together, our results indicate that the PBR is required for DLC1 RhoGAP activity and its antiproliferative tumor suppressive properties.

Inhibition of cell spreading and migration by DLC1 requires an intact PBR

To study in greater detail the contribution of the newly identified lipid interaction motif to DLC1's effects on cytoskeletal remodeling we generated stable HEK293 Flp-In cell lines inducibly expressing either GFP-tagged wild type DLC1 or DLC1 ΔPBR. Due to targeted genomic integration of the cDNA, selected cells contained a single DLC1 copy that can be switched on by the addition of doxycycline. This is advantageous over high expression levels obtained in transient transfections and the growth suppressing and adaption effects encountered when generating stable cell lines. Figure 7A shows that equal amounts of GFP-tagged DLC1 wild type and ΔPBR were expressed upon doxycycline induction of these stable HEK293 Flp-In lines. To study the effect of DLC1 expression on cell morphology and actin cytoskeletal remodeling, we plated cells onto collagen-coated dishes and recorded cell spreading by live cell imaging. Compared to non-induced cells, expression of the DLC wild type protein did not alter cellular adhesion properties but severely impacted on cell spreading (Figure 7B). Cells expressing wild type DLC1 failed to form stable lamellipodia, which were seen in control cells by 15 min after plating (Figure 7B, asterisk), but instead developed abnormal cellular projections (Figure 7B, see arrowhead). These cells furthermore displayed a high degree of rapidly changing protrusive activity (see supplemental movies), which was previously described for HEK293 cells expressing a DLC1 variant lacking the SAM domain (Kim et al., 2008). By contrast, DLC1 ΔPBR expressing cells spread normally in a manner comparable to the control (Figure 7B and supplemental movies).

Transient expression of DLC1 ΔSAM in HEK293 cells was reported to increase the velocity but impair the directionality of migration (Kim et al., 2008). We therefore investigated the impact of DLC1 wild type and DLC1 ΔPBR on directed cell migration by performing Transwell filter assays. Cells were induced with doxycycline and seeded onto collagen-coated Transwell cell culture inserts, and migration was stimulated with a serum gradient (0.5% to 10%). DLC1 WT expression led to a severe decrease in the number of migrated cells, whereas DLC1 ΔPBR expression had only a slight impact on the migratory of cells (Figure 7C). We thus conclude that lipid interaction via the PBR is essential for DLC1 activity and its control of Rho-dependent cellular processes.

Fig. 7: A DLC1 mutant deficient in PI(4,5)P$_2$ binding fails to inhibit cell spreading and directed migration. (A) HEK293 Flp-In DLC1 WT and ΔPBR cells were left untreated (−) or treated (+) with 100 ng/ml doxycycline overnight to induce DLC1 expression. Whole cell extracts were separated by SDS-PAGE and analyzed by Western blotting with GFP-specific (top panel) and tubulin-specific antibodies (bottom panel) as loading control. (B) HEK293 Flp-In DLC1 WT and ΔPBR cells were treated with 100 ng/ml doxycycline overnight. Non-induced HEK293 Flp-In DLC1 WT cells were used as a control. Cells were harvested and plated onto collagen-coated glass bottom dishes. After 5 min, bright field images were taken every 30 seconds for 90 min. The figure shows snapshots of the movies (see online supplemental files) at the indicated time points; asterisks mark cells with lamellipodia; arrowheads point to projections. The scale bar corresponds to 50 μm. (C) HEK293 Flp-In DLC1 WT and ΔPBR cells were left untreated or treated with 100 ng/ml doxycycline. 5 x 10^4 cells were seeded in medium containing 0.5% FCS into the upper chamber of a Transwell. The lower well contained medium supplemented with 10% FCS. Cells that had migrated across the filter after 4 h were fixed and stained. The number of migrated cells was determined by counting five independent microscopic fields (20-fold magnification). Data shown are the mean of duplicate wells and are representative of two independent experiments. Error bars represent SEM.

Discussion

Here we have identified an evolutionarily conserved lipid interaction module within the DLC protein family that is necessary for cellular GAP function. Membrane binding is a common feature of many GTPases that often contain carboxy-terminal lipidation motifs. These can be accompanied by polybasic sequences that aid in localization and specificity to phospholipid membranes (Williams, 2003;Heo et al., 2006). Similarly, effector proteins are often targeted to lipids, due to the necessity of interacting with membrane-localized upstream GTPases (Papayannopoulos et al., 2005;Takahashi and Pryciak, 2007). Finally, GEFs and GAPs which are generally multidomain proteins physically associate with their cognate GTPases and thus often contain different membrane targeting sequences, such as PH, PX, C1, C2, FYVE, ENTH and FERM domains (Hurley, 2006;Bos *et al.*, 2007;Gureasko et al., 2008).

Polybasic sequences generally contain multiple positively charged amino acids that can interact with acidic phospholipids through electrostatic interaction. They further often contain hydrophobic amino acids, present also in the PBR of the DLC proteins, that partition into the hydrophobic core of the lipid bilayer and prevent recognition as nuclear targeting sequences (Heo *et al.*, 2006). The DLC1 PBR from amino acids 614-636 is interspersed by two prolines but may adopt an amphipathic helix in its core section of alternating basic and hydrophobic residues (KFMKRIKV). We show that the DLC1 PBR mediates binding of negatively charged $PI(4,5)P_2$ in an immobilized form and when incorporated into lipid vesicles. $PI(4,5)P_2$ is a phospholipid species enriched in the plasma membrane. Consistent with a previous report (Healy *et al.*, 2008) we observed DLC1 recruitment to the leading edge of migrating cells in addition to localization to focal adhesions, suggesting that Rho inactivation occurs locally at these sites. However, negatively charged phospholipids such as $PI(4,5)P_2$ are unlikely to be the sole determinant of DLC1 plasma membrane localization. Fusion of a peptide encompassing the DLC1 PBR to GFP led to GFP relocation from the nucleus to the cytoplasm, but was not sufficient to promote plasma membrane association (data not shown). Because lipid binding affinities of PBRs are generally rather low, they often act in concert with other interaction domains to promote efficient membrane targeting (Fivaz and Meyer, 2003). This provides an explanation for the similar subcellular distributions of DLC1 ΔN_{long} and ΔN_{short} and DLC1 wild type and ΔPBR proteins. Although SAM and START domains did not contribute to $PI(4,5)P_2$ binding in lipid ELISA assays, these domains may well cooperate in DLC1 membrane localization. It was recently shown that the DLC1 SAM domain associates with membrane ruffles in fibroblast growth factor-stimulated cells (Zhong et al., 2009) and our own experiments with the isolated START domain suggest that this domain strongly interacts with membranes *in vitro* and *in vivo* (data not shown). Furthermore, protein interactions are expected to be critically involved in DLC1 plasma membrane recruitment and activation, perhaps via binding of the Rho GTPase itself. Such activation models have been established for the Ras exchange factor

SOS and the Cdc42 effector N-WASP. In both cases, $PI(4,5)P_2$ and Ras and Cdc42 binding, respectively, act in a cooperative manner to promote full activation (Papayannopoulos *et al.*, 2005;Gureasko *et al.*, 2008).

There are several examples for lipids acting as cofactors in GAP regulation. The importance of phosphoinositides for the GAP activity of the ArfGAPs Arap1 and Arap3 is well established (Krugmann et al., 2002;Miura et al., 2002). Another example is provided by the chimaerins, RacGAP proteins that contain diacylglycerol-binding C1 domains important for membrane recruitment (Colon-Gonzalez and Kazanietz, 2006). Most reported biochemical studies on GAP proteins including those on DLC1 have been conducted with bacterially produced unmodified GTPases. It is known, however, that the lipid environment and prenylation state of the small GTPase are important factors that can modify the substrate specificity of GAPs. For example, p190RhoGAP is a GAP protein which displays *in vitro* activity for Rho and Rac. Interestingly, PS, PI and $PI(4,5)P_2$ inhibited its RhoGAP activity but activated its RacGAP activity when using small GTPases derived from insect cells as substrates (Ligeti *et al.*, 2004). This is in line with our observation that the stimulating effect of $PI(4,5)P_2$-containing membranes on DLC1 GAP activity is only evident for prenylated RhoA. Our results further clarify discrepancies relating to the boundaries of the DLC1 GAP domain. According to SwissProt database information the GAP domain spans amino acids 641-847. The DLC1 GAP domain was recently proposed to extend amino-terminally beyond amino acid 641 because a fragment comprising amino acids 629-1075 failed to produce morphological changes upon expression in cells (Kim *et al.*, 2008). Based on our data, this is attributable to the deletion of a functional PBR motif, since DLC1 ΔN_{short} spanning amino acids 637-1091 lacked *in vivo* activity, while retaining full GAP activity *in vitro* towards unmodified RhoA (Fig. 4A). Rat DLC1 was originally reported to bind and activate phospholipase C δ1 (PLC-δ1) by an unknown mechanism involving the carboxy-terminal half of the protein (Homma and Emori, 1995;Sekimata *et al.*, 1999). Human DLC1 was not found to stimulate phospholipid hydrolysis activity of PLC-δ1 in overexpression assays (Healy et al., 2008), but it cannot be ruled out that DLC1-bound $PI(4,5)P_2$ is utilized locally as a substrate by PLC-δ1.

To examine the importance of the PBR to DLC1 cellular function, we generated DLC1 K626A/R627G and ΔPBR mutants. Although $PI(4,5)P_2$ binding of these mutants was only partially abolished and Rho signaling was only moderately restored, their biological activities were strongly reduced. This proves that subtle changes in Rho-GTP levels can have a significant impact on cellular responses. Indeed, proliferation of MCF7 cells expressing DLC1 ΔPBR was comparable to that of control cells, while proliferation of cells expressing the wild type protein was reduced. To study the role of the DLC1 PBR on actin cytoskeletal remodeling we made use of a doxycycline-inducible cellular system. In HEK293 Flp-In cells expressing the wild type protein, cell spreading associated with lamellipodia and focal adhesion formation and directed migration were severely

compromised. In contrast to this, the cellular actin architecture and migration characteristics of cells expressing DLC1 ΔPBR were more comparable to parental cells, proving that the PBR is required for DLC1 to suppress Rho-dependent biological processes.

Many proteins that are crucial to the assembly of the migration machinery are regulated by $PI(4,5)P_2$. The formation of focal adhesions is dependent on localized $PI(4,5)P_2$ generation and PI(4,5)P2 is enriched at the leading edge (Janmey and Lindberg, 2004;Ling et al., 2006). The establishment and maintenance of local $PI(4,5)P_2$ pools is controlled by the balanced action of phosphatidylinositol phosphate kinases and enzymes that consume $PI(4,5)P_2$, such as phospholipases and phosphatidylinositol-3-kinase as well as $PI(4,5)P_2$ sequestering proteins (Janmey and Lindberg, 2004;Ling *et al.*, 2006). It is conceivable that $PI(4,5)P_2$-dependent DLC1 activation is part of a negative feedback since Rho signaling contributes to $PI(4,5)P_2$ production by activating phosphatidylinositol phosphate kinases (Oude Weernink et al., 2004). We attempted to investigate whether modulation of cellular $PI(4,5)P_2$ levels may influence DLC1 GAP activity and thus RhoA-GTP levels. However, $PI(4,5)P_2$ depletion by activation of phospholipases with 3m3FBS did not restore RhoA-GTP levels in cells expressing DLC1, as determined with Raichu-RhoA biosensor experiments (data not shown). However, such changes may not be seen in overexpression systems and are likely to require analysis by imaging at the single cell level. A challenge for the future is thus the identification of cooperating factors, both lipids and proteins, in DLC1 recruitment to membrane proximal sites in combination with the spatiotemporal analysis of DLC1-regulated Rho signaling events during cell spreading and migration.

Acknowledgements

Abbreviations

DLC (deleted in liver cancer); FRET (fluorescence resonance energy transfer); GAP (GTPase activating protein); GEF (guanine nucleotide exchange factor); PA (phosphatidic acid); PBR (polybasic region); PC (phosphatidylcholine); PI (phosphatidylinositol); $PI(3,4,5)P_3$ (phosphatidylinositol-3,4,5-trisphosphate); PI(4)P (phosphatidylinositol-4-phosphate); $PI(4,5)P_2$ (phosphatidylinositol-4,5-bisphosphate); PLC-δ1 (phospholipase C δ1); PS (phosphatidylserine); SAM (sterile alpha motif); START (StAR-related lipid transfer)

References

Alpy,F., Tomasetto,C. (2005). Give lipids a START: the StAR-related lipid transfer (START) domain in mammals. J.Cell Sci. *118*, 2791-2801.

Bernards,A., Settleman,J. (2005). GAPs in growth factor signalling. Growth Factors *23*, 143-149.

Bos,J.L., Rehmann,H., Wittinghofer,A. (2007). GEFs and GAPs: critical elements in the control of small G proteins. Cell *129*, 865-877.

Ching,Y.P., Wong,C.M., Chan,S.F., Leung,T.H., Ng,D.C., Jin,D.Y., Ng,I.O. (2003). Deleted in liver cancer (DLC) 2 encodes a RhoGAP protein with growth suppressor function and is underexpressed in hepatocellular carcinoma. J.Biol.Chem. *278*, 10824-10830.

Colon-Gonzalez,F., Kazanietz,M.G. (2006). C1 domains exposed: from diacylglycerol binding to protein-protein interactions. Biochim.Biophys.Acta *1761*, 827-837.

Durkin,M.E., Ullmannova,V., Guan,M., Popescu,N.C. (2007a). Deleted in liver cancer 3 (DLC-3), a novel Rho GTPase-activating protein, is downregulated in cancer and inhibits tumor cell growth. Oncogene *26*, 4580-4589.

Durkin,M.E., Yuan,B.Z., Zhou,X., Zimonjic,D.B., Lowy,D.R., Thorgeirsson,S.S., Popescu,N.C. (2007b). DLC-1:a Rho GTPase-activating protein and tumour suppressor. J.Cell Mol.Med. *11*, 1185-1207.

Fivaz,M., Meyer,T. (2003). Specific localization and timing in neuronal signal transduction mediated by protein-lipid interactions. Neuron *40*, 319-330.

Goodison,S., Yuan,J., Sloan,D., Kim,R., Li,C., Popescu,N.C., Urquidi,V. (2005). The RhoGAP protein DLC-1 functions as a metastasis suppressor in breast cancer cells. Cancer Res. *65*, 6042-6053.

Gureasko,J., Galush,W.J., Boykevisch,S., Sondermann,H., Bar-Sagi,D., Groves,J.T., Kuriyan,J. (2008). Membrane-dependent signal integration by the Ras activator Son of sevenless. Nat.Struct.Mol.Biol. *15*, 452-461.

Healy,K.D., Hodgson,L., Kim,T.Y., Shutes,A., Maddileti,S., Juliano,R.L., Hahn,K.M., Harden,T.K., Bang,Y.J., Der,C.J. (2008). DLC-1 suppresses non-small cell lung cancer growth and invasion by RhoGAP-dependent and independent mechanisms. Mol.Carcinog. *47*, 326-337.

Heo,W.D., Inoue,T., Park,W.S., Kim,M.L., Park,B.O., Wandless,T.J., Meyer,T. (2006). PI(3,4,5)P3 and PI(4,5)P2 lipids target proteins with polybasic clusters to the plasma membrane. Science *314*, 1458-1461.

Holeiter,G., Heering,J., Erlmann,P., Schmid,S., Jahne,R., Olayioye,M.A. (2008). Deleted in liver cancer 1 controls cell migration through a Dia1-dependent signaling pathway. Cancer Res. *68*, 8743-8751.

Homma,Y., Emori,Y. (1995). A dual functional signal mediator showing RhoGAP and phospholipase C-delta stimulating activities. EMBO J. *14*, 286-291.

Hurley,J.H. (2006). Membrane binding domains. Biochim.Biophys.Acta *1761*, 805-811.

Jaffe,A.B., Hall,A. (2005). Rho GTPases: biochemistry and biology. Annu.Rev.Cell Dev.Biol. *21*, 247-269.

Janmey,P.A., Lindberg,U. (2004). Cytoskeletal regulation: rich in lipids. Nat.Rev.Mol.Cell Biol. *5*, 658-666.

Kim,C.A., Bowie,J.U. (2003). SAM domains: uniform structure, diversity of function. Trends Biochem.Sci. *28*, 625-628.

Kim,T.Y., Healy,K.D., Der,C.J., Sciaky,N., Bang,Y.J., Juliano,R.L. (2008). Effects of structure of Rho GTPase-activating protein DLC-1 on cell morphology and migration. J.Biol.Chem. *283*, 32762-32770.

Krugmann,S., Anderson,K.E., Ridley,S.H., Risso,N., McGregor,A., Coadwell,J., Davidson,K., Eguinoa,A., Ellson,C.D., Lipp,P., Manifava,M., Ktistakis,N., Painter,G., Thuring,J.W., Cooper,M.A., Lim,Z.Y., Holmes,A.B., Dove,S.K., Michell,R.H., Grewal,A., Nazarian,A., Erdjument-Bromage,H., Tempst,P., Stephens,L.R., Hawkins,P.T. (2002). Identification of ARAP3, a novel PI3K effector regulating both Arf and Rho GTPases, by selective capture on phosphoinositide affinity matrices. Mol.Cell *9*, 95-108.

Lahoz,A., Hall,A. (2008). DLC1: a significant GAP in the cancer genome. Genes Dev. *22*, 1724-1730.

Liao,Y.C., Si,L., deVere White,R.W., Lo,S.H. (2007). The phosphotyrosine-independent interaction of DLC-1 and the SH2 domain of cten regulates focal adhesion localization and growth suppression activity of DLC-1. J.Cell Biol. *176*, 43-49.

Ligeti,E., Dagher,M.C., Hernandez,S.E., Koleske,A.J., Settleman,J. (2004). Phospholipids can switch the GTPase substrate preference of a GTPase-activating protein. J.Biol.Chem. *279*, 5055-5058.

Ling,K., Schill,N.J., Wagoner,M.P., Sun,Y., Anderson,R.A. (2006). Movin' on up: the role of PtdIns(4,5)P(2) in cell migration. Trends Cell Biol. *16*, 276-284.

Miura,K., Jacques,K.M., Stauffer,S., Kubosaki,A., Zhu,K., Hirsch,D.S., Resau,J., Zheng,Y., Randazzo,P.A. (2002). ARAP1: a point of convergence for Arf and Rho signaling. Mol.Cell *9*, 109-119.

Ng,I.O., Liang,Z.D., Cao,L., Lee,T.K. (2000). DLC-1 is deleted in primary hepatocellular carcinoma and exerts inhibitory effects on the proliferation of hepatoma cell lines with deleted DLC-1. Cancer Res. *60*, 6581-6584.

Oude Weernink,P.A., Schmidt,M., Jakobs,K.H. (2004). Regulation and cellular roles of phosphoinositide 5-kinases. Eur.J.Pharmacol. *500*, 87-99.

Papayannopoulos,V., Co,C., Prehoda,K.E., Snapper,S., Taunton,J., Lim,W.A. (2005). A polybasic motif allows N-WASP to act as a sensor of PIP(2) density. Mol.Cell *17*, 181-191.

Qian,X., Li,G., Asmussen,H.K., Asnaghi,L., Vass,W.C., Braverman,R., Yamada,K.M., Popescu,N.C., Papageorge,A.G., Lowy,D.R. (2007). Oncogenic inhibition by a deleted in liver cancer gene requires cooperation between tensin binding and Rho-specific GTPase-activating protein activities. Proc.Natl.Acad.Sci.U.S.A *104*, 9012-9017.

Ridley,A.J. (2006). Rho GTPases and actin dynamics in membrane protrusions and vesicle trafficking. Trends Cell Biol. *16*, 522-529.

Scholz,R.P., Regner,J., Theil,A., Erlmann,P., Holeiter,G., Jahne,R., Schmid,S., Hausser,A., Olayioye,M.A. (2009). DLC1 interacts with 14-3-3 proteins to inhibit RhoGAP activity and block nucleocytoplasmic shuttling. J.Cell Sci. *122*, 92-102.

Sekimata,M., Kabuyama,Y., Emori,Y., Homma,Y. (1999). Morphological changes and detachment of adherent cells induced by p122, a GTPase-activating protein for Rho. J.Biol.Chem. *274*, 17757-17762.

Takahashi,S., Pryciak,P.M. (2007). Identification of novel membrane-binding domains in multiple yeast Cdc42 effectors. Mol.Biol.Cell *18*, 4945-4956.

Wheeler,A.P., Ridley,A.J. (2004). Why three Rho proteins? RhoA, RhoB, RhoC, and cell motility. Exp.Cell Res. *301*, 43-49.

Williams,C.L. (2003). The polybasic region of Ras and Rho family small GTPases: a regulator of protein interactions and membrane association and a site of nuclear localization signal sequences. Cell Signal. *15*, 1071-1080.

Wong,C.M., Lee,J.M., Ching,Y.P., Jin,D.Y., Ng,I.O. (2003). Genetic and epigenetic alterations of DLC-1 gene in hepatocellular carcinoma. Cancer Res. *63*, 7646-7651.

Wong,C.M., Yam,J.W., Ching,Y.P., Yau,T.O., Leung,T.H., Jin,D.Y., Ng,I.O. (2005). Rho GTPase-activating protein deleted in liver cancer suppresses cell proliferation and invasion in hepatocellular carcinoma. Cancer Res. *65*, 8861-8868.

Xue,W., Krasnitz,A., Lucito,R., Sordella,R., Vanaelst,L., Cordon-Cardo,C., Singer,S., Kuehnel,F., Wigler,M., Powers,S., Zender,L., Lowe,S.W. (2008). DLC1 is a chromosome 8p tumor suppressor whose loss promotes hepatocellular carcinoma. Genes Dev. *22*, 1439-1444.

Yam,J.W., Ko,F.C., Chan,C.Y., Jin,D.Y., Ng,I.O. (2006). Interaction of deleted in liver cancer 1 with tensin2 in caveolae and implications in tumor suppression. Cancer Res. *66*, 8367-8372.

Yang,X.Y., Guan,M., Vigil,D., Der,C.J., Lowy,D.R., Popescu,N.C. (2009). p120Ras-GAP binds the DLC1 Rho-GAP tumor suppressor protein and inhibits its RhoA GTPase and growth-suppressing activities. Oncogene.

Yoshizaki,H., Ohba,Y., Kurokawa,K., Itoh,R.E., Nakamura,T., Mochizuki,N., Nagashima,K., Matsuda,M. (2003). Activity of Rho-family GTPases during cell division as visualized with FRET-based probes. J.Cell Biol. *162*, 223-232.

Yuan,B.Z., Jefferson,A.M., Baldwin,K.T., Thorgeirsson,S.S., Popescu,N.C., Reynolds,S.H. (2004). DLC-1 operates as a tumor suppressor gene in human non-small cell lung carcinomas. Oncogene *23*, 1405-1411.

Yuan,B.Z., Zhou,X., Durkin,M.E., Zimonjic,D.B., Gumundsdottir,K., Eyfjord,J.E., Thorgeirsson,S.S., Popescu,N.C. (2003). DLC-1 gene inhibits human breast cancer cell growth and in vivo tumorigenicity. Oncogene *22*, 445-450.

Zhong,D., Zhang,J., Yang,S., Soh,U.J., Buschdorf,J.P., Zhou,Y.T., Yang,D., Low,B.C. (2009). The SAM domain of the RhoGAP DLC1 binds EF1A1 to regulate cell migration. J.Cell Sci. *122*, 414-424.

Zhou,X., Thorgeirsson,S.S., Popescu,N.C. (2004). Restoration of DLC-1 gene expression induces apoptosis and inhibits both cell growth and tumorigenicity in human hepatocellular carcinoma cells. Oncogene *23*, 1308-1313.

8. Acknowledgements

First and foremost I would like to thank Moni Olayioye for giving me the opportunity to do my PhD thesis in her lab. I am thankful for Monis excellent scientific input, her brilliant ideas, great discussions and her patience. She would always support my own ideas adding her knowledge and asking just the right questions.

I also thank Klaus Pfizenmaier for providing the excellent scientific working atmosphere at the IZI and for being my PhD supervisor. I am grateful for excellent discussions with and support from Angelika Hausser.

Furthermore I would like to thank Simone Schmid and Ruth Jähne for their excellent technical assistance in the lab, always supporting my work. Moreover both made life at and beside the "bench" easier in all times. The same applies to all the other members of the MO-lab.

I thank Thomas Günther-Pomorski for agreeing to be part of my PhD committee and for giving me the possibility to learn techniques and perform experiments in his lab. Furthermore I would like to thank Andreas Hermann, Peter Müller, Thomas Korte and all members of the Molecular Biophysics group at the Humbolt University Berlin for their hospitality and advice.

I would to like thank all my colleagues, for stimulating discussions and knowledge exchange and for the very enjoyable working atmosphere at the IZI

At the end I would like to thank my Mum and Dad for everlasting faith and support throughout my studies, my sister Marie (You can do it too!), Karl and Bärbel for their support and interest.

Last but not least I would like to thank Mareike for her love, for giving me all help that she possibly could and for always believing in me.

9. Curriculum vitae

<p align="center">Patrik Erlmann né Schöffler</p>

<p align="center">E-mail: patrikerlmann@gmail.com</p>
<p align="center">Born 11.07.1977 in Filderstadt</p>
<p align="center">Nationality: German</p>

Job History

Since 8/2005	Universität Stuttgart, Institute of Cell Biology and Immunology: PhD thesis on START domain proteins with a special focus on the protein Deleted in Liver Cancer 1.
4/2005 - 6/2005	Friedrich-Löffler-Institut, Tübingen: Research scientist working on Orf virus influence on cell signaling.
2000	Eberhard-Karls-Universität Tübingen: Part-time work as a student assistant in the Organic Chemistry Department
8/1997-9/1998	Bethesda Hospital, Stuttgart: Mandatory civil service

University Education

7/2004 - 2/2005	Diploma thesis at the Friedrich-Löffler-Institut, Tübingen supervised by Prof. Hans-Georg Rammensee and Dr. Hanns-Joachim Rziha titled: Influence of an Orf virus infection on the intracellular signaling pathways in permissive and non-permissive cells.
8/2001 - 7/2002	California State University Long Beach, Biochemistry Department: Biochemistry studies, development of a Candida albicans infection mouse model with Dr. Mason Zhang
10/1998 - 7/2004	Eberhard-Karls-Universität Tübingen: Biochemistry studies with a focus on biochemistry, toxicology and analytical chemistry

School Education

1997	Abitur
8/1988 - 6/1997	Paracelsus-Gymnasium Hohenheim, Stuttgart: Advanced courses in chemistry and mathematics
8/1984 - 7/1988	Grund- und Hauptschule Plieningen, Stuttgart